Novel Approaches in Urethane Acrylate Chemistry

Dissertation

with the aim of achieving the doctoral degree

at the faculty of Mathematics, Informatics and Natural Sciences

submitted to the

Department of Chemistry

University of Hamburg

Niklas Volker Voigt

2022 in Hamburg

The following evaluators recommend the admission of the dissertation:

1. Evaluator: Professor Dr. Gerrit A. Luinstra
2. Evaluator: Professor Dr. Berend Eling

Date of the oral defense: 24.02.2023

Examination committee:

1. Professor Dr. Gerrit A. Luinstra
2. Professor Dr. Volker Abetz
3. Dr. Thomas Hackl

The experimental work described in this thesis has been carried out between May 2017 and July 2020 at the Technical and Macromolecular Chemistry, University of Hamburg in the research group of Prof. Dr. Gerrit A. Luinstra.

Contents

List of Abbreviations

AMA	2-Methylacryloyloxyethyl acrylate
BDMA	*N,N*-Dimethylbenzylamine
BHT	Butylated hydroxytoluene
BuA	Butyl acrylate
BuOH	1-Butanol
c	Concentration
CMC	Critical micelle concentration
CP	Cloud point
Cs Ac	Cesium acetate
Cs Oct	Cesium octoate
DABCO	1,4-Diazabicyclo(2.2.2)octane
DBU	Diazabicyclo(5.4.0)undec-7-ene
DLS	Dynamic light scattering
DMA	Dynamic mechanical analysis
DSC	Differential scanning calorimetry
ESI	Electrospray ionization
EtOH	Ethanol
f	Crosslinker functionality (f_{cor} = corrected)
F_n	Number of functional groups
G	Gel content
G’	Storage modulus
G’’	Loss modulus
GC	Gas chromatography
HDDA	1,6-Hexanediol diacrylate
HDI	Hexamethylene diisocyanate
HexA	Hexyl acrylate
HLB	Hydrophilic-lipophilic balance
HLB	Hydrophilic-lipophilic balance
H_P	Enthalpy of polymerization

IR	Infrared spectroscopy
K Ac	Potassium acetate
K Oct	Potassium octoate
LiCl	Lithium chloride
m	Mass or number of repeating units
M1/M2	Mold 1 or 2
M_c	Average molar mass between crosslinks
MDI	Methylene diphenyl diisocyanate
MeHQ	4-Methoxyphenol
MeOH	Methanol
$MgSO_4$	Magnesium sulfate
1-MI	1-Methylimidazol
M_n	Number average molar mass
MoPEG	Methoxylated poly(ethylene glycol)
MS	Mass spectrometry
mTMI	*meta*-Tolyl isocyanate
n	Amount of substance
N	Number of functional groups
NCO	Isocyanate
NMR	Nuclear magnetic resonance spectroscopy
N_P	Number of latex particles
oTMI	*ortho*-Tolyl isocyanate
p	Pressure
PE	Petroleum ether
PEG	Poly(ethylene glycol)
PEOL	Polyether-based polyol
PESOL	Polyester-based polyol
PETA	Pentaerythritol tetraacrylate
P_n	Degree of polymerization
POE	2-Phenoxyethanol
POEA	Phenoxyethyl acrylate

PPG	Poly(propylene glycol)
PrOH	Propanol
PTHF	Poly(tetrahydrofuran)
pTMI	*para*-Tolyl isocyanate
PU	Polyurethane
Q	Degree of swelling (Q_v = volume related)
R	Universal gas constant
r	Ratio or reaction parameter
Rb Ac	Rubidium acetate
Rb Oct	Rubidium octoate
RT	Room temperature (mostly 20 – 25 °C)
$R_{urethane}$	Residual urethane after purification
S	Sol content
SEM	Scanning electron microscope
SHA	Shore hardness type A
s_n	Number weight particle size
S_P	Entropy of polymerization
s_v	Volume weight particle size
t	Time
T	Temperature
tan(δ)	Dissipation factor
T_{cc}	Temperature of cold crystallization
TDI	Toluene diisocyanate
T_g	Glass transition temperature
TGA	Thermogravimetric analysis
THF	Tetrahydrofuran
T_m	Melting-temperature
T_{max}	Maximum temperature
TMPTA	Trimethylolpropane triacrylate
TMS	Tetramethylsilane
TPU	Thermoplastic polyurethane

ν	Wavenumber
V_s	Molar volume of solvent
X	Conversion or yield
Zn Oct	Zinc octoate
δ	Solubility parameter (s = solvent, p = polymer)
ΔG_P	Gibbs free energy of polymerization
ε_b	Elongation at break
ρ	Density (s = solvent, p = polymer)
σ_b	Stress at break
σ_{CMC}	Surface tension (at CMC)
Φ_p	Volume fraction of polymer
χ	Flory-Huggins interaction parameter

1 Zusammenfassung

Eine kovalente Bindung zwischen Urethan und Acrylat kann lösungsmittelfrei durch eine *aza*-Michael-Additionsreaktion in Gegenwart von *Lewis*-Säuren oder *Brønsted*-Basen erhalten werden. Eine auf monofunktionellen Ausgangsmaterialien basierende Modellstudie ergab, dass Carboxylat-Katalysatoren die gewünschte Addukt-Bildung am effektivsten katalysierten und Umsätze von mindestens 70 % erzielen. Unerwünschte Nebenreaktionen führten mit steigender Katalysatorkonzentration und Reaktionstemperatur zu einer Vielzahl von Nebenprodukten. Die auf Urethan basierenden *aza*-Michael-Addukte zeigten im Vergleich zum ausgehenden Urethan-Edukt eine deutlich erhöhte thermische Stabilität ($\Delta T \approx 100$ °C). Ein Modellsystem aus Isocyanat, Alkohol und Acrylat wurde verwendet, um die *aza*-Michael-Additionsreaktion zu untersuchen. Carboxylat-Katalysatoren katalysierten auch die konkurrierende Bildung von Isocyanurat, welche jedoch durch einen zweifachen Isocyanat-Überschuss kompensiert werden konnte. Der Einsatz der *Lewis*-Säure LiCl als Katalysator führte zu einer deutlich verringerten Isocyanurat-Bildung. Verschiedene tertiäre Amin-Katalysatoren wurden ebenfalls auf katalytische Wirkung untersucht, jedoch zeigte nur 1,4-Diazabicyclo[2.2.2]octan eine gewisse Aktivität für die *aza*-Michael-Reaktion. Poly(ethylenglycol) wurde zur Komplexierung des Alkalikations von Carboxylat-Katalysatoren eingesetzt, was zu erhöhten Reaktionsgeschwindigkeiten bei niedrigen Temperaturen und zu einer erhöhten Selektivität der Reaktion führte. In Untersuchungen zum Einfluss des Methylsubstituenten am aromatischen Ring des Arylisocyanat-Edukts auf den Umsatz wurde der höchste Umsatz für *ortho*-substituierte aromatische Urethane beobachtet (ca. 75 %). Der geringste Umsatz wurde bei einem Derivat mit Methylgruppe in *meta*-Position erzielt (ca. 53 %). Reaktionen basierend auf dem asymmetrischen 2-(Methacryloyloxy)ethylacrylat zeigten, dass das Urethan-N-H-Nukleophil keinerlei Reaktivität gegenüber Methacrylat besitzt. Die Nukleophilie von aliphatisch-aliphatischem und aromatisch-aliphatischem Urethan N-H wurde unter Verwendung von Acrylat-Urethan-Hybridmolekülen analysiert. Das aliphatisch-aliphatische Urethan N-H zeigte keine Reaktion. Ein Monomer basierend auf dem stärkeren N-H-Nukleophil eines aromatisch-aliphatischen Urethans wurde jedoch in kurzkettige *aza*-Michael-Polyadditionsreaktionsprodukte umgewandelt. Es wurde ein Polymerisationsgrad von ca. 11 erzielt (Umsatz von ca. 91 %).

Die *aza*-Michael-Additionsreaktion konnte zur Synthese nicht-ionischer, amphiphiler Moleküle ausgehend von Urethanen und Acrylaten verwendet werden. Es wurde ein allgemeines Syntheseprotokoll mit akzeptablen Ausbeuten ausgearbeitet (ca. 80 – 90 %). Die wasserlöslichen Tenside zeigten kritische Mizellkonzentrationen zwischen 300 bis 900 µmol/L und Trübungspunkte zwischen 25 und 100 °C. Sie führten zudem zu einer starken Reduktion der Oberflächenspannung (ca. 31 – 45 mN/m bei der kritischen Mizellkonzentration). Die stärkste Verringerung der Oberflächenspannung wurde bei einem Tensid auf Basis von methoxyliertem Poly(ethylenglycol) (M_n = 364 g/mol), *para*-Tolylisocyanat und 2-Ethylhexylacrylat beobachtet (31.0 mN/m bei der kritischen Mizellkonzentration). Ausgewählte Tenside wurden in der Synthese von PU-Hartschäumen zur Reduktion der durchschnittlichen Zellgröße von 94±3 Zellen/cm^2 auf 195±26 Zellen/cm^2 eingesetzt (mit/ohne Tensid basierend auf 4-*tert*-Butylcyclohexylacrylat). Normalerweise genutzte Silikon-Tenside führten jedoch zu einer stärkeren Reduktion der durchschnittlichen Zellgröße (648±3 Zellen/cm^2). Bei der Emulsionscopolymerisation von *n*-Butylacrylat und 2-Ethylhexylacrylat wurde die Tensid-Konzentration zwischen 11.6 und 46.3 mmol/L variiert. Die kleinsten Latexpartikel wurden bei der höchsten Tensid-Konzentration beobachtet (zahlenmittlere Partikelgröße von 168 nm bei 46.3 mmol/L).

Das Vorgehen zur Synthese von Modell-Hybridelastomeren basierend auf Polyurethan und Acrylat wurde ebenfalls beschrieben. Lineare Polyurethan-Oligomere wurden durch polyfunktionelle Acrylate unter Verwendung der lösungsmittelfreien *aza*-Michael-Additionsreaktion vernetzt. Elastomere aus dem zweifunktionellen Hexandioldiacrylat und PEG600/MDI/pTMI-Polyurethan zeigten basierend auf Messungen der Gleichgewichtsquellung eine geringe Vernetzung mit einem Sol-Gehalt von S_{max} = 13.1 %. Der Einsatz des vierfunktionellen Pentaerythritoltetraacrylats führte zu einer starken Reduktion des Sol-Gehalts (S_{max} = 2.9 %). Die Zugfestigkeit und Reißdehnung der Modell-Polymere wurde verbessert, indem das PEG600/MDI/pTMI-Polyurethan durch Polyurethan ersetzt wurde, welches partiell aus nicht-*aza*-Michael-reaktiven aliphatisch-aliphatischen Urethangruppen bestand (basierend auf Hexandiisocyanat; 1.35±0.14 MPa bei 36±3 % auf 1.47±0.13 MPa bei 68±4 %). Die unvollständige Umsetzung des Acrylats bei der Vernetzung mittels *aza*-Michael-Additionsreaktion erwies sich als größte Herausforderung. Eine optimierte Katalyse ist zur weiteren Verbesserung der Polymereigenschaften erforderlich.

2 Summary

A covalent bond between urethane and acrylate can be obtained in bulk by an *aza*-Michael addition reaction in the presence of *Lewis*-acids or *Brønsted*-bases. A model study based on monofunctional starting materials revealed that carboxylate-type catalysts were the most effective towards the desired adduct formation, reaching conversions of at least 70 %. Undesired side reactions led to a broad range of byproducts with increasing catalyst concentration and temperature. The urethane-based *aza*-Michael adducts, however, showed a significantly increased thermal stability over the original urethane ($\Delta T \approx 100$ °C). A model system based on isocyanate, alcohol and acrylate was used to characterize the *aza*-Michael addition reaction. Carboxylate catalysts also catalyzed a competing isocyanurate formation but a two-fold isocyanate-excess was useful for compensation. This isocyanurate formation was slow when using the *Lewis*-acid LiCl as a catalyst. Different tertiary amine catalysts were also studied for catalytic action but only 1,4-diazabicyclo[2.2.2]octane showed some activity for the *aza*-Michael reaction. The ability of poly(ethylene glycol) to complex the alkali cation in carboxylate-type catalysts led to increased reaction rates at low temperatures and a higher reaction selectivity was obtained. The highest conversion was obtained for *ortho* substituted aromatic urethanes (approx. 75 %) in a study about the influence of the methyl substituent on the aromatic ring of the aryl isocyanate educt. The lowest conversion was observed for derivatives with a methyl group in the *meta*-position (approx. 53 %). Reactions conducted with the asymmetric 2-(methacryloyl oxy) ethyl acrylate showed that the urethane-N-H nucleophile did not show any reactivity towards methacrylates. Acrylate-urethane hybrid-molecules were used to map the nucleophilicity of aliphatic-aliphatic and aromatic-aliphatic urethane N-H. The aliphatic-aliphatic urethane N-H showed no reaction. A monomer containing the stronger N-H nucleophile of an aromatic-aliphatic urethane was converted to short *aza*-Michael polyaddition reaction polymers. A degree of polymerization was reached of approx. 11 (conversion of approx. 91 %).

The *aza*-Michael addition reaction proved suitable for the synthesis of non-ionic amphiphilic molecules from urethanes and acrylates. A general synthesis protocol was elaborated that provided adequate product yields (approx. 80 – 90 %). All water-soluble surfactants showed critical micelle concentrations in the range of about 300 to 900 µmol/L, cloud-points between 25 and 100 °C and a strong surface tension reduction (approx. 31 – 45 mN/m at the critical micelle concentrations). The

strongest reduction of surface tension (31.0 mN/m at critical micelle concentration) was found for a surfactant from methoxylated poly(ethylene glycol) (M_n = 364 g/mol), *para*-tolyl isocyanate and 2-ethylhexyl acrylate. The surfactants were used in reducing the average cell size of PU rigid foams from 94±3 cells/cm^2 to 195±26 cells/cm^2 (with and without surfactant from 4-*tert*-butylcyclohexyl acrylate, respectively). Commonly applied silicone surfactants led to a stronger reduction of the average cell size (648±3 cells/cm^2). The surfactant concentration was varied in the range of 11.6 to 46.3 mmol/L in the emulsion copolymerization of *n*-butyl acrylate and 2-ethylhexyl acrylate. The smallest latex particles were found for the highest surfactant concentration (number weight particle size of 168 nm at 46.3 mmol/L).

A protocol for the preparation of model polyurethane-acrylate hybrid-elastomers was also established. The solvent-free *aza*-Michael addition reaction was used to crosslink linear polyurethane oligomers with polyfunctional acrylates. Elastomers based on the two-functional hexanediol diacrylate and PEG600/MDI/pTMI-polyurethane showed poor crosslinking as determined by equilibrium swelling with a sol content of S_{max} = 13.1 %. It was strongly reduced to S_{max} of 2.9 % when tetra-functional pentaerythritol tetraacrylate was employed. The tensile strength and elongation at break were improved by substituting the PEG600/MDI/pTMI-polyurethane with partly non-*aza*-Michael reactive hexane diisocyanate containing polyurethane (1.35±0.14 MPa at 36±3 % to 1.47±0.13 MPa at 68±4 %). The major drawback of the *aza*-Michael addition crosslinking technology was the incomplete conversion of the acrylate. Improved catalysis is required to further improve the polymer properties.

3 Introduction

3.1 Polyurethane chemistry

A polymer based on the polyaddition reaction of polyfunctional alcohols (polyols) and polyfunctional isocyanates is called a polyurethane (PU, Figure 1 (a)). Polyurethanes were first described by OTTO BAYER and his team of researchers at I.G. Farben AG in 1937.[1] In the following years, the properties of this new class of polymers were intensively investigated and developed.[2] Today, polyurethane represents one of the most important specialty polymers with a global production of 27 million tons in 2015.[3,4] Most often PU is prepared in the presence of various additives such as catalysts, flame retardants and blowing agents.[5] Industrial polyurethane chemistry also includes additional isocyanate reactions such as the formation of urea, the reaction product of an amine and isocyanate, Figure 1 (b), the dimerization and trimerization of isocyanate leading to uretdione and isocyanurate, Figure 1 (c) and (d), respectively, or the subsequent reactions of isocyanate with urethane and urea to allophanate, Figure 1 (e), and biuret, Figure 1 (f), respectively.[6]

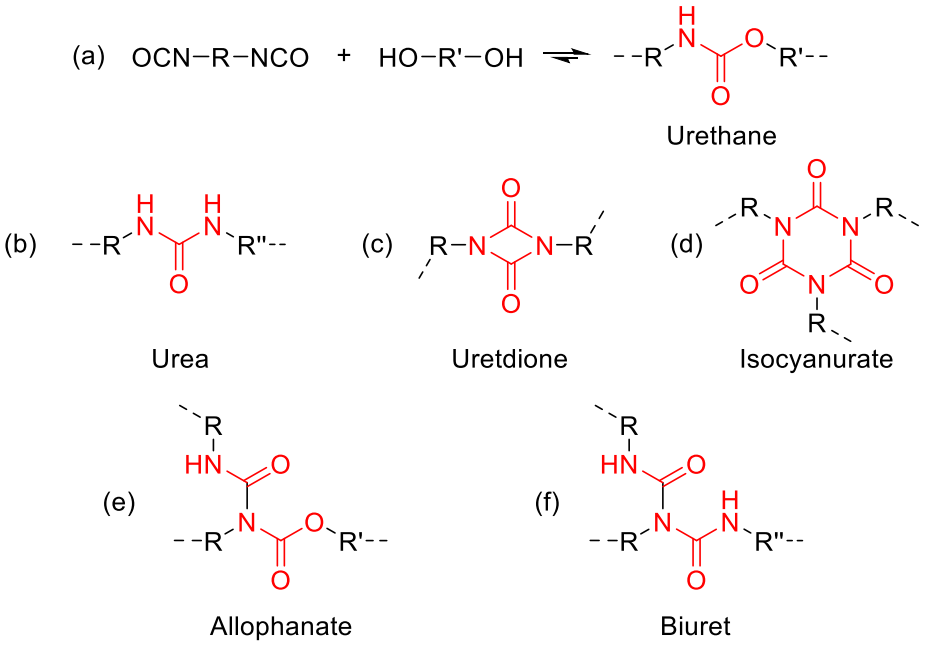

Figure 1. Isocyanate addition reaction products.

PU can be found in many applications in the daily life which is justified by the wide range of different material properties that can be achieved through the use of different starting materials or reactions.[7] Polymers with different network topologies and polymer morphologies can be obtained, depending on the structure of the starting materials. The usage of only two-functional components leads to the formation of linear

thermoplastic polyurethanes (TPU).[8] Thermosets will be formed, when the functionality F_n of one of the components is higher than 2. Depending on the crosslink density, the polymers can either be soft and elastomeric ($F_n > 2$) or hard and rigid ($F_n >> 2$).[9] The addition of blowing agent leads to the formation of rigid or flexible foams. The blowing agent can be of physical (e.g., cyclohexane) or chemical (e.g., water) origin.[10] Polyurethane foams are used, for example, as insulating materials or mattress foams. Polyurethane elastomers benefit from the characteristic phase separation between hard and soft segments during polymerization. The polyol-rich soft phase provides excellent elasticity, while the urethane-rich hard phase acts as physical crosslinker and ensures toughness. The extent of phase separation depends heavily on the polarity, structure and functionality of the starting materials as well as on the processing.[5,11–21] Polyurethane elastomers can be found, e.g., in the cable industry as sheathing material,[10] in shock absorbers providing damping properties,[22,23] as elastic yarns in the textile industry[24] or soling material in the manufacturing of shoes.[25] Sustainability has become increasingly important in recent years. A more environmentally benign polyurethane life cycle can be obtained when using bio-based raw materials such as 1,4-butanediol and poly(tetrahydrofuran). Also recycling of PU materials at the end of their service life becomes increasingly important.[26]

3.2 Polyacrylate chemistry

Polyacrylates are formed by the polymerization or copolymerization of acrylic acid and/or its salts, esters, amides, and nitriles.[27] The world annual production of acrylic acid was about 8 million tons in 2017.[28] Most often these acrylates are produced from oil-based petrochemicals and more recently also from renewable resources. For example, crude glycerol as a byproduct of the biodiesel production can be converted to acrylic acid.[29] The oxidative dehydration of glycerol with oxygen allows its formation in a single stage process. Vanadosilicate catalysts proved to be highly effective in latter process.[30]

Polyacrylates are used in many applications. They are employed as water absorbent materials (e.g., in disposable diapers),[31] in paint and coating applications[32–34] or in adhesives.[35,36] Polyacrylates are utilized in pressure sensitive adhesive applications because of their strong cohesion, high temperature and UV stability and solubility in common solvents. They are prepared either in bulk or solution polymerizations. A polymerization can be inflicted by for example UV radiation.[36] Binders for acrylic paints

are often prepared by emulsion copolymerization of ethyl acrylate and methyl methacrylate. Drying of the water-based dispersion (polyacrylate latex) leads to a continuous film.[37] Poor tensile properties and water resistance were reported to be the major shortcomings of films from simple polyacrylate latexes.[38] Their performance is commonly improved by combining them with further chemicals or materials (polymers or fillers) either by physical blending or, more preferably, by copolymerization of the acrylates with other vinylic monomers.[39–42] Polyurethanes are frequently used for acrylate modification.[27,43]

3.3 Conventional urethane-acrylate chemistry

Isocyanate-terminated urethane-prepolymers can be reacted with hydroxy-terminated acrylic monomers to give a set of acrylate monomers, i.e., the resulting polyurethane chains become terminated with acrylate functionalities (“conventional approach”). Such functionalities can participate in radical polymerizations after proper initiation by for instance photo initiators or exposure to UV-radiation.[44–46] Because of their high viscosities acrylate-terminated urethanes are often diluted down by addition of reactive diluents to adjust viscosity and reactivity. Reactive diluents are for example low molecular weight mono- or polyfunctional acrylates and methacrylates such as butyl acrylate[47], dipropyleneglycol diacrylate[46] and methyl methacrylate.[48] The combination of acrylate and urethane, so called hybrid-chemistry, allows further extension of the properties range of conventional polyurethanes and polyacrylates. Such copolymers are used in several applications[49–53] and have recently been reviewed (2018).[44] For example, coating formulations are often produced by mixing aqueous polyurethane and polyacrylate dispersions. Polyurethane-based coatings combine high elasticity with a superior abrasion resistance and can be custom tailored.[54] Urethane-acrylate hybrid coatings could not only be produced at lower costs than polyurethanes, they also showed increased solvent and chemical resistance and improved mechanical properties such as increased hardness, modulus and tensile strength.[48,55] Polyfunctional reactive diluents reinforce the film build by the urethane chains by crosslinking.[48] In the context of this work, it is important to emphasize that in this conventional urethane-acrylate chemistry the incorporation of acrylate-functionalities is obtained by coupling the acrylate by an urethane-linkage (Figure 2).

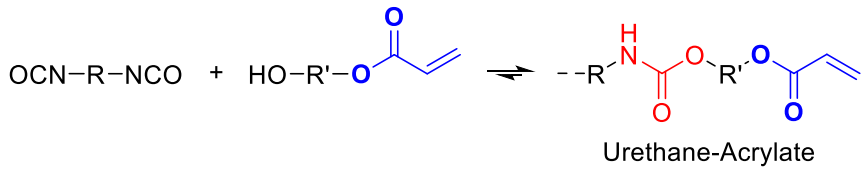

Figure 2. Conventional urethane-acrylate chemistry.

3.4 Non-conventional covalent connection of urethane and acrylate

Two putative reaction mechanisms have been put forward for reaching a direct, covalent connection of urethane and acrylate (non-conventional), i.e., by an interaction of the polyurethane with acrylic functionality. Firstly, a radical type of reaction was proposed. The commonly applied aromatic isocyanates methylene diphenyl diisocyanate (MDI) and toluene diisocyanate (TDI) contain benzylic entities, CH_2- and CH_3-group, respectively. They can, in principle, undergo radical transfer reactions (Figure 3). MAYO showed already in 1943 that in radical polymerization reactions of styrene in toluene, transfer of radicals from the propagating chain to the resonance stabilized methyl group of toluene could occur.[56]

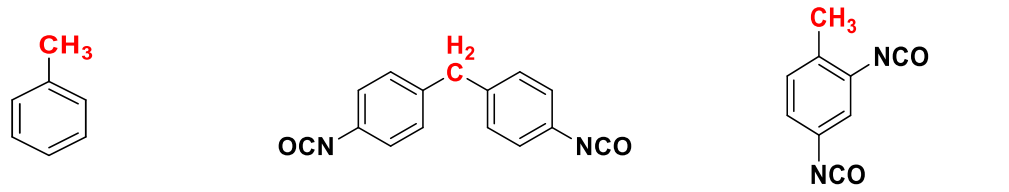

Toluene | 4,4-Methylene diphenyl diisocyanate | 2,4-Toluene diisocyanate

Figure 3. Methyl and methylene groups (red) in aromatic isocyanates.

A covalent bonding between an aromatic polyurethane and an acrylate can be expected after a reaction of an intermediate benzylic radical and the vinyl group. The methyl or methylene radical can initiate a radical polyaddition reaction of acrylate thereby forming a polyurethane with a grafted polyacrylate chain.

The second proposed pathway is a Michael-addition reaction that proceeds between an amine entity and the acrylate. The Michael-addition reaction is in general a (catalyzed) cross-coupling reaction of an electron-rich nucleophile (Michael-donor) and an electron-poor *α*,*β*-unsaturated compound (Michael-acceptor).[57] The reaction sequence of the Michael-addition reaction is shown exemplary for the reaction of ethyl acetoacetate with methyl acrylate (Figure 4).[58] Each reaction step in this scheme is dependent on the applied Michael-donor precursor and its relative base strength. The

action of the catalyst is understood in that it deprotonates the donor, thus providing an enolate anion which then reacts in an 1,4-addition with the Michael-acceptor. The final step is a protonation of the carbanion leading to the final Michael-adduct, and liberation of the catalyst.[57]

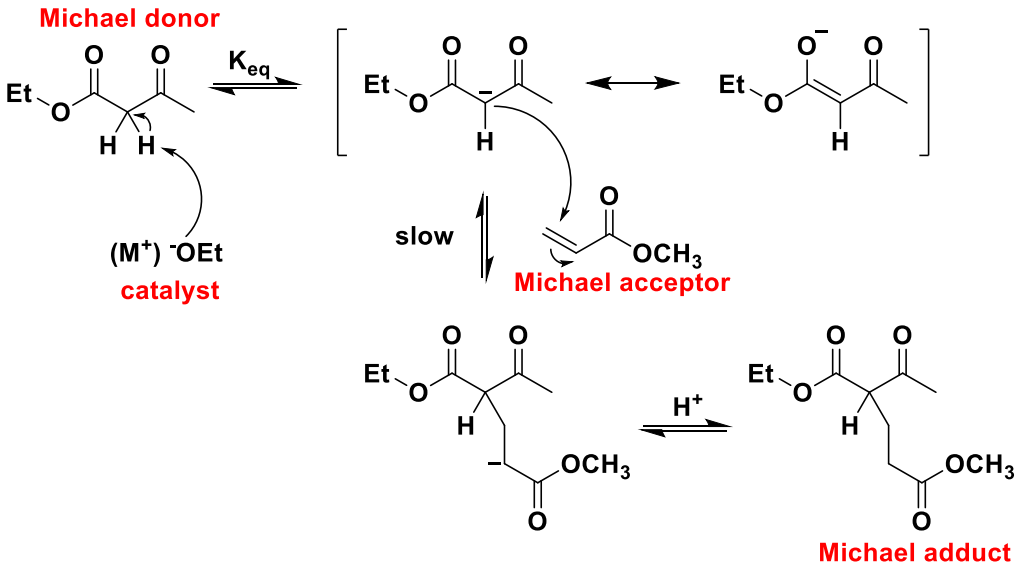

Figure 4. Michael-addition reaction pathway for ethyl acetoacetate and methyl acrylate.[57,58]

The prefix *aza* indicates, that the nucleophile in the Michael addition reaction is a primary or a secondary amine, i.e., *aza*-Michael-addition.[59] Catalyst-free and/or solvent-free *aza*-Michael-additions were reported, in general however, tertiary amines are used as catalysts.[60–62] The *α,β*-unsaturated double bond of acrylates are known to be potential *aza*-Michael-acceptors because of their electron deficiency.[63,64] The secondary amine of an urethane could directly act as an *aza*-Michael-donor and a covalent link between the urethane and acrylate can be formed, when it is sufficient nucleophilic. The nitrogen atom in the urethane group, however, is a rather poor nucleophile as it is directly connected to an electron-withdrawing carbonyl group[65] and consequently urethane is expected to be a poor coupling agent in this addition reaction. Nevertheless, some cases were described in which an activated *α,β*-unsaturated system was coupled with a carbamate-amine in a Michael-type reaction. An intramolecular ring-closing *aza*-Michael addition reaction was reported in the preparation of hydroindolenone from carbamyl-N-protected tyrosine. Hydroindolenone is a key intermediate in the synthesis of stemona alkaloids.[66,67] The strongly activated Michael-acceptor 2-chloro-2-cyclopropylideneacetate could be coupled with a substituted cyclic carbamate (oxazolidinone).[68,69] A base catalysis was used in both solvent based syntheses.

A Brønsted acid catalysis was applied in the preparation of *dl*-deoxyfebrifugine and a model for cylindrospermopsin through a Michael-addition.[70,71] Protonic acids were catalytically active by activation of the carbonyl-group.[72] Some *aza*-Michael addition reactions were catalyzed using polymer-supported acids, such as polystyrene-based Amberlyst®-15, solid perfluorinated resin-bound sulfonic acids, e.g., Nafion-H® and Nafion® SAC-13, the latter being a silica-nanocomposite with improved surface area.[73]

Lewis acidic transition metal salts were used as catalysts in the addition reaction of various enones to carbamates. Especially group 7 – 11 transition metal salts in higher oxidation states were effective catalysts.[74] Even the poor nucleophile benzyl carbamate was successfully converted by a Pd(II)-based catalyst.[75]

Organocatalyzed *aza*-Michael additions of carbamates were also reported, for instance of *N*-silyl-oxycarbamates.[76] Camphor sulfonyl hydrazine was used as a catalyst in the conversion of methoxy and benzyloxy carbamates.[77] A broad spectrum of asymmetric organocatalytic *aza*-Michael additions is known, some of them with carbamates as nucleophiles.[78]

To the best of my knowledge, *aza*-Michael addition reactions have not been described before in polymer forming reaction systems in the context of polyurethane and acrylate, or alternatively polyol, polyisocyanate and acrylate, where the urethane-NH acts as a Michael-donor. Therefore, the covalent bonding reaction between urethane and acrylate was studied using inexpensive and environmentally benign catalysts free from radical initiators. The reactions were carried out in bulk, anticipating potential use of the chemistry in polymer applications.

4 Motivation

Interest preceding this work was to expand the well-established urethane-chemistry by introducing the bulk *aza*-Michael addition reaction of urethane and acrylate. Concomitantly, it seemed to open an option for the development of possible applications in the context of polyurethanes, e.g., as non-ionic (gemini-) surface-active agents, or as novel crosslinking agents. It also seemed appealing expanding scientific knowledge to build an understanding of the *aza*-Michael addition reaction between urethane and acrylate and to identify the reaction channels (Figure 5). This all led to this dissertation.

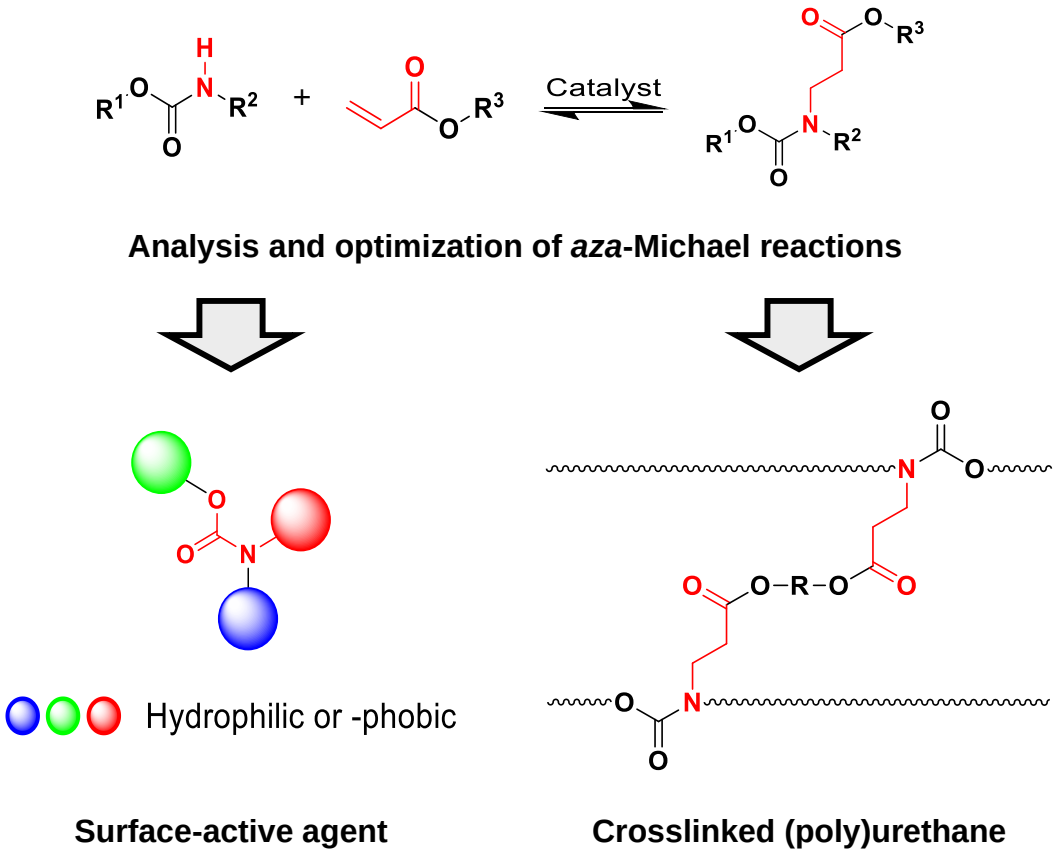

Figure 5. Flowchart representing the structure of this thesis.

5 Results and discussion

5.1 *Aza*-Michael addition of urethane onto acrylates

5.1.1 *Aza*-Michael addition of urethane onto acrylates

A molecular model reaction system was chosen to investigate the coupling reaction of acrylate and urethane. Reactions carried out using this model system allowed a detailed ^{1}H-NMR spectroscopic analysis of the compounds involved and thus of the chemistry that takes place. Two putative reaction mechanisms were considered for explaining the result, a radical mechanism and an anionic *aza*-Michael addition reaction.

A bifunctional urethane compound and a mono-functional acrylate were chosen. Potassium acetate was used as a catalyst. The urethane model compound dibutyl (methylenebis(4,1-phenylene)) dicarbamate was prepared by reaction of 1-butanol (BuOH) and 4,4'-methylene diisocyanate (Chapter 6.2.1). Two equivalents of 2-phenoxyethyl acrylate and 0.5 wt% (0.04 eq.) potassium acetate (K Ac) were added to 1 eq. of the dibutyl diurethane. The reaction mixture was stirred under an inert gas atmosphere (Ar) at 160 °C for 3 h. The resulting highly viscous and yellowish reaction mixture was treated with acetone at room temperature to remove the insoluble catalyst and filtrated. The acetone was evaporated, and the reaction mixture was analyzed using ^{1}H-NMR spectroscopy. Two products were identified besides minor traces of polyacrylate and some unreacted starting material. The crude reaction product was purified by column chromatography. The colorless and highly viscous liquids were characterized by ^{1}H-NMR and ESI-MS spectra (Chapter 6.2.2). Two molecular structures were identified (Figure 6). No radical coupling products at the central methylene bridge of the model compound were observed. The ^{1}H-NMR spectroscopic analysis of the crude product (Figure 96, Chapter 6.2.2) revealed that the molar ratio of non-reacted urethane to mono- and di-*aza*-Michael-adduct was approximated to 1.0:1.9:1.7 corresponding to 22:41:37 mol%, respectively.

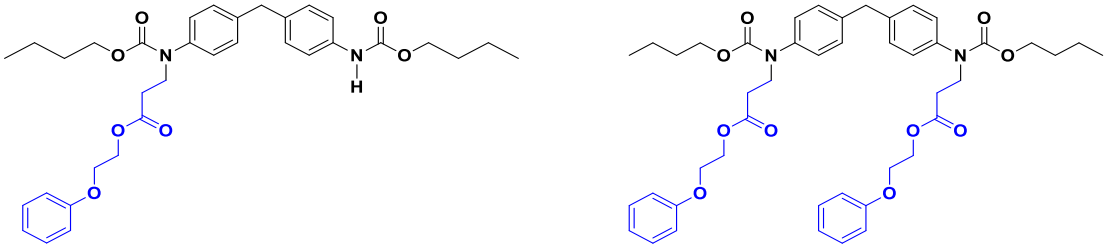

Figure 6. (left) Mono- and (right) di-*aza*-Michael adduct (^{1}H-NMR spectra in Chapter 6.2.2).

The reaction pathway will be similar to that in Figure 4. The N-H functional group of the urethane may partially be deprotonated by the basic acetate. The resulting amide anion would attack at the electrophilic *β*-position of the *α,β*-unsaturated acrylate. The final *aza*-Michael addition product is formed after a proton transfer from a further urethane entity or acetic acid, followed by a keto-enol reorganization.

A second model reaction was studied to further support the proposed reaction pathway. A deuterium transfer instead of a proton transfer would lead to a reduction of integrals of transfer-related peaks in proton NMR spectroscopy. The starting components were *para*-tolyl isocyanate (pTMI), phenoxyethyl acrylate (POEA) and either *n*-butanol (BuOH) or fully deuterated *n*-butanol (d_9-*n*-BuOD). Potassium 2-ethylhexanoate (K Oct) was used as catalyst. The reaction was carried out at 110 °C.

The products are the expected ones from a scheme wherein at first the urethane is formed, and consecutively an *aza*-Michael addition takes place with the acrylate (Figure 7a, b). A proton- (a) and a deuterium-transfer (b) leads to the formation of the two addition products which showed indeed the expected differences in ^{1}H-NMR and ESI-MS spectra (Figure 8; Table 1; Chapter 6.2.3.3 and 6.2.3.4). An integral of 1 was found in *α*-position to the former acrylic carbonyl functionality (C12-position) when using d_9-*n*-BuOD and 2 when using BuOH. No radical coupling products were detected. In conclusion, the coupling of acrylate and urethane in the presence of the potassium carboxylate proceeds predominantly by an *aza*-Michael addition reaction.

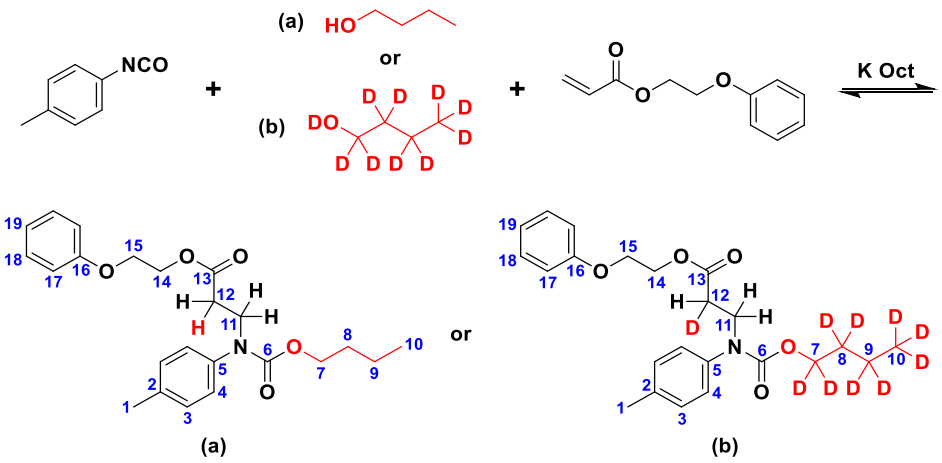

Figure 7. Model reaction to protonated (a) or deuterated (b) *aza*-Michael adducts.

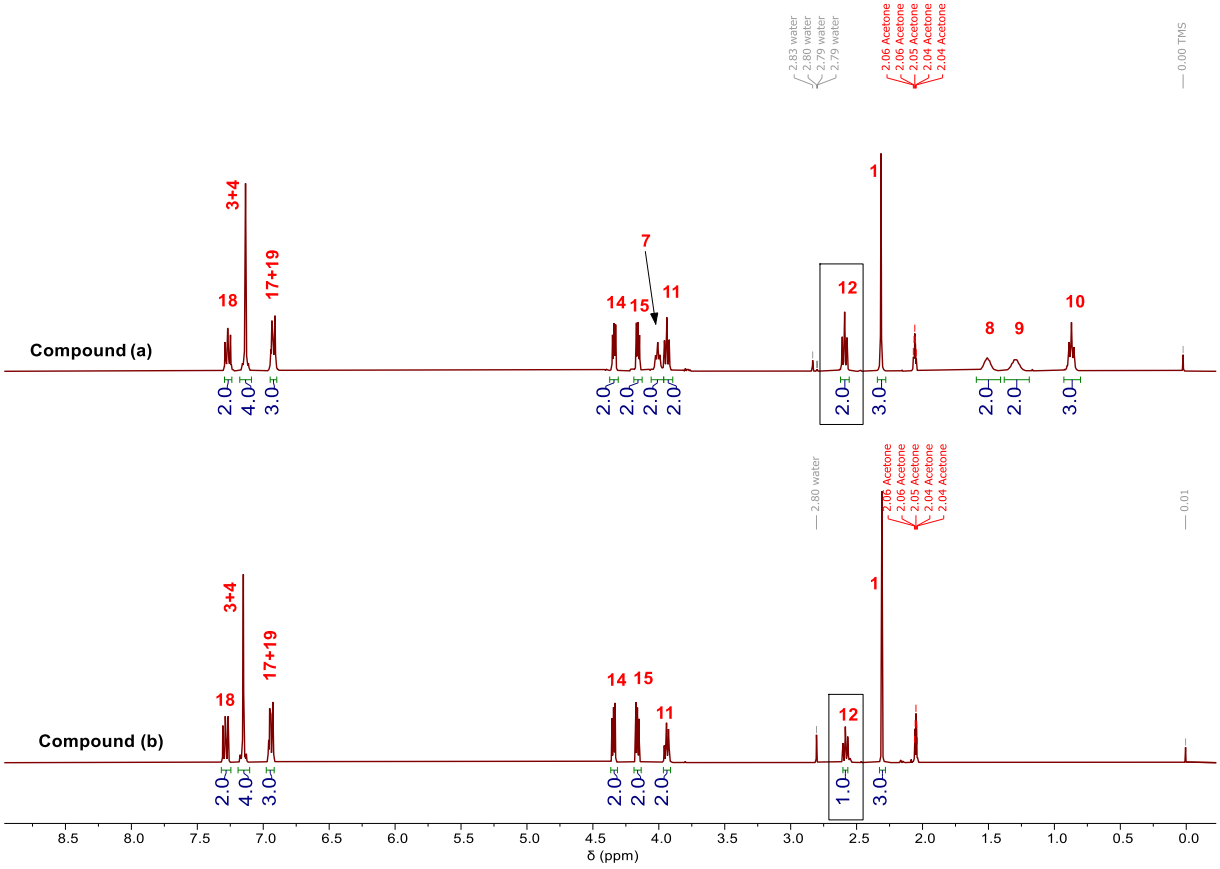

Figure 8. ^{1}H-NMR spectra of (top) fully protonated or (bottom) fully deuterated alcohol-based *aza*-Michael adducts (Figure 7).

Table 1. ESI-MS data for adducts (a) and (b) (Figure 7).

Substance	Formula	m/z_{calc} [g/mol]	m/z_{found} [M + H$^+$] [g/mol]
Adduct (a)	$C_{23}H_{29}NO_5$	399.20	400.20
Adduct (b)	$C_{23}H_{19}D_{10}NO_5$	409.27	410.26

5.1.2 Further *aza*-Michael reactions with model systems

The potential formation of the *aza*-Michael-adduct **6** was mapped in bulk from monofunctional reactants in form of isocyanate **1**/alcohol **2**/acrylate **3** or urethane **4**/acrylate **3** (Figure 9) and potassium acetate (K Ac) as a catalyst. A two-step procedure was applied using **1** – **3**. A low reaction temperature (T_1) was selected at the start of the reaction in which predominantly urethane **4** should form. The use of catalyst K Ac, however, also led to the formation of some tri(*p*-tolyl) isocyanurate **5**. The temperature was subsequently increased to T_2 to yield the *aza*-Michael addition product **6** (Figure 10).

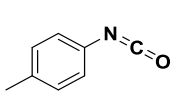

p-Tolyl isocyanate

1

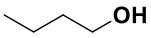

1-Butanol

2

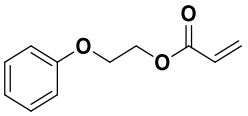

2-Phenoxyethyl acrylate

3

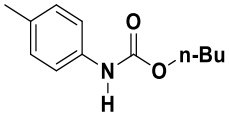

n-Butyl *p*-tolylcarbamate

4

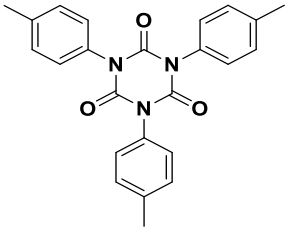

Tri(*p*-tolyl) isocyanurate

5

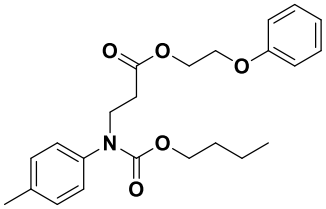

2-Phenoxyethyl 3-((butoxycar-bonyl)(*p*-tolyl)amino) propanoate

6

Figure 9. Starting materials and characteristic reaction products.

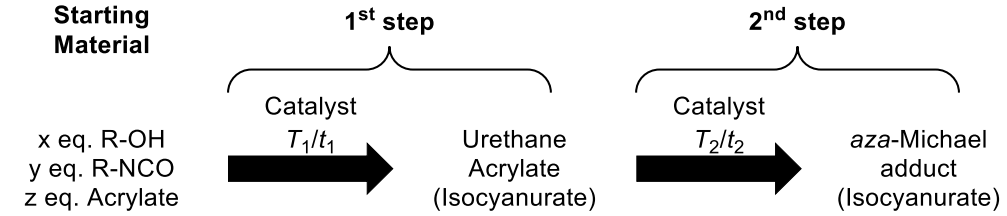

Figure 10. Two-step model reaction system.

Reactions with monofunctional low molecular mass starting materials allow quantification of the product ratios by ^{1}H-NMR spectroscopy (Figure 11). The characteristic proton signals for **3** - **6** are highlighted. The starting materials **1** and **2** were fully converted. The reaction products were also prepared or isolated from product mixtures to secure peak assignment in the individual compounds (Chapter 6.2.3).

K Ac has a poor solubility in the reaction mixture, even the employed catalytic quantities were not dissolved at room temperature. The catalyst quantity was soluble at the chosen T_1 of 90 °C. A coupling reaction did not take place at T_1. The conversion of isocyanate into urethane **4** and isocyanurate **5** was completed after 1 h. The acrylate concentration remained untouched. Next the temperature was increased to T_2 to induce the formation of the *aza*-Michael adduct (Figure 12). No significant conversion to the *aza*-Michael-adduct **6** occurred when T_2 was below 130 °C whereas **6** was formed in significant amounts at temperatures of 130 °C and above. The highest conversion of about 70 % was obtained after 3 h at 130 °C.

The yield in **6** gradually started to decrease above this temperature because of side reactions of which two could be identified, the homo-polymerization of the acrylate and transesterification of the adduct. Homo-polymerization of acrylate can also become the dominant acrylate-consuming reaction when the formation rate of the *aza*-Michael-adduct **6** is slow. This was observed for $T_2 < 130$ °C. The acrylate polymerization reduces the amount of acrylate available for the adduct formation and as a result the adduct yield will be smaller. A further side reaction is indicated by a steady decline of the concentration of *aza*-Michael adduct at higher temperatures. This was caused by transesterification reactions.

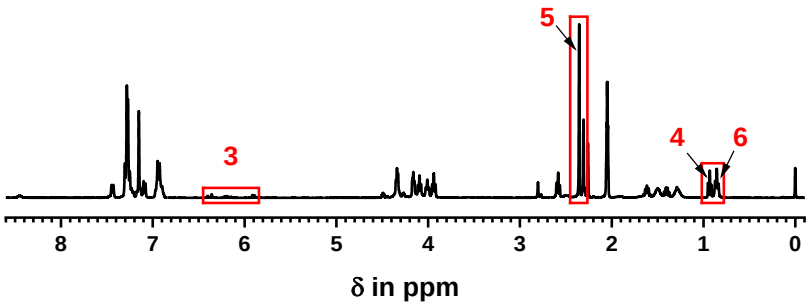

Figure 11. ^{1}H-NMR spectrum of the crude reaction product with characteristic proton signals (acetone-d_6).

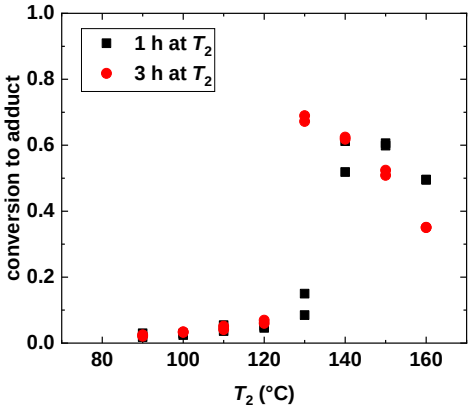

Figure 12. K Ac catalyzed conversion of urethane **4** to *aza*-Michael-adduct **6** (≈ 0.5 wt%, NCO:OH:acrylate = 2:1:1).

The formation of polyacrylate was attributed to a thermally induced radical homo-polymerization and probably proceeds by a diradical self-initiation mechanism.[79] Three acrylate containing reaction mixtures were prepared with and without the radical inhibitor 4-methoxyphenol (MeHQ) and reacted at 160 °C for 3 h to gain some information on the pathway:

1. acrylate **3** (used as received)
2. acrylate **3** + 10 mol% MeHQ
3. acrylate **3** + 0.5 wt% K Ac + 10 mol% MeHQ

Reaction 1 gave a colorless and slightly yellowish solid while the reaction mixture of reaction 2 and 3 remained liquid. The interpretation is that only in the first reaction a solid polyacrylate is formed. The suppression of the polymerization by addition of radical inhibitor supports the radical acrylate polymerization. No polymerization occurred when potassium acetate and a radical inhibitor were present (reaction 3). This indicates that an ionic pathway as an alternative for the polymerization is unlikely. Addition of radical inhibitors is a common method to suppress radical polymerizations. Processes with a slow conversion to *aza*-Michael-adduct **6** can favor the radical polymerization of the acrylate, unless radical inhibitors were added.

The aromatic hydroxyl group in the radical inhibitor MeHQ is sterically unhindered and could react with an NCO moiety. Alternatively, 2,6-di-*tert*-butyl-4-methylphenol (BHT) could be used as a radical inhibitor that is less reactive towards NCO, since the hydroxyl entity is sterically more hindered. MeHQ turned out to be more reactive than BHT. This is irrespective of the use of the catalyst DABCO (Table 2).[80]

Table 2. Equimolar reaction of MeHQ or BHT with pTMI in toluene.

Inhibitor	Catalyst	*T*	*t*	Yield (urethane)
MeHQ	-	70 °C/RT	6 h/10 h	12 %
MeHQ	DABCO (4 mol%)	90 °C	5 h	98 %
BHT	-	70 °C/RT	6 h/10 h	0 %
BHT	DABCO (4 mol%)	90 °C	5 h	31 %

The reactivity of BHT towards isocyanate and its ability to suppress the radical reaction was also analyzed in the context of an *aza*-Michael model reaction. The molar amount of acrylate was 4 times higher than that of alcohol (NCO:OH:acrylate = 2:1:4, Chapter 6.2.4) and the reaction was catalyzed by K Ac. The reaction mixture gelled without BHT already after 1 h during the first heating step at 90 °C. The same reaction was repeated in the presence of 12.5 mol% BHT and no radical reaction occurred. BHT was found to be quantitatively converted at 90 °C (T_1) to the corresponding urethane **7** (Figure 13) but fully liberated at 160 °C (T_2).

In summary, the addition of BHT allows the suppression of a radically initiated acrylate polymerization. The addition of radical inhibitor was required when the *aza*-Michael reaction was slow, i.e., in the case of acrylate equivalent amounts ≤ 1 relative to urethane, or at high reaction temperatures (e.g., $T > 130$ °C). The relatively high amount of radical inhibitor of 12.5 mol% was reduced in subsequent experiments: An amount of 0.1 mol% proved to be effective.

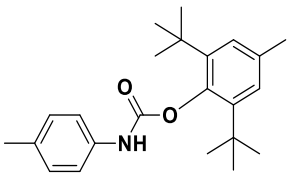

2,6-Di-*tert*-butyl-4-methylphenyl *p*-tolylcarbamate

7

Figure 13. Structure of BHT-pTMI-urethane **7** (Chapter 6.2.4).

The transesterification rate as second major side reaction was strongly depended on the catalyst concentration and temperature - the higher the temperature and catalyst concentration the more pronounced the transesterification. Transesterification led to a plurality of by-products (Figure 14, **8** – **10**) resulting from a cascade of reactions (Figure 20).

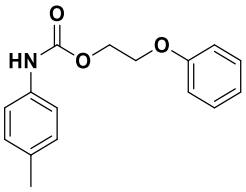

2-Phenoxyethyl *p*-tolyl carbamate

8

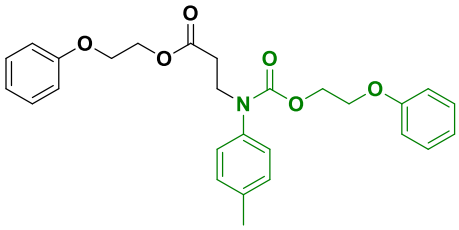

2-Phenoxyethyl *N*-(2-phenoxyethoxy carbonyl)-*N*-(*p*-tolyl) glycinate

9

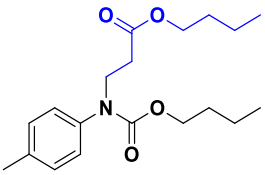

Butyl 3-(butoxycarbonyl) *p*-tolyl amino propanoate

10

Figure 14. Transesterification products urethane **8** (Chapter 6.2.5.2), adduct **9** based on **8** (green part) and adduct **10** from intermediate *n*-butyl acrylate (blue part).

Transesterification of esters is generally inflicted at higher temperatures and under basic conditions.[81–83] Two scenarios need to be considered. A temperature dependent liberation of alcohol may lead to various transesterification products. The alcohol could origin from the reverse reaction of the urethane into free isocyanate and alcohol (Figure 15).[6]. Only little evidence was found for the involvement of free isocyanate by ^{1}H-NMR spectroscopy. That may be attributed to the trimerization of liberated isocyanate to isocyanurate under the given catalysis or its recombination to other species (e.g., urethane). Transesterification can also occur by the rearrangement of two esters of different kind. It does not necessarily require free alcohol.[84,85] The possibility of transesterification under the given catalysis was confirmed by treating urethane **4** with a 4-fold excess of 2-phenoxyethanol (POE). The reaction was carried out with and without the presence of 5 wt% catalyst at 160 °C for 3 h in an open round bottom flask (K Ac, Figure 16, Chapter 6.2.5.1). The presence of catalyst strongly enhanced the rate of transesterification. Without catalyst only about 11 % of the urethane-groups were transesterified whereas in the presence of catalyst this increased to 93 %.

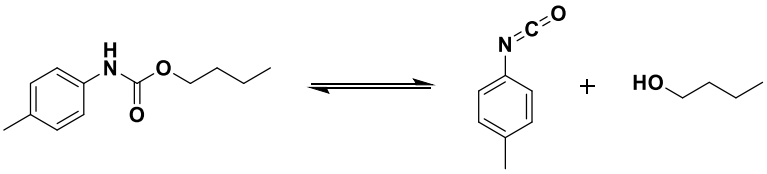

Figure 15. Degradation of urethane to NCO and alcohol.

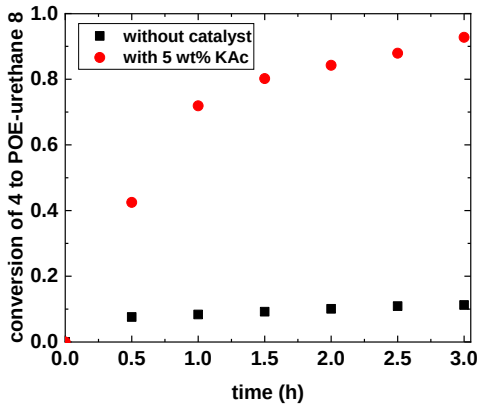

Figure 16. Conversion of urethane **4** to transesterified urethane **8**.

Transesterification can lead to a scrambling of the various alkyl groups (Figure 9). Liberated alcohol **2** could undergo transesterification with acrylic ester **3** to form *n*-butyl acrylate (BuA) and phenoxyethanol (POE). POE could subsequently react with isocyanate **1** to yield urethane **8**. **8** may also be formed by direct exchange of the alkyl groups from urethane **4** and acrylic ester **3**. Both pathways lead to *aza*-Michael adduct **9**. Similarly, urethane **4** and product BuA can convert to adduct **10** (Figure 14). Adducts **6**, **9** and **10** were synthesized also directly from urethane **4** and acrylate **3**, urethane **8** and acrylate **3** or urethane **4** and BuA, respectively, at 140 °C using K Oct as a catalyst (Chapter 6.2.3.3 and Chapters 6.2.5.2 - 6.2.5.4). These products could be identified in ^{1}H-NMR and ESI-MS spectra. The raw mixture contained all of the aforementioned transesterified products (Figure 17 and Figure 18; Table 3). The formation of *aza*-Michael adduct **11** from transesterified urethane **8** and BuA could not be observed (Figure 19).

The degradation of model adduct **6** is also the result of transesterification. It was kept at 160 °C for 2 h to investigate its thermal stability in the presence and absence of catalyst. Virtually no retro-*aza*-Michael addition had occurred in the absence of catalyst, and no other products were detected. However, in the presence of 4 mol% of K Oct, the transesterification products as discussed above were obtained (^{1}H-NMR spectra in Chapter 6.2.5.5). The decrease in the concentration of adduct **6** with time (Figure 12, T > 130 °C) thus is most likely the result of transesterification (Figure 20).

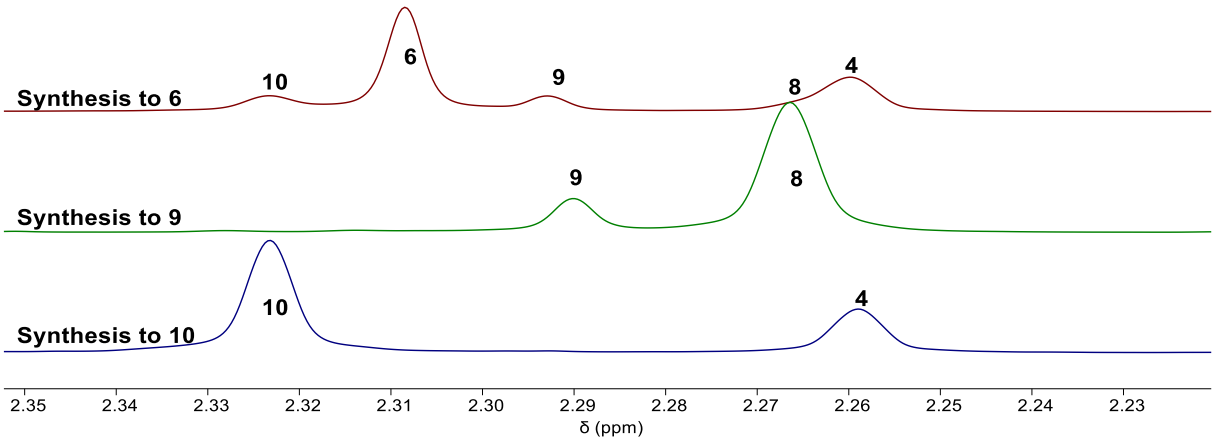

Figure 17. ^{1}H-NMR spectra of reaction to adduct **6** (based on **4**), adduct **9** (based on **8** and **3**) and adduct **10** (based on **4** and butyl acrylate).

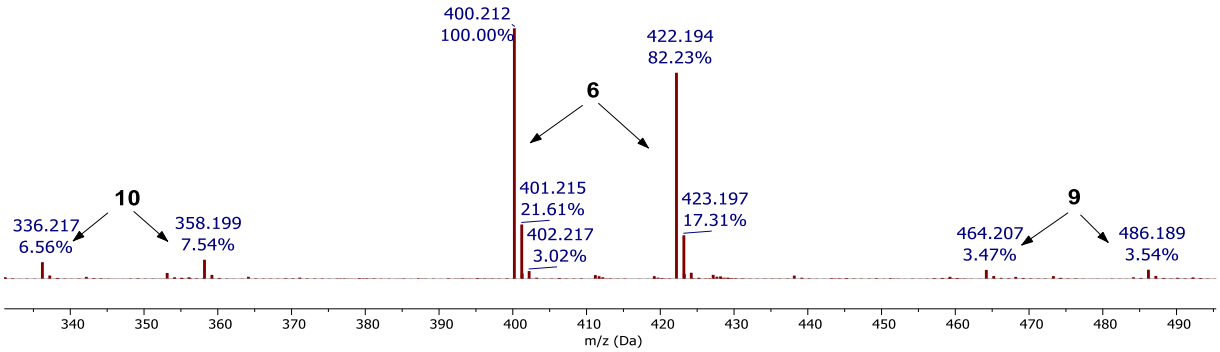

Figure 18. ESI-MS spectrum of the crud product to adduct **6** with by-products **9** and **10**.

Table 3: ESI-MS data of the crud product to adduct **6** with by-products **9** and **10**.

	[M]	$[M+H]^+$	$[M+Na]^+$
Adduct 6	399.20 g/mol	400.21 g/mol	422.19 g/mol
Adduct 9	463.20 g/mol	464.21 g/mol	486.19 g/mol
Adduct 10	335.21 g/mol	336.22 g/mol	358.20 g/mol

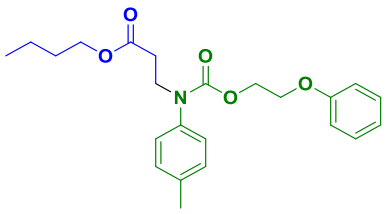

Butyl 3-(((2-phenoxyethoxy) carbonyl)(*p*-tolyl)amino)propanoate

11

Figure 19. Adduct **11** based on **8** (green part) and *n*-butyl acrylate (blue part).

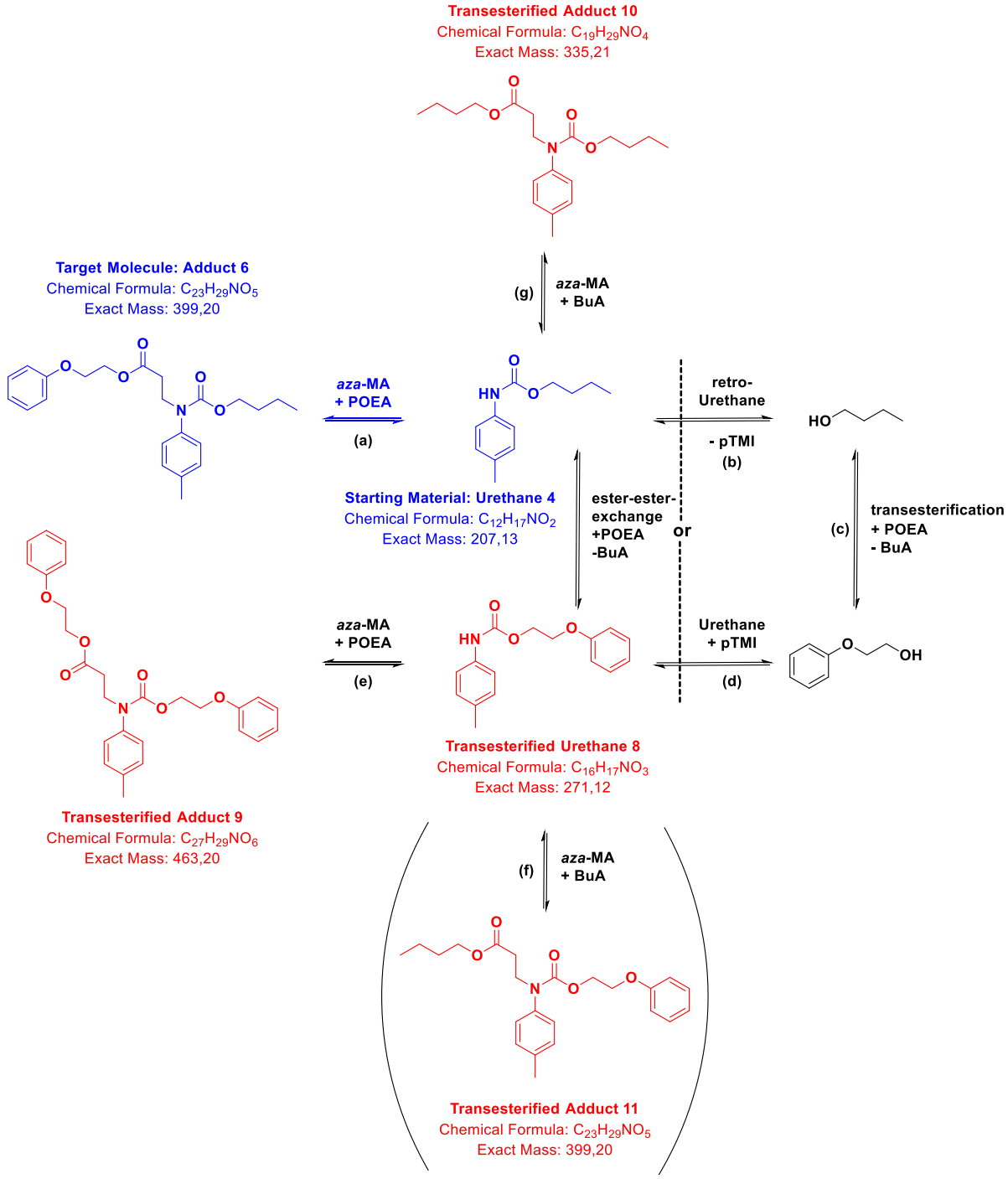

Figure 20. Reaction pathways to different transesterified adducts.

The thermal behavior of adduct **6** and urethane **4** was also analyzed by thermogravimetric analysis (TGA). Samples with and without 4 mol% K Oct were heated to 400 °C at a heating rate of 10 °C/min in air (Figure 21, Table 4). The temperature $T_{1\ wt\%}$ at which a weight loss of 1 % had occurred was defined as the starting point of thermal degradation. $T_{5wt\ \%}$ and $T_{50\ wt\%}$ (temperatures at which a weight loss had occurred of 5 and 50 %, respectively) were used as indicators for the rate of degradation. Compound **6** proved to be significantly more stable than **4** (ΔT = 95 °C)

in the absence of catalyst. The Δ*T* values at $T_{5\ wt\%}$ and $T_{50\ wt\%}$ amounted to 104 and 113 °C, respectively. The steadily increase in Δ*T* indicates that the rate of degradation of **6** is slower than that of **4**. N-substituted urethanes are known to be more thermally stable than non-substituted urethanes[86] - the alkyl group impedes the urethane decomposition to isocyanate and alcohol.[6,87] The thermal stability of the *aza*-Michael adduct is significantly reduced in the presence of catalyst (4 mol% K Oct), whereas the stability of the urethane is only marginally affected. The urethane-based *aza*-Michael adduct is nevertheless still significantly more stable than the corresponding urethane.

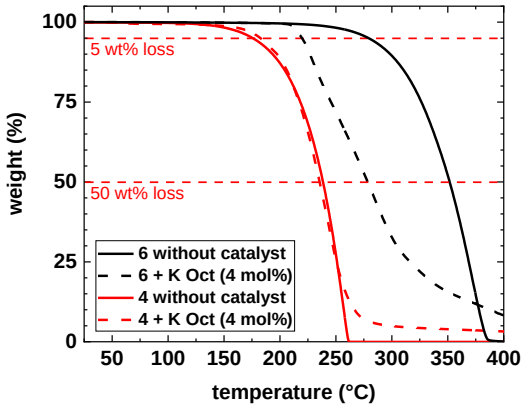

Figure 21. TGA of *aza*-Michael adduct **6** (black) and urethane **4** (red).

Table 4. TGA data from Figure 21.

Compound	$T_{1\ wt\%}$ [°C]	$T_{5\ wt\%}$ [°C]	$T_{50\ wt\%}$ [°C]
Adduct	233	280	352
Adduct + K Oct	210	219	278
Urethane	138	176	239
Urethane + K Oct	142	182	235

5.1.3 Catalyst study

One objective of this work was to identify highly selective *aza*-Michael catalysts that were active at lower temperatures. It was shown in the previous chapter that the reaction of the starting materials **1** - **3** to adduct **6** using K Ac as a catalyst only occurred at relatively high temperatures ($T \geq 130$ °C). A reduction of the reaction temperature by simply increasing the catalyst concentration was not favorable as the transesterification reactions became more significant.

The ionic bond strength between the cation and anion of salt catalysts becomes weaker with increasing size of the cation.[88,89] This can be used to improve the catalytic activity at lower temperatures as the catalytic active anion becomes more accessible with increasing cation size. Potassium acetate was therefore replaced by cesium and rubidium acetate (Cs Ac, Rb Ac).

Rb Ac and Cs Ac showed a better solubility in the reaction medium than K Ac and led to a reduction of T_1 for Rb Ac and Cs Ac to 80 °C respectively to 60 °C. The formation of adduct **6** did not occur at these temperatures. The conversion of urethane **4** to adduct **6** was studied as a function of the temperature T_2. Equimolar catalyst concentrations and equal reaction times of 3 h were used at a 2:1:1 reactant ratio of NCO, OH and acrylate (Figure 22). The reaction temperature to convert urethane **4** to adduct **6** could be reduced by about 20 °C to a T_2 of 110 °C when using Rb Ac[90] and by about 50 °C to a T_2 of 80 °C for Cs Ac. All three catalysts catalyzed the transesterification reactions to a similar extent. This was presumably because all three catalysts are based on the same carboxylate.

The extent to which transesterification occurs could only be reduced by using less catalyst at higher temperatures. This was shown in a series of experiments in which the concentration of Cs Ac was reduced by more than two orders of magnitude (Figure 23 and Figure 24). T_2 had to be increased to at least 140 °C to convert urethane **4** to adduct **6** at comparable rates, when using a tenth of the original catalyst concentration. Almost no product degradation occurred at these conditions. A further reduction of the catalyst concentration to one-hundredth resulted in no catalytic activity, not even at T_2 for 5 h.

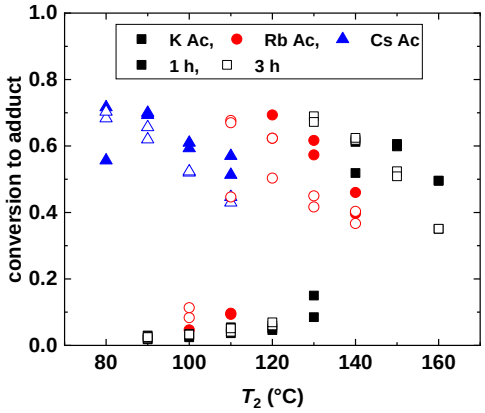

Figure 22. Conversion of urethane **4** to adduct **6** with 0.027 eq. of acetate catalysts.

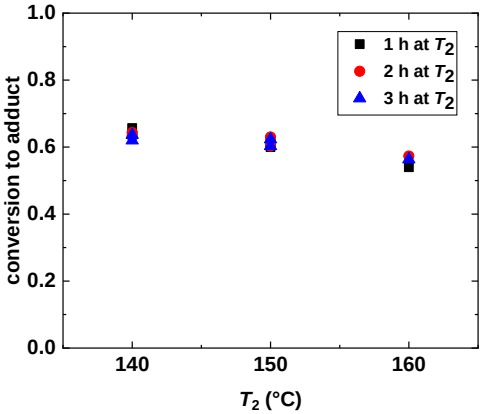

Figure 23. Conversion of **4** to **6** with reduced Cs Ac catalyst concentration (1/10).

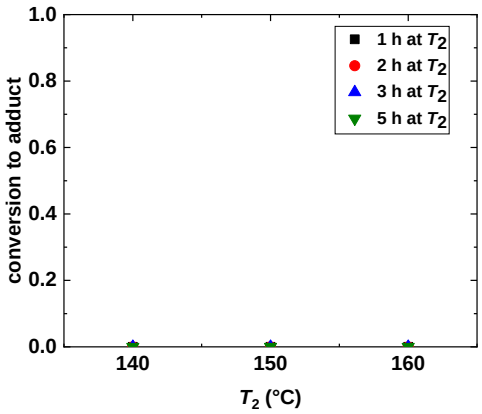

Figure 24. Conversion of **4** to **6** with reduced Cs Ac catalyst concentration (1/100).

The acetate salts were poorly soluble in the reaction medium at lower temperatures (i.e., below T_1). That might also have limited their low-temperature activity. Octoate salts were chosen as an alternative to acetate. Octoates show a similar basicity/ nucleophilicity whereas the larger aliphatic substituent will enhance its solubility in the mixture.

Reactions were carried out employing potassium, rubidium and cesium octoate (K Oct, Rb Oct and Cs Oct) at equimolar catalyst concentrations and starting material composition (NCO:OH:acrylate = 2:1:1) applying the two-temperature procedure. The octoate salts (notably Cs Oct) were soluble in the mixture at temperatures below 50 °C. T_1 was kept at 60 °C for one hour for all screens in the comparative catalyst study. The reaction mixture was then heated to T_2 at which conversions of about 70 % were obtained for all three catalysts after sufficiently long reaction times, i.e., between 1 to 19.5 h. The reaction time to final state was dependent on the catalyst (Figure 25).

The trends were similar to that of the acetate-based catalysts (Figure 22), but the octoate catalysts were less reactive. Cs Ac showed for instance a conversion to adduct **6** of about 70 % after 1 h at 80 °C whereas under the same conditions the conversion for Cs Oct only amounted to 21 %. Reaction times of 3 h were required for obtaining a conversion of 62 %. Conversions of about 40 % could be obtained at 60°C for the octoates after 19.5 h of reaction time. Reactions carried out at 80°C and above usually yielded products with a yellowish color. The reaction products that were obtained at lower temperatures were colorless.

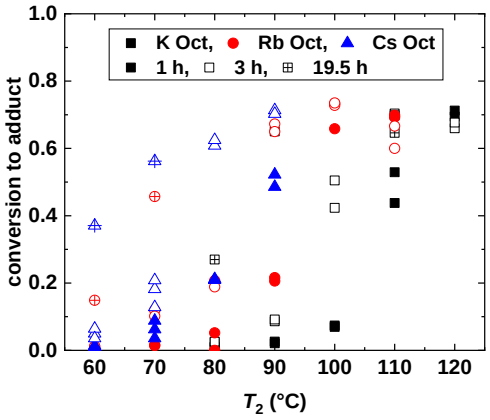

Figure 25. Conversion of urethane **4** to adduct **6** with 0.027 eq. of octoate catalysts.

Tertiary amines are known catalysts for urethane and isocyanurate formation from isocyanate and alcohols. The catalytic activity is attributed to their basic and nucleophilic properties.[91–94] These properties are also important in the catalysis of the *aza*-Michael formation from urethane and acrylate. The tertiary amine catalysts Diazabicyclo(5.4.0)undec-7-ene (DBU), 1-methylimidazol (1-MI), *N,N*-dimethylbenzylamine (BDMA) and diazabicyclo(2.2.2)octane (Figure 26) differ in nucleophilicity and basicity[91–94] and their catalytic activity should also differ.

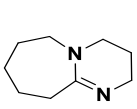

DBU

Diazabicyclo(5.4.0)-undec-7-ene

1-MI

1-Methylimidazol

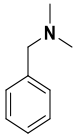

BDMA

N,N-Dimethyl-benzylamine

DABCO

Diazabicylco(2.2.2)-octane

Figure 26. Tertiary amines.

The ability of these amine catalysts to catalyze the formation to **6** was analyzed after 1 h of reaction time at T_1 = 90 °C and 3 h at T_2 = 140 °C and 160 °C (Figure 27 and

Figure 28). Equimolar catalyst concentrations were used at a 3:1:1.5 reactant ratio of NCO, OH and acrylate. DABCO showed the highest catalytic activity in the formation of adduct **6**, whereas BDMA and 1-MI induced no reaction. DABCO and DBU also catalyze the trimerization of isocyanate **1** to isocyanurate **4** which puts limits on their use as *aza*-Michael catalysts in this context.

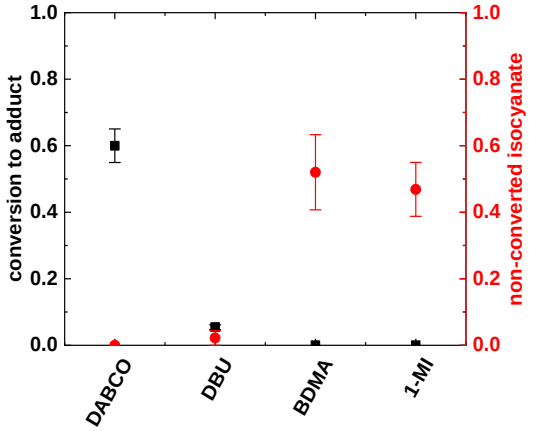

Figure 27. Comparisons of amine-catalysts at T_2 = 140 °C.

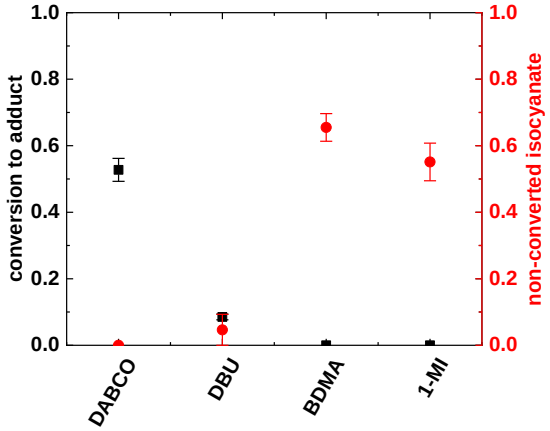

Figure 28. Comparisons of amine-catalysts at T_2 = 160 °C.

Metal cations can be used as catalysts in reactions where complexes of the metal ion and a carbonyl oxygen atom can be formed. The increased electrophilicity of the carbonyl carbon atom leads to an enhanced reactivity.[95–99] The activation of the acrylic carbonyl group in Michael-addition reactions through complexation could be an approach for catalysis.[96,99] LiCl as catalyst is interesting in that regard: it catalyzes the urethane-formation[98] but not the formation of isocyanurate. Isocyanurate was a major by-product in all previous *aza*-Michael addition reactions of this study. It was therefore investigated whether LiCl can catalyze the formation of **6** while avoiding the formation of isocyanurate.

Alcohol **2** was quantitatively converted to urethane **4** after 1 h at T_1 = 80 °C and no isocyanurate **5** was formed using the “standard conditions” (0.027 eq. of catalyst and ratios of NCO:OH:acrylate = 2:1:1). Approx. 50 % of isocyanate **1** remained unreacted and no adduct **6** was formed. Unreacted **1** was thermally converted to **5** only at $T_2 \geq 150$ °C accompanied by minor formation of **6** (approx. 30 % after 7 h to 21 h, Figure 29). This allowed to reduce the ratio of isocyanate to equimolar amounts of alcohol and acrylate. The resulting system is nearly isocyanurate-free after the urethane formation (< 1 mol%) as isocyanate **1** was fully consumed at T_1 (Figure 30). Traces of isocyanurate **5** after a given time at T_2 were most likely formed after

unzipping of urethane **4** liberating isocyanate **1**. The overall catalytic activity of LiCl for the *aza*-Michael reaction was poor; a yield of about 20 to 30 % was obtained at 160°C and 24 h of reaction.

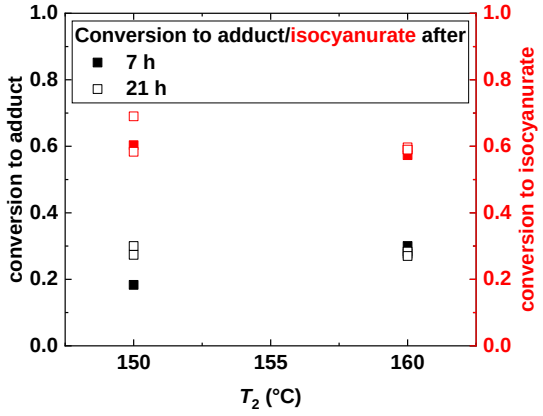

Figure 29. Standard conditions with LiCl as a catalyst.

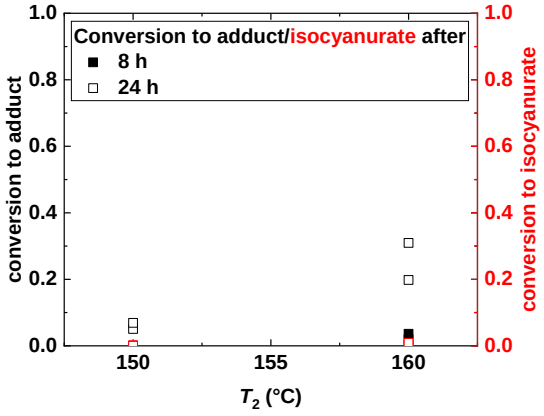

Figure 30. Isocyanurate-free reaction with LiCl as a catalyst.

5.1.4 Complexing agents

It was shown in Chapter 5.1.3 that the catalytic activity of the alkali metal carboxylates increased with increasing size of the cation. That was explained by the smaller Coulomb forces between the two ions and a greater basicity of the carboxylate-anion. The latter is believed to be essential in the catalysis to form the *aza*-Michael bond formation. The separation of the ion-pair can in principle also be obtained by addition of complexing agents for the cation. Crown ethers – cyclic oligomers of poly(ethylene glycol) – are well-known as complexing agents for cations of elements such as K, Rb and Cs.[100,101] Crown ethers, however, are toxic and their use is not desired.[102] Less toxic linear poly(ethylene glycol) can be used alternatively.[103,104]

The *aza*-Michael adducts from urethane and acrylate are partially built from two alcoholic species which can be used for the incorporation of poly(ethylene glycol)-groups. Monofunctional poly(ethylene glycol) (MoPEG) was thus introduced by an urethane and/or an ester linkage with a molecular weight of 510 g/mol (Figure 31).

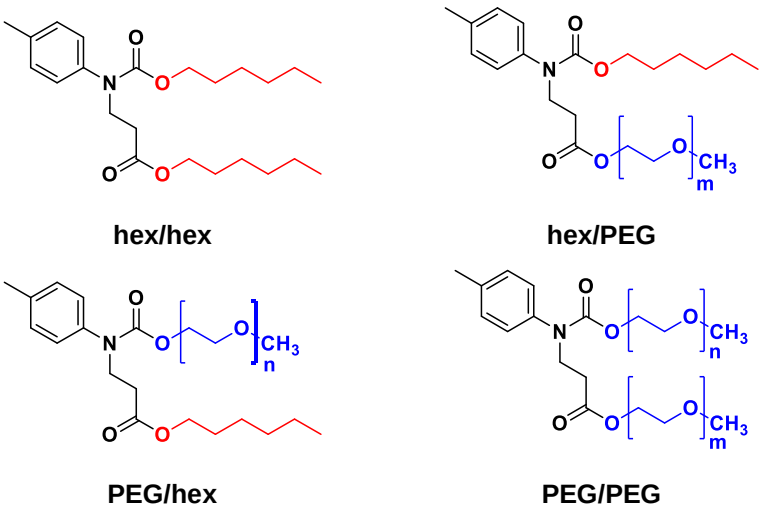

Figure 31. *Aza*-Michael adducts of the complexing agent study.

A one-pot synthesis was conducted at 90 °C for 7 h using 1 eq. alcohol, 2 eq. pTMI and 1 eq. acrylate in the presence of BHT and K Oct (Chapter 6.2.7). The conversion to the *aza*-Michael adduct was monitored as a function of the reaction time by ^{1}H-NMR spectroscopy (Figure 32).

The reaction rate was dependent on the presence of the PEG chains. The conversion after 7 h for hex/hex (black curve) amounted to 27 %. Conversions of about 70 % could be achieved for the PEG-containing systems in the same reaction time (red curve: 68±3 %, blue curve: 69±3 %, and green curve: 72±1 %). The acceleration of the

reaction and the higher yields for the MoPEG-modified systems are attributed to the complexation of the cation to the educt. The conversion was also dependent on the way MoPEG was introduced. The fastest reaction was obtained for PEG/hex (blue curve), followed by hex/PEG (green curve) and PEG/PEG (red curve), respectively. The urethane N-H-entity needs to be activated by the carboxylate to form the *aza*-Michael bond. This proceeds most efficiently when the MoPEG is introduced with a urethane cap. PEG/PEG shows the lowest reactivity of the three.

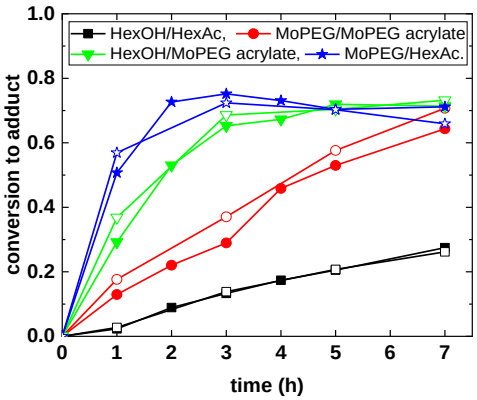

Figure 32. Adduct-formation of the complexing agent study.

5.1.5 Isocyanate substitution pattern

The aromatic diisocyanates MDI and TDI are used most often in industrial applications. These isocyanates can contain *ortho*- and *meta*-positioned NCO groups with different reactivities (e.g. in 2,4'-MDI and 2,4- or 2,6-TDI).[26] The reaction of *in-situ* formed urethane from *ortho*-, *meta*- and *para*-tolyl isocyanate (oTMI, mTMI and pTMI; Figure 33) with acrylate was used to study the influence of the substitution pattern on the *aza*-Michael addition.

Methoxylated poly(ethylene glycol) ($M_n \approx 510$ g/mol, 1 eq.) and BuA (1 eq.) were chosen for the alcohol and the acrylate. Reactions to the corresponding *aza*-Michael adduct were carried out in the presence of the radical inhibitor BHT and catalyzed by K Oct (Figure 34; Chapter 6.2.8). The compounds were reacted at 90 °C for 5 h. Sampling was carried out every hour to monitor the conversion (Figure 35). Each reaction was also repeated without sampling in order to detect the effect of sampling on the result.

The NCO group was fully converted to urethane and isocyanurate after 1 h of reaction. This was independent of the position of the methyl isocyanate substituent. The highest conversion of the urethane to the corresponding *aza*-Michael adduct was found for products derived from oTMI ($X_{5\,h} = 75 \pm 2$ %), followed from those from pTMI ($X_{5\,h} = 60 \pm 1$ %) and mTMI ($X_{5\,h} = 53 \pm 0$%). The *ortho*-isomer also appeared to react faster ($t_{X(max)} \leq 1$ h) than the *meta*- ($t_{X(max)} \approx 2$ h) and *para*-isomer ($t_{X(max)} \approx 3$ h).

All urethanes from different isomers showed some reactivity in the *aza*-Michael addition. This observation supports the assumption that all N-H-functionalities in urethanes derived from 2,4'-MDI, 4,4'-MDI and related isocyanates can in principle be used as donors in *aza*-Michael reactions since their substitution pattern is similar to that of the model isomers. Some reactivity is also expected for urethanes from 2,4-/ 2,6-TDI even if they differ slightly in their substitution patterns.

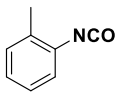

ortho-Tolyl isocyanate (oTMI)

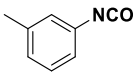

meta-Tolyl isocyanate (mTMI)

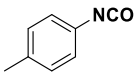

para-Tolyl isocyanate (pTMI)

Figure 33. Tolyl isocyanate with methyl residual in *ortho*-, *meta*- or *para*-position.

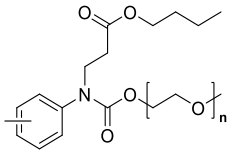

Figure 34. Targeted *aza*-Michael adduct with methyl residual in *ortho*-, *meta*- or *para*-position

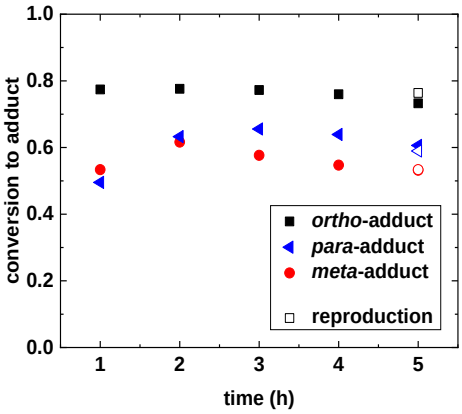

Figure 35. Adduct-formation of the methyl residual study.

5.1.6 Acrylate vs. methacrylate

Methacrylates are less electrophilic than acrylates because of an inductive effect by the methyl group that enhances the electron density in the carbon-carbon double bond.[105]

One equivalent of 2-(methacryloyloxy) ethyl acrylate (AMA, Figure 36) was reacted in a first series of reactions with 1 eq. 1-butanol and 2 eq. *para*-tolyl isocyanate. K Oct was used as a catalyst. The mixtures were heated at T = 90, 100, 110 and 120 °C for 3 h and changes were analyzed using ^{1}H-NMR spectra (Chapter 6.2.9, Figure 112). The acrylate-methacrylate molecule could react along the pathway in option a (Figure 36, red) and/or in option b (Figure 36, blue).

Only additions according to option a were observed. Addition to the methacrylate did not occur. This was also not obtained when an excess of *in-situ* formed urethane was used (1 eq. 1-BuOH, 0.5 eq. AMA and 2 eq. pTMI; Chapter 6.2.9, Figure 113). Methacrylates are too poor Michael-acceptors for reactions with aromatic carbamates.[57]

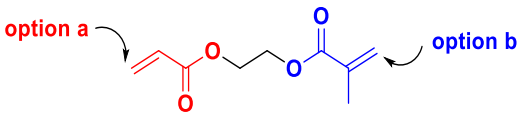

2-(Methacryloyloxy)ethyl acrylate

Figure 36. Acrylate-methacrylate model compound.

5.1.7 Reactivity of urethanes from aromatic vs. aliphatic isocyanate

The acidity of the urethane N-H is significantly different for urethanes produced from aromatic or aliphatic isocyanates. The electron density at the nitrogen atom is significantly higher in aromatic amines and hence in amides.

The commercially available 2-[(butylcarbamoyl)oxy] ethyl acrylate was chosen as a model system for the analysis of the reactivity of aliphatic-aliphatic urethanes in an *aza*-Michael addition reaction (Figure 37, left). The substance contains an acrylate functionality. A second model compound was synthesized by treating pTMI with 2-hydroxyethyl acrylate resulting in a colorless, crystalline product (Figure 37, right, Chapter 6.2.10.1). That aromatic-aliphatic model urethane also contains an acrylate functionality. Both model compounds are solids with melting temperatures below 90 °C. They were treated with catalyst K Oct and inhibitor BHT. The reaction mixtures were heated to 110, 120 or 130 °C. An [AB]-type (poly)addition reaction would occur in case of an *aza*-Michael reaction and an oligo- or polymer could be formed. No polyaddition was observed for 2-[(butylcarbamoyl)oxy] ethyl acrylate, not even after 39 h at 130 °C. 2-[(*p*-Tolylcarbamoyl)oxy] ethyl acrylate, however, could readily be converted to an oligomeric product at 110 °C for 8 h (Figure 38, Figure 39).

The monomer exhibits two (sharp) aromatic signals for H_3 and H_4, one signal for H_7 and H_8 and another signal for H_1. The polymerization led to a broadening of the signals. Unreacted monomer could still be detected after 15 h of reaction, after 111 h no monomer was left. Only traces of unidentified by-products were found in the range from 4.5 – 4.4 ppm and 3.7 – 3.5 ppm. The by-product formation during the polymerization can be explained by the transesterification-degradation reactions as discussed before (Chapter 5.1.2).

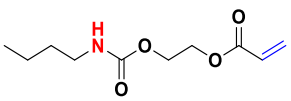

2-[(Butylcarbamoyl)oxy]ethyl acrylate

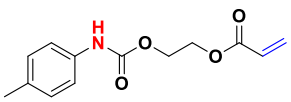

2-[(*p*-Tolylcarbamoyl)oxy]ethyl acrylate

Figure 37. (left) Aliphatic and (right) aromatic isocyanate-based urethane-acrylates.

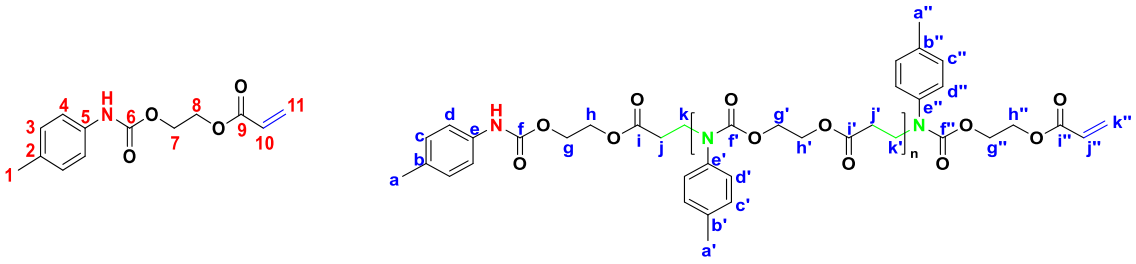

2-[(*p*-Tolylcarbamoyl) oxy]ethyl acrylate

Poly(2-[(*p*-Tolylcarbamoyl)oxy]ethyl acrylate)

Figure 38. ^{1}H-NMR-assignments for the [AB]-type monomer (A = red, B = blue) and the polymeric species (new bond = green).

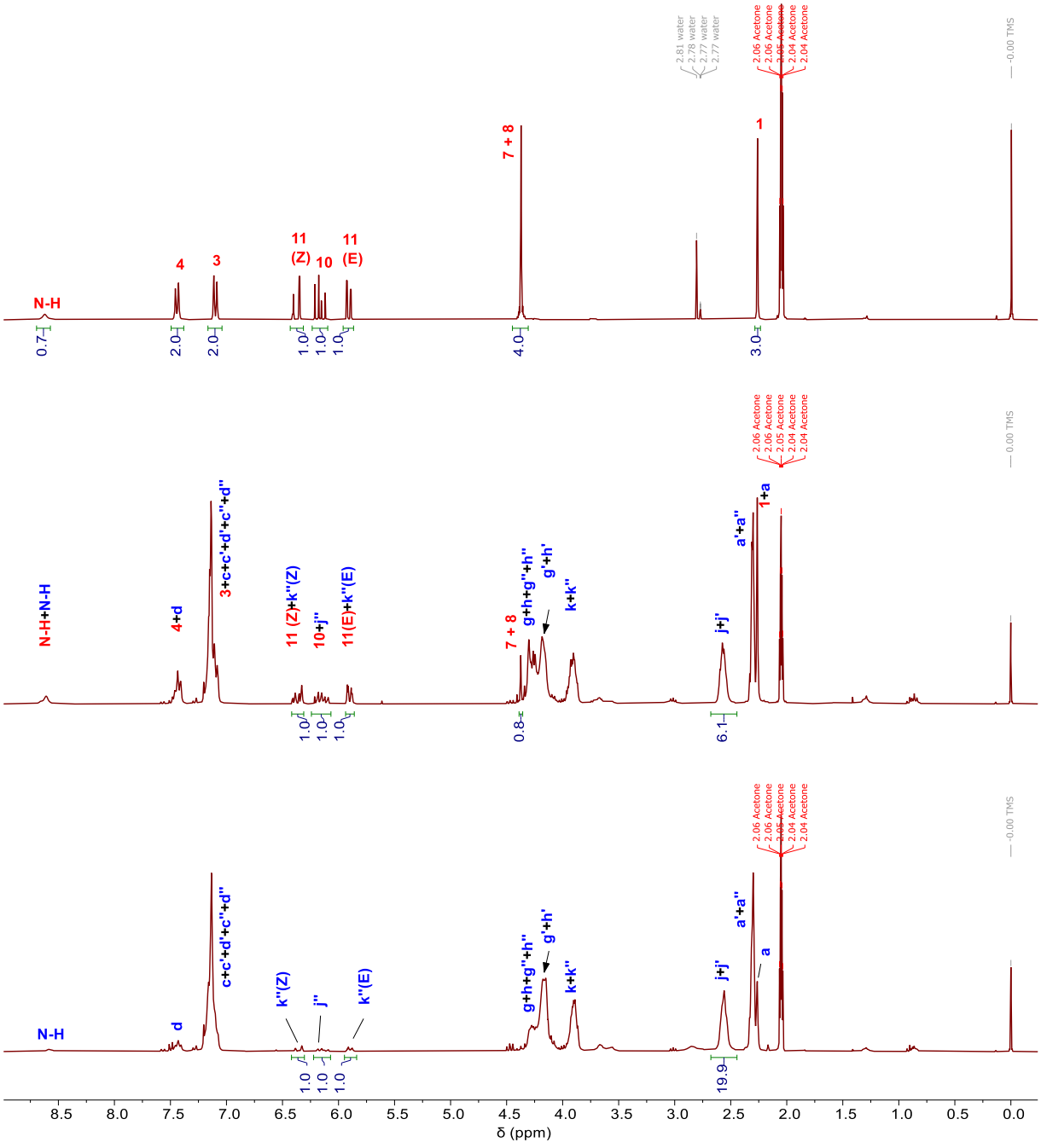

Figure 39. ^{1}H-NMR spectra of (top) pure monomer, (middle) after 15 h and (bottom) after 111 h at 110 °C (acetone-d_6, assignments according to Figure 38).

The catalyzed [AB]-type (poly)addition of the aromatic-aliphatic species was studied in more detail in the temperature range between 90 and 120 °C. Reactions without catalyst were conducted at 130 °C (Chapter 6.2.10.3).

The viscosity of the reaction mixtures increased with time but only in the presence of catalyst. The highest degree of polymerization P_n amounted to $P_n \approx 11$ and was achieved after about 100 h at temperatures in the range of 110 °C to 120 °C. It was determined by ^{1}H-NMR spectroscopy using the integral-ratio of the olefinic monomer, the end-group proton signals (e.g., $H_{11(E)}$ and $H_{k''(E)}$) and the backbone-proton signals (e.g., $H_{j+j'}$; Equation 1). The monomer conversion X at different reaction times was determined by frequent sampling and determination of P_n for each sample. X was then calculated from P_n using the Carothers equation (Equation 2). The monomer conversion could reasonably be approximated by a hyperbolic curve (Figure 40). The maximum conversion amounted to approximately 91 %. The obtained polymers were solid at room temperature, transparent and had a yellowish color. No reaction was observed without catalyst.

$$P_n = \left(\frac{\int H_{j+j'}}{2} + 1 \right) \qquad \text{Equation 1}$$

$$X = 1 - \frac{1}{P_n} = 1 - \frac{1}{\left(\frac{\int H_{j+j'}}{2} + 1 \right)} \qquad \text{Equation 2}$$

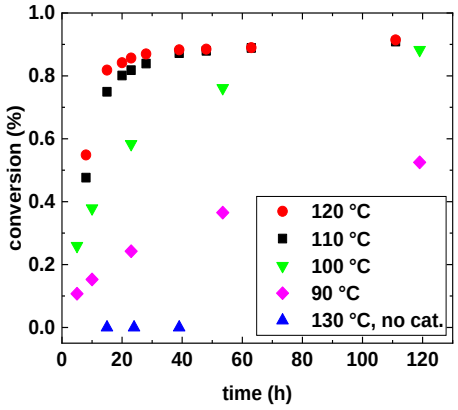

Figure 40. [AB]-type *aza*-Michael polyaddition reactions of 2-[(*p*-tolylcarbamoyl)oxy]ethyl acrylate.

5.1.8 Conclusions on chapter 5.1

A covalent bond between urethane and acrylate can be obtained in bulk by an *aza*-Michael addition reaction in the presence of *Lewis*-acids or *Brønsted*-bases. The urethane-based *aza*-Michael adducts showed a significantly increased thermal stability over the original urethane ($\Delta T \approx 100$ °C).

A model study based on monofunctional starting materials revealed that carboxylate-type catalysts were the most effective towards the *aza*-Michael adduct formation. Conversions were reached of at least 70 %. Undesired side reactions led to a range of byproducts, in increasing concentration with increasing catalyst concentration and temperature. Carboxylate catalysts also catalyzed a competing isocyanurate formation, but the use of a two-fold excess of isocyanate was sufficient to compensate for this. This isocyanurate formation was slow when using the *Lewis*-acid LiCl as a catalyst. That allowed the nearly NCO-trimer free formation of the aza-Michael adduct but required higher temperatures and was significantly slower. Various tertiary amines were studied as catalysts but only 1,4-diazabicyclo[2.2.2]octane showed some catalytic activity for the *aza*-Michael reaction. The ability of poly(ethylene glycol) to complex to the alkali cation in carboxylate-type catalysts led to increased reaction rates at low temperatures and a higher reaction selectivity was obtained.

The substitution pattern of tolyl isocyanate was influencing the *aza*-Michael reaction. The highest conversion was obtained when the urethane was derived from *ortho*-tolyl isocyanate (approx. 75 %) and the lowest when from *meta*-tolyl isocyanate (approx. 53 %).

Reactions conducted with the asymmetric 2-(methacryloyl oxy) ethyl acrylate indicated that the urethane-N-H nucleophile did not possess any reactivity towards methacrylates. Aliphatic urethane N-H moieties showed no comparable addition reaction. A monomer containing the N-H nucleophile of an aromatic-aliphatic urethane was converted in a polyaddition to short *aza*-Michael polymers. A degree of polymerization was reached of approx. 11.

5.2 Application in the synthesis of novel surface-active agents

Surface active agents (surfactants) are ionic or non-ionic amphiphilic molecules with the ability to interact with interfaces between phases of different polarity (e.g., air and water; Figure 41 a). Non-ionic surfactants find application in a variety of systems, e.g., in vaccines, coatings and hair dyes.[106–108] Typical non-ionic surfactants are alkyl ethylene glycols, alkyl glucosides, poly(ethylene oxide)-iso-octylphenyl ethers (Triton) or poly(ethylene oxide) sorbitan monoalkanoates (Tween).[109] Physical parameters of surfactant containing solutions change in dependence of its structure and concentration. Examples are the molar conductivity or the surface tension.[110] An increase in surfactant concentration will cause a reduction in interface surface tension at low concentrations. Surfactant molecules will be located at the interface and some will be dissolved in the bulk solvent (Figure 41 b). The interface will largely be saturated with surfactant molecules after having reached a specific concentration known as the critical micelle concentration (CMC; Figure 41 c). Additional surfactant will form structures above this concentration in the bulk solution such as micelles (Figure 41 d). A further increase in surfactant concentration above the CMC will not lead to a further decrease in surface tension. Aggregates of different shapes may be formed instead.[110–112] A critical surfactant packing parameter was defined that correlates the molecular geometry of a surfactant with the shape of the formed aggregates (spherical and non-spherical). Large head groups are required to form spherical micelles. Small head groups may lead to differently shaped aggregates (e.g., disc or rod shaped).[113]

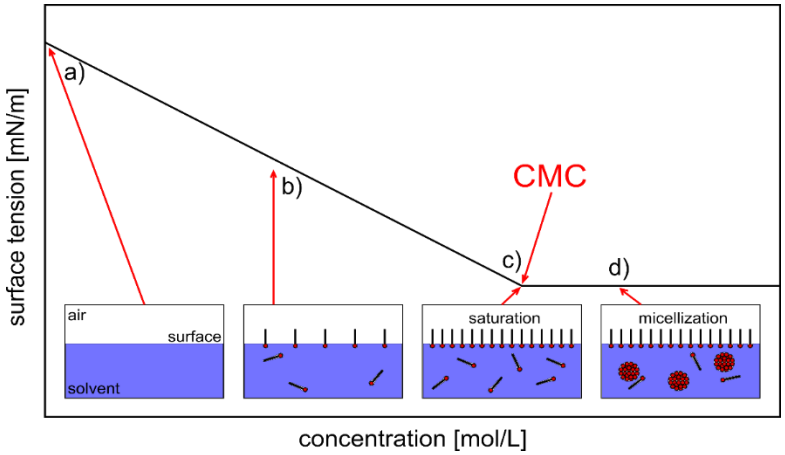

Figure 41. Surface tension as a function of surfactant concentration.[reproduced with permission from: [112]]

The CMC of non-ionic, poly(ethylene oxide)-based (PEG) surfactants is largely independent of the temperature up to the so-called cloud point temperature (CP). Large aggregates can precipitate into a separate phase above the CP. This is the result

of two different processes:[111,114,115] Firstly, the solubility of the non-ionic surfactants below the CP is based on hydrogen bonding between the water and the ether oxygen atoms.[115–120] Only specific ethylene oxide-chain conformations interact favorably with water which lowers the conformational entropy of the EO-chain in solution. These conformations are preferred at comparatively low temperature but become less probable at high temperature. The solubility is then decreased because of higher conformational entropy for the pure EO-EO-interactions.[117–120] Eventually a dewetting occurs where intramolecular interactions between water molecules and surfactant molecules are most dominant.[115–120] Secondly, the forming of aggregates can be induced by changes in the micellar phase.[115] A PEG-based surfactant with PEG-chains of a higher molecular weight generally has a higher CP but a higher lipophilic volume leads to a lower CP.[121] PEG-chains with terminal alkyl groups reduce the CP (by 20 – 30 °C for shorter chains).[115] The CP is also sensitive to impurities.[122,123] Polar organic liquids which were fully miscible with the surfactant, for instance, increased the CP of the non-ionic surfactant Triton X-100.[123]

The ability of surfactants to aggregate at interfaces can be estimated from its hydrophile-lipophile balance (*HLB*).[124,125] This is used to parameterize amphiphilic molecules by the weight fraction of their hydrophilic (polar) functional groups.[126–129] The *HLB*-value is calculated by dividing the molar mass of the hydrophilic chain M_h by the molar mass M (or M_n for polymeric surfactants) and multiplying the result by 20 (Equation 3).[125] The *HLB*-value allows the prediction of the properties of a surface active agent and whether it will form an oil-in-water (o/w) or a water-in-oil (w/o) emulsion.[124] The *HLB*-value scale ranges from 1 to 40; most surface-active compounds have values of around 10. Experimental work indicated that *HLB*-values above 18 are too high for the surfactant to show surface activity (Table 5).[124]

$$HLB = 20 \cdot \frac{M_h}{M_n} \qquad \text{Equation 3}$$

Table 5. *HLB*-values and corresponding applications (GRIFFIN).[124]

HLB	**Application**
1 – 3	Antifoaming agents
4 – 6	w/o emulsifier
7 – 9	Wetting agents
8 – 18	o/w emulsifier
13 – 15	Detergents
15 – 18	Solubilizing

Many different surfactant structures are described in literature to cover the broad range of applications. Conventional surfactants are based on one polar head group and a non-polar tail. Surfactants, however, can also consist of two head groups and two tails which are connected by a spacer.[130,131] Such surfactants are called gemini- or dimeric surfactants. These gemini-surfactants often exhibit a reduced critical micelle concentration in comparison to the corresponding conventional surfactants (Figure 42). Tri- or polymeric surfactants as well as surfactants based on di- or multiblock-copolymers are also used instead of dimeric surfactants (e.g., PEG-PPG-PEG).[109]

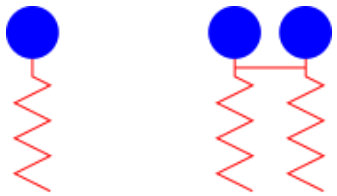

Figure 42. (left) Conventional surfactant and (right) gemini surfactant.

Typical applications for non-ionic surfactants are as additives in PU rigid foams or emulsion (co-) polymerizations. Three steps can be distinguished in the production of PU foam and a surfactant can play a role in each step. They are i) component mixing and nucleation, ii) bubble growth and iii) bubble packing and foam stabilization.

The A and B components used to prepare PU foams are in general incompatible. Surfactants can improve the emulsification of the two components during mixing by reducing the surface tension of interfaces of the different components. That facilitates molecular mixing. Small bubbles (nuclei) may be formed when gas is introduced into the mixture. This process is called nucleation in the context of PU-foam formation. The gas used for nucleation can originate from gasses dissolved in the reactants, purposely

entrained gas in the mixing and/or blowing agents. The process of nucleation may be described from free energy considerations of a liquid/gas system. The fully unmixed state is given by a gas and liquid phase which are separated by a single interface. An energetically higher state is reached when energy is introduced to the system. Energy input by a mixing procedure may lead to a redistribution of the gas and the liquid phase with formation of new interfaces. Some of the mixing energy goes into the work necessary to form gas bubbles in the liquid. A surfactant reduces the surface tension at the interface which leads to the stabilization of the gas-liquid system. The addition of surfactant to the system therefore thermodynamically promotes the formation of bubbles.[132] The energy for the formation of a bubble scales with the reciprocal value of the radius and a system with smaller bubbles will have a higher free energy content than one with larger bubbles.[132] The spontaneous formation of small nuclei would consequently require higher amounts of energy, which have a higher driving force to relax to a system with larger bubbles. That is why the total number of cells in the final foam is in general smaller than the number of nuclei produced during nucleation.

The size of the spherical bubbles increases in the second or bubble growth step. This is caused by multiple processes such as the diffusion of the dissolved gas out of the liquid phase, evaporation of blowing agents and gas-forming reactions. Inhomogeneous bubble growth results in a broad cell size distribution. It is part of an Ostwald ripening (diffusion of gas from adjacent bubbles) and coalescence process (rupture of interlayer between adjacent bubbles).[132,133] Both processes are induced by cell-pressure differences in the bubbles of different size and lead to bubble growth at the expense of the number of bubbles. The cell pressure is proportional to the surface tension of the liquid phase. This is the reason why these processes are influenced by the presence of surfactants.[132] The (kinetic) bubble stability is also dependent on the viscosity of the reaction mixture, and thus on the progress of the polymerization reaction to polyurethane.[134]

Bubble packing starts when the volume fraction occupied by the gas in the bubbles exceeds 74 %. Cell membranes are formed at that point and further bubble size growth results in the formation of polyhedral spheres. Most of the polymer mass retracts into the nodes and cell struts are formed. Surfactants mediate at this stage the mass transport within the cell window and thereby stabilize the cell. This last phase iii) ends with the complete cure of the polymeric matrix.[132] In summary, surfactants have the

roles of emulsifying incompatible reaction components, promoting nucleation during mixing and assisting in film drainage. They also function as foam stabilizers.[132,135,136]

Non-ionic polyalkylsiloxanepolyoxyalkylene copolymers are commonly applied in rigid and flexible PU foams as surfactants.[137,138] These consist of a PDMS backbone grafted with poly(oxyalkylene) chains. The silicone to polyether ratio determines the performance of the surfactant.[139] Non-silicone surfactants are rarely used in the PU foam technology (e.g., Spans, Tweens and Emulphors) since they show poor foam stabilizing properties.[137]

Another important application for non-ionic surfactants is emulsion polymerization. Water-insoluble monomer is typically added to an aqueous surfactant solution, where the surfactant concentration is above its CMC. Multiple phases can be distinguished in such a system. The first phase consists of small amounts of surfactant and monomer that are dissolved in the aqueous medium. A second phase consists of large monomer-droplets (1 – 10 µm diameter). They cover the majority of monomer molecules. These droplets are formed by agitation and stabilized by surfactant molecules. The third phase is one of micelles formed by the surface-active molecules, which are slightly swollen by monomer-molecules. These micelles have a size in the range of nanometers (5 – 10 nm diameter) and are of a much higher quantity than the monomer-droplets (several orders of magnitudes) but contain only a minority of monomers.[140,141] Surfactants play also an important part during the polymerization after initiation. They mediate and stabilize different processes and are key to a good product quality of emulsion polymers (latexes).[140,142,143]

Nonylphenol-based non-ionic surfactants were widely used in the past decades to prepare latexes. A recommendation, however, was made by the European Union to stop using these surfactants because of environmental concerns. That is why alternative surfactants are desired.[144] Fatty alcohol polyglycol ethers (Disponil AFX-series) were successfully applied in emulsion polymerizations.[145] The application of a lignin-based surfactant for emulsion polymerization showed a comparable performance to nonylphenol-containing additives.[146] Poly(ethylene glycol)$_{20}$ oleyl ether (Brij98) was used to produce mini-emulsions with improved transportation properties in the RAFT-polymerization of styrene.[147]

5.2.1 *Aza*-Michael addition-based urethane/acrylate-surfactants

The structure of the surfactant is key to surface tension dependent processes. Tailor-made surfactants for a given application can be desirable. The *aza*-Michael addition of urethane and acrylate can be used as a means to prepare urethane/acrylate-based surface-active agents. A literature search showed no matches to any of the surfactants and related structures presented in this thesis. It is therefore conceivable that these compounds have not been prepared before.

5.2.2 Surfactant synthesis

A novel one-pot synthesis protocol for surfactants was developed. The synthesis was based on the previous results regarding the *aza*-Michael addition reaction of urethane and acrylate. A three-fold excess of a non-polar acrylate was required to obtain close to 100 % conversions of urethane to the corresponding amphiphilic adduct. The carboxylate catalyst for the *aza*-Michael addition was activated using the polar MoPEG (1 eq.) alcohol as inherent complexing agent. The intramolecular catalysis allowed reaction temperatures as low as 90 °C for the addition and minimized side-reactions. pTMI (2 eq.) was used as isocyanate.

The formation of isocyanurate as a by-product could not be prevented because of the nature of the catalyst (Chapters 5.1.2 to 5.1.4; Figure 43). The purification of the end product was challenging because of the amphiphilic nature. All liquid-liquid extraction attempts failed. The main products could be isolated with high purity when the crude product was filtered over silica, since other than the by-products the desired products could not migrate through the silica and were retained on the surface. The reaction mixture was therefore dissolved in a mixture of petroleum ether and ethyl acetate and filtered over silica. The silica was then washed with a mixture of petroleum ether and ethyl acetate before the purified product was re-dissolved in acetone. Only traces of non-converted urethane (≈ 1 %) remained after purification in the product of the reaction of 2-ethylhexyl acrylate, pTMI and MoPEG500. Residual acrylate and the by-product isocyanurate were completely removed as confirmed by a recorded ^{1}H-NMR spectrum (Figure 44). The reaction was scaled up to 30 g where a yield of approx. 91 % could be obtained (Chapter 6.3.1).

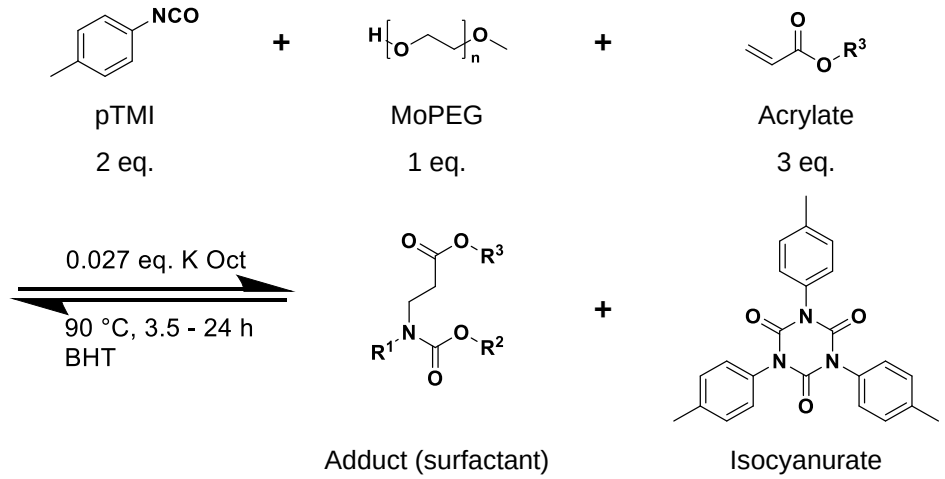

Figure 43. General synthesis protocol to surfactant molecules.

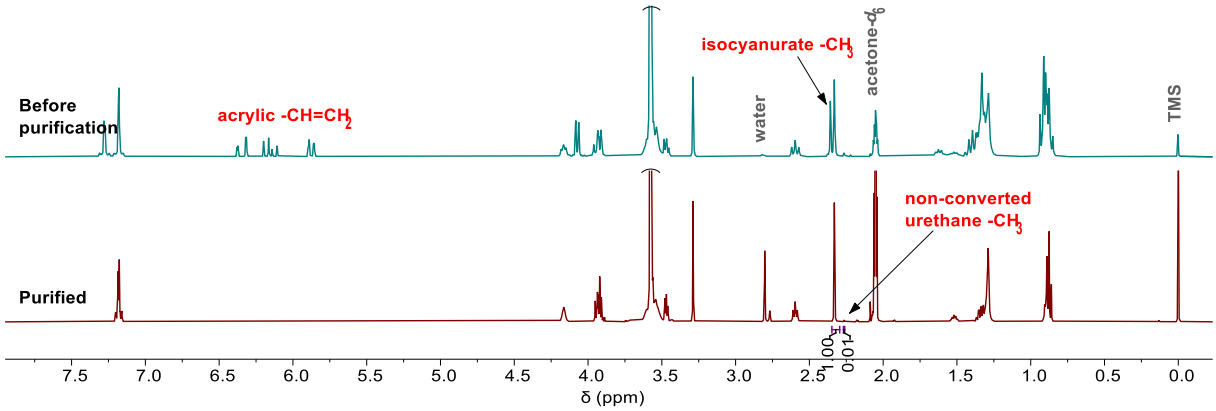

Figure 44. ^{1}H-NMR spectra of (blue) crude product and (red) purified product (acetone-d_6).

Several novel amphiphilic molecules were produced (Table 6 and Table 7). Yields of approx. 80 – 90 % could be achieved after purification with residual urethane entities ($R_{urethane}$) of about 1 to 7 %. The structures of the synthesized surface-active molecules are in accordance to ^{1}H-NMR and ESI-MS spectra (Table 7). The M_n of the surfactants determined by ^{1}H-NMR spectroscopy (in brackets) were close to the M_n values calculated from the starting materials.

Table 6. Results for reactions to different surfactant molecules.

Surfactant	Acrylate	*t* [h]	*X* [%]	$R_{urethane}$ [%]
S1[b]	Butyl acr.	3.5 h	81 %	7 %
S2[b]	Hexyl acr.	5 h	79 %	6 %
S3[b]	Stearyl acr.	24 h	83 %	5 %
S4[b]	2,4-dimethyl-3-pentyl acr.	8 h	82 %	7 %
S5[b]	2-ethylhexyl acr.	4.5 h	91 %	1 %
S6[b]	4-tert-butylcyclohexyl acr.	4.5 h	87 %	5 %
S7[b]	Phenoxyethyl acr.	5.5 h	82 %	4 %
S8[b]	2-(Methyacryl-oyloxy)ethyl acr.	7 h	77 %	4 %
S9[a]	2-ethylhexyl acr.	7.5 h	88 %	4 %
S10[c]	2-ethylhexyl acr.	7.5 h	80 %	5 %

[a]MoPEG350 (M_n = 363.5 g/mol), [b]MoPEG500 (M_n = 510.0 g/mol) or [c]MoPEG750 (M_n = 793 g/mol) was used.

Table 7. Non-ionic surfactants.

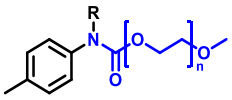

R =

M_n = 643.2 g/mol (656.4 g/mol)

Urethane-backbone

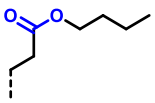

M_n = 771.3 g/mol (747.1 g/mol)

S1 (butyl acrylate)

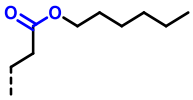

M_n = 799.4 g/mol (816.3 g/mol)

S2 (hexyl acrylate)

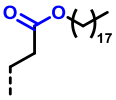

M_n = 967.8 g/mol (965.6 g/mol)

S3 (stearyl acrylate)

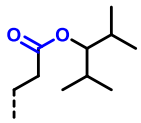

M_n = 813.5 g/mol (832.2 g/mol)

S4 (2,4-dimethyl-3-pentyl acrylate)

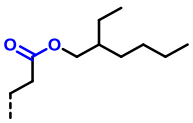

M_n = 827.5 g/mol (833.0 g/mol)

S5 (2-ethylhexyl acrylate)

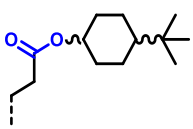

M_n = 853.5 g/mol (846.9 g/mol)

S6 (4-*tert*-butylcyclohexyl acrylate)

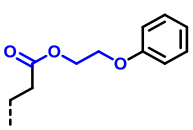

M_n = 835.4 g/mol (844.2 g/mol)

S7 (phenoxyethyl acrylate)

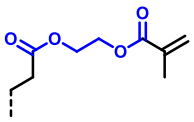

M_n = 827.4 g/mol (842.1 g/mol)

S8 (methacryloyloxyethyl acrylate)

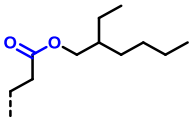

M_n = 681.0 g/mol (699.7 g/mol)

S9 (2-ethylhexyl acrylate)

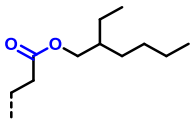

M_n = 1110.5 g/mol (1061.0 g/mol)

S10 (2-ethylhexyl acrylate)

*M_n calculated and determined by ^{1}H-NMR spectroscopy (in brackets). Parts that were additionally used for the calculation of HLB_{hydro} are marked in blue.

The synthesis protocol could be extended to the preparation of gemini-surfactants. The mono-hydroxy-functional MoPEG was replaced for these surfactants by di-functional PEG600. It was mixed with POEA, pTMI and catalytic amounts of K Oct. The gemini-surfactant **S11** (Figure 45, left) was obtained after 5 h of reaction at 90 °C. The reaction mixture was purified using the same purification method as before. A yield of approx. 86 % was obtained (Chapter 6.3.2.1). Approx. 96 % of the urethane groups were converted to the corresponding *aza*-Michael adduct. The purified product consisted of approx. 92 % di-adduct and 8 % mono-adduct. ESI-MS data showed only some minor traces (<< 1 %) of non-reacted di-urethane.

2-Ethylhexyl acrylate was also used for the synthesis of a gemini-surfactant (**S12**, Figure 45, right). The target molecule was prepared at 90 °C and a reaction time of 6.5 h. A conversion of 97 % in urethane was achieved (Chapter 6.3.2.2). Minor traces (<< 1 %) of non-reacted di-pTMI-PEG600-urethane were detected in ESI-MS spectra. **S12** was calculated to consist of approx. 94 % di-adduct and 6 % mono-adduct.

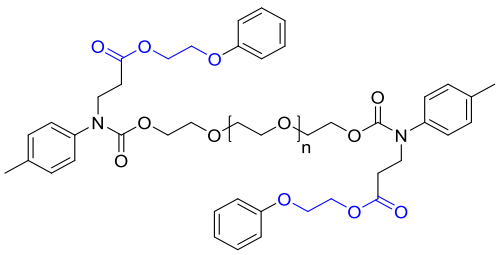

M_n = 1259.8 g/mol (1267.5 g/mol)

S11 (phenoxyethyl acrylate)

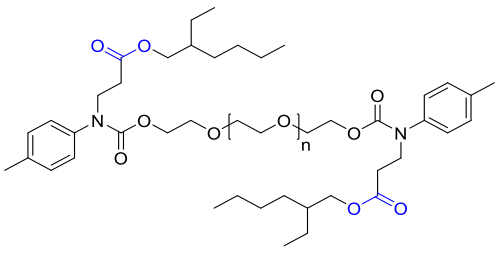

M_n = 1244.1 g/mol (1207.7 g/mol)

S12 (2-ethylhexyl acrylate)

Figure 45. Non-ionic gemini-surfactants.

5.2.3 Properties of the novel surfactants

5.2.3.1 Hydrophilic-lipophilic balance (HLB-value)

The *HLB*-value of a surfactant allows an estimation of its behavior in solution. It was originally defined for structures such as fatty acid esters that show a clear transition between the hydrophobic and hydrophilic parts (e.g., polar poly(ethylene oxide) and non-polar aliphatic fatty acid-based residue).[124,125] That allows a clear definition of the molar mass of the hydrophilic chain segment, M_h, which is required for the calculation of *HLB*. The surfactants **S1** – **S12** are different in that the coupling of the acrylic ester integrated an additional polar ester group as well as polar ethylene oxide units into the "traditionally" purely lipophilic segment (Table 7, highlighted in blue). This makes the determination of M_h more complex and requires the definition of two extrema: $M_{h(lipo)}$ and $M_{h(hydro)}$. Only the carbamate-functionality and the PEG-chain are counted as the hydrophilic chain segment for $M_{h(lipo)}$ (Figure 46 left). $M_{h(hydro)}$ includes additionally the molar mass of the acrylic ester group and in some cases further polar segments (Figure 46 right; i.e., **S7**, **S8** and **S11**). Derived *HLB*-values are therefore divided into HLB_{lipo} and HLB_{hydro} (Equation 3; Table 8).

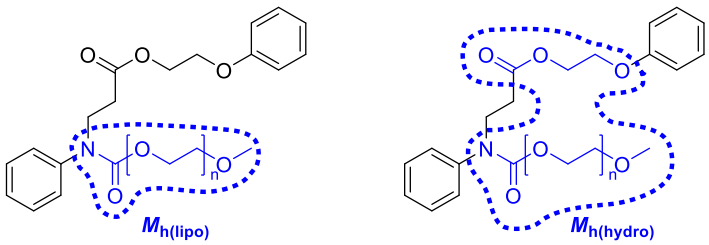

Figure 46. Difference between $M_{h(lipo)}$ and $M_{h(hydro)}$.

The surfactants **S1** – **S12** have *HLB*-values in range from 12.3 to 16.1 (HLB_{hydro}) or 11.0 to 15.0 (HLB_{lipo}). These *HLB*-values are typical for o/w-emulsifiers.[124,125] The properties are determined by the chain length of the polar MoPEG (**S5**, **S9**, **S19**) and by the alcohol part of the acrylic ester (**S1** – **S8**). Prepared surfactants showed water solubilities of at least several grams per liter, e.g., **S5** with more than 33.2 g/L. The gemini-surfactants **S11** and **S12** had a poor water solubility and were not further studied.

Table 8. *HLB*-values for the surfactants of this study.

Surfactant	M_n [g/mol]	$M_{h(hydro)}$ [g/mol]	$M_{h(lipo)}$ [g/mol]	HLB_{hydro}	HLB_{lipo}
Urethane	643.2	552.0	-	17.2	-
S1	771.3	595.0	551.0	15.4	14.3
S2	799.4	595.0	551.0	14.9	13.8
S3	967.8	595.0	551.0	12.3	11.5
S4	813.5	595.0	551.0	14.6	13.6
S5	827.5	595.0	551.0	14.4	13.4
S6	853.5	595.0	551.0	13.9	13.0
S7	835.4	640.1	551.0	15.3	13.4
S8	827.4	667.1	551.0	16.1	11.5
S9	681.0	448.6	404.5	13.2	11.9
S10	1110.5	878.0	834.0	15.8	15.0
S11	1259.8	867.2	691.1	13.8	11.0
S12	1244.1	779.3	691.1	12.5	11.1

5.2.3.2 Critical micelle concentration (CMC)

The CMC is an important parameter in describing a surface active molecule as it represents the surface activity of the surfactant.[111,148] The surfactants in Table 6 contained some unreacted urethane. It was pertinent to study the effect of the free urethane building block on the CMC of the surfactant.

The corresponding urethane was synthesized by reacting pTMI with MoPEG500 (Figure 47, Chapter 6.3.1.11). This urethane was subsequently mixed in different molar ratios with the surfactant **S5** based on 2-ethylhexyl acrylate. **S5** had a negligible residual urethane content of about 1 %. The surface tension was measured as a function of the concentration at various molar ratios of urethane to surfactant using the Wilhelmy-Plate-Method (Figure 48, r = n(urethane)/n(surfactant) = 1/0, 50/50, 20/80, 0/1, Chapter 6.1.3). Measurements were at least performed twice.

The surface tension was dependent on the absolute concentration and the molar ratios of the two components (Figure 48). At first, the surface tension decreased with increasing surfactant concentration at low concentrations. The surface tension then became nearly independent of the concentration (e.g., > 400 µmol/L for **S5**, black curve). This concentration dependent behavior is typical for the formation of micelles.

The CMC and its corresponding surface tension value σ_{CMC} were determined for all molar ratios, r, using the intersection of two regression lines of the concentration dependent and independent part of each curve (Table 9; Chapter 6.1.4). The experimental error given was determined from the difference of the values obtained in two consecutive measurements. The experimental error for the calibration was estimated to be 0.1 mN/m.

The neat urethane showed weak surface activity and a relatively high CMC. The surfactant **S5** showed a lower surface tension and a low value for the CMC. This clearly demonstrates that coupling of the urethane with 2-ethylhexyl acrylate provides molecules of high surface activity. It results from the substitution of the hydrogen-bonding N-H functionality and the increase in lipophilic volume. The CMC slightly increased with increasing urethane-fraction whereas the surface tension at the CMC remained almost constant. In summary, additional urethane in **S5** reduced the surface-active properties but the deterioration was negligible up to 20 mol% of urethane.

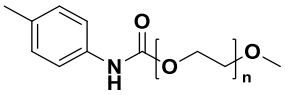

Figure 47. Urethane from MoPEG500 and pTMI.

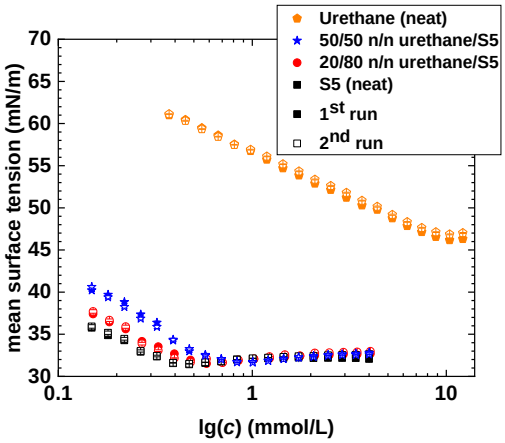

Figure 48. Influence of various molar ratios of urethane and **S5** on mean surface tension (T = 26±1 °C).

Table 9. CMC and σ_{CMC} values for different molar ratios of urethane and **S5**.

r **[n(urethane)/n(surfactant)]**	**CMC [µmol/L]***	**σ_{CMC} [mN/m]***
1/0	9194±6	46.4±0.3
50/50	683±22	30.4±0.1
20/80	546±8	31.4±0.1
0/1	406±5	31.4±0.1

*The error is the deviation of 2 measurements.

Surfactants **S1** to **S10** had free urethane contents ranging from 1 to 7 % (Table 6). This should also have only little effect on their surface-active properties.

The surface tension is strongly dependent on the type of acrylate used in the *aza*-Michael addition. A broad transition concentration is sometimes found rather than a sharp CMC (Figure 49; e.g., **S1**, **S7**, **S8**). The CMC and σ_{CMC} are then derived from a linear plot of the surface tension as a function of the surfactant concentration (Figure 50).[149,150]

All surfactants from ethylene oxide-free acrylates significantly reduced the surface tension of the aqueous solutions (Table 10; Figure 49, butyl acr. (**S1**/orange), hexyl acr. (**S2**/red), stearyl acrylate (**S3**/purple), 2,4-dimethyl-3-pentyl acr. (**S4**/blue), 2-ethylhexyl acr. (**S5**/black), 4-*tert*-butylcyclohexyl acr. (**S6**/green)). The two surfactants

that contained an ethylene oxide-unit in the acrylate moiety were less effective in reducing the surface tension (phenoxyethyl acr. (**S7**/turquoise), methacryloyloxyethyl acr. (**S8**/yellow)).

The σ_{CMC} was strongly dependent on the number of carbon atoms in the lipophilic moiety (Figure 51, black). A V-shaped pattern was obtained with a minimum in σ_{CMC} at 8 carbon atoms (**S5**). The CMC was largely independent from the number of carbon atoms for $n = 4 - 10$. Sample **S3** with 18 carbon atoms showed the highest CMC (Figure 51, red).

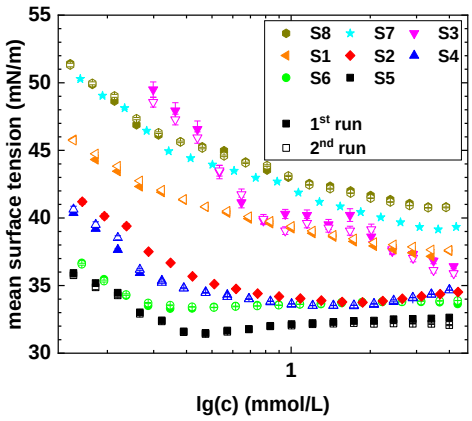

Figure 49. Influence of surfactants **S1** – **S8** on mean surface tension (T = 27±2 °C).

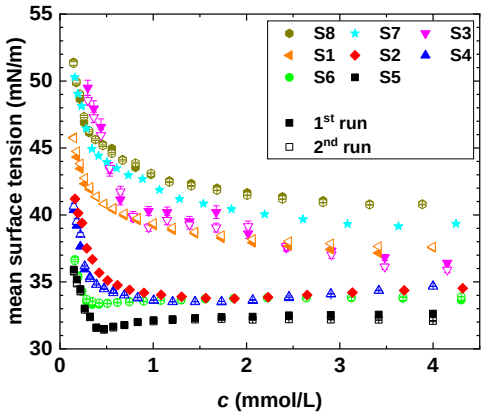

Figure 50. Non-logarithmic plot of the influence of surfactants **S1** – **S8** on mean surface tension (T = 27±2 °C).

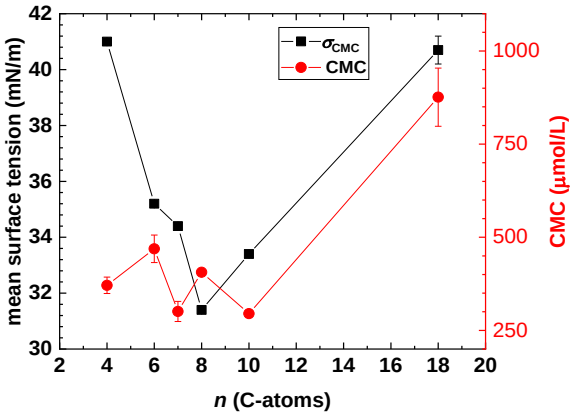

Figure 51. Dependency of the number of C-atoms in the lipophilic moiety on the mean surface tension and CMC (**S1** – **S6**).

Table 10. CMC and σ_{CMC} values of surfactants **S1** – **S8**.

Surfactant	Acrylate	CMC [µmol/L][a]	σ_{CMC} [mN/m][a]
S1	Butyl acr.	371±22	41.0±0.1
S2	Hexyl acr.	469±37	35.2±0.1
S3	Stearyl acr.	876±78	40.7±0.5
S4	2,4-dimethyl-3-pentyl acr.	301±27	34.4±0.1
S5	2-ethylhexyl acr.	406±5	31.4±0.1
S6	4-tert-butylcyclohexyl acr.	295±10	33.4±0.1
S7	Phenoxyethyl acr.	369±29	44.1±0.1
S8	2-Methyacryloyloxyethyl acr.	316±3	44.9±0.1

[a] Error as deviation of 2 measurements.

2-Ethylhexyl acrylate-based **S5** showed the lowest σ_{CMC} and reasonably low CMC. **S5** was therefore taken to study the effect of the molar mass of the hydrophilic methoxypolyethylene glycol-segment on the CMC and σ_{CMC} (Figure 52). The M_n was varied from 364 g/mol to 793 g/mol. The average number of ethylene oxide units in the chain was therefore varied from 7.5 to 17.3.

The lowest values for CMC and σ_{CMC} were obtained for the surfactant based on the shortest hydrophilic chain (**S9**). These values slightly increased with increasing chain length (Table 11) which is common for non-ionic surface-active agents based on poly(ethylene oxide).[114,149] The σ_{CMC} only decreased marginally when the chain length was decreased from 510 g/mol to 364 g/mol (**S5** to **S9**, $\Delta\sigma_{CMC}$ = -0.4 mN/m). The length of the hydrophilic chain cannot be decreased much further for solubility issues. The lower limit of the surface tension is therefore about 31.0 mN/m for this class of surfactants.

The surface tension for **S10** increased strongly with increasing surfactant concentration after reaching the CMC. Non-ionic surfactants from rather long ethylene oxide chains having a broad molar mass distribution often show this behavior. Surfactants with a low degree of ethoxylation are very effective in reducing the surface tension at low concentrations. These surfactant molecules adsorb into the micelles at concentrations above the CMC and the surface tension increases.[149,151]

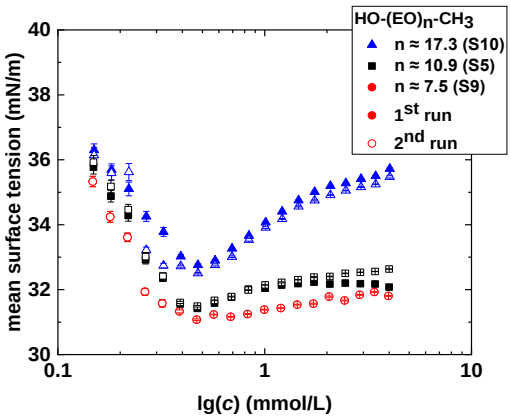

Figure 52. Influence of surfactants from MoPEG of different M_n on mean surface tension (T = 26±1 °C).

Table 11.CMC and σ_{CMC} of surfactants from MoPEG of different M_n.

Surfactant	M_n (MoPEG) [g/mol]	CMC [µmol/L]	σ_{CMC} [mN/m]
S9	364 g/mol	337±2	31.0±0.1
S5	510 g/mol	406±5	31.4±0.1
S10	793 g/mol	467±23	32.5±0.1

5.2.3.3 Cloud Point (CP)

The cloud point (CP) specifies for surfactants from PEG the temperature at which large aggregates precipitate and the solution turns cloudy.[111,114,116,122,123] The CP therefore gives the temperature limit at which the additive can be used as surfactant.

The effect of residual urethane on the CP was studied using **S5** from 2-ethylhexyl acrylate ($R_{urethane} \approx 1$ %) and its corresponding urethane (Figure 47). Aqueous solutions were prepared of different molar ratios from urethane and **S5** (r = n(urethane)/n(surfactant): 1/0, 50/50, 20/80, 0/1). All solutions had a cumulating concentration of c = 2 mM. The CP was determined as described in Chapter 6.1.1 (Table 12).

The aqueous solution containing only urethane did not show a CP and the solutions remained clear up to 98 °C. The solution containing **S5** showed a CP of 42 °C. All mixtures of urethane and **S5** exhibited similar CPs but differed in turbidity. The solutions became opaquer with increasing surfactant concentration. The CPs of mixtures were equal to that of neat **S5** even at a urethane/surfactant ratio of 50/50 (n/n). **S4** was the most impure surfactant with a residual urethane content of $R_{urethane} \approx 7$ %. It is assumed that the CP values obtained for the as-produced surfactants should be same as that of the neat surfactants. This is because even impurities of up to 50 mol% did not affect the CP.

Table 12. Influence of various molar ratios of urethane and **S5** on CP.

***r* [n(urethane)/n(surfactant)]**	**CP [±0.5 °C]**
1/0	>98 °C[a]
50/50	42 °C[b]
20/80	42 °C[c]
0/1	42 °C[c]

[a] Clear solution, [b] only slightly opaque at CP, [c] strongly opaque at CP.

The CP values of **S1 – S8** were determined at a concentration of c = 2 mM (Table 13). Sample **S1** did not show a cloud point and was therefore not further analyzed. The lowest CP was found for the phenoxyethyl acrylate-based surfactant **S7**. This surfactant already showed some turbidity at room temperature. The CPs of **S5** (2-ethylhexyl acrylate-based), **S4** (2,4-dimethyl-3-pentyl acrylate-based) and **S6** (4-tert-butylcyclohexyl acrylate-based) were found at somewhat higher temperatures

(42 – 45 °C), followed by **S3** (49.5 °C, stearyl acrylate-based) and **S2** (51 °C, hexyl acrylate-based). The highest cloud point was found for **S8** from 2-methylacryloyloxyethyl acrylate (68 °C). The CP was therefore dependent on the former acrylate structure of the surfactant (Figure 53).

Table 13. CP values of surfactants **S1** – **S8**.

Surfactant	Acrylate	CP [±0.5 °C]
S1	Butyl acr.	-[a]
S2	Hexyl acr.	51 °C
S3	Stearyl acr.	49.5 °C
S4	2,4-dimethyl-3-pentyl acr.	45 °C
S5	2-ethylhexyl acr.	42 °C
S6	4-tert-butylcyclohexyl acr.	45 °C
S7	Phenoxyethyl acr.	< 25 °C
S8	2-Methyacryloyloxyethyl acr.	68 °C

[a] No cloud point was detected (either too weak or CP > 98 °C).

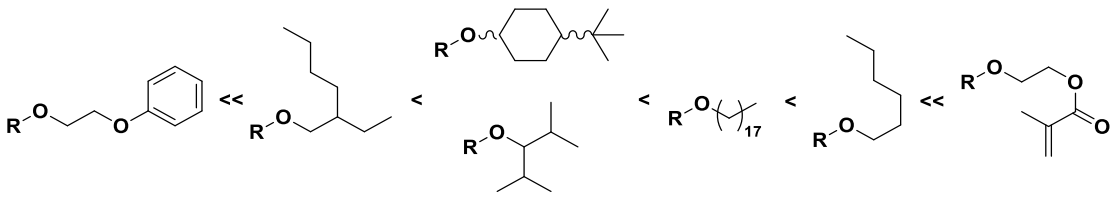

Figure 53. Order of surfactants sorted by CP in dependency of their acrylic residual.

The influence of the hydrophilic chain length on the CP was analyzed next using **S9**, **S5** and **S10** (Table 14; M_n(MoPEG) = 364 g/mol, 510 g/mol and 793 g/mol, respectively). The CP increased with increasing EO-chain length. This is ascribed to the increasing solubility because of the increasing hydrophilicity.[114,115,152]

HLB-value and CP increase with increasing number of ethylene oxide units for non-ionic surfactants with the same lipophilic moiety.[153] This correlation was verified for **S2** – **S6** and **S8** – **S10** using HLB_{hydro} (Figure 54). **S7** was excluded as no CP could be determined. The cloud points of **S2**, **S4** – **S6** and **S8** – **S10** were found to linearly correlate with their HLB_{hydro}-values. The stearyl acrylate-based **S3** deviated from linearity, probably because of its relatively large lipophilic volume.[116,121] This surfactant was consequently also excluded from the study. Summarizing, the novel urethane based non-ionic surfactants showed the expected correlation between CP and HLB-value.[153]

Table 14. CPs in dependency on the number of ethylene oxide units.

Surfactant	M_n (MoPEG) [g/mol]	*n*	CP [±0.5 °C]
S9	364 g/mol	7.5	32 °C
S5	510 g/mol	10.9	42 °C
S10	793 g/mol	17.3	74.5 °C

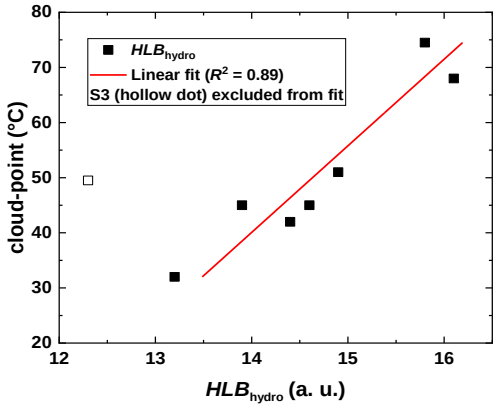

Figure 54. Correlation of HLB_{hydro} and CP (linear fit: $y = 11.45 + 0.06364 \cdot x$; $R^2 = 0.89$).

5.2.4 Application of *aza*-Michael adducts as emulsifier in PU rigid foam formulations

The novel non-silicone surfactants from urethane and acrylate were tested in a polyetherol-MDI-based standard rigid foam system. The non-ionic silicone-surfactant Niax Silicone L-6900 was used as a reference for the state of the art. The A-component contained two different polyetherols, catalyst (Jeffcat ZR-70) and surfactant. Lupranol 1100/1 and Lupranol 3423 were used as polyols in a 35/65 w/w-ratio. The A-component was mixed with polymeric MDI (Lupranat M20S) using a mechanical stirrer at 1400 rpm for 15 s. Bubble nuclei were generated in the mixing step. The reaction mixture was poured into a cup in which the foam expansion took place (Figure 55). The foam-rise time and the tack-free time were measured ($t_{\text{end-of-rise}}$ and $t_{\text{tack-free}}$, respectively). Foams were also produced without the presence of a surfactant (Chapter 6.3.4).

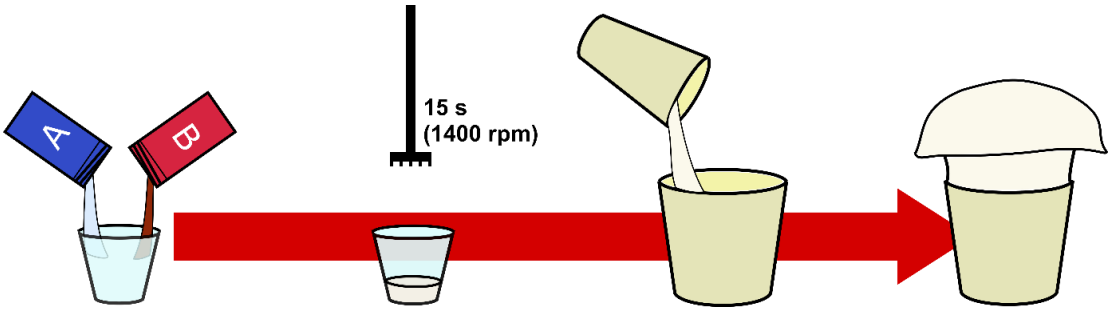

Figure 55. Schematic representation of the foam synthesis.

The catalyst concentration influences the bubble stabilization.[134] Higher catalyst concentrations speed up the urethane forming reaction rate and gel build-up. The faster gel build-up prevents bubble collapse, hence with increasing rate the foams will be more fine celled.[134]

Surfactant-free foams were prepared containing 0.82 pph, 1.22 pph and 1.64 pph of catalyst (pph is based on the total amount of polyol in the A-component). All foams were prepared at least twice and analyzed by SEM-imaging (Figure 56). The absolute number of cells per cm^2 were determined. All images were taken at a resolution of 0.89 cm x 0.62 cm (0.55 cm^2) and 32-fold magnification. At least four images were taken of each foam at different positions and cell counts were made using the open-source software *ImageJ* (Table 15). Foams with smaller cells were obtained at higher catalyst concentration, as expected. The lowest catalyst concentration of 0.82 pph was used in all further foaming experiments.

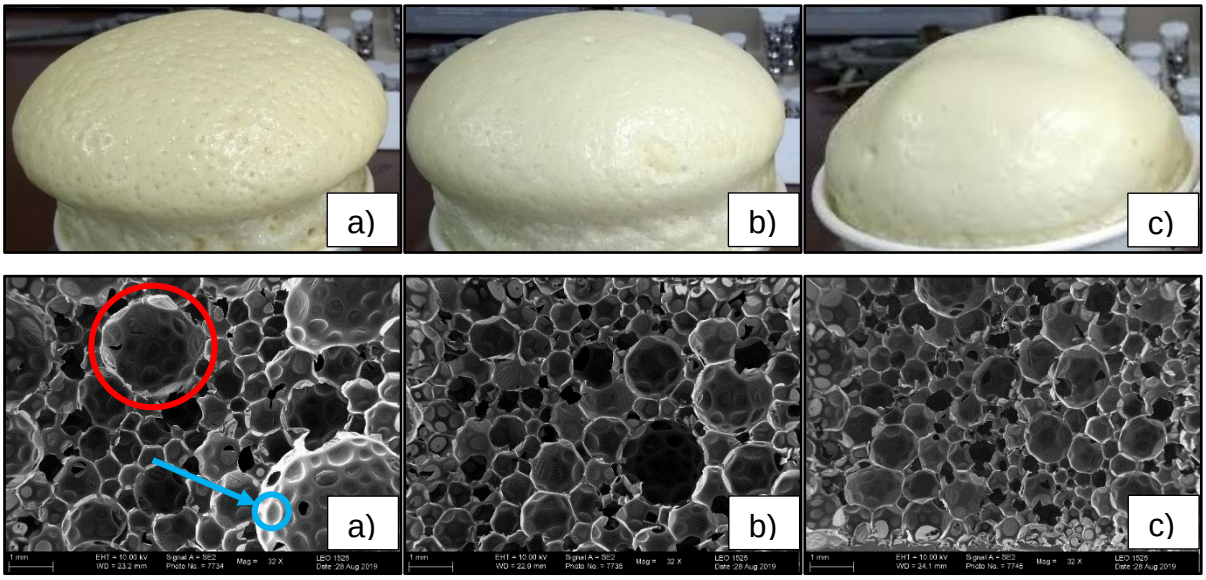

Figure 56. (top) Pictures and (bottom) SEM images at 32-fold magnification of blank PU rigid foams with (a) 0.82 pph, (b) 1.22 pph and (c) 1.64 pph catalyst (red circle = cell; blue circle and arrow = cell window).

Table 15. Influence of catalyst concentration.

$c_{catalyst}$ [pph]	$t_{end\text{-}of\text{-}rise}$ [s][a]	$t_{tack\text{-}free}$ [s][a]	N [cells/cm^2][a]
0.82	210±10	613±13	94±3
1.22	162±1	243±4	155±5
1.64	130±1	188±3	192±7

[a] Error as mean deviation of two foams of the same composition.

Similar recipes were used to prepare foam in the presence of surfactant. At first, silicone-benchmark Niax Silicone L-6900 was used at a concentration of 2 pph, which is typical for PU foam production.[138,139,154,155] 2 pph of **S2** (hexyl acrylate based) were used in the same way. All other surfactants of this study (**S5 – S8**) were applied at the same molar concentration as that of **S2**. The number of cells per cm^2 was determined by SEM (Table 16 and Figure 57).

The presence of a surfactant resulted in a higher number of cells per cm^2. The best performing novel surfactant **S6** (N = 195±26 cells/cm^2) with respect to the density of cells, however, was largely inferior to the standard silicone surfactant (N = 648±3 cells/cm^2).[156] Silicone surfactants reduce the surface tension and stabilize the cells. This results in less cells being lost during foaming, leading to smaller cell sizes.[155] The silicon-free surfactants described in this work were effective in reducing the surface tension of aqueous solutions but not that of polyols. The surface tension of the neat polyol blend was determined using a drop volume tensiometer (Chapter 6.1.3). It amounted to 32.4±0.2 mN/m. The addition of 2 pph of the silicon surfactant significantly reduced the surface tension of the polyol blend

(22.4±0.3 mN/m). The addition of **S2**, **S5** and **S6** had no effect on the surface tension (33.1±0.5 mN/m, 32.9±0.4 mN/m and 32.9±0.3 mN/m, respectively; Figure 58). The addition of the novel surfactants still led to a somewhat smaller cell size. This is explained as follows: The polyol blend is incompatible with the isocyanate. Only the continuous phase can be nucleated in mixing the A- and B-components. The novel surfactants can be considered as A-B block-copolymers with one polyol- and one isocyanate-compatible part. Such copolymers are effective in reducing the interfacial tension between the two incompatible phases. Compatibilization as brought about by the surfactants increases the effective volume for nucleation and leads to the formation of more nuclei, resulting in finer cells.

Table 16. Influence of different surfactants on cell size.

Surfactant	$c_{surfactant}$ **[pph]**[a]	$n_{surfactant}$**/80 g [mol/80 g]**	***N*** **[cells/cm²]**[b]
Blank sample	0	0	94±3
S2 (hexyl acr.)	2.00	$2.03 \cdot 10^{-3}$	156±12
S5 (2-ethylhexyl acr.)	2.09	$2.05 \cdot 10^{-3}$	163±14
S6 (4-*tert*-butylcyclohexyl acr.)	2.08	$2.00 \cdot 10^{-3}$	195±26
S7 (phenoxyethyl acr.)	2.11	$2.05 \cdot 10^{-3}$	166±1
S8 (methacryloyloxyethyl acr.)	2.11	$2.05 \cdot 10^{-3}$	142±8
Niax Silicon L-6900	2.00	unknown	648±3

[a] Parts per hundred A-component. [b] Error as mean deviation of two foams of the same composition.

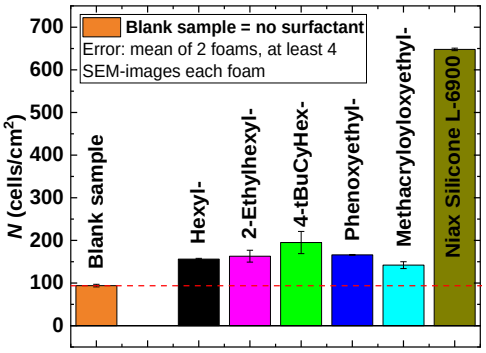

Figure 57. Influence of different surfactants on *N*.

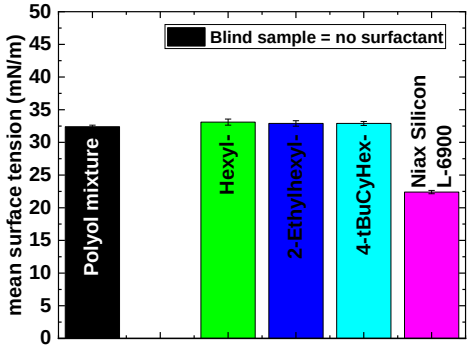

Figure 58. Influence of different surfactants on mean surface tension of the polyol mixture.

5.2.5 Application as emulsifier in emulsion polymerization

The novel class of surfactants from urethane and acrylate showed surface activity in aqueous solutions. These surfactants could potentially be of use in emulsion polymerizations. Surfactant **S5** was used as emulsifier in an emulsion copolymerization of *n*-butyl acrylate and 2-ethylhexyl acrylate to study their applicability.

A 20 wt% monomer emulsion was prepared from 24.0 g 2-ethylhexyl acrylate (c = 0.415 mol/L, 1 eq.), 56.0 g *n*-butyl acrylate (c = 1.39 mol/L, 3.4 eq.) and 2-ethylhexyl acrylate-based *aza*-Michael surfactant **S5** in 312 g of demineralized water at 30 °C under a nitrogen atmosphere. The concentration of **S5** was applied at 11.6 to 23.1, 34.7 and 46.3 mmol/L. The employed concentrations were above the CMC of **S5** (406 µmol/L). The polymerization was carried out in a glass reactor using a 6-blade agitator (blade angle 45 °) at 400 rpm. The polyreaction was initiated after homogenization for 30 min. A red-ox initiator system was used from ascorbic acid (c = 15.1 mmol/L), iron(II)-sulfate (c = 0.285 mmol/L) and *t*-butyl hydroperoxide (c = 21.6 mmol/L, Chapter 6.3.5). It allows the initiation at temperatures close to room temperature. The temperature profiles were constantly monitored for the different surfactant concentrations (Figure 59).

The emulsion turned from colorless to cloudy-opaque during the polymerization.[157] The temperature increased after initiation (t = 0, T_{start} = 30 °C) until a maximum (T_{max}) was reached. Then, T started to decrease and approached T_{start} after a given amount of time. T_{max} was higher at higher surfactant concentration (Table 17). The time required to reach T_{start} after the maximum ($t_{T=start}$) was significantly shorter for higher surfactant concentrations. Conversions of almost 100 % were achieved (Table 17).

These observations may be explained by the SMITH-EWART-theory of emulsion polymerization. The number of latex particles, N_P, is proportional to the surfactant concentration ($N_p \propto c_s^{0.6}$).[140,158] Higher surfactant concentrations lead to a higher number of micelles in the emulsion and to a higher rate. More energy is released at higher surfactant concentrations in a shorter period of time leading to higher T_{max}. The high polymerization rate shortens the duration of the polymerization and $t_{T=start}$ is reached earlier. The amount of monomer available for each individual latex particle is less because more particles grow simultaneously. This results in a decrease in number

and volume weighted particle sizes with increasing surfactant concentration (Table 17, Figure 60).

In summary, the dependency of the surfactant concentration on the temperature profile and the particle size show that the novel surfactants can be utilized for emulsion polymerizations.

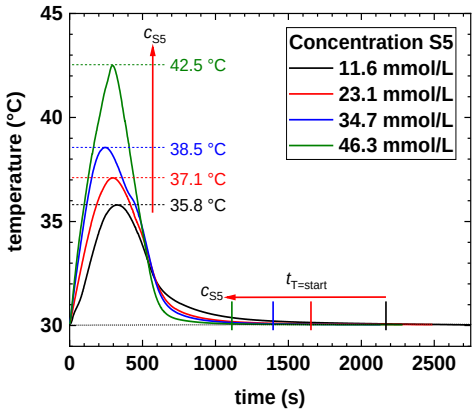

Figure 59. Temperature profile for emulsion copolymerizations at different **S5** concentrations.

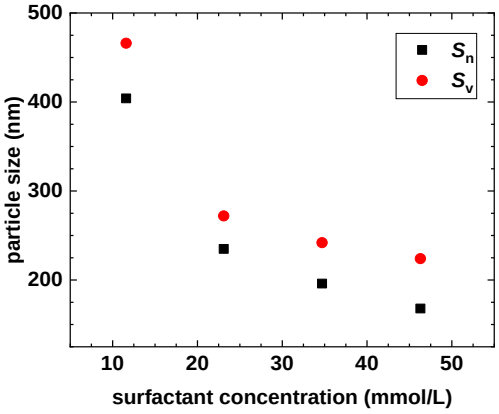

Figure 60. Number and volume weighted particle size s_n and s_v as a function of **S5**.

Table 17. Results from emulsion polymerizations employing **S5**.

c_{S5} [mmol/L]	T_{max} [°C]	$t_{T=start}$ [s]	s_n [nm]	s_v [nm]	X [%]
11.6	35.8	2158	404	466	97.4
23.1	37.1	1648	235	272	98.4
34.7	38.5	1388	196	242	99.9
46.3	42.5	1122	168	224	99.9

5.2.6 Conclusions on chapter 5.2

Non-ionic amphiphilic molecules can be obtained in bulk from urethanes and acrylates by the *aza*-Michael addition reaction. A general synthesis protocol was elaborated that provided adequate product yields (approx. 80 – 90 %). All water-soluble surfactants showed critical micelle concentrations in the range of about 300 to 900 µmol/L, cloud-points between 25 and 100 °C, and a strong surface tension reduction (approx. 31 – 45 mN/m at the critical micelle concentrations). The strongest reduction of the surface tension (31.0 mN/m at CMC) was found for a surfactant from methoxylated poly(ethylene glycol) (M_n = 364 g/mol), *para*-tolyl isocyanate and 2-ethylhexyl acrylate.

The surfactants were used in reducing the average cell size of PU rigid foams from 94±3 cells/cm^2 to 195±26 cells/cm^2 (with and without surfactant from 4-*tert*-butylcyclohexyl acrylate, respectively), but were found ineffective. This is related to the mediocre reduction of polyol surface tension by the novel compounds. A small advantage in compatibilizing A- and B-component was found.

The surfactant concentration was varied in the range of 11.6 to 46.3 mmol/L in the emulsion copolymerization of *n*-butyl acrylate and 2-ethylhexyl acrylate. The smallest latex particles were found for the highest surfactant concentration (number weight particle size of 168 nm at 46.3 mmol/L).

5.3 Application as novel crosslinking mechanism in polyurethane chemistry

The most critical part in preparing polyurethanes is the handling of isocyanate because they are toxic and sensitizing.[159] The reaction of isocyanates with proton acidic components is also highly exothermic. Strict handling procedures for isocyanates exist.[159,160] Polyurethane is therefore produced in specialized companies with adequate expertise and equipment to handle isocyanates. The preparation of a PU is best carried out in a controlled environment.[161–163]

Chemical crosslinking in polyurethanes is most easily realized by using polyols and isocyanates with a functionality $F_n > 2$ or by employing an excess of isocyanate. The excess isocyanate is used to form branched structures such as allophanate and isocyanurate.[4,9,164]

The handling of isocyanate can be circumvented by using thermoplastic polyurethane (TPU).[165] TPU is commercially available as solid granulate, which is safe to use. The customer melts the TPU in an extruder to produce polymer articles such as engineering parts, films or fibers.[166] TPU is not chemically crosslinked and hence products from it have a limited thermal form stability.[167,168]

Several methods to post-crosslink linear polyurethane have been developed to reach higher service temperatures. Crosslinks are obtained, for example, by using chain extenders containing thiol-functionalities (1,4-dithiothreitol) in the form of disulfide bridges after oxidation of the thiols.[169] Crosslinking is also achieved by reacting hydroxy-terminated TPU with polyfunctional isocyanates.[170] Acrylate-terminated star-shaped urethanes (e.g., Laromers®) can be cured by photoinitiation and crosslinked products are obtained.[171] PU chain-extended with hydrazine gives hydrazinyl-functionalities in the polymer backbone. Such a polymer can be crosslinked using a polyacrylate containing diacetone acrylamide through formation of hydrazone-groups.[172] Blocked isocyanates may also be used to post-crosslink PU.[173]

5.3.1 *Aza*-Michael addition-based PU/acrylate-crosslinking

Post-crosslinking of polyurethanes is thus of interest. The *aza*-Michael addition reaction of the carbamyl-N-H and acrylate was employed to crosslink polyurethanes. A literature search showed no matches for crosslinking of urethane using an *aza*-Michael addition reaction of the carbamate-N-H-functionality with acrylate. It is therefore conceivable that this approach has not yet been reported.

The preparation of *aza*-Michael post-crosslinked polyurethane elastomers should be at best similar to the established industrial processes for PU-thermosets. A homogenous mixture of all components has to be prepared first (e.g., polyurethane-precursor, acrylate-crosslinker, catalyst and inhibitor). High viscosity components such as the polyurethane precursor need preheating to reduce the viscosity prior to mixing with other components. The reaction mixture is then poured into a mold and cured at the selected reaction temperature. The reaction mixture should ideally not react at temperatures below the curing temperature. The parts can be demolded after solidification (Figure 61).

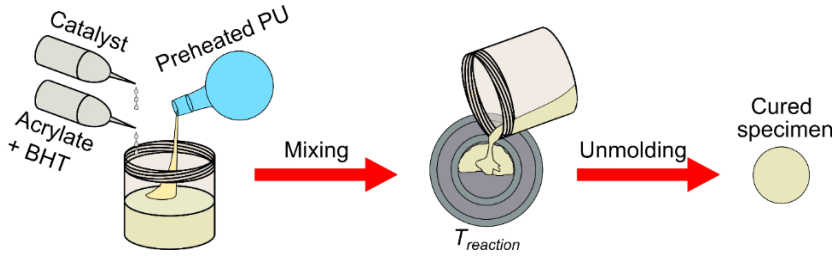

Figure 61. Preparation of *aza*-Michael addition crosslinked polyurethane.

A quantitative conversion could previously not be obtained for the reaction of urethane to the corresponding adduct at equimolar acrylate to N-H-ratios. A conversion of about 60 to 80 % could be achieved at best. At least one compound must therefore have a functionality of $F_n > 2$ to obtain a dense network (preferably $F_n >> 2$). The high functionality can be achieved through either the polyurethane, the acrylate or both. Numerous low-viscosity polyfunctional acrylates are commercially available that could be suitable as crosslinker (e.g., 1,6-hexanediol diacrylate (HDDA, $F_n = 2$), trimethylolpropane triacrylate (TMPTA, $F_n = 3$) and pentaerythritol tetraacrylate (PETA, $F_n = 4$)). The thermally induced radical homo-polymerization of acrylates as a potential side-reaction can be sufficiently suppressed by the addition of radical stabilizers such as BHT (Chapter 5.1.2). The *aza*-Michael crosslinking-reaction should furthermore be carried out at temperatures below the degradation temperature of polyurethanes ($T \approx 150$ °C) to prevent chain degradation.[174] Additional catalyst activation by using

poly(ethylene glycol) as catalyst complexing agent resulted previously in coupling reactions at temperatures well below the degradation temperature (Chapter 5.1.4).

5.3.2 Influence of polyol on *aza*-Michael crosslinking conditions of model substances

A polyurethane is in general accessible from a diisocyanate and polyol. PU products are thus attainable with a range of properties that derive from the choice of the components. Most variations of the motive are traditionally based on variation of the polyol structure. The relevance of the polyol structure in the polyurethane for the *aza*-Michael addition was mapped first. The catalyst for the *aza*-Michael addition was previously activated using methoxylated poly(ethylene glycol) as inherent complexing agent for a coupling reaction at reduced temperatures (Chapter 5.1.4 and Chapter 5.2.2).

Low molecular mass difunctional urethanes from pTMI and different difunctional polyalcohols were synthesized. The following polyether diols were selected: poly(ethylene glycol) (PEG600), poly(propylene glycol) (PPG450) and poly(tetrahydrofuran) (PTHF1400) (Figure 62, synthesis in Chapter 6.4.1). The corresponding urethane compound was then mixed with 2 eq. HexA, catalyst K Oct and 100 ppm BHT. The mixture was poured into a round bottom flask and stirred at temperatures between 120 and 160 °C for 5 h (in steps of 10 °C, Chapter 6.4.1.4). The catalyst concentration was doubled when no reaction occurred (Table 18). The degree of conversion was determined by analyzing ^{1}H-NMR spectra. The formation of by-products can adequately be derived from the ^{1}H-NMR signal of the methylene-group in alpha-position to the former acrylic carbonyl group ($\delta \approx 2.60 – 2.50$ ppm, Table 19).

The PEG- and PPG-based urethanes were readily converted to *aza*-Michael adducts at $T = 120$ °C using 0.027 eq. K Oct. No reaction was observed for PTHF-based urethane at this catalyst concentration and temperatures between 120 to 160 °C. An *aza*-Michael adduct from pTHF-urethane was only present when the catalyst concentration was increased to 0.055 eq. at $T \geq 150$ °C. The number of by-products increased with increasing temperature for all polyols as observed in ^{1}H NMR spectra.

The PEG-urethane containing formulations showed high reactivity at comparatively low temperatures. This may possibly be related to their complexation to the cation of the catalyst ($X_{120\,°C} \approx 64$ %).[103,104,175] The PPG450-urethane showed a conversion of

approx. 41 % at the same temperature (approx. 57 % at 130 °C). PPG is therefore also able to activate the carboxylate catalyst in the *aza*-Michael reaction.[176] The methyl substituent next to the ether oxygen might hinder the interaction with the cation. No activation was observed for PTHF-urethanes ($X_{PTHF(160\ °C)} \approx 50$ %).

It was concluded that the urethane precursor for the present *aza*-Michael addition crosslinking systems should be based on urethanes of PEG- or PPG-type. Coupling reactions can then be performed at low temperatures and, consequently, with a low rate of by-product formation.

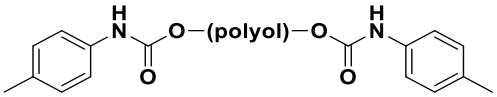

Figure 62. Structure of model compounds used in this study.

Table 18. Model *aza*-Michael reactions with hexyl acrylate.

Polyol-component	***T* [°C]**	**$c_{catalyst}$ [eq.]**	***X* [%]**
PEG600	120	0.027	64
	130	0.027	64 [a]
	140 – 160	0.027	not determined [b]
PPG450	120	0.027	41
	130	0.027	57
	140 – 160	0.027	not determined [b]
PTHF1400	120 – 160	0.027	no reaction
	120	0.055	3 [a]
	130	0.055	4 [a]
	140	0.055	10 [a]
	150	0.055	34 [a]
	160	0.055	50 [a]

[a] Approximations because of overlaying signals in ^{1}H-NMR spectra.
[b] Not determinable by multiple overlaying signals in ^{1}H-NMR spectra.

Table 19. ^{1}H-NMR-area of methylene-group in alpha-position to the former acrylic carbonyl group (selected experiments from Table 18, acetone-d_6).

T [°C]	PEG600 0.027 eq. K Oct	PPG450 0.027 eq. K Oct	PTHF1400 0.055 eq. K Oct
160 °C	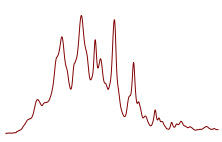	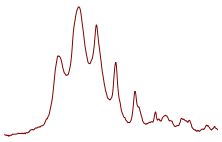	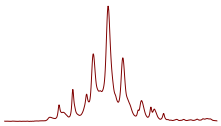
150 °C	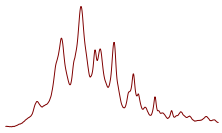	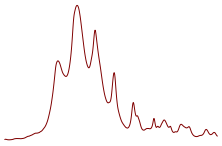	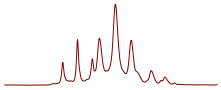
140 °C	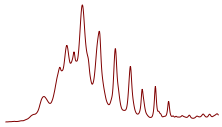	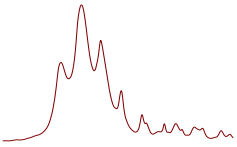	
130 °C	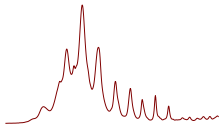	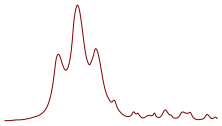	
120 °C	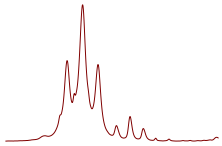	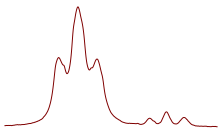	
	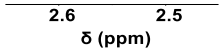	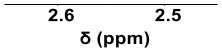	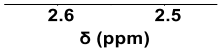

5.3.3 Polymer-forming *aza*-Michael addition reactions

A stepwise approach was used to validate the polymer forming reaction of polyurethane and polyfunctional acrylate. The complexity of the studied systems was gradually increased. At first, various short diurethanes were synthesized and converted to the corresponding *aza*-Michael adducts using mono-functional acrylate. The conversion and structure of the still soluble oligo-adducts were analyzed using ^{1}H-NMR spectroscopy. Secondly, an addition polymerization reaction was studied using bi-functional acrylates and IR spectroscopy (Chapter 6.4.1).

A difunctional, urethane-capped compound of medium-viscosity was synthesized from poly(ethylene glycol) ($M_n \approx 600$ g/mol, PEG600) and pTMI (Figure 63 (left) and Figure 64 (top)). The obtained product was of high purity and had a number average molar mass of $M_n \approx 886$ g/mol. The *aza*-Michael addition reaction was subsequently inflicted using two equivalents of mono-functional HexA, 100 ppm BHT and 0.03 eq. K Oct. The solvent-free mixture was stirred at 120 °C for 5 h and analyzed using ^{1}H-NMR spectroscopy (Figure 64 (bottom)). Approx. 64 % of all the urethane groups were converted to the corresponding adduct (Figure 63 (right)). Unreacted acrylate (e.g., at $\delta = 6.4 – 6.0$ ppm) and some minor amounts of by-products (e.g., at $\delta = 7.7$ ppm) were detected as well. The by-products may have originated from transesterification-reactions as previously discussed (Chapter 5.1.2). The formation of polyacrylate was inhibited by the addition of the radical inhibitor BHT.

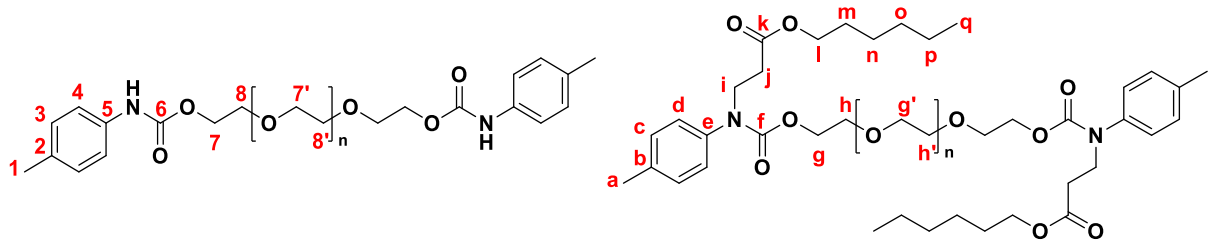

Figure 63. (left) pTMI/PEG600-based diurethane and (right) targeted model adduct.

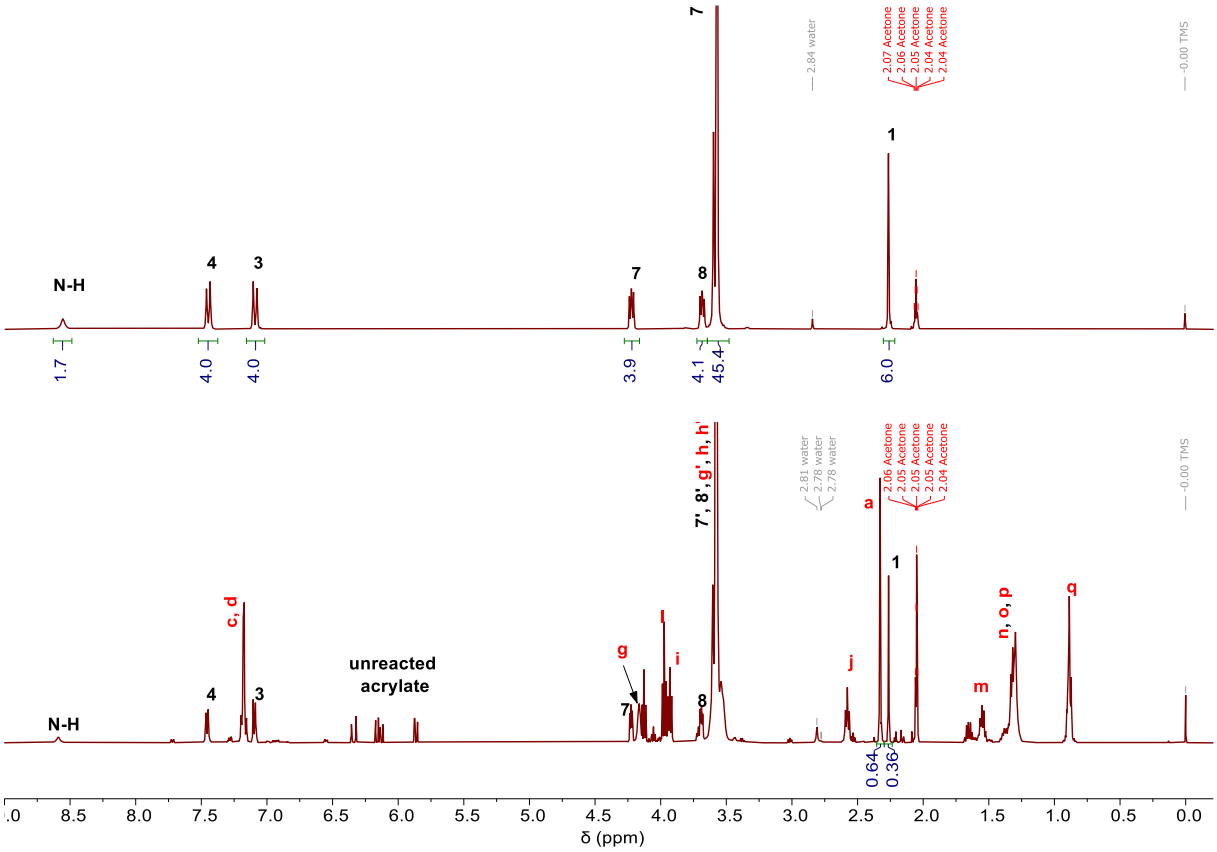

Figure 64. ^{1}H-NMR spectrum of (top) pTMI/PEG600-based diurethane and (bottom) raw-spectrum of the reaction to the model adduct at 120 °C (acetone-d_6).

PU1 and **PU2** – oligo-urethanes containing mor than two urethane groups – were prepared by reacting PEG600 with mono-functional pTMI and di-functional 4,4'-MDI at different molar ratios (Table 20 and Figure 66; Chapter 6.4.2). The number of repeating units *m* required for the calculation of M_n was also determined from ^{1}H-NMR spectra.

Table 20. Molar composition of PU-oligomers **PU1** and **PU2**.

#	*eq.* (PEG600)	*eq.* (pTMI)	*eq.* (4,4'-MDI)	*m**	M_n [g/mol]*
PU1	2	2	1	1	1781
PU2	3	2	2	2	2738

*Calculation of *m* and M_n based on ^{1}H-NMR data (Chapter 6.4.2).

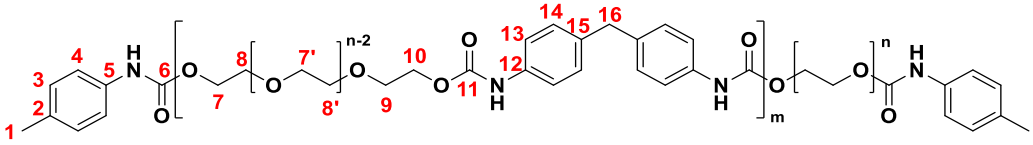

Figure 65. Oligo-urethanes **PU1** and **PU2** from pTMI, 4,4'-MDI- and PEG600.

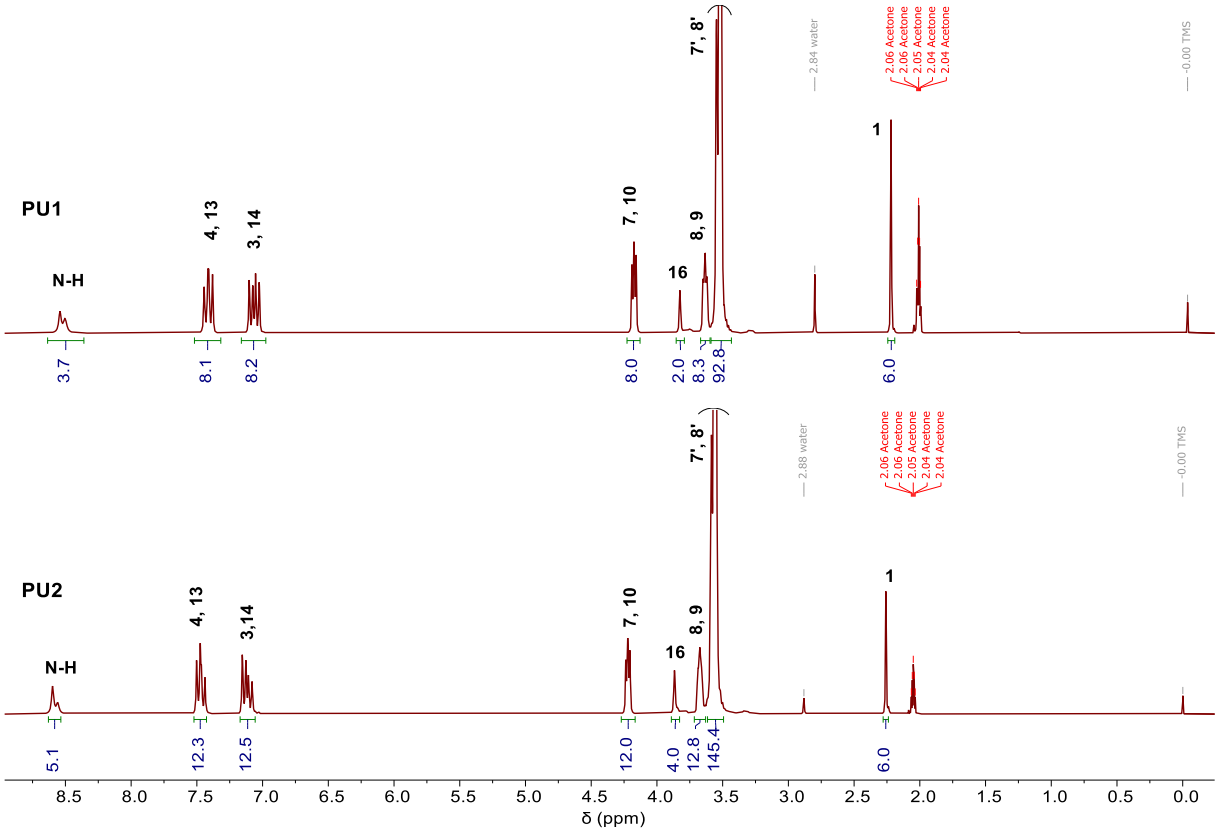

Figure 66. ^{1}H-NMR spectra of pTMI, 4,4'-MDI- and PEG600-based oligo-urethanes **PU1** (top) and **PU2** (bottom).

Four equivalents of HexA, 100 ppm BHT and 0.03 eq. K Oct were added to 1 eq. of **PU1** (*n*(NH)/*n*(acrylate) ≈ 1). The reaction mixture was homogenized at 80 °C and stirred at 120 °C for 5 h to yield the targeted *aza*-Michael product (Figure 67). The conversion *X* of the pTMI- and 4,4'-MDI-based urethane-NH-functionalities was calculated from ^{1}H-NMR spectroscopic data (Table 21 and Figure 68; Chapter 6.4.2).

Table 21. Conversion of pTMI- or MDI-based urethane to the corresponding *aza*-Michael adduct.

$X_{\text{pTMI adduct}}$	$X_{\text{MDI mono adduct}}$	$X_{\text{MDI bi adduct}}$	X_{total}
55 %	55 %	25 %	54 %

Approx. 54 % of both the pTMI and MDI-based urethane groups were converted to the corresponding *aza*-Michael adducts. This was about 10 % less than that obtained previously for the bis-functional urethane compounds. No polyacrylate was formed in this reaction.

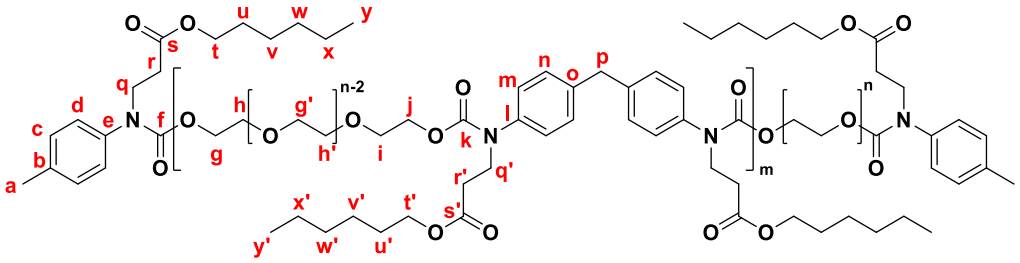

Figure 67. Model adduct from **PU1** and hexyl acrylate.

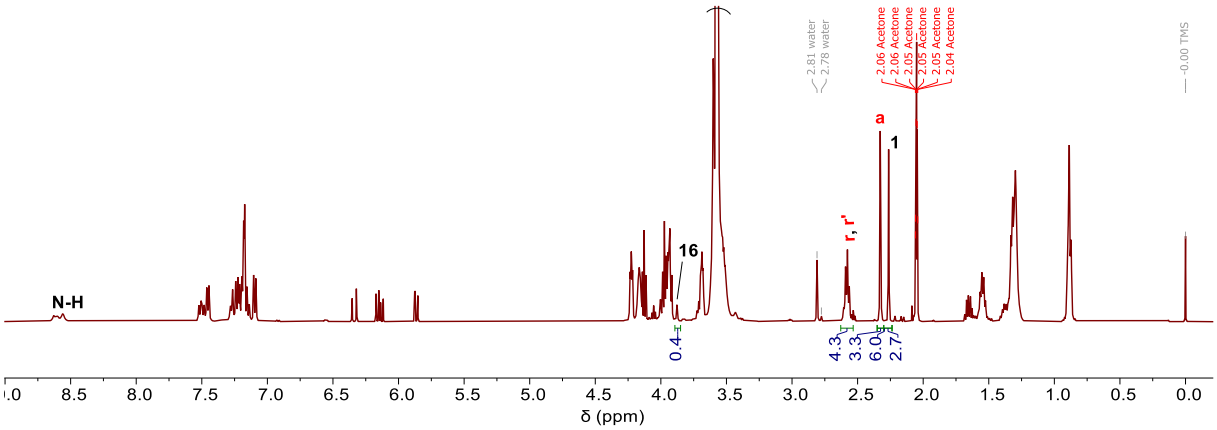

Figure 68. ^{1}H-NMR spectrum of **PU1-**hexyl acrylate-based model adduct (acetone-d_6).

Bifunctional HDDA allows the preparation of crosslinked model-products. Three equivalents of HDDA, 100 ppm BHT and 0.08 eq. K Oct were subsequently added to 1 eq. of **PU2** (*n*(NH)/*n*(acrylate) ≈ 1). The reaction mixture was homogenized at 80 °C and cured in an oven in molds at 120 °C for 9 h (M2-type, Figure 73). It was sampled hourly for the first 7 h and then again after 9 h. The samples were analyzed by IR spectroscopy (*v*(C=O) Figure 69; *v*(N-H) Figure 70). The IR spectra were normalized to the peak area assigned to C-H vibrations from 3000 to 2760 cm^{-1}.

The urethane carbonyl peak at $v \approx 1721$ cm^{-1} decreased during reaction while a new peak arose at $v \approx 1702$ cm^{-1} (red arrows). The N-H vibration at $v \approx 3305$ cm^{-1} (red arrow) was reduced to approximately 30 % of its original height in the process. The spectral changes were ascribed to the *aza*-Michael addition reaction of the carbamoyl N-H to the acrylate-double bond. The formation of a weak signal at $v \approx 3320$ cm^{-1} (blue arrow) was attributed to the slow thermal decomposition of urethane. This degradation can lead to the formation of amines.[177] The absorbance of the IR peak at $v \approx 3305$ cm^{-1} followed a sigmoidal decay curve running into a plateau value (Figure 71). The data cannot be evaluated quantitatively but a clear correlation was observed between the reaction progress and the solidification of the sample. The reaction rate decreased after solidification. The point of solidification was defined as

the moment at which the surface of the castings became dry to the touch (tack-free time). A complete conversion of all the carbamoyl-N-H groups was not achieved. This is indicated by the presence of residual N-H-absorptions (Figure 70).

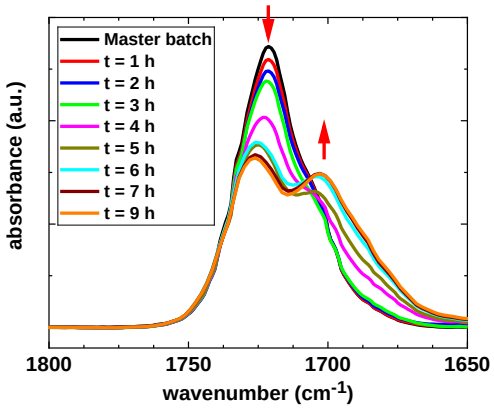

Figure 69. IR analysis: Magnification of *v*(C=O).

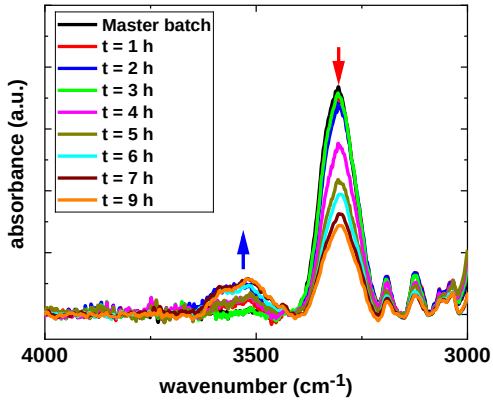

Figure 70. IR analysis: Magnification of *v*(N-H).

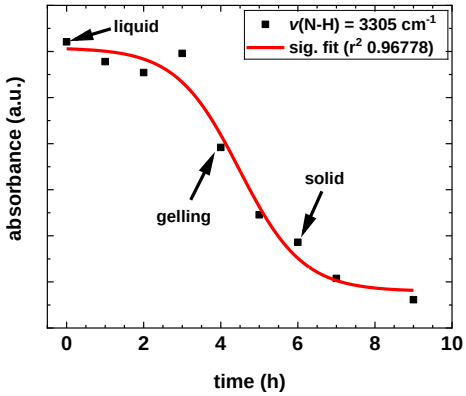

Figure 71. Absorbance of IR peak at $\nu \approx 3305$ cm^{-1} vs. time.

The observed changes in IR spectra and their correlation with the *aza*-Michael addition reaction were further studied. A model urethane based on pTMI and methoxylated poly(ethylene glycol) ($M_n \approx 516$ g/mol) was used in reaction with 2,4-dimethyl-3-pentyl acrylate. The purified reaction product was identified as the *aza*-Michael adduct (Chapter 6.3.1.4). The carbonyl and amine regions in the IR spectrum (Figure 72) of the adduct (red) were compared to that of an equimolar physical mixture of the employed starting materials urethane and acrylate (black).

It was found that the urethane carbonyl peak at $\nu \approx 1721$ cm^{-1} decreased whereas a new peak at $\nu \approx 1702$ cm^{-1} emerged and the amine-signal from $\nu = 3720$ to 3160 cm^{-1} had disappeared. The obtained results support that the oligomeric urethane had reacted with the di-acrylate by means of the *aza*-Michael addition reaction.

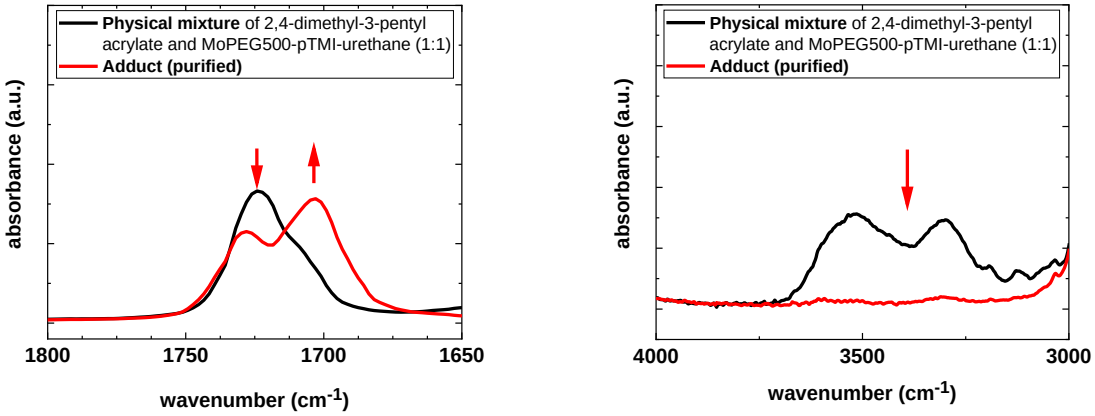

Figure 72. (left) *v*(C=O) and (right) *v*(N-H) region of low-molar mass adduct (red line: purified adduct, black line: physical mixture).

5.3.4 Experimental design of *aza*-Michael polyaddition reactions

Two different types of molds were used (M1 and M2, Figure 73). Mold M1 allowed the fast screening of various reaction mixtures and conditions (diameter = 40 mm, thickness = 2 mm). Mold M2 was used for the preparation of test specimens for the employed testing methods (thickness = 2 mm; e.g., SHA, DMA, S2-tensile bars (DIN 53504), swelling, …).

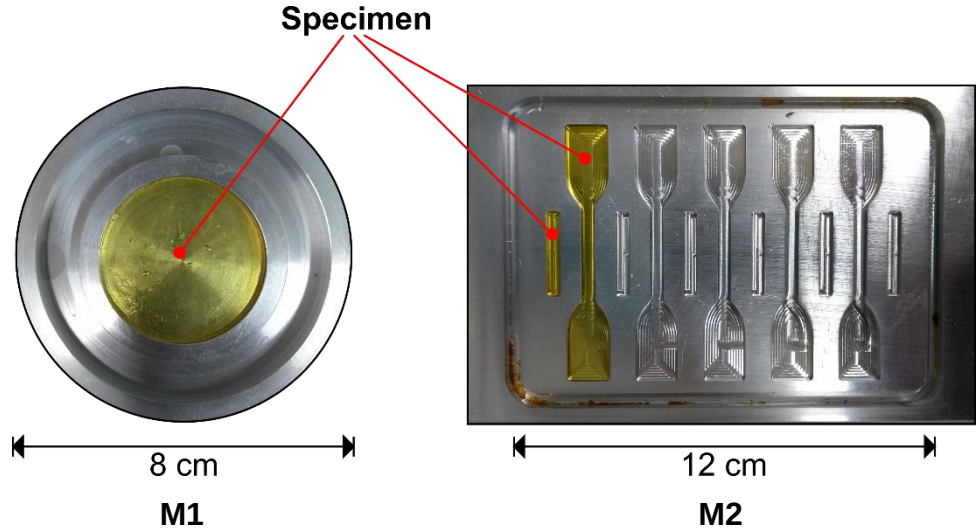

Figure 73. Molds used for sample preparation.

The crosslink reactions were at first catalyzed by K Ac. The mixtures were homogenized, poured into a mold (M1) and cured on a heating plate at T = 160 – 170 °C for 4 h. The employed catalyst did not give substantial conversions at lower temperatures. A greyish-to-white vapor was emitted during the curing process, and strong bubble-formation occurred (Figure 74, 1st step). The bubble formation was only slightly reduced when degassing the reaction mixture prior to use. Solidification always occurred from the edge to the center and resulted in a patterned surface (Figure 75).[90]

1st step
- Blistering
- Patterned surface
- Vapor emission

2nd step
- Blistering but smooth surface
- Vapor emission

3rd step
- No blistering and smooth surface
- No vapor emission

Figure 74. Effects of process improvements.

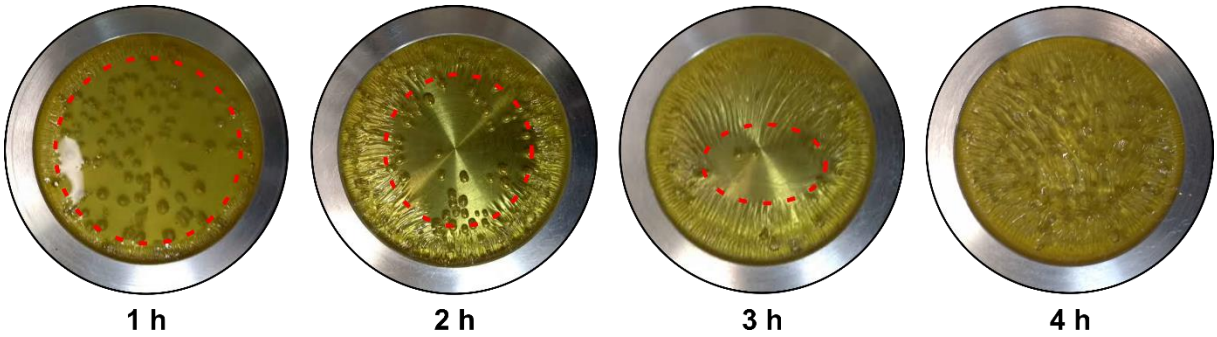

Figure 75. Inhomogeneous solidification of specimens.

A glass lid was used in the next step to cover the mold completely. Samples with a smooth surface were obtained, exemplary, for a system from polyurethane (PPG450 and 2,4'-/4,4'-MDI (n/n: 50/50)), PETA (F_n = 4), BHT and K Ac after curing at 170 °C (Figure 74, 2nd step). The use of the lid also led to a significant reduction in the cure time (e.g., 1 h instead of 4 h).[90] Both observations were ascribed to a more homogeneous temperature distribution across the sample. Condensate on the inner side of the glass lid was identified by ^{1}H-NMR spectroscopy as majorly acrylate with traces of PPG-chains (Figure 76). The weight loss caused by evaporation of reactants typically amounted to $m(\text{loss})_{\text{total}} \approx 1 - 2$ wt% or expressed in acrylate $\Delta m(\text{loss})_{\text{acrylate}} \approx 6 - 11$ wt%. The number average molar mass as determined by ^{1}H-NMR spectroscopy of the neat PPG450 starting material and the condensed PPG amounted to $M_n \approx 443$ and $M_n \approx 330$ g/mol, respectively. The unzipping of the urethane bond commences at temperatures of about 150 °C.[167] The PPG oligomers in the condensate are therefore attributed to urethane degradation. The reduction in M_n is ascribed to the lower vapor pressure of the higher MW polypropylene glycol chains; the low MW fragments evaporate, whereas the high MW fragments stay behind in the resin. Free NCO was not observed by ^{1}H-NMR spectroscopy, which is the complementary primary product of the polyurethane unzipping reaction.

The polymer preparation method was further improved by applying K Oct as catalyst and covering the mold with a metal lid, before placing it in an oven to cure (Chapter 6.4.4, Figure 74, 3rd step). K Oct allowed reactions at curing temperatures well below 160 °C.

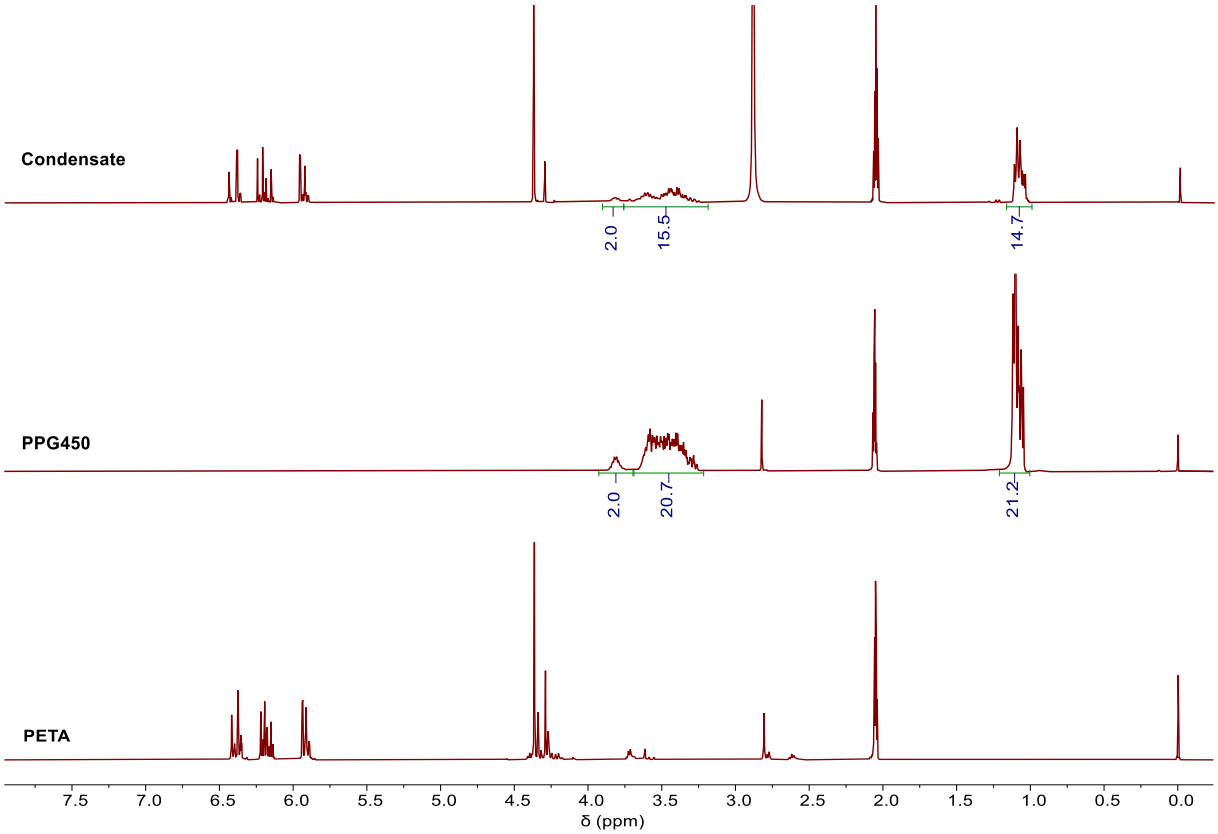

Figure 76. ^{1}H-NMR spectra of (top) the condensate, (middle) PPG450 and (bottom) PETA (acetone-d_6).

5.3.5 Properties of *aza*-Michael cross-linked polyurethane

5.3.5.1 Influence of crosslinker functionality

The properties of an *aza*-Michael addition crosslinked polyurethane system were analyzed as a function of the crosslinker functionality. A polyurethane from 2 eq. PEG600, 1.5 eq. MDI and 1 eq. pTMI was subsequently mixed with HDDA (F_n = 2), TMPTA (F_n = 3) or PETA (F_n = 4). BHT and K Oct were used as additive, respectively, as catalyst. The number of added acrylate groups was always equivalent to the number of urethane groups in the polyurethane. The viscosity of the reaction mixture increased with increasing F_n of the acrylate. The reaction mixtures were cured at 120 °C for 5, 21 or 23 h (HDDA, TMPTA or PETA, respectively).

The elongation at break, ε_b, was lower and the stress at break, σ_b, higher for crosslinker with a higher functionality. The Young's modulus and the shore hardness increased at the same time (Figure 77; Table 22).

These observations are attributed to a higher crosslinking density with increasing F_n of the acrylate. This is commonly observed for natural rubbers with different crosslinking densities.[178,179] It is important to recall that the conversion of the *aza*-Michael addition reaction is not complete and ranges from 60 to 80 % (e.g., Chapter 5.1.3). The material would contain some amount of sol next to crosslinks and dangling chain ends. The probability of crosslink formation would be higher with an increasing functionality of the acrylate.

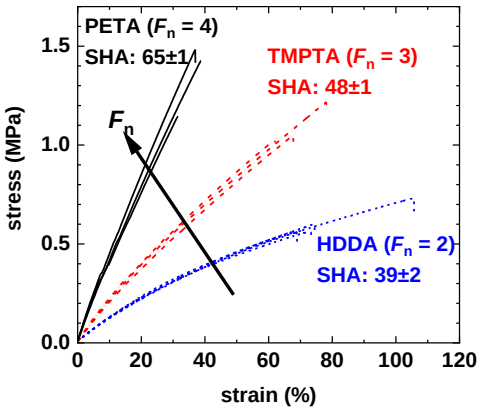

Figure 77. Influence of the crosslinker functionality on tensile properties and hardness.

Table 22: Mechanical properties.

Acrylate	F_n	ε_b [%]	σ_b [MPa]	SHA [a. u.]
HDDA	2	78±11	0.60±0.05	39±2
TMPTA	3	69±6	1.09±0.08	48±1
PETA	4	36±3	1.35±0.14	65±1

The sol content, *S*, gel content, *G*, and volume related degree of swelling, Q_v, were determined by equilibrium swelling measurements in petroleum ether (PE), toluene, tetrahydrofuran (THF), acetone, iso-propanol (*i*-PrOH), ethanol (EtOH), methanol (MeOH) and water (Chapter 6.1.9; Equation 7 to Equation 9; Table 34). The sol content is lower with higher functionality of the acrylate crosslinker and the gel content increased (Table 23, Figure 78), as expected. This was observed for all the organic solvents. The highest sol contents, S_{max}, and hence the lowest gel contents were obtained when using MeOH as a solvent. The results show that the crosslink density is higher with increasing functionality of the acrylate.

The results from the swelling experiments in methanol provide further evidence that the crosslink density increases with increasing functionality of the acrylate. Non-crosslinked/slightly branched urethane chains and unreacted polyfunctional acrylate can be extracted using a good solvent like methanol and analyzed using ^{1}H-NMR spectroscopy. The highest amount of *aza*-Michael adduct-related signals (e.g., at 2.56 – 2.62 ppm) was found for samples crosslinked with the two-functional HDDA (Figure 79; blue curve). Nearly none was found for the four-functional PETA (black curve).

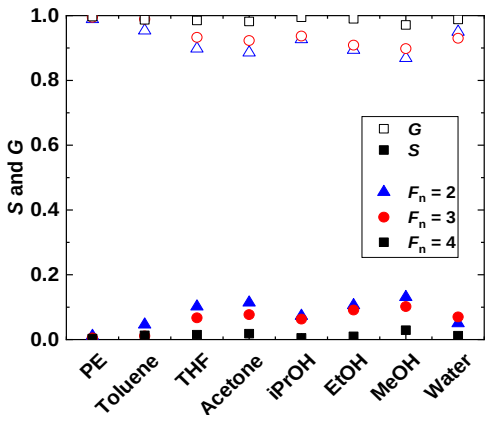

Figure 78. Equilibrium swelling experiments in various solvents.

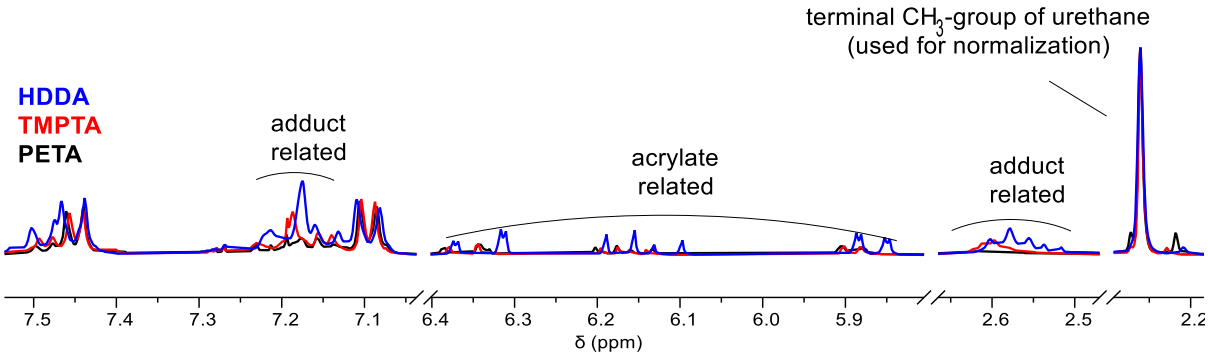

Figure 79. ^{1}H-NMR spectra of sol fractions from different crosslinkers (acetone-d_6).

The highest degree of swelling, $Q_{v,max}$, (Table 23, Figure 80) was obtained if THF (δ_s = 18.6 MPa$^{0.5}$) was used as a solvent. The highest swelling values were obtained for the HDDA-crosslinked samples, followed by samples from TMPTA- and PETA-crosslinking. A second swelling maximum was found for MeOH (Table 23). The bimodal swelling behavior is explained as follows: The polymer/solvent interaction is described by the Flory-Huggins interaction parameter χ. It is calculated from the solvent and polymer solubility parameter δ_s and δ_p (Equation 4, with temperature T, universal gas constant R and the solvent molar volume V_s).[180]

$$\chi \approx 0.34 + \frac{V_s}{R \cdot T} \left(\delta_p - \delta_s\right)^2 \qquad \text{Equation 4}$$

χ needs to be smaller than 0.5 for solvent-polymer miscibility. Swelling of a polymer then occurs when the difference between the two solubility parameters is small. This means that the chemical structures of the polymer chain and the solvent should be alike.[180,181] The urethane of this study was based on 2 eq. PEG600 (M_n ≈600 g/mol), 1.5 eq. MDI (M = 250.26 g/mol) and 1 eq. pTMI (M = 133.15 g/mol). The polymer backbone mainly consists, by mass, of PEG and ether solvents should be good swelling agents. The second maximum at high δ_s is related to the presence of the urethane groups in the polymer. These can be solvated when more polar solvents like alcohols are used. The decrease in physical crosslinking allows higher swelling ratios. The Q_v is also dependent on the level of polymer crosslinking. High crosslinking reduces the swelling.[182–184] The lowest degree of crosslinking is therefore obtained for the HDDA and highest for the PETA-samples.

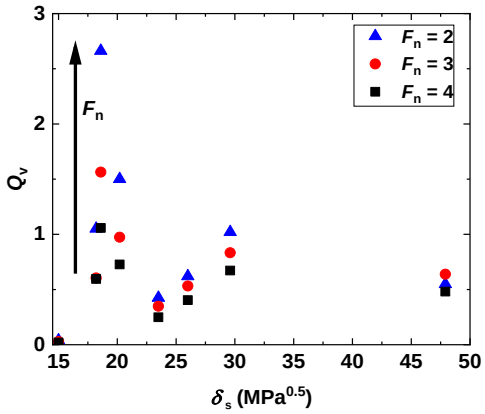

Figure 80. Degree of swelling as a function of the solvent solubility parameters.

Table 23: Swelling properties.

Acrylate	F_n	S_{max} [%]	$Q_{v,max}$ [-]	$Q_{v,2nd\ max}$ [-]
HDDA	2	13.1	2.66	1.02
TMPTA	3	10.2	1.56	0.83
PETA	4	2.9	1.06	0.67

The molar mass between crosslinks M_c was determined using the FLORY and REHNER equation. It is based on thermodynamic considerations to describe the swelling behavior of a polymer in a solvent.[181,184,185] A more detailed discussion on the FLORY-REHNER swelling theory and the underlying calculations and assumptions can be found in the appendix (Chapter 6.1.10).

The M_c was the lowest for PETA (M_c = 622 g/mol), medium for TMPTA (M_c = 960 g/mol) and highest for HDDA (M_c = 2200 g/mol). These experimental values are close to calculated M_c numbers from the molecular structure (Figure 81).

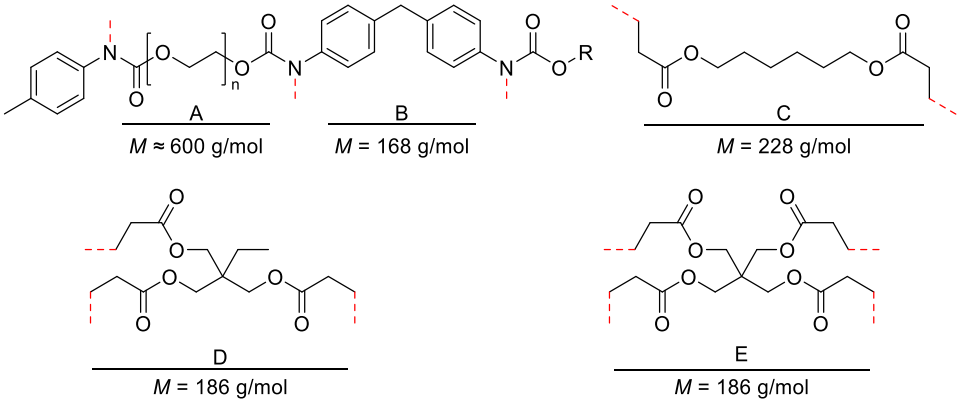

Figure 81. Theoretically minimal distances between junction points in g/mol (A – E).

The degree of crosslinking and the presence of dangling side chain ends affects the polymer chain mobility and polymer stiffness.[186–189] The storage modulus G', loss

modulus $G^{''}$ and dissipation factor tan(δ) were determined as a function of the temperature for the three model polymers of this study using DMA (Figure 82). All specimens show a sharp glass-transition and broad rubber-elastic plateau which is typical for crosslinked elastomers.[181,190] The maximum of tan(δ) shifts to higher temperatures resulting from increasing chain stiffening with increasing crosslinker functionality (Table 24). *G*' of the rubber-elastic plateau shows the expected increase with increasing crosslinker functionality (e.g., at 25 °C; Table 24).[186,188,191,192] Dangling ends of side chains and an unbound sol in the polymer crosslinked by HDDA result in the β-transition at T_β = -57.7 °C (tan(δ) = 0.39).[189] The high thermal stability of the *aza*-Michael crosslink ($T \approx 230$ °C; Chapter 5.1.2) and dense crosslinking prevented polymers branched by PETA and TMPTA from early softening at elevated temperatures. This for thermosets typical behavior was different for the sample branched by HDDA.[193] It showed softening already at $T_{(HDDA)} \geq 140$ °C putatively because of a beginning aliphatic–aromatic urethane linkage degradation of the non-reacted urethane groups in the polymer backbone ($T \approx 150$ °C).[167] The DMA results support the equilibrium swelling results and provide further evidence that use of HDDA leads to dangling ends of side chains rather than the formation of crosslinks, as it is the case with TMPTA and PETA.

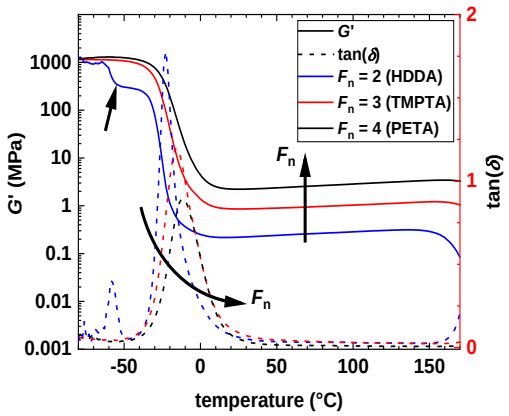

Figure 82. Influence of crosslinker functionality on DMA.

Table 24. DMA properties.

Acrylate	F_n	G' (25 °C) [MPa]	$T_{g,\alpha}$ [°C]	$T_{g,\beta}$ [°C]
HDDA	2	0.22	-22.6	-57.7
TMPTA	3	0.86	-15.8	-
PETA	4	2.22	-11.6	-

5.3.5.2 Influence of urethane precursor

The topology and molecular mass of the oligomers was changed in three steps by varying the ratio of PEG600 to 4,4'-MDI and pTMI (Table 25). Only the low and the medium molar mass polyurethanes were soluble in acetone-d_6. The M_n could therefore be determined analytically only from these two (M_n(low) ≈ 2738 g/mol, M_n(medium) ≈ 3792 g/mol). The M_n of the oligomers was also calculated using the Carothers equation (Equation 5). The reaction ratio, or *r*-parameter, was redefined (Equation 6) to take into account that the monofunctional isocyanate acts as a terminus (with the number of functional groups *N*).[194] The calculated M_n for the low (M_n ≈ 2896 g/mol) and medium molar mass PU (M_n ≈ 3629 g/mol) were in good agreement with the experimentally determined M_n. The M_n for the high molar mass oligomer was calculated to be 4692 g/mol. Polyurethanes of a higher molar mass could not be used in this study as their high viscosities did not allow the preparation of formulations using the synthesis protocol presented previously (Chapter 5.3.1).

$$P_n = \frac{1 + r}{1 + r - 2\,r\,X} \qquad \text{Equation 5}$$

$$r = \frac{N_{OH}}{N_{NCO(MDI)} + 2\,N_{NCO(pTMI)}} \qquad \text{Equation 6}$$

Table 25. Molar composition of precursors with low, medium and high molar mass.

Molar mass	*n*% (PEG600)	*n*% (4,4'-MDI)	*n*% (pTMI)	P_n*	M_n (NMR) [g/mol]	M_n (calc) [g/mol]
low	42.8	28.5	28.7	6.9	2738	2896
medium	44.1	33.8	22.1	8.5	3792	3629
high	45.5	36.3	18.2	11.0	-	4692

*Degree of polymerization P_n according to Equation 5 and Equation 6.[194]

Model polymers from HDDA showed the formation of side chains rather than network formation. A precursor with a comparatively small number of *aza*-Michael reactive urethane groups per chain is expected to give only a loosely crosslinked network with a high amount of sol. An increase in the number of urethane groups per chain in the polyurethane precursor can enhance network formation and should reduce sol. The properties of the cured polymers would become rather independent of the number of urethane groups per chain at some point.

The polyurethane precursors of different P_n were crosslinked employing HDDA. K Oct was added as catalyst and curing was carried out at 120 °C for 20 h. The number of acrylate-groups added was always equivalent to the number of urethane groups in the PU. Some BHT was added to suppress radical reactions (Chapter 6.4.4).

The elastomer from the PU with the lowest P_n showed a somewhat higher ε_b but lower σ_b, tensile modulus and hardness than elastomers prepared from the medium and high P_n. The tensile and hardness properties were about the same for medium and high (Figure 83; Table 26).

The poor mechanical properties of polymers prepared from the PU with the smallest P_n can be ascribed to the formation of mainly dangling side chains instead of network formation. An increase in P_n increased the crosslinking density which led to higher hardness and improved tensile strength.

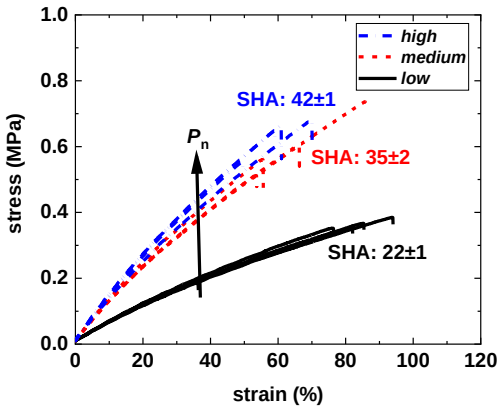

Figure 83. Influence of P_n of the PU-precursor on tensile properties and hardness.

Table 26: Mechanical properties.

Molar mass	P_n	ε_b [%]	σ_b [MPa]	SHA [a. u.]
low	6.9	72±18	0.32±0.07	22±1
medium	8.5	65±11	0.60±0.07	35±2
high	11.0	60±6	0.64±0.04	42±1

The sol content, S, gel content, G, and volume related degree of swelling, Q_v, were determined by equilibrium swelling measurements in petroleum ether (PE), toluene, tetrahydrofuran (THF), acetone, iso-propanol (*i*-PrOH), ethanol (EtOH), methanol (MeOH) and water (Chapter 6.1.9, Table 35). The polymer from the PU precursor with the lowest P_n contains the expected highest sol content in all solvents (Figure 84; Table 27). The sol contents for the products of P_n(medium) and (high) are similar and

somewhat lower. The highest sol content was obtained for P_n(low) in MeOH and for P_n(medium) and (high) in acetone. The strongest swelling was always observed in THF. The highest degree of swelling was found for the polymer from P_n(low) (Figure 85; Table 27). It was about the same for the samples from P_n(medium) and (high). The values of $Q_{v,max}$ were decreasing with increasing precursor length. The results for S_{max} and Q_v show that the crosslinking density increases significantly for the castings prepared from P_n(low) to (medium). A further improvement is not obtained by increasing the P_n of the polyurethanes. The residual sol of 14 % is ascribed to the presence of low molecular weight polyurethane oligomers which exist in all precursors.

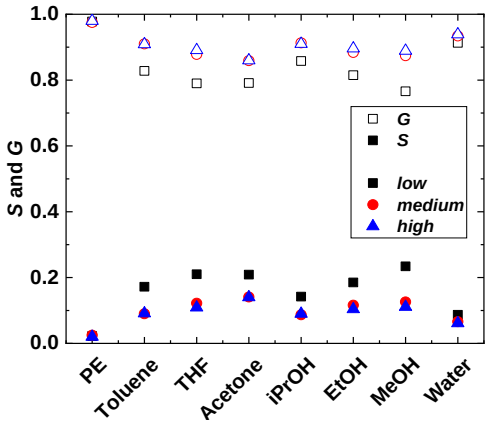

Figure 84. Equilibrium swelling experiments in various solvents.

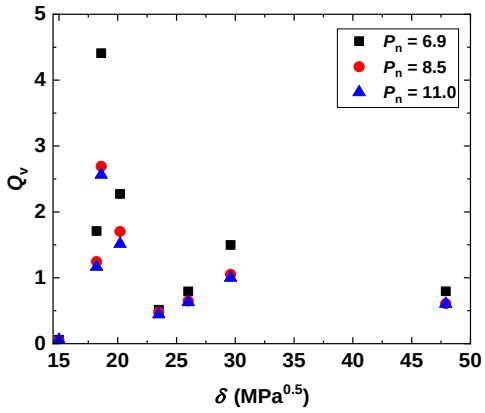

Figure 85. Degree of swelling as a function of the solvent solubility parameters.

Table 27. Swelling properties.

M_c	P_n	S_{max} [%]	$Q_{v,max}$ [-]
low	6.9	23.4	4.41
medium	8.5	14.1	2.69
high	11.0	14.0	2.56

Polyurethane oligomers were also prepared from MDI/pTMI mixtures and PEG600, PEG1500 or a hydroxy-terminated HDI-prepolymer (Table 28; Chapter 6.4.3). The HDI-prepolymer was based on equimolar amounts of PEG600, 1,6-hexanediol and HDI. The approximate number of reactive aromatic-aliphatic urethanes per chain in the *aza*-Michael addition remained a constant (aliphatic-aliphatic urethane groups are not undergoing *aza*-Michael reactions; Chapter 5.1.7). The three PU oligomers were crosslinked with equimolar amounts of PETA under the action of K Oct catalyst. Some BHT was added to suppress radical reactions. The viscosity of the urethane oligomers based on PEG1500 and the HDI-prepolymer was significantly higher than that of the

PEG600 based variant. The reaction temperature was therefore increased from 120 to 130 or 140 °C. The reaction time, however, was kept the same (20 – 24 h).

Table 28. Molar composition of the modified urethane precursors.

Polyol	mol% (polyol)	mol% (4,4'-MDI)	mol% (pTMI)	P_n^*
PEG600	44.1	33.8	22.1	8.5
PEG1500	44.2	33.1	22.6	8.7
HDI-prepolymer	44.4	33.3	22.2	8.9

*P_n was calculated for all castings according to Equation 5 and Equation 6.[194]

Improved extensibility and tensile strength were expected for *aza*-Michael crosslinked polyurethane elastomers made from the PEG1500 PU-precursor compared to products from the PEG600 PU-precursor with similar P_n because of the increased M_c and the potential of soft segment crystallization.[195–197] The incorporation of *aza*-Michael addition unreactive aliphatic-aliphatic urethane units should improve the tensile properties compared to products from PEG600. This is because of an increasing distance between the formed crosslinks and the remaining purely aliphatic urethane groups that can form reinforcing hydrogen bonds.

The sol content, S, gel content, G, and volume related degree of swelling, Q_v, were determined by equilibrium swelling measurements in petroleum ether (PE), toluene, tetrahydrofuran (THF), acetone, ethanol (EtOH), methanol (MeOH) and water as a measure for the conversion of the *aza*-Michael crosslinking reaction and the crosslinking density of the samples (Chapter 6.1.9, Table 36). The sol content was highest for samples from PEG1500 and lowest for samples from PEG600 (Table 29, Figure 86). The high compatibility of PEG with ethers and urethane with polar alcohols leads to a bimodal swelling behavior for all castings (Figure 87). The degree of swelling is always the highest in THF (Table 29). The strong swelling of the PEG1500-system is attributed to the high amount of sol and the relatively high molar mass of the PEG polyol. The low values of S and Q_v for the system containing PEG600 indicate the highest conversion and also highest level of crosslinking.

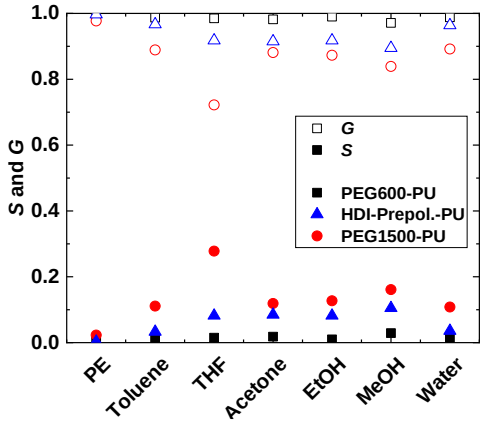

Figure 86. Equilibrium swelling experiments in various solvents.

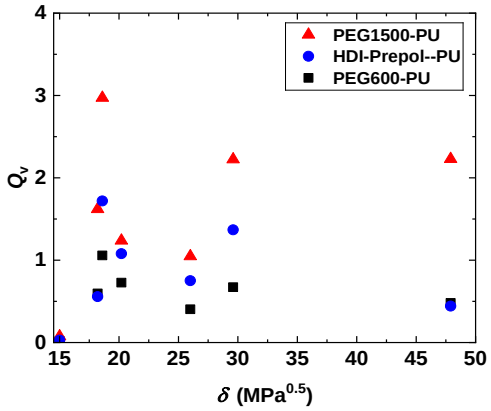

Figure 87. Degree of swelling as a function of the solvent solubility parameters.

Table 29. Swelling properties.

M_c	P_n	S_{max} [%]	$Q_{v,max}$ [-]
PEG600	8.5	2.9	1.06
PEG1500	8.7	28.8	2.97
HDI-prepolymer	8.9	10.5	1.72

Elastomeric properties at room temperature can be expected for all three elastomers with glass transition below about -20 °C (Table 30, Figure 88, DSC from -80 → 200 °C, ΔT = 10 K/min, Chapter 6.1.5). The highest T_g was found for the system with the smallest M_c (PEG600)[198] followed by the HDI-prepolymer-based system. The lowest T_g was found for the PEG1500-system.[12,198] The appearance of a cold-crystallization peak can often be observed for PEG-based polymers of a certain chain length (PEG1500, T_{cc}).[195–197] It is commonly explained by microphase separation.[198,199] Cold-crystallization is not observed for the PEG600-based system because a minimum chain length needs to be exceeded.[199] The observation of an exotherm at high temperatures, viz. T_{high}, cannot be explained by the melting of polyurethane hard phases as no chain extender was applied.[165,183,199] T_{high} might originate from exothermal polymerization processes of some free acrylate groups. Once reacted, no further energy can be liberated and, thus, T_{high} is absent in the 2nd heating run (Figure 89). The presence of free acrylate functionalities was already indicated by considerable sol contents in the castings.

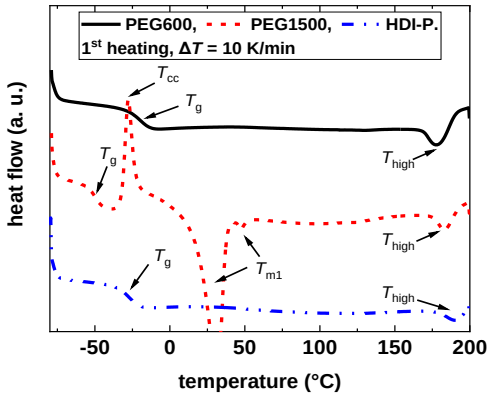

Figure 88. DSC curves (1st heating run).

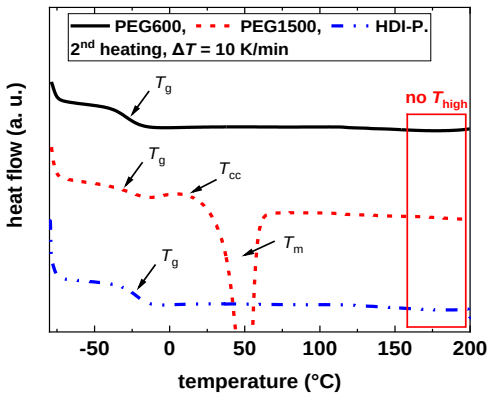

Figure 89. DSC curves (2nd heating run).

Table 30. Thermophysical properties of 1st. heating run.

Polyol	T_g [°C]	T_{cc} [°C]	ΔH_{cc} [J/g]	T_m [°C]	ΔH_m [J/g]	T_{high} [°C]	ΔH_{high} [J/g]
PEG600	-19.9	-	-	-	-	178	-14.8
PEG1500	-49.6	-27.7	31.7	30.44	-59.0	183	-7.1
HDI-prepolymer	-26.9	-	-	-	-	191	-6.2

The differences in the conversion of the *aza*-Michael crosslinking reaction and the increasing molecular weight between crosslinks, M_c, are reflected in the improved extensibility, ε_b, for both the PEG1500 and HDI modified elastomers if compared to the PEG600 based sample (Table 31; Figure 90). High M_c also reduces the polymer hardness (Table 31).[200] The lower conversion and higher M_c of the PEG1500 sample compared to PEG600 has also affected the tensile strength, σ_b, which decreases (Table 31). This was despite soft phase crystallization of the PEG1500-containing specimens (Figure 88). The HDI modified system combined high extensibility with comparatively high tensile strength despite an increase in M_c. This is ascribed to the reinforcing effect of hydrogen bonding chain interactions between the non-*aza*-Michael-active aliphatic-aliphatic urethane groups.

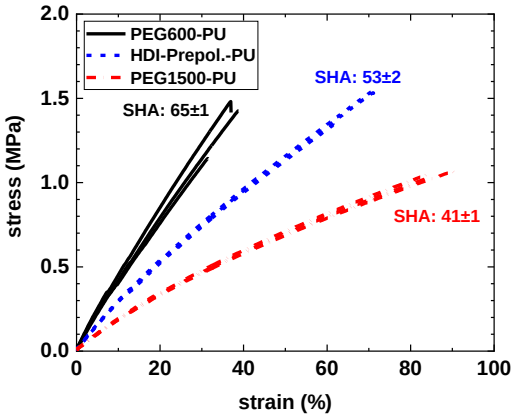

Figure 90. Tensile properties and hardness of castings from modified urethane precursors.

Table 31. Mechanical properties.

Polyol	σ_b [MPa]	ε_b [%]	SHA [a. u.]
PEG600	1.35±0.14	36±3	65±1
PEG1500	1.05±0.02	86±3	41±1
HDI-prepolymer	1.47±0.09	68±4	53±2

5.3.6 Conclusions on chapter 5.3

A protocol for the preparation of model polyurethane-acrylate hybrid-elastomers was established. The solvent-free *aza*-Michael addition reaction was used to crosslink linear polyurethane oligomers with polyfunctional acrylates. Elastomers based on the two-functional hexanediol diacrylate and PEG600/MDI/pTMI-polyurethane showed little crosslinking as determined from equilibrium swelling measurements. The sol content, *S*, had a maximum of 13.1 %. The increase of the acrylate functionality to pentaerythritol tetraacrylate led to a lower S_{max} of 2.9 %. The tensile strength and elongation at break were improved by substituting the PEG600/MDI/pTMI-polyurethane with partly non-*aza*-Michael reactive hexane diisocyanate containing polyurethane. The major drawback of the *aza*-Michael addition crosslinking technology was the incomplete conversion of the coupling reaction. Improved rates are required to further enhance the polymer properties.

6 Experimental part

6.1 Analytical procedure

6.1.1 Cloud point

The cloud point (CP) of all surfactants and surfactant mixtures was determined visually by using the melting point detector *M-565* (Büchi Labortechnik GmbH). A heating rate of 2 °C/min was applied. The temperature was noted at which turbidity was observed. It was sometimes challenging to determine the cloud point. The temperature was decreased in such cases and the heating rate reduced to 1 °C/min. The procedure was repeated as long as it took to reduce the possible error to approx. ±0.5 °C.

6.1.2 Column chromatography

All eluents were distilled at least once prior to use. As a stationary phase *silica gel 60* of a 0.04 – 0.063 mm mash size (Merck Millipore) was used. The progress of separation was monitored using thin layer chromatography-plates of *silica gel F254* (Merck Millipore)-type.

6.1.3 Critical micelle concentration (CMC) – drop volume tensiometry

CMC-measurements using drop volume tensiometry were thankfully conducted by BASF Polyurethanes GmbH (Lemförde) using an *Easy Drop* (Krüss)-tensiometer at 23 °C. It was assumed for the measurement that the density of the solutions (1.071 g/L) was not changed upon the addition of 2 pph of surfactant. Ten drops of each composition were analyzed using *Advance 1.8.0.4* (Krüss). The error is given as the standard deviation.

6.1.4 Critical micelle concentration (CMC) – Wilhelmy-Plate Method

The CMC of all surfactants and surfactant mixtures was determined by measuring the surface tension of an aqueous surfactant solution by a *Force Tensiometer – K100* (Krüss GmbH) using the *Krüss Laboratory Desktop* (Krüss GmbH) software if not stated otherwise. The surface tension in dependency of the surfactant concentration was measured in the reverse CMC mode using the Wilhelmy-Plate method (plate material: Pt). The Wilhelmy-Plate was cleaned before each measurement with acetone and heated until the plate glowed using a Bunsen burner. The surface tension of double distilled water was measured for calibration once a day prior to use.

An aqueous solution was prepared of each surfactant. 5 mL were transferred to an *SV23 Al/PTFE Conic Vessel* (Krüss GmbH) with a maximum volume of V = 165.794 mL. This solution was automatically diluted in 19 nonlinear steps (linear factor: 0.7, exponential factor: 0.085) using a *Dosimat 765* (Metrohm AG)-type dosing unit. The solution was homogenized after each dosing step for 10 s using a magnetic stirrer at half speed. That was followed by an equilibration time of 10 s. The surface tension of each concentration was then measured for 10 consecutive times. The last 5 data points were used to calculate the mean surface tension. The CMC was determined using the intersection of two regression lines of the concentration dependent and independent section (exemplarily shown for 1st run of **S5** in Figure 91). The equations of all linear fits to determine CMC and σ_{CMC} are shown in Table 32.

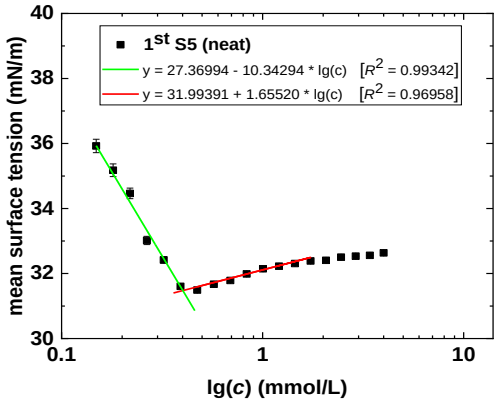

Figure 91. Exemplary determination of the critical micelle concentration (CMC) and surface tension at CMC (σ_{CMC}).

Table 32. Linear fit functions for CMC determination.

Surf. No.	y-Intercept	Slope	R^2	y-Intercept	Slope	R^2
Urethane (1st run)	56.53669	-10.8271	0.99928	44.25276	1.90448	1.0000
Urethane (2nd run)	56.66303	-10.29592	0.99946	44.48079	2.34398	1.00000
1 (1st run)	36.72929	-10.45220	0.99340	39.26871	-4-28995	0.99863
1 (2nd run)	36.91178	-10.52637	0.96298	39.42996	-4-77475	0.99415
2 (1st run)	30.66550	-13.04782	0.99139	34.13079	-1.91873	0.97945
2 (2nd run)	30.53964	-12.49781	0.93922	34.06781	-2.96014	0.98228
3 (1st run)	37.17295	-24.16494	0.98794	40.10106	-5.76488	0.98426
3 (2nd run)	37.89432	-21.12842	0.99229	39.62711	-5.53981	0.94807
4 (1st run)	25.18916	-18.53063	0.99509	33.5887	-2.76100	0.99309
4 (2nd run)	27.01148	-16.26341	0.95674	33.66272	-2.12612	0.98913
5 (1st run)	27.36994	-10.34294	0.99133	32.11248	1.60141	0.93581
5 (2nd run)	27.54089	-9.82645	0.99342	31.99391	1.65520	0.96958

6 (1st run)	27.26767	-11.55935	0.99341	33.59193	0.63877	0.97884
6 (2nd run)	28.15834	-10.22072	0.98474	33.58881	0.72487	0.98337
7 (1st run)	37.45646	-16.23831	0.99103	42.05271	-5.53392	0.98584
7 (2nd run)	37.95333	-15.58807	0.98693	41.82543	-5.27247	0.98160
8 (1st run)	38.49345	-14.74557	0.98484	43.21831	-5.04701	0.98285
8 (2nd run)	39.07661	-14.23135	0.99244	43.10634	-5.82544	0.99107
9 (1st run)	24.26179	-14.36051	0.97744	31.35437	1.12920	0.99415
9 (2nd run)	25.54848	-11.70576	0.95618	31.39092	0.92592	0.95213
10 (1st run)	30.52210	-6.73116	0.97232	33.99276	4.50306	0.99766
10 (2nd run)	30.02856	-6.43981	0.74866	33.83091	4.32025	0.99390
11 (1st run)	poor solubility in water			poor solubility in water		
11 (2nd run)	poor solubility in water			poor solubility in water		
12 (1st run)	poor solubility in water			poor solubility in water		
12 (2nd run)	poor solubility in water			poor solubility in water		
n(urethane)/ n(surf. 4)	**y-Intercept**	**Slope**	R^2	**y-Intercept**	**Slope**	R^2
1/0 (1st run)	56.53669	-10.8271	0.99928	44.25276	1.90448	1.00000
1/0 (2nd run)	56.66303	-10.29592	0.99946	44.48079	2.34398	1.00000
5/5 (1st run)	27.54089	-9.82645	0.99342	31.99391	1.65520	0.96958
5/5 (2nd run)	27.36994	-10.34294	0.99133	32.11248	1.60141	0.93581
2/8 (1st run)	28.49139	-10.67387	0.99405	31.95636	1.74906	0.98644
2/8 (2nd run)	28.09630	-11.06945	0.96661	32.09683	2.77757	0.98112
0/1 (1st run)	27.36994	-10.34294	0.99133	32.11248	1.60141	0.93581
0/1 (2nd run)	27.54089	-9.82645	0.99342	31.99391	1.65520	0.96958

6.1.5 Differential scanning calorimetry (DSC)

DSC-samples were weighed into an aluminum crucible (m = 12.9±0.9 mg) and analyzed using a *DSC 1* (Mettler Toledo)-type calorimeter according to following protocol: *RT* (ΔT = 20 °K/min) → -80 °C (ΔT = 10 °K/min) → 200 °C (ΔT = 10 °K/min) → -80 °C (ΔT = 10 °K/min)→ 200 °C, equilibrium time = 3 min. The thermograms were analyzed using *STARe* (Mettler Toledo). The glass transition temperature, T_g, was obtained as the half-height (midpoint) of the jump in the heat capacity.[195] Temperatures of crystallization- (T_c) or melt-processes (T_m) were taken as the peak maximum or minimum, respectively.[195]

6.1.6 Drying of solvents and components

All dried solvents were distilled at least once for purification, dried by the addition of molecular sieves (4 Å) and stored for at least three days. Reactants were dried as received by the addition of molecular sieves (4 Å) and stored for at least three days.

6.1.7 Dynamic light scattering (DLS)

Dynamic light scattering was performed on a *Zetasizer nano ZS* (Malvern). Two to three droplets of a sample were diluted in deionized water and measured. The obtained data was processed to extract the number and volume weight particle sizes using the software Zetasizer v7.02 (Malvern).

6.1.8 Dynamic mechanical analysis (DMA)

DMA-measurements were conducted on a *Haake Mars II Modular Advanced Rheometer System* (Thermo Fisher Scientific) with solid clamps using software *RheoWin Job Manager* (Thermo Fisher Scientific). A DMA-specimen was prepared using the mold-type M2 (Figure 75). The storage modulus, *G*', loss modulus, *G*'', and dissipation factor, tan(*δ*), were recorded as a function of temperature in the range of -80 – 170 °C at a heating rate of 5 K/min using torsion mode with a frequency of 1.000 Hz and a CD-autostrain of 0.005 %.

6.1.9 Equilibrium swelling

A specimen of known density was weighed to give the *pre*-swollen mass m_1. It was then submerged in a solvent of known solubility parameter, δ_s (Table 33)[201] at 25 °C for at least 7 days.

Table 33. Solubility parameters δ_s for solvents used in swelling experiments.[201]

Solvent	PE[a]	Toluene	THF	Acetone	*i*PrOH	EtOH	MeOH	Water
δ_s [MPa$^{0.5}$]	≈ 15.0	18.2	18.6	20.2	23.5	26.0	29.6	47.9

[a] Mean of hexane (14.9) and pentane (15.1).

A sample was carefully blotted subsequently with filter paper to remove residual solvent on the polymer surface. The swollen sample was weighed immediately to determine m_2. It was dried for at least 2 days at 50 °C under reduced pressure to obtain the *post*-swollen mass m_3. The sol content, *S*, gel content, *G,* and volume related

degree of swelling, Q_v, were determined according to Equation 7 – Equation 9, respectively (with solvent density ρ_s at 25 °C and polymer density, ρ_p).[202] The results regarding the sol content, S, gel content, G, and the degree of swelling, Q_v, are shown in Table 34 to Table 36.

$$S = \frac{m_1 - m_3}{m_1} \qquad \text{Equation 7}$$

$$G = \frac{m_3}{m_1} \qquad \text{Equation 8}$$

$$Q_v = \frac{m_2 - m_3}{m_3} \cdot \frac{\rho_p}{\rho_s} \qquad \text{Equation 9}$$

Table 34. Sol content S, gel content G and volume related degree of swelling Qv for specimens crosslinked by HDDA, TMPTA and PETA. The polymer density δ_p was determined by weighing of at least 5 samples of a known dimension and is δ_p(HDDA) = 1.20±0.03 g/cm³, δ_p(TMPTA) = 1.13±0.03 g/cm³ and δ_p(PETA) = 1.23±0.02 g/cm³.

Acrylate	F_n	Solvent	S	G	Qv
HDDA	2	PE	0.011	0.989	0.040
TMPTA	3	PE	0.005	0.995	0.029
PETA	4	PE	0.003	0.997	0.020
HDDA	2	Toluene	0.046	0.954	1.05
TMPTA	3	Toluene	0.011	0.989	0.605
PETA	4	Toluene	0.013	0.987	0.596
HDDA	2	THF	0.102	0.898	2.66
TMPTA	3	THF	0.067	0.933	1.56
PETA	4	THF	0.015	0.985	1.06
HDDA	2	Acetone	0.114	0.886	1.50
TMPTA	3	Acetone	0.077	0.923	0.974
PETA	4	Acetone	0.018	0.982	0.727
HDDA	2	^{i}PrOH	0.073	0.927	0.425
TMPTA	3	^{i}PrOH	0.063	0.937	0.349
PETA	4	^{i}PrOH	0.005	0.995	0.249
HDDA	2	EtOH	0.106	0.894	0.620
TMPTA	3	EtOH	0.091	0.909	0.532
PETA	4	EtOH	0.010	0.990	0.404
HDDA	2	MeOH	0.131	0.869	1.02
TMPTA	3	MeOH	0.102	0.898	0.833
PETA	4	MeOH	0.029	0.971	0.672

HDDA	2	Water	0.050	0.950	0.549
TMPTA	3	Water	0.070	0.930	0.639
PETA	4	Water	0.012	0.988	0.481

Table 35. Sol content *S*, gel content *G* and volume related degree of swelling *Q*v for specimens crosslinked by HDDA but with different urethane chain length. The polymer density δ_p was determined by weighing of at least 5 samples of a known dimension and is $\delta_p(P_n = 6.9) = 1.23\pm0.03$ g/cm^3, $\delta_p(P_n = 8.5) = 1.20\pm0.03$ g/cm^3 and $\delta_p(P_n = 11.0) = 1.17\pm0.05$ g/cm^3.

Chain length	P_n	Solvent	S	G	Qv
short	6.9	PE	0.022	0.978	0.060
medium	8.5	PE	0.025	0.975	0.050
long	11.0	PE	0.020	0.980	0.058
short	6.9	Toluene	0.172	0.828	1.71
medium	8.5	Toluene	0.090	0.910	1.25
long	11.0	Toluene	0.091	0.909	1.17
short	6.9	THF	0.210	0.790	4.41
medium	8.5	THF	0.122	0.878	2.69
long	11.0	THF	0.109	0.891	2.56
short	6.9	Acetone	0.209	0.791	2.27
medium	8.5	Acetone	0.141	0.859	1.70
long	11.0	Acetone	0.140	0.860	1.52
short	6.9	^{i}PrOH	0.142	0.858	0.515
medium	8.5	^{i}PrOH	0.087	0.913	0.478
long	11.0	^{i}PrOH	0.090	0.910	0.444
short	6.9	EtOH	0.185	0.815	0.793
medium	8.5	EtOH	0.116	0.884	0.647
long	11.0	EtOH	0.104	0.896	0.629
short	6.9	MeOH	0.234	0.766	1.50
medium	8.5	MeOH	0.126	0.874	1.05
long	11.0	MeOH	0.111	0.889	1.00
short	6.9	Water	0.087	0.913	0.794
medium	8.5	Water	0.066	0.934	0.608
long	11.0	Water	0.061	0.939	0.604

Table 36. Sol content *S*, gel content *G* and volume related degree of swelling *Q*v for specimens crosslinked by PETA but with different soft segments. The polymer density δ_p was determined by weighing of at least 5 samples of a known dimension and is δ_p(PEG600) = 1.23±0.02 g/cm^3, δ_p(PEG1500) = 1.19±0.03 g/cm^3 and δ_p(HDI-prepolymer) = 1.22±0.04 g/cm^3.

Polyol	Solvent	S	G	Qv
PEG600	PE	0.003	0.997	0.020
PEG1500	PE	0.023	0.977	0.075
HDI-prepolymer	PE	0.003	0.997	0.029
PEG600	Toluene	0.013	0.987	0.596
PEG1500	Toluene	0.111	0.889	1.62
HDI-prepolymer	Toluene	0.033	0.967	0.558
PEG600	THF	0.015	0.985	1.06
PEG1500	THF	0.278	0.722	2.97
HDI-prepolymer	THF	0.082	0.918	1.72
PEG600	Acetone	0.018	0.982	0.727
PEG1500	Acetone	0.119	0.881	1.24
HDI-prepolymer	Acetone	0.085	0.915	1.08
PEG600	EtOH	0.010	0.990	0.404
PEG1500	EtOH	0.127	0.873	1.05
HDI-prepolymer	EtOH	0.082	0.918	0.751
PEG600	MeOH	0.029	0.971	0.672
PEG1500	MeOH	0.161	0.839	2.22
HDI-prepolymer	MeOH	0.105	0.895	1.37
PEG600	Water	0.012	0.988	0.481
PEG1500	Water	0.108	0.892	2.23
HDI-prepolymer	Water	0.036	0.964	0.442

6.1.10 Flory-Rehner swelling theory

A model proposed by FLORY and REHNER allows the determination of the molar mass between crosslinks, M_c. It is based on thermodynamic considerations for swollen polymers. The mixing and elastic components of the free energy of the system are additive and separable in swollen state.[185] The contribution by mixing can then be described by the Flory-Huggins mixing theory and the elastic contribution by molecular theory. The elastic forces of a network compensate the solvent driven expansion in the equilibrium swollen state.[181,184] It is assumed in the affine model (Equation 10) that

the mean position of the network junctions deforms affinely to the chains end-to-end vectors (e.g., similar to the macroscopic deformation). No fluctuation of the network junctions around their mean positions is allowed (with the molar volume of the solvent, V_s, and the crosslinker functionality, f, as defined by FLORY and REHNER).[181] The volume fraction of the polymer, Φ_p, is defined by Equation 11.[184]

$$\ln(1 - \Phi_p) + \Phi_p + \chi\Phi_p^2 = -\frac{\rho_p}{M_c} V_s \left(\Phi_p^{1/3} - \frac{2\,\Phi_p}{f}\right) \qquad \text{Equation 10}$$

$$\Phi_p = \frac{\frac{m_3}{\rho_p}}{\frac{m_3}{\rho_p} + \frac{m_2 - m_3}{\rho_p}} \qquad \text{Equation 11}$$

At first, the Flory-Huggins interaction parameter was estimated using Equation 4. The highest degree of swelling was obtained in THF (Chapter 5.3.5.1, Figure 80). The Flory-Huggins interaction parameter is approximated to be $\chi \approx 0.34$ assuming that the solubility parameter of the polymer is close to that of THF. It is further assumed, that the conversion of acrylate functionalities is similar to that of the model reactions shown in Chapter 5.1. Only 70 % of the functional groups are crosslink active following this rationale. The crosslinker functionality, f, was therefore corrected to a value of f_{cor} = 2.8, 4.2 and 5.6 for HDDA, TMPTA and PETA instead of 4, 6 and 8, respectively. The results are shown in Table 37. The M_c value represent the mean distance between crosslinks in the model system. The M_c is lowest for PETA (M_c = 622 g/mol) and highest for HDDA (M_c = 2200 g/mol) based networks.

Table 37. Parameters and M_c for specimens crosslinked by HDDA, TMPTA and PETA.

Acrylate	f_{cor}	Φ_p	M_c **[g/mol]**
HDDA	2.8	0.273	2200
TMPTA	4.2	0.390	960
PETA	5.6	0.486	622

6.1.11 Gas chromatography (GC)

GC-measurements were conducted on a *7820A GC* (Agilent Technologies). A sample consisting of 500 mg of the reaction mixture and 50 mg of the internal standard toluene was diluted with 5 mL THF and separated using a column of type *Varian CP8760* (30 m x 0.32 mm, CP-Sil 5 CB, df = 1.0 µm).

6.1.12 Infrared spectroscopy (IR)

ATR-FT-IR spectra were obtained using a *Vertex 70* (Bruker) at room temperature in the range of 450 – 4000 cm^{-1} with a resolution of 4 cm^{-1} (32 scans) using an ATR-unit of the *A225 platinum diamond* (Bruker)-type. The data was analyzed using *OPUS* or *OriginPro 2019 (64-bit) 9.6.0.172*.

6.1.13 Mass spectrometry (MS)

ESI-MS was performed on an *Agilent 6224 ESI-TOF* (Agilent) coupled to an *Agilent HPLC 1200*-series (Agilent) with direct injection. Samples were dissolved in acetone (HPLC-grade) and filtered using a syringe filter. Spectrograms were analyzed using *MestReNova 14.0.1*.

6.1.14 Nuclear magnetic resonance spectroscopy (NMR)

NMR spectra (^{1}H, ^{13}C, H,H-Cosy, HSQC) were measured on either a *FourierHD 300 MHz* (Bruker), *Avance I 400 MHz* (Bruker) or *Avance I 500 MHz* (Bruker)-type spectrometer in chloroform-*d* or acetone-d_6 containing 0.03 wt% tetramethylsilane as internal standard if not stated otherwise. The spectra were analyzed using *MestReNova 14.0.1*.

6.1.15 Scanning electron microscopy (SEM)

SEM images were analyzed by a *Leo 1525 Gemini* (LEO Electron Microscopy Inc.) field emission scanning microscope using an electron beam of 10.00 kV at a 32-fold magnification. Samples were sputtered with platinum using a *Polaron SC7640 Sputter Coater* (Quorum Technologies) to obtain conductive samples. Images were analyzed by *ImageJ 1.48*.

6.1.16 Shore hardness A (SHA)

At least five samples with a thickness of about 6 mm were tested according to DIN ISO 7619-1 (2012-05). A force was applied for 15 s using a durometer of the *HBA 100-0* (Sauter)-type at 16.0 – 19.0 °C and 30 – 55 % humidity. The durometer was calibrated by an *AHBA-01* (Sauter)-type test-kit.

6.1.17 Tensile testing

At least 5 specimens of the S2-type were prepared according to DIN ISO 23529 using the S2-part of an M2-type mold and tested using a *Z1.0* (Zwick Roell) at 16.0 – 20.0 °C and 30 – 60 % humidity (preload: 0.01 MPa, speed for E-modulus: 10 mm/min, test speed: 200 mm/min). *OriginPro 2019 (64-bit) 9.6.0.172* was used for analysis.

6.1.18 Thermogravimetric analysis (TGA)

Thermograms were measured on a *TGA 209 F1 Iris* (Netzsch) in a temperature range from 25 to 400 °C at a heating rate of 10 K/min under atmospheric conditions using ceramic aluminum oxide crucibles. *OriginPro 2019 (64-bit) 9.6.0.172* was used for analysis.

6.2 Study on the *aza*-Michael addition reaction

6.2.1 Synthesis of dibutyl (methylenebis(4,1-phenylene)) dicarbamate

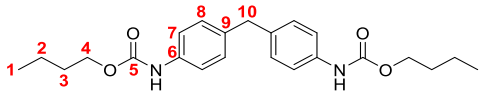

Dibutyl (methylenebis(4,1-phenylene)) dicarbamate

The following reaction was carried out under an inert gas atmosphere (Ar), 1-butanol was dried prior to use over molecular sieves (4 Å) for at least three days.

A flask containing 70 mL 1-butanol (n = 7.6 · 10^{-1} mol, 27 eq) was heated to 60 °C. Then 7.12 g of molten 4,4'-methylene diphenyl diisocyanate (n = 2.85 · 10^{-2} mol, 1 eq.) was added dropwise while stirring. The formation of a colorless precipitate was observed. The mixture was cooled to room temperature after 1 h and filtrated. The precipitate was washed with cold ethanol and recrystallized in ethanol. The purified product was received after filtration and drying under reduced pressure.

Dibutyl (methylenebis(4,1-phenylene)) dicarbamate was obtained as colorless, needle-like crystals (10.89 g, n = 2.73 · 10^{-2} mol, ***X* ≈ 96 %**, T_m = 117.8 °C).

^{1}H-NMR (400.13 MHz, acetone-d_6): δ [ppm] = 8.49 (s, 2 H, N-H), 7.47 (d, ^3J(H,H) = 8.4 Hz, 4 H, H_7), 7.14 (d, ^3J(H,H) = 8.8 Hz, 4 H, H_8), 4.09 (t, ^3J(H,H) = 6.6 Hz, 4 H, H_4), 3.87 (s, 2 H, H_{10}). 1.71 – 1.53 (m, 4 H, H_3), 1.49 – 1.29 (m, 4 H, H_2), 0.93 (t, ^3J(H,H) = 7.4 Hz, 6 H, H_1).

ESI-MS: $m/z_{calc.}$ [$C_{23}H_{30}N_2O_4$] = 398.22 g/mol, m/z_{found} [M + H^+] = 399.23 g/mol.

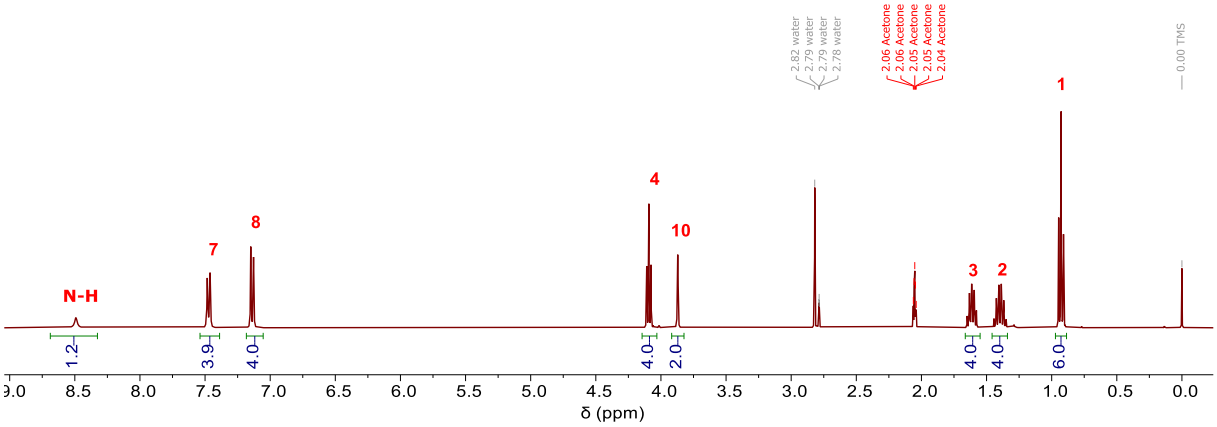

Figure 92. ^{1}H-NMR spectrum of di-*n*-butyl (methylenebis(4,1-phenylene)) dicarbamate (acetone-d_6).

6.2.2 Covalent bonding using dibutyl (methylenebis(4,1-phenylene)) dicarbamate

The following reaction was carried out under an inert gas atmosphere (Ar), phenoxyethyl acrylate was dried prior to use over molecular sieves (4 Å) for at least three days.

0.264 g 2-phenoxyethyl acrylate ($n = 1.37 \cdot 10^{-3}$ mol, 2 eq) were added to a flask containing 0.274 g dibutyl (methylenebis(4,1-phenylene)) dicarbamate ($n = 6.863 \cdot 10^{-4}$ mol, 1 eq.) and 0.003 g potassium acetate ($n = 3 \cdot 10^{-5}$ mol, ≈0.5 wt%). The reaction mixture was stirred under argon at 160 °C for 3 h. The resulting highly viscous and yellowish reaction mixture was cooled to room temperature, treated with acetone and filtered. The filtrate was dried under reduced pressure to obtain the catalyst free crude product mixture. The products were separated using column chromatography (PE:EE, 2:1). Three different products were isolated: mono-, di-adduct and poly(phenoxyethyl acrylate).

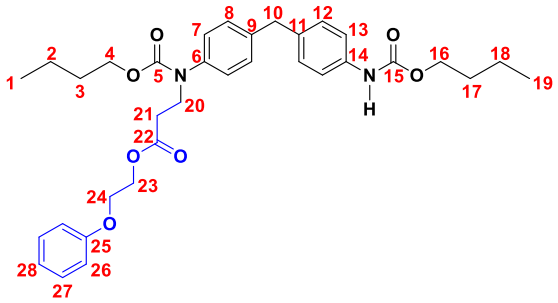

2-Phenoxyethyl 3-((butoxycarbonyl) (4-(4-((butoxycarbonyl)amino) benzyl)phenyl)amino) propanoate

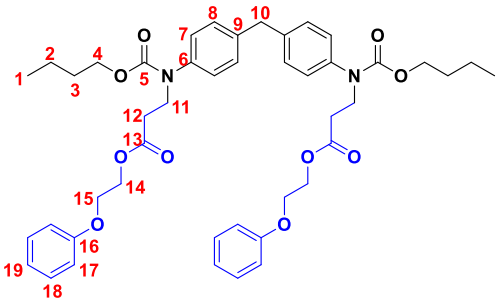

Bis(2-phenoxyethyl) 3,3'-((methylenebis (4,1-phenylene)) bis((butoxycarbonyl) azanediyl)) dipropionate

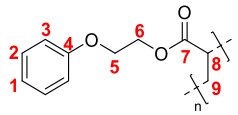

Poly(phenoxyethyl acrylate)

^{1}H-NMR (mono-adduct, 400.13 MHz, acetone-d_6, Figure 93): δ [ppm] = 8.52 (s, 1 H, N-H), 7.49 (d, ^3J(H,H) = 8.1 Hz, 2 H, H_{13}), 7.30 – 7.24 (m, 2 H, H_{27}), 7.24 – 7.14 (m, 6 H, H_7, H_8, H_{12}), 7.00 – 6.85 (m, 3 H, H_{26}, H_{28}), 4.33 – 4.25 (m, 2 H, H_{24}), 4.15 – 4.11 (m, 2 H, H_{23}), 4.09 (t, ^3J(H,H) = 6.7 Hz, 2 H, H_{16}), 4.01 (t, ^3J(H,H) = 6.5 Hz, 2 H, H_4), 3.95 (t, ^3J(H,H) = 7.1 Hz, 2 H, H_{20}), 3.92 (s, 2 H, H_{10}), 2.58 (t, ^3J(H,H) = 7.1 Hz, 2 H, H_{21}), 1.65 – 1.56 (m, 2 H, H_{17}), 1.55 – 1.45 (m, 2 H, H_3), 1.45 – 1.35 (m, 2 H, H_{18}), 1.34 – 1.23 (m, 2 H, H_2), 0.93 (t, ^3J(H,H) = 7.4 Hz, 3 H, H_{19}), 0.85 (t, ^3J(H,H) = 7.4 Hz, 3 H, H_1).

^{1}H-NMR (bi-adduct, 400.13 MHz, acetone-d_6, Figure 94): δ [ppm] = 7.30 – 7.25 (m, 4 H, H_{18}), 7.24 – 7.18 (m, 8 H, H_7, H_8), 6.95 – 6.89 (m, 6 H, H_{17}, H_{19}), 4.32 – 4.28 (m, 4 H, H_{15}), 4.16 – 4.11 (m, 4 H, H_{14}), 4.00 (t, ^3J(H,H) = 6.6 Hz, 4 H, H_4), 3.97 (s, 2 H, H_{10}), 3.94 (t, ^3J(H,H) = 7.1 Hz, 4 H, H_{11}), 2.58 (t, ^3J(H,H) = 7.1 Hz, 4 H, H_{12}), 1.55 – 1.45 (m, 4 H, H_3), 1.34 – 1.23 (m, 4 H, H_2), 0.85 (t, ^3J(H,H) = 7.4 Hz, 6 H, H_1).

^{1}H-NMR (P(POEA), 400.13 MHz, acetone-d_6, Figure 95): δ [ppm] = 7.23 (t, ^3J(H,H) = 7.8 Hz, 2 H, H_2), 6.91 (d, ^3J(H,H) = 7.6 Hz, 3 H, H_1, H_3), 4.33 (s, 2 H, H_6), 4.09 (s, 2 H, H_5), 2.49 (s, 1 H, H_8), 1.91 (s, 0.5 H, H_9), 1.79 – 1.40 (m, 1.5 H, H_9).

ESI-MS (mono-adduct): $m/z_{calc.}$ [$C_{34}H_{42}N_2O_7$] = 590.30 g/mol, m/z_{found} [M + H$^+$] = 591.31 g/mol.

ESI-MS (bi-adduct): $m/z_{calc.}$ [$C_{45}H_{54}N_2O_{10}$] = 782.38 g/mol, m/z_{found} [M + H$^+$] = 783.38 g/mol.

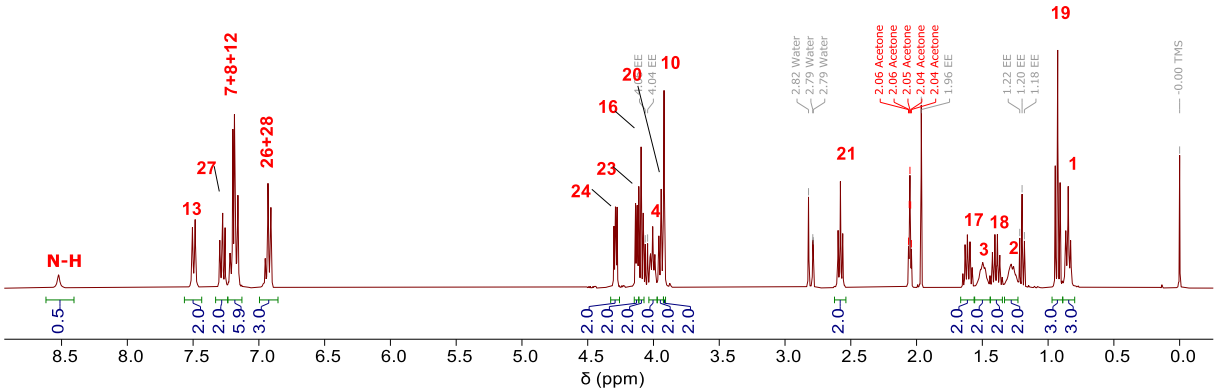

Figure 93. ^{1}H-NMR spectrum of 2-phenoxyethyl 3-((butoxycarbonyl)(4-(4-((butoxycarbonyl)amino) benzyl)phenyl)amino) propanoate (mono-adduct, acetone-d_6).

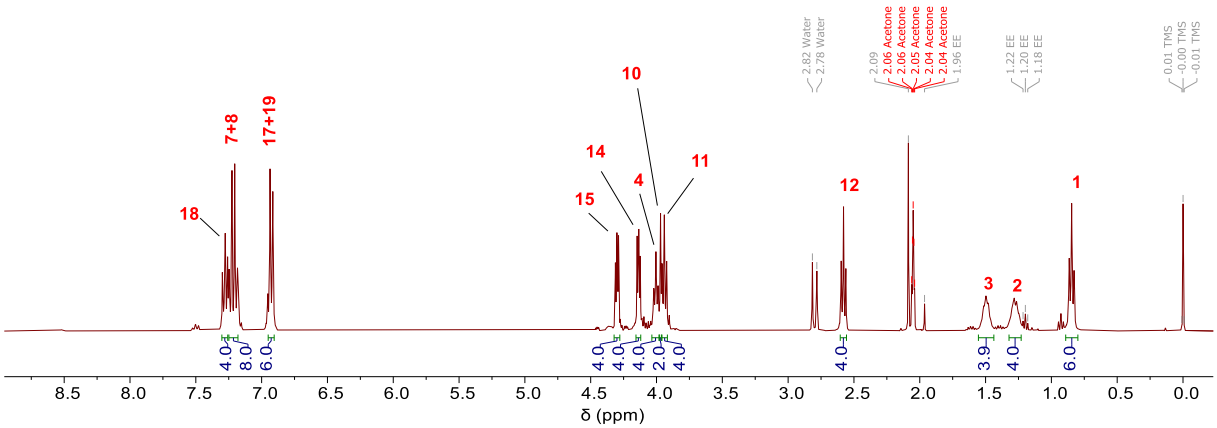

Figure 94. ^{1}H-NMR spectrum of Bis(2-phenoxyethyl) 3,3'-((methylenebis(4,1-phenylene))bis((butoxy carbonyl)azanediyl)) dipropionate (bi-adduct, acetone-d_6).

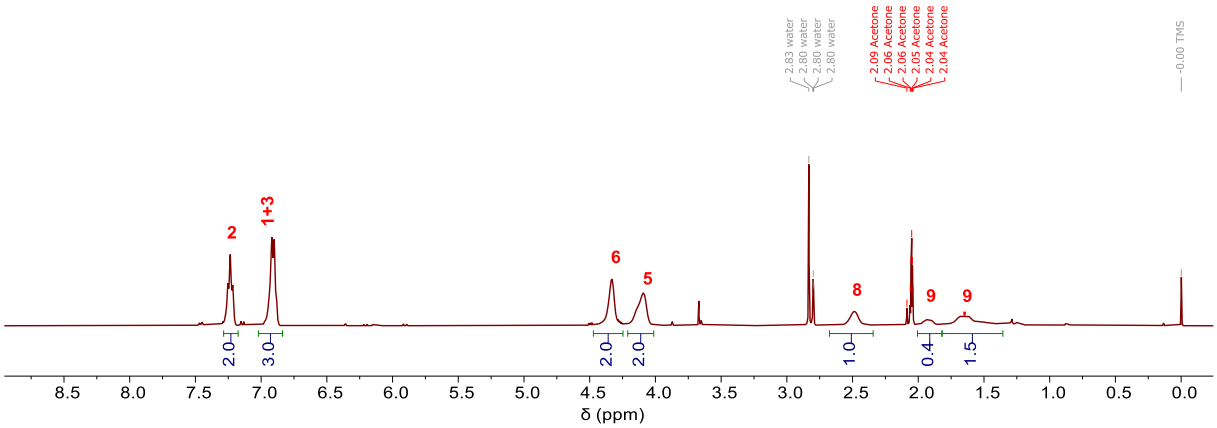

Figure 95. ^{1}H-NMR spectrum of poly(phenoxyethyl acrylate) (acetone-d_6).

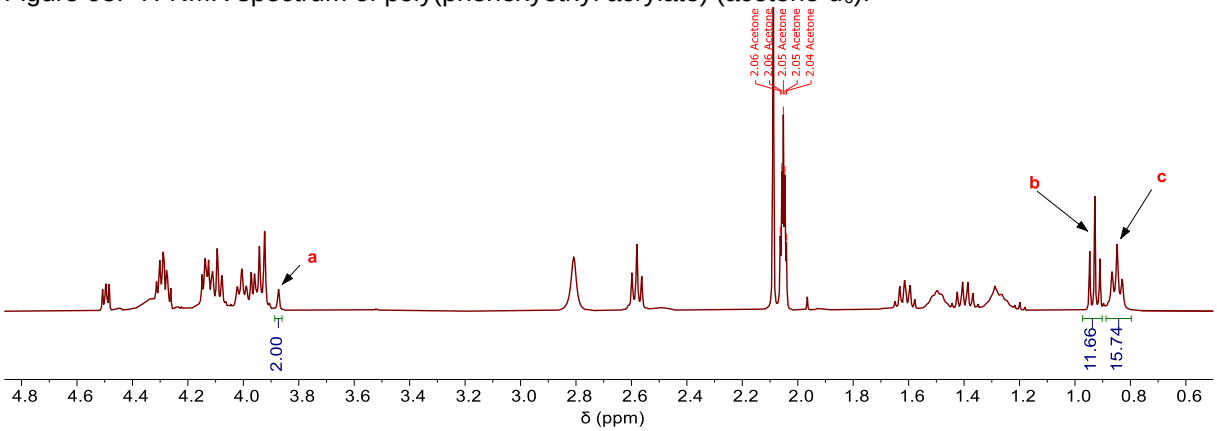

Figure 96. Crude ^{1}H-NMR spectrum for approximation of product ratio. Signal a corresponds to the central methylene-protons of urethane (2 H, H_{10}, Figure 92), signal b to terminal methyl-protons of urethane (6 H, H_3, Figure 92) and mono-adduct (non-coupled moiety, 3 H, H_{19}, Figure 93), signal c to terminal methyl-protons of mono- and di-adduct (coupled moiety, 3 or 6 H, H_1, Figure 93 and Figure 94) (acetone-d_6). Integral a is set to 2. The contribution of urethane to integral b is then 6. The residual integral of 5.66 correspond to mono-adduct and with a value of 5.66 to integral c. The residual value of 10.12 in integral c is contributed by the di-adduct. The molar ratio is 22 to 41 to 37 mol% of urethane to mono- to di-adduct, respectively.

6.2.3 Synthesis of model compounds used in catalyst study

6.2.3.1 Synthesis of *n*-butyl *p*-tolylcarbamate

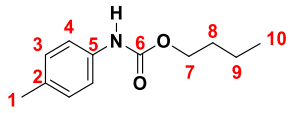

***n*-Butyl *p*-tolylcarbamate**

The following reaction was carried out under an inert gas atmosphere (Ar), 1-butanol was dried prior to use over molecular sieves (4 Å) for at least three days.

A flask containing 11.984 g 1-butanol (n = 1.617 · 10^{-1} mol) was heated to 80 °C and stirred. Subsequently 6.914 g *para*-tolyl isocyanate (n = 5.192 · 10^{-2} mol) was added dropwise. The excess 1-butanol was evaporated after 5 h under reduced pressure and yellowish needle-like crystals were obtained. These crystals were recrystallized twice in PE.

n-Butyl *p*-tolylcarbamate was obtained as colorless, needle-like crystals (9.877 g, n = 4.765 · 10^{-2} mol, ***X* ≈ 91 %**).

^{1}H-NMR (400.13 MHz, acetone-d_6): δ [ppm] = 8.45 (s, 1 H, N-H), 7.44 (d, ^3J(H,H) = 8.5 Hz, 2 H, H_4), 7.09 (d, ^3J(H,H) = 8.4 Hz, 2 H, H_3), 4.09 (t, ^3J(H,H) = 6.6 Hz, 2 H, H_7), 2.26 (s, 3 H, H_1). 1.71 – 1.53 (m, 2 H, H_8), 1.52 – 1.29 (m, 2 H, H_9), 0.93 (t, ^3J(H,H) = 7.3 Hz, 3 H, H_{10}).

ESI-MS: $m/z_{calc.}$ [$C_{12}H_{17}NO_2$] = 207.13 g/mol, m/z_{found} [M + H^+] = 208.13 g/mol.

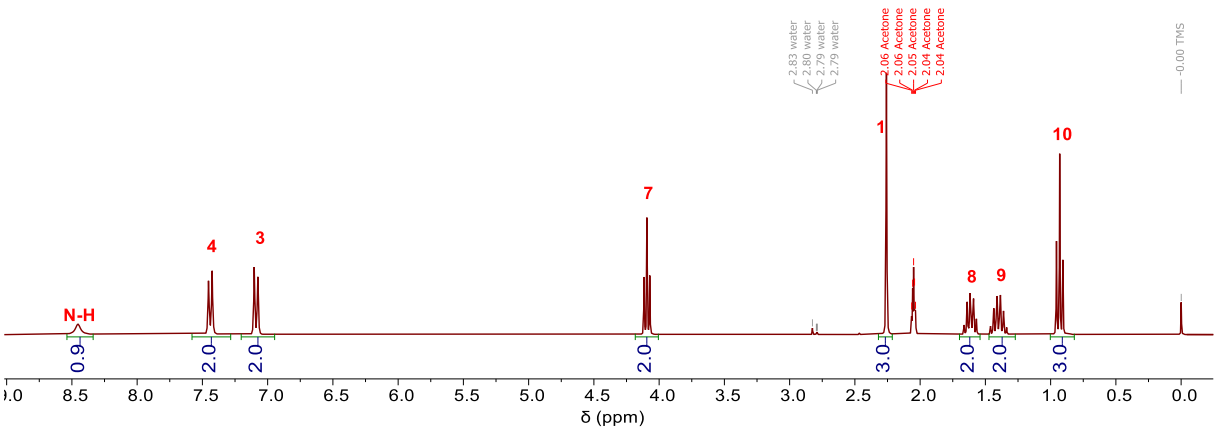

Figure 97. ^{1}H-NMR spectrum of *n*-butyl *p*-tolylcarbamate (acetone-d_6).

6.2.3.2 Synthesis of 1,3,5-tri-*p*-tolyl isocyanurate

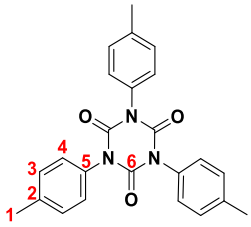

1,3,5-Tri-*p*-tolyl isocyanurate

1,3,5-Tri-*p*-tolyl isocyanurate was not directly synthesized since it was a common by-product in the adduct-synthesis. It was instead isolated from adduct mixtures by precipitation in 2-propanol. The precipitate was recrystallized in 2-propanol for further purification, filtrated and dried under reduced pressure.

1,3,5-Tri-*p*-tolyl isocyanurate was obtained as colorless, needle-like crystals.

^{1}H-NMR (300.21 MHz, acetone-d_6): δ [ppm] = 7.38 – 7.18 (m, 12 H, H_3, H_4), 2.36 (s, 9 H, H_1).

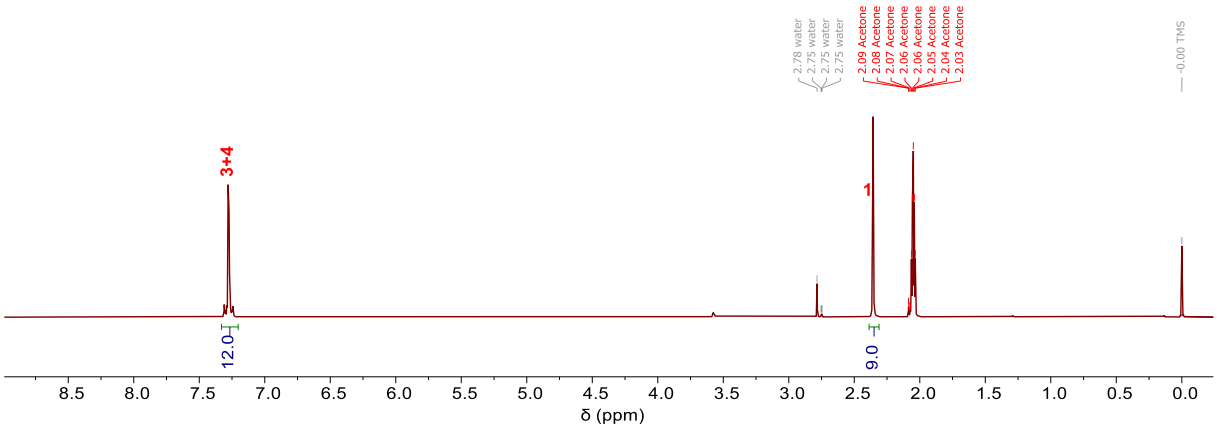

Figure 98. ^{1}H-NMR spectrum of 1,3,5-tri-*p*-tolyl isocyanurate (acetone-d_6).

6.2.3.3 Synthesis of 2-phenoxyethyl 3-((butoxycarbonyl)(p-tolyl)amino) propanoate

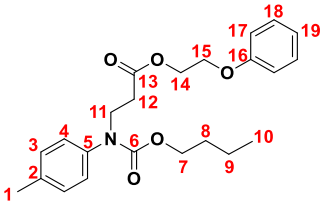

2-Phenoxyethyl 3-((butoxycarbonyl)(p-tolyl)amino) propanoate

A flask containing 1.999 g *n*-butyl *p*-tolylcarbamate ($n = 9.642 \cdot 10^{-3}$ mol, 1 eq.), 1.961 g phenoxyethyl acrylate ($n = 1.020 \cdot 10^{-2}$ mol, 1.05 eq.), 0.041 g potassium octoate ($n = 2.3 \cdot 10^{-4}$ mol, 0.023 eq.) and < 0.001 g butylated hydroxytoluene ($n < 5 \cdot 10^{-6}$ mol, < 0.0005 eq) was heated to 140 °C and stirred for 17.5 h. The product was purified by column chromatography (silica: 0.04 – 0.063 mm, eluent PE/EE, 5:1 → 4:1) and dried under reduced pressure.

2-Phenoxyethyl 3-((butoxycarbonyl)(p-tolyl)amino) propanoate was obtained as a colorless, medium viscosity liquid (2.014 g, $n = 5.041 \cdot 10^{-3}$ mol, ***X* ≈ 53 %**).

^{1}H-NMR (400.13 MHz, acetone-d_6): δ [ppm] = 7.35 – 7.23 (m, 2 H, H_{18}), 7.15 (s, 4 H, H_3, H_4), 7.00 – 6.88 (m, 3 H, H_{17}, H_{19}), 4.40 – 4.30 (m, 2 H, H_{14}), 4.21 – 4.11 (m, 2 H, H_{15}), 4.01 (t, ^3J(H,H) = 6.6 Hz, 2 H, H_7), 3.94 (t, ^3J(H,H) = 7.2 Hz, 2 H, H_{11}), 2.58 (t, ^3J(H,H) = 7.2 Hz, 2 H, H_{12}), 2.30 (s, 3 H, H_1), 1.49 (p, ^3J(H,H) = 7.2, 6.9 Hz 2 H, H_8), 1.28 (m, 2 H, H_9), 0.85 (t, ^3J(H,H) = 7.4 Hz, 3 H, H_{10}).

ESI-MS: $m/z_{calc.}$ [$C_{23}H_{29}NO_5$] = 399.20 g/mol, m/z_{found} [M + H^+] = 400.20 g/mol.

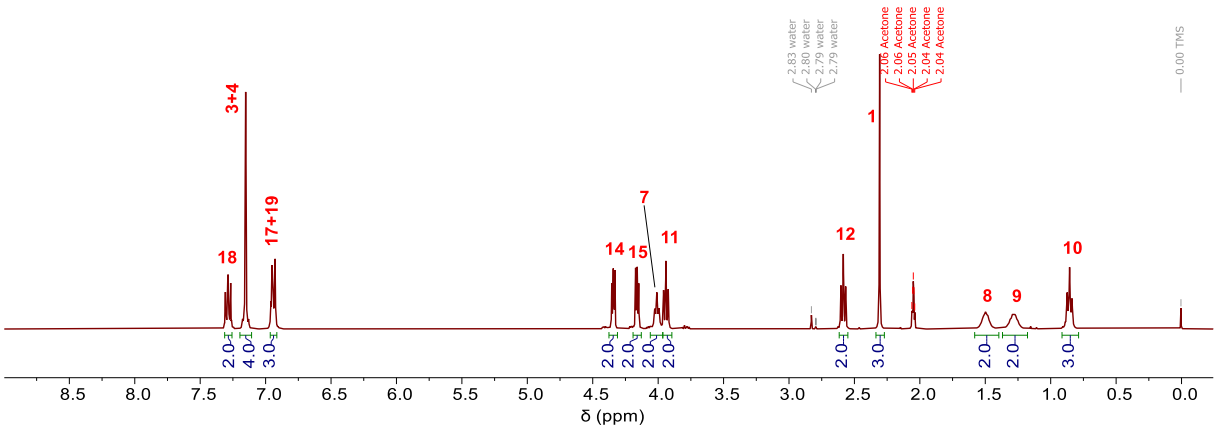

Figure 99. ^{1}H-NMR spectrum of 2-phenoxyethyl 3-((butoxycarbonyl)(p-tolyl)amino) propanoate (acetone-d_6).

6.2.3.4 Synthesis of 2-phenoxyethyl 3-(((butoxy-*d*$_9$)carbonyl)(p-tolyl)amino) propanoate-2-*d*

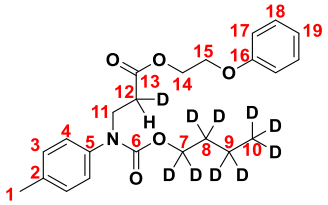

2-Phenoxyethyl 3-(((butoxy-*d*$_9$)carbonyl)(p-tolyl)amino) propanoate-2-*d*

A flask containing 0.501 g 1-butanol-*d*$_{10}$ ($n = 5.90 \cdot 10^{-3}$ mol, 1 eq), 3.424 g phenoxyethyl acrylate ($n = 1.78 \cdot 10^{-2}$ mol, 3 eq.), 0.031 g potassium octoate ($n = 1.7 \cdot 10^{-4}$ mol, 0.03 eq.), 0.002 g butylated hydroxytoluene ($n = 7 \cdot 10^{-6}$ mol, 0.001 eq) and 1.582 g *para*-tolyl isocyanate ($n = 1.19 \cdot 10^{-2}$ mol, 2 eq) was heated up to 110 °C and stirred for 5 h. The product was isolated by column chromatography (silica: 0.04 – 0.063 mm, eluent PE/EE, 4:1) and dried under reduced pressure.

2-Phenoxyethyl 3-(((butoxy-*d*$_9$)carbonyl)(p-tolyl)amino) propanoate-2-*d* was obtained as a colorless, medium viscosity liquid.

^{1}H-NMR (400.13 MHz, acetone-*d*$_6$): δ [ppm] = 7.32 – 7.23 (m, 2 H, *H*$_{18}$), 7.14 (s, 4 H, *H*$_3$, *H*$_4$), 7.00 – 6.87 (m, 3 H, *H*$_{17}$, *H*$_{19}$), 4.39 – 4.29 (m, 2 H, *H*$_{14}$), 4.22 – 4.10 (m, 2 H, *H*$_{15}$), 4.00 – 3.88 (m, 2 H, *H*$_{11}$), 2.59 (t, ^3J(H,H) = 7.2 Hz, 1 H, *H*$_{12}$), 2.31 (s, 3 H, *H*$_1$).

ESI-MS: $m/z_{calc.}$ [$C_{23}H_{19}D_{10}NO_5$] = 409.27 g/mol, m/z_{found} [M + H$^+$] = 410.26 g/mol.

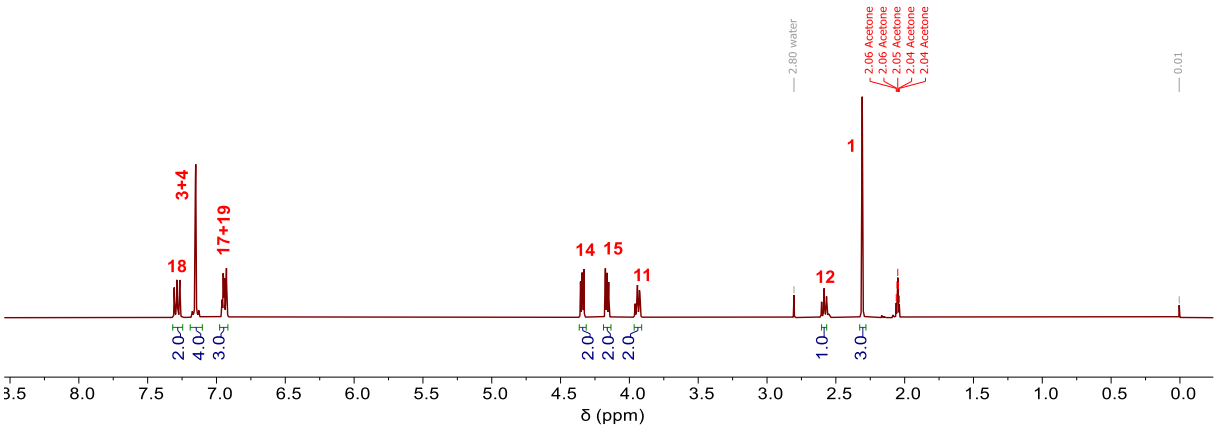

Figure 100. ^{1}H-NMR spectrum of 2-phenoxyethyl 3-((butoxycarbonyl)(p-tolyl)amino) propanoate (deuterated) (acetone-*d*$_6$).

6.2.4 Inhibitor study of model system

1-Butanol and phenoxyethyl acrylate were dried prior to use over molecular sieves (4 Å) for at least three days. Butylated hydroxytoluene was recrystallized in 2-propanol.

A mixture was prepared in a flask containing 1 eq. 1-butanol (BuOH), 4 eq. phenoxyethyl acrylate (POEA) and 0.008 eq. potassium acetate (K Ac). The mixture was stabilized w or w/o 0.5 eq. of the radical inhibitor butylated hydroxytoluene (BHT). 2 eq. *para*-tolyl isocyanate (pTMI) was added to the mixtures w and w/o BHT and heated to 90 °C for 1 h and subsequently to 160 °C for 3 h. The reaction mixture stayed liquid during the entire reaction when BHT was added. The reaction already gelled during the first reaction step at 90 °C in the absence of BHT. It turned yellowish in the second heating step.

The mass balance of both reactions is shown in the tables below. The inhibitor-urethane products were synthesized according to the synthesis protocols shown in the following subchapters and subsequently characterized and identified.

Table 38. Weights for a reaction containing the radical inhibitor BHT.

	BuOH	**POEA**	**BHT**	**K Ac**	**pTMI**
***m* [g]**	0.073	0.752	0.107	0.006	0.260
***n* [mol]**	$9.78 \cdot 10^{-4}$	$3.91 \cdot 10^{-3}$	$4.86 \cdot 10^{-4}$	$6 \cdot 10^{-5}$	$1.96 \cdot 10^{-3}$

Table 39. Weights for a reaction without the radical inhibitor BHT.

	BuOH	**POEA**	**BHT**	**K Ac**	**pTMI**
***m* [g]**	0.073	0.752	-	0.006	0.260
***n* [mol]**	$9.78 \cdot 10^{-4}$	$3.91 \cdot 10^{-3}$	-	$6 \cdot 10^{-5}$	$1.96 \cdot 10^{-3}$

6.2.4.1 Synthesis of 4-methoxyphenyl *p*-tolylcarbamate

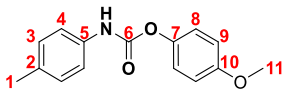

4-Methoxyphenyl *p*-tolylcarbamate

Toluene was dried prior to use over molecular sieves (4 Å) for at least three days.

A flask containing 1.001 g 4-methoxyphenol ($n = 8.062 \cdot 10^{-3}$ g/mol, 1 eq.) and 0.014 g DABCO ($n = 1.2 \cdot 10^{-4}$ g/mol, 0.03 eq.) in toluene was heated to 90 °C. 1.077 g *para*-tolyl isocyanate ($n = 8.090 \cdot 10^{-3}$ g/mol, 1 eq.) was added to the solution while stirring. The solvent was evaporated after completion of the reaction under reduced pressure.

4-Methoxylphenyl *p*-tolylcarbamate was obtained as colorless, needle-like crystals (1.973 g, $n = 7.668 \cdot 10^{-3}$ mol, ***X* ≈ 95 %**).

^{1}H-NMR (400.13 MHz, acetone-d_6): δ [ppm] = 8.95 (s, 1 H, N-H), 7.48 (d, ^3J(H,H) = 8.1 Hz, 2 H, H_4), 7.14 (d, ^3J(H,H) = 8.5 Hz, 2 H, H_3), 7.11 (d, ^3J(H,H) = 9.1 Hz, 2 H, H_8), 6.93 (d, ^3J(H,H) = 9.1 Hz, 2 H, H_9), 3.80 (s, 3 H, H_{11}), 2.28 (s, 3 H, H_1).

ESI-MS: $m/z_{calc.}$ [$C_{15}H_{15}NO_3$] = 257.11 g/mol, m/z_{found} [M + H$^+$] = 258.12 g/mol.

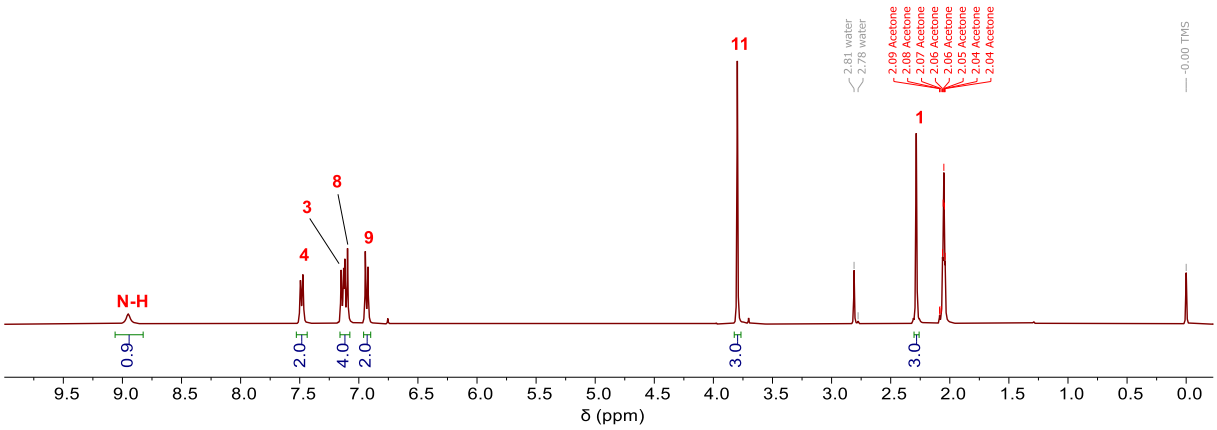

Figure 101. ^{1}H-NMR spectrum of 4-methoxyphenyl *p*-tolylcarbamate (acetone-d_6).

6.2.4.2 Synthesis of 2,6-di-*tert*-butyl-4-methylpenyl *p*-tolylcarbamate

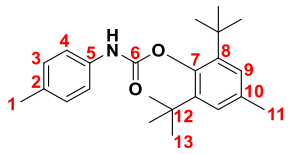

2,6-di-*tert*-butyl-4-methylpenyl *p*-tolylcarbamate

Toluene was dried prior to use over molecular sieves (4 Å) for at least three days. Butylated hydroxytoluene was recrystallized in acetone.

A flask containing 1.000 g butylated hydroxytoluene ($n = 4.54 \cdot 10^{-3}$ mol, 1 eq.), 0.014 g potassium octoate ($n = 1.354 \cdot 10^{-4}$ mol, 0.03 eq.) and 2 mL toluene was heated to 90 °C. 1.821 g *para*-tolyl isocyanate ($n = 1.37 \cdot 10^{-2}$ mol, 3 eq.) was added to the solution while stirring. The turbid, yellowish solution was cooled to room temperature after 4 h and filtrated. The filtrate dried by evaporation under reduced pressure. The resulting powder was washed with petroleum ether to remove traces of non-converted butylated hydroxytoluene. The purified product was isolated by column chromatography (silica: 0.04 – 0.063 mm, eluent: petroleum ether/ethyl acetate 4/1).

2,6-Di-*tert*-butyl-4-methylphenyl *p*-tolylcarbamate was obtained as a colorless powder (1.271 g, $n = 3.59 \cdot 10^{-3}$ mol, ***X* ≈ 79 %**).

^{1}H-NMR (300.21 MHz, acetone-d_6): δ [ppm] = 9.21 (s, 1 H, N-H), 7.57 – 7.40 (m, 2 H, H_4), 7.23 – 7.04 (m, 4 H, H_3, H_9), 2.30 (s, 3 H, H_1), 2.27 (s, 3 H, H_{11}), 1.36 (s, 18 H, H_{13}).

ESI-MS: $m/z_{calc.}$ [$C_{23}H_{31}NO_2$] = 353.24 g/mol, m/z_{found} [M + H^+] = 354.25 g/mol.

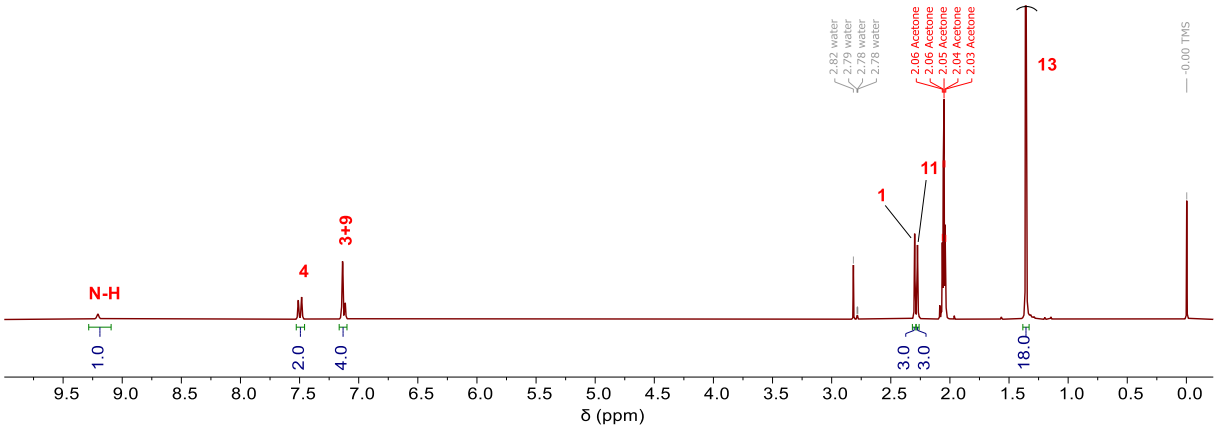

Figure 102. ^{1}H-NMR spectrum of 2,6-di-*tert*-butyl-4-methylphenyl *p*-tolylcarbamate (acetone-d_6).

6.2.5 Studies on by-product formation caused by transesterification

6.2.5.1 Transesterification of *n*-butyl *p*-tolylcarbamate to phenoxyethyl *p*-tolylcarbamate

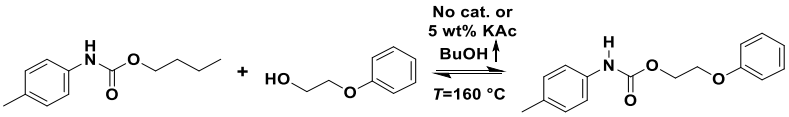

Transesterification reaction to phenoxyethyl *p*-tolylcarbamate

The following reactions were carried out in an open flask to allow evaporation of *n*-BuOH in case of an unzipping reaction.

1-Butyl *p*-tolylcarbamate ($m = 0.21$ g, $n = 1.0 \cdot 10^{-3}$ mol, 1 eq.) was dissolved in 0.51 mL 2-phenoxyethanol ($n = 4.1 \cdot 10^{-3}$ mol, 4 eq.) and heated to 160 °C while stirring. A colorless vapor was observed. 1-Butyl *p*-tolylcarbamate ($m = 0.21$ g, $n = 1.0 \cdot 10^{-3}$ mol, 1 eq.) and potassium acetate ($m = 0.040$ g, $n = 4.0 \cdot 10^{-4}$ mol, 0.4 eq.) were dissolved in a similar reaction in 0.51 mL 2-phenoxyethanol ($n = 4.1 \cdot 10^{-3}$ mol, 4 eq.) and heated to 160 °C while stirring. A heavy, colorless vapor was observed. Both reactions were sampled every 30 min for 3 h and analyzed by ^{1}H-

NMR spectroscopy. Phenoxyethyl *p*-tolylcarbamate was also directly synthesized from pTMI and 2-phenoxyethanol as described below for characterization.

6.2.5.2 Synthesis of phenoxyethyl *p*-tolylcarbamate

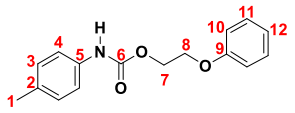

Phenoxyethyl *p*-tolylcarbamate

The following reaction was carried out under an inert gas atmosphere (Ar), all solvents and chemicals were dried prior to use over molecular sieves (4 Å) for at least three days.

2-Phenoxyethanol (m = 6.692 g, n = 4.844 · 10^{-2} mol, 2 eq.) was heated to 60 °C and 3.110 g *p*-tolyl isocyanate (2.335 · 10^{-2} mol, 1 eq.) was added dropwise while stirring. The mixture was heated to 120 °C after 2 h and the excess of 2-phenoxyethanol was removed under reduced pressure. The remaining colorless precipitate was purified by recrystallization in 2-propanol.

Phenoxyethyl *p*-tolylcarbamate was obtained as colorless, needle-like crystals (5.551 g, n = 2.046 · 10^{-2} mol, ***X* ≈ 88 %**).

^{1}H-NMR (400.13 MHz, acetone-d_6): δ [ppm] = 8.64 (s, 1 H, N-H), 7.46 (d, ^3J(H,H) = 8.1 Hz, 2 H, H_4), 7.38 – 7.25 (m, 2 H, H_{11}), 7.11 (d, ^3J(H,H) = 8.4 Hz, 2 H, H_3), 7.04 – 6.91 (m, 3 H, H_{10}, H_{12}), 4.55 – 4.38 (m, 2 H, H_7), 4.29 – 4.16 (m, 2 H, H_8), 2.27 (s, 3 H, H_1).

ESI-MS: $m/z_{calc.}$ [$C_{16}H_{17}NO_3$] = 271.12 g/mol, m/z_{found} [M + Na^+] = 294.10 g/mol.

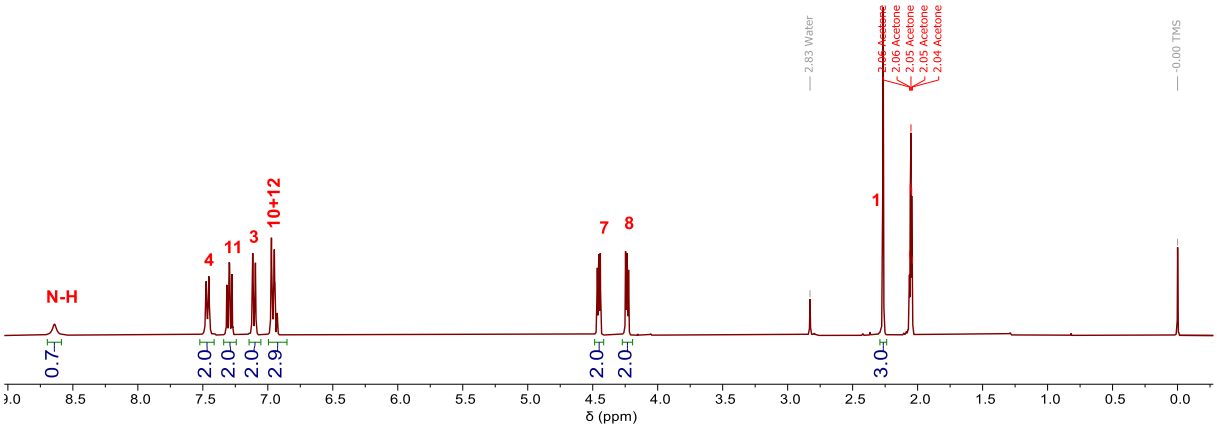

Figure 103. ^{1}H-NMR spectrum of phenoxyethyl *p*-tolylcarbamate (acetone-d_6).

6.2.5.3 Synthesis of 2-phenoxyethyl 3-(((2-phenoxyethoxy)carbonyl)(*p*-tolyl)amino)propanoate

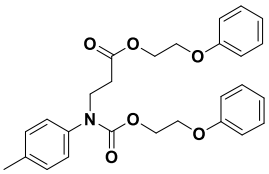

2-phenoxyethyl 3-(((2-phenoxyethoxy)carbonyl) (*p*-tolyl)amino)propanoate

A flask containing 0.500 g phenoxyethyl *p*-tolylcarbamate ($n = 1.84 \cdot 10^{-3}$ mol, 1 eq.), 0.008 g potassium octoate ($n = 4 \cdot 10^{-5}$ mol, 0.02 eq.), approx. 0.001 g butylated hydroxytoluene ($n \approx 5 \cdot 10^{-6}$ mol, 0.003 eq.) and 0.388 g phenoxyethyl acrylate ($n = 2.02 \cdot 10^{-3}$ mol, 1.1 eq.) was stirred at 140 °C for 22 h. No further purification was conducted, the crude product was directly analyzed by ^{1}H-NMR and ESI-MS spectra. The conversion calculated from ^{1}H-NMR spectroscopic data amounted to ***X* ≈ 18 %**.

ESI-MS: $m/z_{calc.}$ [$C_{27}H_{29}NO_6$] = 463.20 g/mol, m/z_{found} [M + H^+] = 264.21 g/mol, [M + Na^+] = 486.19 g/mol.

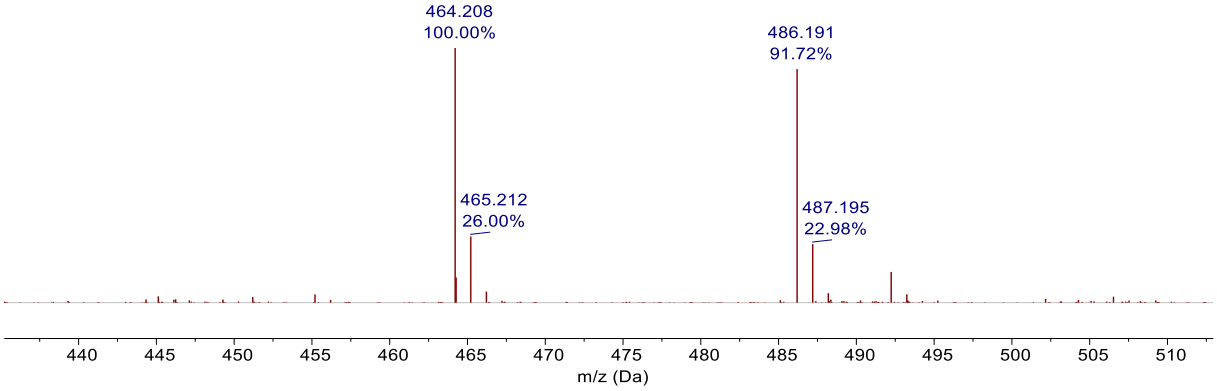

Figure 104. ESI-MS spectrogram of 2-phenoxyethyl 3-(((2-phenoxyethoxy)carbonyl)(*p*-tolyl) amino)propanoate.

6.2.5.4 Synthesis of *n*-butyl 3-((butoxycarbonyl)(*p*-tolyl)amino) propanoate

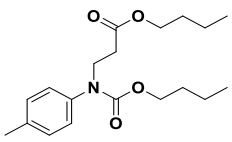

***n*-Butyl 3-((butoxycarbonyl)(*p*-tolyl)amino) propanoate**

A flask containing 0.498 g *n*-butyl *p*-tolylcarbamate ($n = 2.40 \cdot 10^{-3}$ mol, 1 eq.), 0.010 g potassium octoate ($n = 5.5 \cdot 10^{-5}$ mol, 0.04 eq.), approx. 0.001 g butylated

hydroxytoluene ($n \approx 5 \cdot 10^{-6}$ mol, 0.003 eq.) and 0.399 g *n*-butyl acrylate ($n = 3.12 \cdot 10^{-3}$ mol, 1.3 eq.) was stirred at 140 °C for 22 h. No further purification was conducted, the crude product was directly analyzed by ^{1}H-NMR and ESI-MS spectra. The conversion based on ^{1}H-NMR spectroscopic data amounted to ***X* ≈ 71 %**.

ESI-MS: $m/z_{calc.}$ [$C_{19}H_{29}NO_4$] = 335.21 g/mol, m/z_{found} [M + H^+] = 336.21 g/mol, [M + Na^+] = 358.20 g/mol.

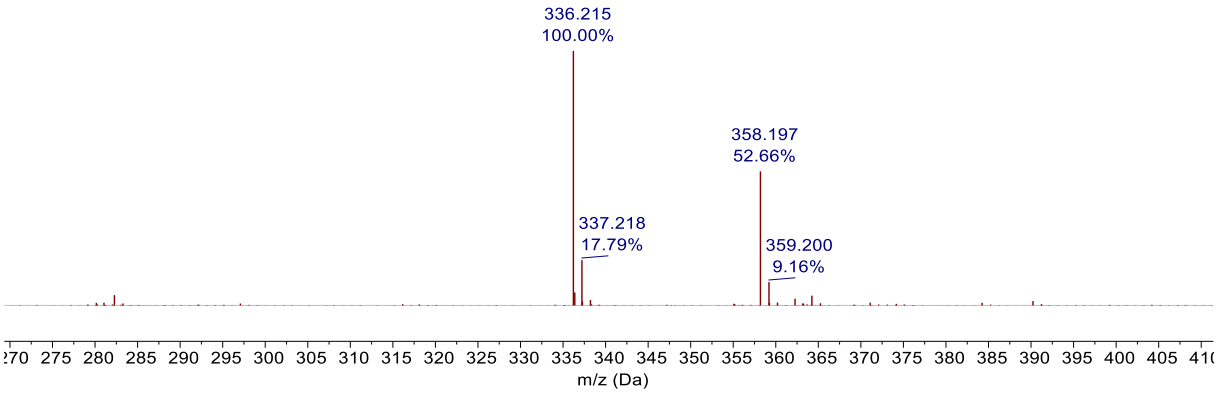

Figure 105. ESI-MS spectrogram of *n*-Butyl 3-((butoxycarbonyl)(*p*-tolyl)amino) propanoate.

6.2.5.5 Degradation of adduct 6

(a) 0.089 g 2-Phenoxyethyl 3-((butoxycarbonyl)(*p*-tolyl)amino)propanoate (adduct **6**, $n = 2.2 \cdot 10^{-4}$ mol, 1 eq.) or (b) 0.094 g adduct **6** ($n = 2.4 \cdot 10^{-4}$ mol, 1 eq.) were stirred at 160 °C for 2 h in a sealed flask containing 0.002 g potassium octoate ($n = 1 \cdot 10^{-5}$ mol, 0.04 eq.). A sample of the crude mixture was dissolved in acetone-d_6 and analyzed by ^{1}H-NMR spectroscopy (Figure 106; (top) neat adduct **6**, (middle) reaction (a) and (bottom) reaction (b)). Without catalyst no reaction took place whilst in the presence of catalyst degradation occurred. Various by-products were formed (formation of 2-phenoxythyl acrylate (POEA), *n*-butyl acrylate (BuA), *n*-BuOH-urethane **4**, POE-urethane **8** (shoulder in signal of **4**), 2-POE/POEA-adduct **9** and *n*-BuOH/BuA-adduct **10** (shoulder in signal of **6**).

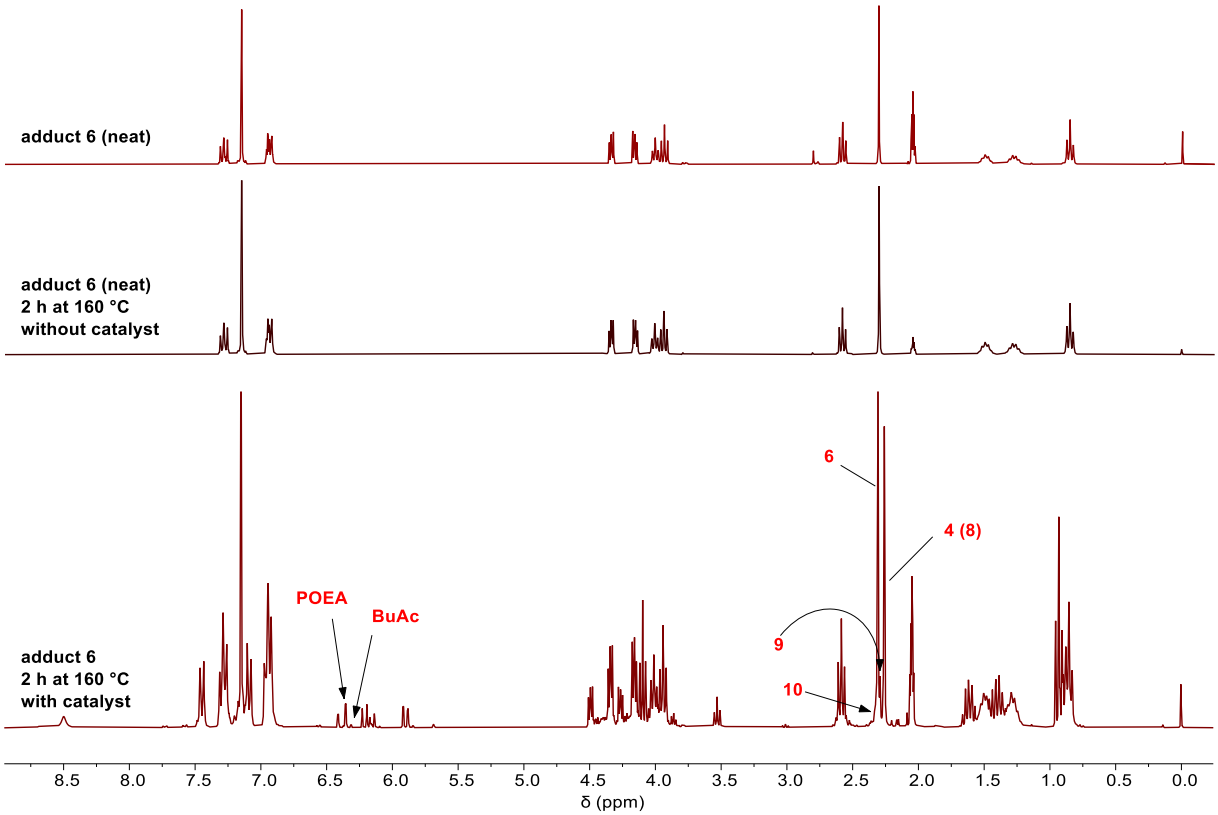

Figure 106. ^{1}H-NMR spectra of (top) neat adduct **6** (before reaction), (middle) neat adduct **6** after 2 h at 160 °C and (bottom) adduct **6** in the presence of catalyst after 2 h at 160 °C (acetone-d_6). The different degradation-related by-products are marked: 2-phenoxythyl acrylate (POEA), *n*-butyl acrylate (BuA), *n*-BuOH-urethane **4**, POE-urethane **8** (shoulder in signal of **4**), 2-POE/POEA-adduct **9** and *n*-BuOH/BuA-adduct **10** (shoulder in signal of **6**).

6.2.5.6 Synthesis of 1,3-di-*p*-tolylurea

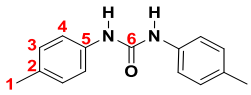

1,3-Di-*p*-tolylurea

The following reaction was carried out under an inert gas atmosphere (Ar), dichloromethane and *p*-toluidine were dried prior to use over molecular sieves (4 Å) for at least three days.

1.242 g *p*-tolyl isocyanate ($n = 9.328 \cdot 10^{-3}$ mol, 1 eq.) was added dropwise to a solution of 1.000 g *p*-toluidine ($n = 9.332 \cdot 10^{-3}$ mol, 1 eq.) in dichloromethane at room temperature while stirring. The precipitate was filtrated after 64.5 h, washed with dichloromethane and dried under reduced pressure.

1,3-Di-*p*-tolylurea was obtained as colorless crystals (2.132 g, $n = 8.872 \cdot 10^{-3}$ mol, ***X* ≈ 95 %**).

^{1}H-NMR (500.13 MHz, acetone-d_6): δ [ppm] = 7.93 (s, 2 H, N-H), 7.52 – 7.26 (m, 4 H, H_4), 7.17 – 6.93 (m, 4 H, H_3), 2.26 (s, 6 H, H_1).

ESI-MS: $m/z_{calc.}$ [$C_{15}H_{16}N_2O$] = 240.13 g/mol, m/z_{found} [M + H^+] = 241.13 g/mol.

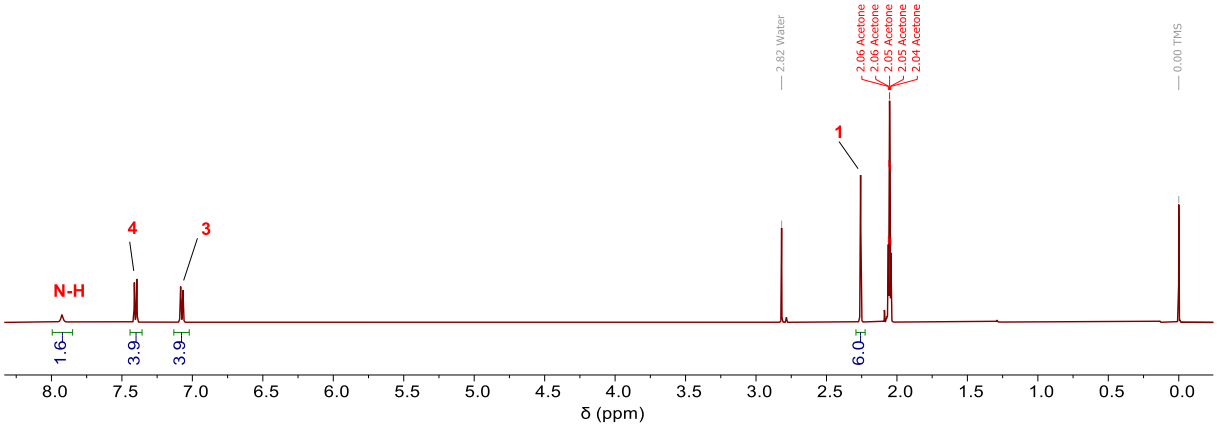

Figure 107. ^{1}H-NMR spectrum of 1,3-di-*p*-tolylurea (acetone-d_6).

6.2.6 Catalyst study

1-Butanol and phenoxyethyl acrylate were dried prior to use over molecular sieves (4 Å) for at least three days. All moisture-sensitive catalysts were dried and stored under inert gas atmosphere (Ar). The standard procedure is given below. The catalyst weight is given in Table 40 – Table 53.

para-Tolyl isocyanate (pTMI) was added to a sealed flask containing 1-butanol (1-BuOH), phenoxyethyl acrylate (POEA) and catalyst. Hygroscopic catalysts were added as a solution in 1-BuOH. The mixture was placed in an oil bath at temperature T_1 and stirred for 1 h. It was then transferred into another oil bath at temperature T_2 and stirred for at least another 3 h. The lid was removed for sampling and a sample taken. The whole process of sampling took place in less than 10 s. The mixture turned yellowish (lower temperatures) or to dark-red (higher temperature) with time depending on the reaction temperature and employed catalyst.

Table 40. Weights for potassium acetate (K Ac) as catalyst. K Ac was added as a solution in 1-BuOH. The weight given below is the absolute amount of K Ac added to the reaction mixture.

Catalyst: K Ac	**1-BuOH**	**POEA**	**pTMI**	**K Ac**
***m* [g]**	0.138	0.357	0.495	0.005
***n* [mol]**	$1.86 \cdot 10^{-3}$	$1.86 \cdot 10^{-3}$	$3.72 \cdot 10^{-3}$	$5 \cdot 10^{-5}$

Table 41. Weights for rubidium acetate (Rb Ac) as catalyst (T_1 = 80 °C). Rb Ac was added as a solution in 1-BuOH. The weight given below is the absolute amount of Rb Ac added to the reaction mixture.

Catalyst: Rb Ac	**1-BuOH**	**POEA**	**pTMI**	**Rb Ac**
***m* [g]**	0.138	0.358	0.496	0.0073
***n* [mol]**	$1.86 \cdot 10^{-3}$	$1.86 \cdot 10^{-3}$	$3.73 \cdot 10^{-3}$	$5.1 \cdot 10^{-5}$

Table 42. Weights for cesium acetate (Cs Ac) as catalyst (T_1 = 60 °C). Cs Ac was added as a solution in 1-BuOH. The weight given below is the absolute amount of Cs Ac added to the reaction mixture.

Catalyst: Cs Ac	**1-BuOH**	**POEA**	**pTMI**	**Cs Ac**
***m* [g]**	0.138	0.357	0.495	0.0097
***n* [mol]**	$1.86 \cdot 10^{-3}$	$1.86 \cdot 10^{-3}$	$3.72 \cdot 10^{-3}$	$5.1 \cdot 10^{-5}$

Table 43. Weights for cesium acetate (Cs Ac) as catalyst at 1/10th of the standard concentration (T_1 = 60 °C). Cs Ac was added as a solution in 1-BuOH. The weight given below is the absolute amount of Cs Ac added to the reaction mixture.

Catalyst: Cs Ac	**1-BuOH**	**POEA**	**pTMI**	**Cs Ac**
***m* [g]**	0.138	0.357	0.495	0.00097
***n* [mol]**	$1.86 \cdot 10^{-3}$	$1.86 \cdot 10^{-3}$	$3.72 \cdot 10^{-3}$	$5.1 \cdot 10^{-6}$

Table 44. Weights for cesium acetate (Cs Ac) as catalyst at 1/100th of the standard concentration (T_1 = 60 °C). Cs Ac was added as a solution in 1-BuOH. The weight given below is the absolute amount of Cs Ac added to the reaction mixture.

Catalyst: Cs Ac	**1-BuOH**	**POEA**	**pTMI**	**Cs Ac**
***m* [g]**	0.138	0.357	0.495	0.000097
***n* [mol]**	$1.86 \cdot 10^{-3}$	$1.86 \cdot 10^{-3}$	$3.72 \cdot 10^{-3}$	$5.1 \cdot 10^{-7}$

Table 45. Weights for potassium octoate (K Oct) as catalyst (T_1 = 60 °C). K Oct was added as a solution in 1-BuOH. The weight given below is the absolute amount of K Oct added to the reaction mixture.

Catalyst: K Oct	**1-BuOH**	**POEA**	**pTMI**	**K Oct**
***m* [g]**	0.138	0.358	0.495	0.0092
***n* [mol]**	$1.86 \cdot 10^{-3}$	$1.86 \cdot 10^{-3}$	$3.72 \cdot 10^{-3}$	$5.0 \cdot 10^{-5}$

Table 46. Weights for rubidium octoate (Rb Oct) as catalyst (T_1 = 60 °C). Rb Oct was added as a solution in 1-BuOH. The weight given below is the absolute amount of Rb Oct added to the reaction mixture.

Catalyst: Rb Oct	**1-BuOH**	**POEA**	**pTMI**	**Rb Oct**
***m* [g]**	0.138	0.357	0.494	0.011
***n* [mol]**	$1.86 \cdot 10^{-3}$	$1.86 \cdot 10^{-3}$	$3.71 \cdot 10^{-3}$	$5.0 \cdot 10^{-5}$

Table 47. Weights for cesium octoate (Cs Oct) as catalyst (T_1 = 60 °C). Cs Oct was added as a solution in 1-BuOH. The weight given below is the absolute amount of Cs Oct added to the reaction mixture.

Catalyst: Cs Oct	**1-BuOH**	**POEA**	**pTMI**	**Cs Oct**
***m* [g]**	0.137	0.356	0.493	0.014
***n* [mol]**	$1.85 \cdot 10^{-3}$	$1.85 \cdot 10^{-3}$	$3.70 \cdot 10^{-3}$	$5.0 \cdot 10^{-5}$

Table 48. Weights for diazabicylco(2.2.2)-octane (DABCO) as catalyst (T_1 = 90 °C).

Catalyst: DABCO	**1-BuOH**	**POEA**	**pTMI**	**DABCO**
***m* [g]**	0.097	0.376	0.521	0.006
***n* [mol]**	$1.31 \cdot 10^{-3}$	$1.96 \cdot 10^{-3}$	$3.92 \cdot 10^{-3}$	$5 \cdot 10^{-5}$

Table 49. Weights for diazabicyclo(5.4.0)undec-7-ene (DBU) as catalyst (T_1 = 90 °C).

Catalyst: DBU	**1-BuOH**	**POEA**	**pTMI**	**DBU**
***m* [g]**	0.102	0.398	0.551	0.008
***n* [mol]**	$1.38 \cdot 10^{-3}$	$2.07 \cdot 10^{-3}$	$4.14 \cdot 10^{-3}$	$5 \cdot 10^{-5}$

Table 50. Weights for 1-methylimidazol (1-MI) as catalyst (T_1 = 90 °C).

Catalyst: 1-MI	**1-BuOH**	**POEA**	**pTMI**	**1-MI**
***m* [g]**	0.097	0.377	0.522	0.004
***n* [mol]**	$1.31 \cdot 10^{-3}$	$1.96 \cdot 10^{-3}$	$3.92 \cdot 10^{-3}$	$5 \cdot 10^{-5}$

Table 51. Weights for N,N-dimethylbenzylamine (BDMA) as catalyst (T_1 = 90 °C).

Catalyst: BDMA	**1-BuOH**	**POEA**	**pTMI**	**BDMA**
***m* [g]**	0.100	0.391	0.541	0.007
***n* [mol]**	$1.36 \cdot 10^{-3}$	$2.03 \cdot 10^{-3}$	$4.07 \cdot 10^{-3}$	$5 \cdot 10^{-5}$

Table 52. Weights for lithium chloride (LiCl) as catalyst. The catalyst was added as a 13.87 wt% LiCl-solution in propylene glycol because of its low molar mass. The weight given below is the absolute amount of LiCl added to the reaction mixture. The composition is for BHT-stabilized (< 1 mg) reactions with a 1 eq. 1-BuOH, 1 eq. POEA and 2 eq. pTMI ratio (T_1 = 80 °C).

Catalyst: LiCl	**1-BuOH**	**POEA**	**pTMI**	**LiCl**
***m* [g]**	0.139	0.360	0.499	0.002
***n* [mol]**	$1.87 \cdot 10^{-3}$	$1.87 \cdot 10^{-3}$	$3.75 \cdot 10^{-3}$	$5 \cdot 10^{-5}$

Table 53. Weights for lithium chloride (LiCl) as catalyst. The catalyst was added as a 13.87 wt% LiCl-solution in propylene glycol because of its low molar mass. The weight given below is the absolute amount of LiCl added to the reaction mixture. The composition is for BHT-stabilized (≈ 10 mg) reactions with a 1 eq. 1-BuOH, 1 eq. POEA and 1 eq. pTMI ratio (T_1 = 80 °C).

Catalyst: LiCl	**1-BuOH**	**POEA**	**pTMI**	**LiCl**
***m* [g]**	0.185	0.480	0.333	0.002
***n* [mol]**	$2.50 \cdot 10^{-3}$	$2.50 \cdot 10^{-3}$	$2.50 \cdot 10^{-3}$	$5 \cdot 10^{-5}$

6.2.6.1 Synthesis of *n*-butyl 1,3-di-*p*-tolyl allophanate

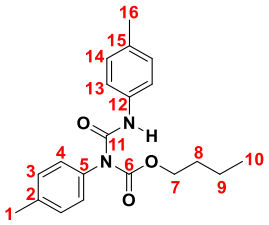

***n*-Butyl 1,3-di-*p*-tolyl allophanate**

The preparation of *n*-butyl 1,3-di-*p*-tolyl allophanate was carried out according to KUMAR *et al*.[203]

The following reaction was carried out under an inert gas atmosphere (Ar), all solvents and chemicals were dried prior to use over molecular sieves (4 Å) for at least three days.

A solution of zirconium(IV) *n*-butoxide (1.65 g, 80 wt% in 1-butanol, *n*(zirconium(IV) *n*-butoxide) = $3.44 \cdot 10^{-3}$ mol, 1 eq.) was heated under reduced pressure at 110 °C to remove 1-butanol. The resulting yellowish paste was dissolved in 10 mL tetrahydrofuran and heated to 35 °C. 4.30 mL *para*-tolyl isocyanate ($n = 3.41 \cdot 10^{-2}$ mol, 10 eq.) were added. The solvent was evaporated after 46.75 h. The mixture was then redissolved in 20 mL dichloromethane and washed with demineralized water (3 times). The organic layer was dried over magnesium sulfate. The crude product was extracted by evaporation of the solvent. The pure product was isolated by column chromatography (PE:EE, 6:1) and recrystallization in acetone.

n-Butyl 1,3-di-*p*-tolyl allophanate was obtained as colorless crystals (2.48 g, $n = 7.29 \cdot 10^{-3}$ mol, ***X* ≈ 53 %**).

^{1}H-NMR (400.13 MHz, acetone-d_6): δ [ppm] = 10.82 (s, 1 H, N-H), 7.45 (d, ^3J(H,H) = 8.5 Hz, 2 H, H_4), 7.23 (d, ^3J(H,H) = 8.1 Hz, 2 H, H_{13}), 7.18 (d, ^3J(H,H) = 8.3 Hz, 2 H, H_{14}), 7.13 (d, ^3J(H,H) = 8.2 Hz, 2 H, H_3), 4.15 (t, ^3J(H,H) = 6.5 Hz, 2 H, H_7), 2.37 (s, 3 H, H_{16}), 2.28 (s, 3 H, H_1), 1.50 (p, ^3J(H,H) = 6.7 Hz, 2 H, H_8), 1.22 (h, ^3J(H,H) = 7.4 Hz, 2 H, H_9), 0.82 (t, ^3J(H,H) = 7.4 Hz, 3 H, H_{10}).

ESI-MS: $m/z_{calc.}$ [$C_{20}H_{24}N_2O_3$] = 340.18 g/mol, m/z_{found} [M + H^+] = 841.19 g/mol.

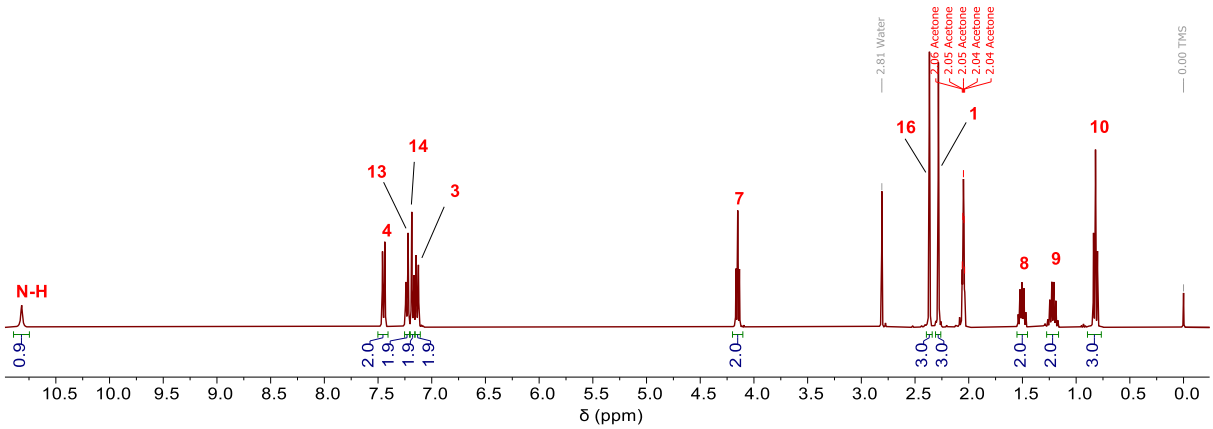

Figure 108. ^{1}H-NMR spectrum of *n*-butyl 1,3-di-*p*-tolyl allophanate (acetone-d_6).

6.2.7 Influence of complexing agents on *aza*-Michael addition

All chemicals were dried prior to use over molecular sieves (4 Å) for at least three days.

A round bottom flask was filled with 1 eq. alcohol (MoPEG500 or 1-hexanol), 1. eq. acrylate (hexyl acrylate or MoPEG480 acrylate), 0.027 eq. potassium octoate and 0.0015 eq. 3,5-di-*tert*-butyl-4-hydroxytoluene (BHT). 2 eq. *para*-tolyl isocyanate (pTMI) was added to this mixture. The flask was closed and stirred at 90 °C for 7 h. Sampling took place hourly for the first 5 h and the final sample was taken after 7 h. All reactions were reproduced once with different sampling times (1, 3, 5 and 7 h). The exact weights and the corresponding amount of substance for each reaction are shown in Table 54, Table 55, Table 56 and Table 57.

Table 54. Exact weights and amount of substance for reactions to determine the influence of polarity (apolar/apolar).

Substance	**1-Hexanol**	**Hexyl acrylate**	**BHT**	**K Oct**	**pTMI**
***m* [g]**	0.512	0.782	0.001	0.026	1.343
***n* [mol]**	$5.01 \cdot 10^{-3}$	$5.01 \cdot 10^{-3}$	$5 \cdot 10^{-6}$	$1.4 \cdot 10^{-4}$	$1.01 \cdot 10^{-2}$
***m* [g]**	0.511	0.780	0.001	0.026	1.336
***n* [mol]**	$5.00 \cdot 10^{-3}$	$4.99 \cdot 10^{-3}$	$5 \cdot 10^{-6}$	$1.4 \cdot 10^{-4}$	$1.00 \cdot 10^{-2}$

Table 55. Exact weights and amount of substance for reactions to determine the influence of polarity (polar/polar).

Substance	MoPEG500	MoPEG480 acrylate	BHT	K Oct	pTMI
***m* [g]**	1.548	1.443	0.001	0.015	0.797
***n* [mol]**	$3.00 \cdot 10^{-3}$	$3.01 \cdot 10^{-3}$	$5 \cdot 10^{-6}$	$8.4 \cdot 10^{-5}$	$5.99 \cdot 10^{-3}$
***m* [g]**	1.555	1.443	0.001	0.015	0.797
***n* [mol]**	$3.01 \cdot 10^{-3}$	$3.01 \cdot 10^{-3}$	$5 \cdot 10^{-6}$	$8.4 \cdot 10^{-5}$	$5.99 \cdot 10^{-3}$

Table 56. Exact weights and amount of substance for reactions to determine the influence of polarity (apolar/polar).

Substance	1-Hexanol	MoPEG480 acrylate	BHT	K Oct	pTMI
***m* [g]**	0.306	1.443	0.001	0.016	0.801
***n* [mol]**	$3.00 \cdot 10^{-3}$	$3.01 \cdot 10^{-3}$	$5 \cdot 10^{-6}$	$8.3 \cdot 10^{-5}$	$6.01 \cdot 10^{-3}$
***m* [g]**	0.306	1.446	0.001	0.015	0.799
***n* [mol]**	$3.00 \cdot 10^{-3}$	$3.01 \cdot 10^{-3}$	$5 \cdot 10^{-6}$	$8.1 \cdot 10^{-5}$	$6.00 \cdot 10^{-3}$

Table 57. Exact weights and amount of substance for reactions to determine the influence of polarity (polar/apolar).

Substance	MoPEG500	Hexyl acrylate	BHT	K Oct	pTMI
***m* [g]**	1.551	0.468	0.001	0.016	0.799
***n* [mol]**	$3.01 \cdot 10^{-3}$	$3.00 \cdot 10^{-3}$	$5 \cdot 10^{-6}$	$8.3 \cdot 10^{-5}$	$6.00 \cdot 10^{-23}$
***m* [g]**	1.553	0.470	0.001	0.015	0.798
***n* [mol]**	$3.01 \cdot 10^{-3}$	$3.01 \cdot 10^{-3}$	$5 \cdot 10^{-6}$	$8.1 \cdot 10^{-5}$	$6.00 \cdot 10^{-23}$

6.2.8 Analysis of isocyanate substitution pattern

Methoxylated poly(ethylene glycol) (MoPEG) and 1-butyl acrylate (BuA) were dried prior to use over molecular sieves (4 Å) for at least three days.

2 Eq. *ortho*-, *meta*- or *para*-tolyl isocyanate (TMI) were added to a flask containing 1 eq. methoxylated poly(ethylene glycol) ($M_n \approx 510$ g/mol), 1 eq. 1-butyl acrylate, 0.003 eq. butylated hydroxytoluene and 0.027 eq. potassium octoate (K Oct). The mixture was heated to 90 °C while stirring for 5 h. Samples were taken hourly or, in case of the reproduction, after 5 h. The reaction mixtures turned yellowish to reddish during the reactions. A precipitate was formed when the para-isomer was used during

the reaction. It was identified as isocyanurate. The employed weights of the reactants for the reaction are shown in Table 58.

The syntheses and characterizations of the corresponding *aza*-Michael adducts are shown in the following subchapter.

Table 58. Weights for reactions based on *ortho*-, *meta*- and *para*-tolyl isocyanate (TMI) (5 h at 90 °C).

	MoPEG	**BuA**	**BHT**	**K Oct**	**TMI**
***m* [g]**	1.000	0.248	0.001	0.010	0.516
***n* [mol]**	$1.94 \cdot 10^{-3}$	$1.94 \cdot 10^{-3}$	$6 \cdot 10^{-6}$	$5.5 \cdot 10^{-5}$	$3.88 \cdot 10^{-3}$

6.2.8.1 *ortho*-Tolyl isocyanate based adduct

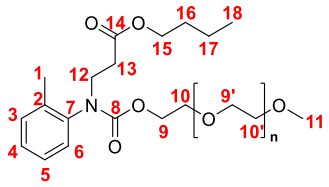

***ortho*-Tolyl isocyanate based adduct**

Methoxylated poly(ethylene glycol) and butyl acrylate were dried prior to use over molecular sieves (4 Å) for at least three days.

0.516 g *ortho*-tolyl isocyanate ($n = 3.88 \cdot 10^{-3}$ mol, 2 eq.) was added to a mixture containing 1.001 g methoxylated poly(ethylene glycol) ($M_n \approx 510$ g/mol, $n = 1.96 \cdot 10^{-3}$ mol, 1 eq.), 0.748 g butyl acrylate ($n = 5.83 \cdot 10^{-3}$ mol, 3 eq.), 0.001 g butylated hydroxytoluene ($n = 5 \cdot 10^{-6}$ mol, 0.003 eq.) and 0.010 g potassium octoate ($n = 5.3 \cdot 10^{-5}$ mol, 0.03 eq.). The reaction was heated to 90 °C and stirred for 3.5 h. The crude product was dissolved in a mixture of petroleum ether and ethyl acetate (2/1) after cooling to room temperature and filtered over silica (0.04 – 0.063 mm, eluent: petroleum ether/ethyl acetate 2/1). The silica was washed with a mixture of petroleum ether and ethyl acetate (2/1). It was then slurried in acetone for at least three times. The dry and purified product was obtained after evaporation of the organic solvent at reduced pressure.

The *aza*-Michael adduct was obtained as a colorless and low-viscosity liquid (1.242 g, $1.610\ 10^{-3}$ mol, ***X* ≈ 82 %**).

^{1}H-NMR (500.13z MHz, acetone-d_6): δ [ppm] = 7.31 – 7.25 (m, 1 H, H_5), 7.25 – 7.17 (m, 3 H, H_3, H_4, H_6), 4.31 – 4.14 (m, 1 H, H_{9a}), 4.10 – 4.01 (m, 2 H, H_{9b}, H_{12a}), 3.99 (t,

^3J(H,H) = 6.7 Hz, 2 H, H_{15}), 3.80 – 3.67 (m, 1 H, H_{12b}), 3.67 – 3.36 (m, 36 H, $H_{9'}$, H_{10}, $H_{10'}$), 3.29 (s, 3 H, H_{11}), 2.70 – 2.52 (m, 2 H, H_{13a}, H_{13b}), 2.22 (s, 3 H, H_1), 1.59 – 1.49 (m, 2 H, H_{16}), 1.34 (h, 2 H, ^3J(H,H) = 7.4 Hz, H_{17}), 0.90 (t, ^3J(H,H) = 7.4 Hz, 3 H, H_{18}).

ESI-MS: $m/z_{calc.}$ [$C_{36}H_{63}NO_{14}$] = 733.42 g/mol, m/z_{found} [M + NH_4^+] = 751.46 g/mol.

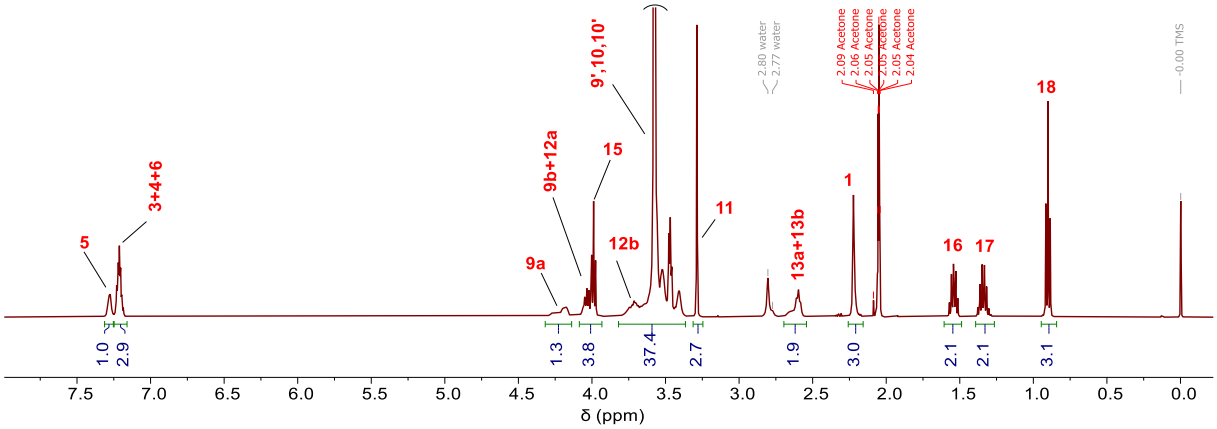

Figure 109. ^{1}H-NMR spectrum of *ortho*-Tolyl isocyanate *aza*-Michael adduct (acetone-d_6).

6.2.8.2 *meta*-Tolyl isocyanate based adduct

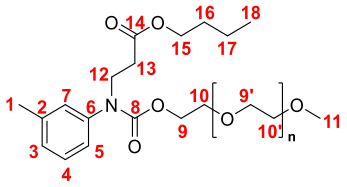

***meta*-Tolyl isocyanate based adduct**

Methoxylated poly(ethylene glycol) and butyl acrylate were dried prior to use over molecular sieves (4 Å) for at least three days.

0.518 g *meta*-Tolyl isocyanate (n = 3.89 · 10^{-3} mol, 2 eq.) was added to a mixture containing 1.007 g methoxylated poly(ethylene glycol) (M_n ≈ 510 g/mol, n = 1.96 · 10^{-3} mol, 1 eq.), 0.746 g butyl acrylate (n = 5.82 · 10^{-3} mol, 3 eq.), 0.001 g butylated hydroxytoluene (n = 5 · 10^{-6} mol, 0.003 eq.) and 0.011 g potassium octoate (n = 6.1 · 10^{-5} mol, 0.03 eq.). The reaction was heated to 90 °C and stirred for 3.5 h. The crude product was cooled to room temperature, dissolved in a mixture of petroleum ether and ethyl acetate (2/1) and filtered over silica (0.04 – 0.063 mm, eluent: petroleum ether/ethyl acetate 2/1). The silica was washed with a mixture of petroleum ether and ethyl acetate (2/1). It was then slurried in acetone for at least three times. The dry and purified product was obtained after evaporation of the organic solvent at reduced pressure.

The *aza*-Michael adduct was obtained as a colorless and low-viscosity liquid (1.135 g, $1.47 \cdot 10^{-3}$ mol, ***X* ≈ 75 %**).

^{1}H-NMR (500.13z MHz, acetone-d_6): δ [ppm] = 7.26 (t, ^3J(H,H) = 7.7 Hz, 1 H, H_4), 7.12 (s, 1 H, H_7), 7.10 – 7.06 (m, 2 H, H_3, H_5), 4.17 (t, ^3J(H,H) = 4.9 Hz, 2 H, H_9), 3.98 (t, ^3J(H,H) = 6.7 Hz, 2 H, H_{15}), 3.94 (t, ^3J(H,H) = 7.3 Hz, 2 H, H_{12}), 3.65 – 3.45 (m, 37 H, $H_{9'}$, H_{10}, $H_{10'}$), 3.29 (s, 3 H, H_{11}), 2.59 (t, ^3J(H,H) = 7.3 Hz, 2 H, H_{13}), 2.34 (s, 3 H, H_1), 1.58 – 1.51 (m, 2 H, H_{16}), 1.39 – 1.30 (m, 2 H, H_{17}), 0.90 (t, ^3J(H,H) = 7.4 Hz, 3 H, H_{18}).

ESI-MS: $m/z_{calc.}$ [$C_{36}H_{63}NO_{14}$] = 733.42 g/mol, m/z_{found} [M + NH_4^+] = 751.46 g/mol.

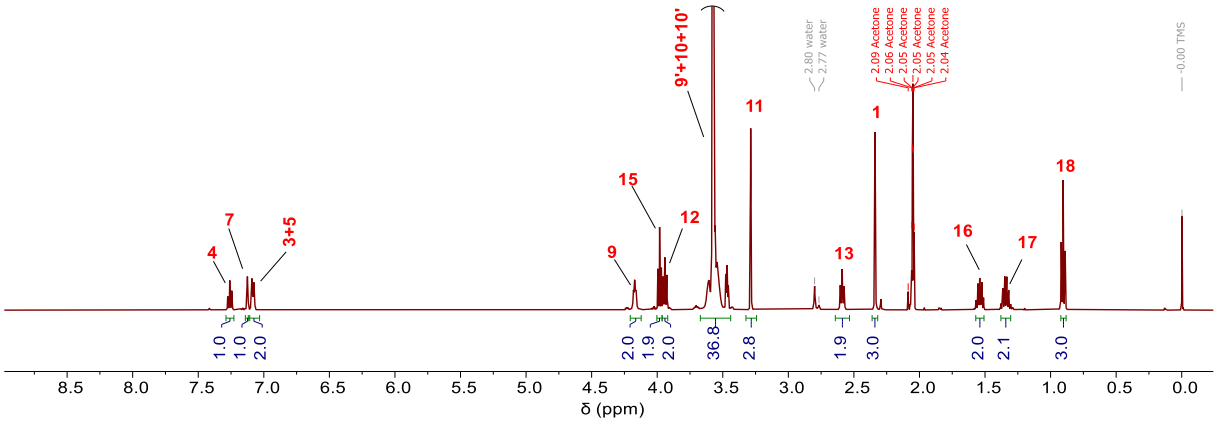

Figure 110. ^{1}H-NMR spectrum of *meta*-Tolyl isocyanate *aza*-Michael adduct (acetone-d_6).

6.2.8.3 *para*-Tolyl isocyanate based adduct

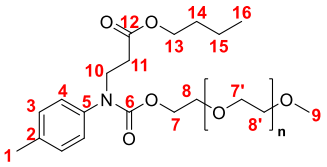

***para*-Tolyl isocyanate based adduct**

Methoxylated poly(ethylene glycol) and butyl acrylate were dried prior to use over molecular sieves (4 Å) for at least three days.

0.523 g *para*-Tolyl isocyanate ($n = 3.93 \cdot 10^{-3}$ mol, 2 eq.) was added to a mixture containing 1.001 g methoxylated poly(ethylene glycol) ($M_n \approx 510$ g/mol, $n = 1.96 \cdot 10^{-3}$ mol, 1 eq.), 0.756 g butyl acrylate ($n = 5.90 \cdot 10^{-3}$ mol, 3 eq.), 0.001 g butylated hydroxytoluene ($n = 5 \cdot 10^{-6}$ mol, 0.003 eq.) and 0.011 g potassium octoate ($n = 6.1 \cdot 10^{-5}$ mol, 0.03 eq.). The reaction was heated quickly to 90 °C and stirred for 7 h. The crude product was cooled to room temperature, dissolved in a mixture of petroleum ether and ethyl acetate (2/1) and filtered over silica (0.04 – 0.063 mm,

eluent: petroleum ether/ethyl acetate 2/1). The silica was washed with a mixture of petroleum ether and ethyl acetate (2/1). It was then slurried in acetone for at least three times. The dry and purified product was obtained after evaporation of the organic solvent at reduced pressure.

The *aza*-Michael adduct was obtained as a colorless and low-viscosity liquid (1.193 g, $1.55 \cdot 10^{-3}$ mol, ***X* ≈ 79 %**).

^{1}H-NMR (500.13z MHz, acetone-d_6): δ [ppm] = 7.32 – 7.13 (m, 4 H, H_3, H_4), 4.16 (t, ^3J(H,H) = 4.9 Hz, 2 H, H_7), 3.98 (t, ^3J(H,H) = 6.6 Hz, 2 H, H_{13}), 3.93 (t, ^3J(H,H) = 7.2 Hz, 2 H, H_{10}), 3.67 – 3.43 (m, 40 H, $H_{7'}$, H_8, $H_{8'}$), 3.29 (s, 3 H, H_9), 2.58 (t, ^3J(H,H) = 7.3 Hz, 2 H, H_{11}), 2.33 (s, 3 H, H_1), 1.58 – 1.48 (m, 2 H, H_{14}), 1.44 – 1.26 (m, 2 H, H_{15}), 0.90 (t, ^3J(H,H) = 7.3 Hz, 3 H, H_{16}).

ESI-MS: $m/z_{calc.}$ [$C_{36}H_{63}NO_{14}$] = 733.42 g/mol, m/z_{found} [M + H^+] = 734.43 g/mol.

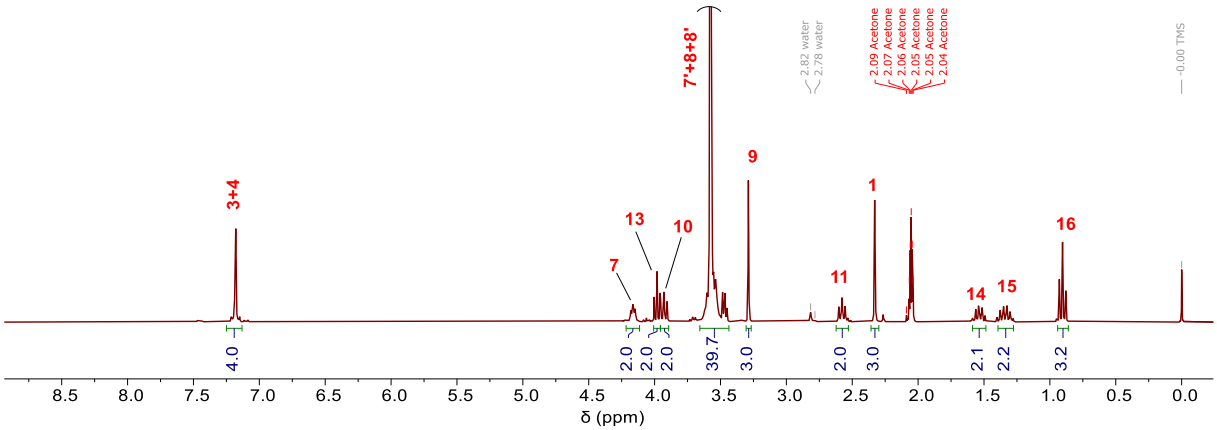

Figure 111. ^{1}H-NMR spectrum of *para*-Tolyl isocyanate *aza*-Michael adduct (acetone-d_6).

6.2.9 Competitive reactions with AMA

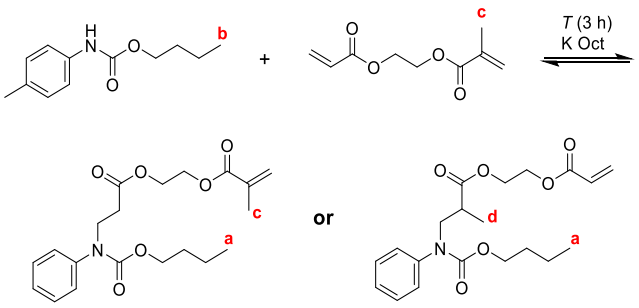

Competitive reactions with 2-methylacryloylethyl acrylate

All substances were dried prior to use by addition of molecular sieve (4 Å) and storage for several days (at least three).

A sealed round bottom flask containing either 1 eq. 1-butanol, 1 eq. 2-methylacryloyloxyethyl acrylate, 2 eq. *p*-tolyl isocyanate and 0.27 eq. potassium acetate or 1 eq. 1-butanol, 0.5 eq. 2-methylacryloyloxyethyl acrylate, 2 eq. *p*-tolyl isocyanate and 0.27 eq. potassium acetate was stirred in a preheated oil bath (either T = 90 – 120 °C, ΔT = 10 °C or T = 120 °C) for 3 h. A sample was taken, dissolved in acetone-d_6 and analyzed by ^{1}H-NMR spectroscopy.

The weights for all reactions are given in the following tables.

Table 59. Competitive reaction at 90 °C with 1-butanol (1-BuOH), 2-methylacryloyloxyethyl acrylate (AMA), potassium octoate (K Oct) and *p*-tolyl isocyanate (pTMI).

Substance	**1-BuOH**	**AMA**	**K Oct**	**pTMI**
***m* [g]**	0.141	0.346	0.010	0.504
***n* [mol]**	$1.89 \cdot 10^{-3}$	$1.88 \cdot 10^{-3}$	$5.4 \cdot 10^{-5}$	$3.78 \cdot 10^{-3}$

Table 60. Competitive reaction at 100 °C with 1-butanol (1-BuOH), 2-methylacryloyloxyethyl acrylate (AMA), potassium octoate (K Oct) and *p*-tolyl isocyanate (pTMI).

Substance	**1-BuOH**	**AMA**	**K Oct**	**pTMI**
***m* [g]**	0.143	0.346	0.010	0.506
***n* [mol]**	$1.93 \cdot 10^{-3}$	$1.88 \cdot 10^{-3}$	$5.4 \cdot 10^{-5}$	$3.80 \cdot 10^{-3}$

Table 61. Competitive reaction at 110 °C with 1-butanol (1-BuOH), 2-methylacryloyloxyethyl acrylate (AMA), potassium octoate (K Oct) and *p*-tolyl isocyanate (pTMI).

Substance	**1-BuOH**	**AMA**	**K Oct**	**pTMI**
***m* [g]**	0.142	0.346	0.009	0.502
***n* [mol]**	$1.92 \cdot 10^{-3}$	$1.88 \cdot 10^{-3}$	$5.1 \cdot 10^{-5}$	$3.77 \cdot 10^{-3}$

Table 62. Competitive reaction at 120 °C with 1-butanol (1-BuOH), 2-methylacryloyloxyethyl acrylate (AMA), potassium octoate (K Oct) and *p*-tolyl isocyanate (pTMI).

Substance	**1-BuOH**	**AMA**	**K Oct**	**pTMI**
***m* [g]**	0.145	0.348	0.010	0.509
***n* [mol]**	$1.95 \cdot 10^{-3}$	$1.89 \cdot 10^{-3}$	$5.4 \cdot 10^{-5}$	$3.82 \cdot 10^{-3}$

Table 63. Competitive reaction at 120 °C with 1-butanol (1-BuOH), 2-methylacryloyloxyethyl acrylate (AMA), potassium octoate (K Oct) and *p*-tolyl isocyanate (pTMI).

Substance	**1-BuOH**	**AMA**	**K Oct**	**pTMI**
***m* [g]**	0.170	0.216	0.009	0.612
***n* [mol]**	$2.29 \cdot 10^{-3}$	$1.17 \cdot 10^{-3}$	$5.1 \cdot 10^{-5}$	$4.59 \cdot 10^{-3}$

^{1}H-NMR spectra of the reaction at 90 – 120 °C were normalized to the terminal methyl group of the product (a). The ratio of (a), urethane (b) and the methyl-group of the

methacrylate functionality (c) were compared. Signal (c) should be equal to the sum of (a) + (b) in case the methacrylic double bond would not react. Signal (c), however, should shift and thereby its integral would be reduced if the methacrylic double reacted. The sum of (a) + (b) was always similar to signal (c). Only additions according to option a were observed. Addition to the methacrylate did not occur (Figure 112).

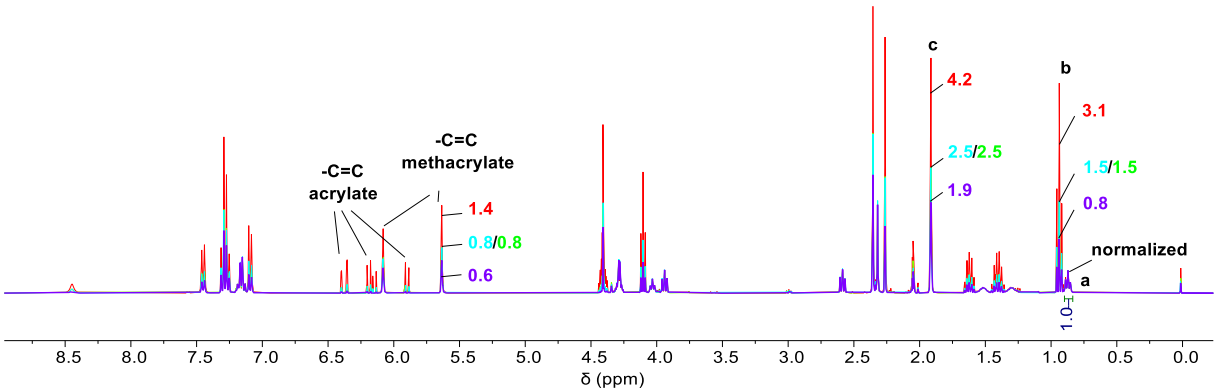

Figure 112. ^{1}H-NMR spectra of experiments based on 1 eq. 1-BuOH, 1 eq. AMA and 2 eq. pTMI as a function of *T* (after 3 h at red = 90 °C, turquoise = 100 °C, green = 110 °C, purple = 120 °C, normalized to adduct; spectra in acetone-d_6).

Signal (c) was equal to (a) indicating no conversion when an excess of *in-situ* formed urethane was used (Figure 113).

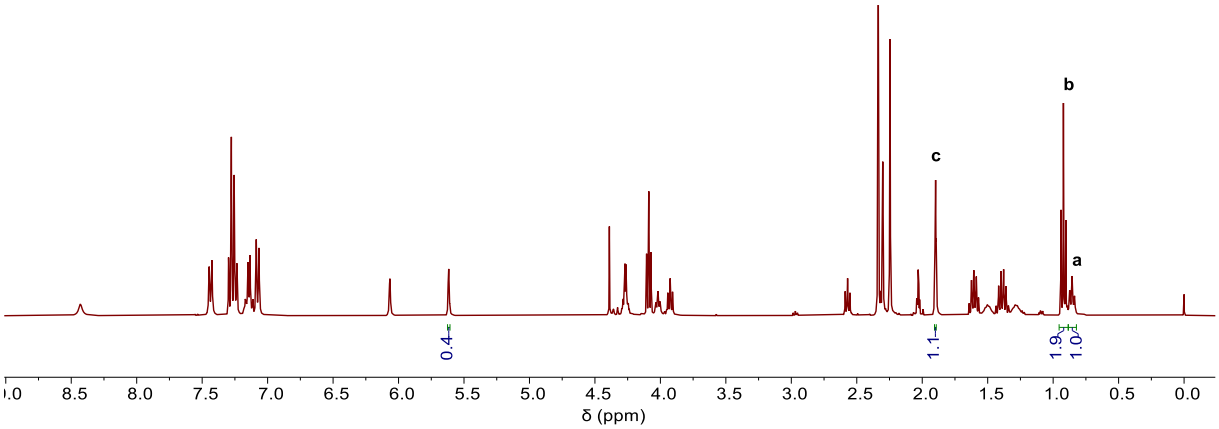

Figure 113. ^{1}H-NMR spectrum of experiment based on 1 eq. 1-BuOH, 0.5 eq. AMA and 2 eq. pTMI after 3 h at 120 °C (acetone-d_6).

6.2.10 Synthesis of [AB]-type monomers and polymerizations thereof

6.2.10.1 2-[(*p*-Tolylcarbamoyl)oxy]ethyl acrylate

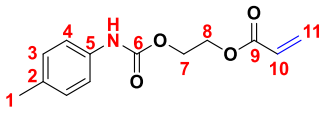

2-[(*p*-Tolylcarbamoyl)oxy]ethyl acrylate

5.159 g *para*-Tolyl isocyanate ($n = 3.874 \cdot 10^{-2}$ mol, 1 eq.) was added dropwise to a flask containing 4.782 g 2-hydroxyethyl acrylate ($n \approx 4.118 \cdot 10^{-2}$ mol, 1.06 eq.) at 40 °C. The mixture was stirred for 16 h before the temperature was raised to 60 °C. The reaction was stopped after 2 h. The crystalline crude product was purified by multiple dispersing steps in boiling water and rapid mixing. The water was decanted off. The colorless crystals were then dissolved in acetone and dried over $MgSO_4$. The product was isolated by evaporation of the solvent under reduced pressure.

2-[(*p*-Tolylcarbamoyl)oxy]ethyl acrylate was isolated as colorless crystals (6.728 g, $n = 2.670 \cdot 10^{-2}$ mol, ***X* ≈ 70 %**).

^{1}H-NMR (300.21 MHz, acetone-d_6): δ [ppm] = 8.63 (s, 1 H, N-H), 7.45 (d, ^3J(H,H) = 8.5 Hz, 2 H, H_4), 7.10 (d, ^3J(H,H) = 8.5 Hz, 2 H, H_3), 6.38 (dd, ^3J(H,H) = 17.3 Hz, ^2J(H,H) = 1.7 Hz, 1 H, $H_{11(Z)}$), 6.17 (dd, ^3J(H,H) = 17.3, 10.3 Hz, 1 H, H_{10}), 5.91 (dd, ^3J(H,H) = 10.3 Hz, ^2J(H,H) = 1.7 Hz, 1 H, $H_{11(E)}$), 4.48 – 4.25 (m, 4 H, H_7, H_8), 2.27 (s, 3 H, H_1).

ESI-MS: $m/z_{calc.}$ [$C_{13}H_{15}NO_4$] = 249.10 g/mol, m/z_{found} [M + Na^+] = 272.09 g/mol.

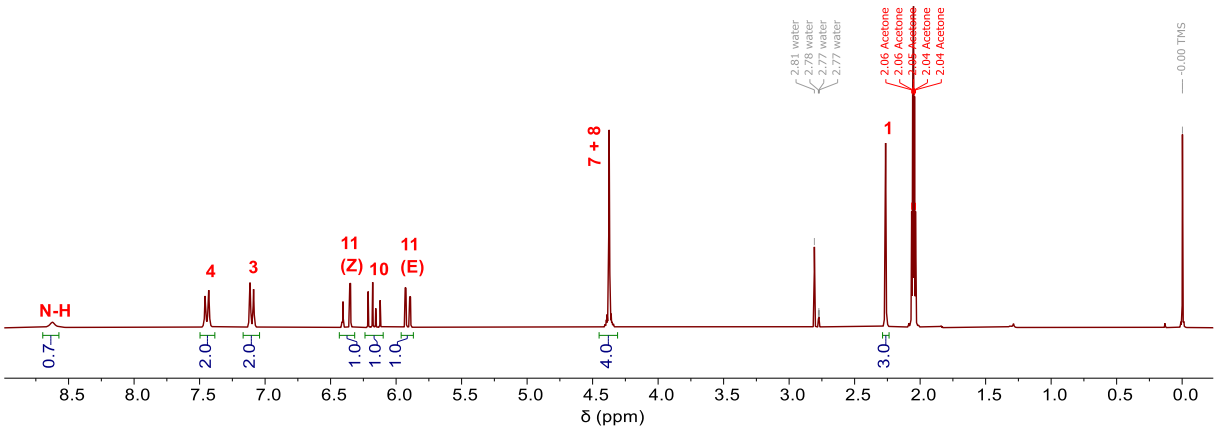

Figure 114. ^{1}H-NMR spectrum of 2-[(*p*-tolylcarbamoyl)oxy]ethyl acrylate (acetone-d_6).

6.2.10.2 2-[(*p*-Tolylcarbamoyl)oxy]ethyl methacrylate

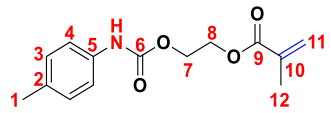

2-[(*p*-Tolylcarbamoyl)oxy]ethyl methacrylate

5.058 g *para*-Tolyl isocyanate (n = 3.799 · 10^{-2} mol, 1 eq.) was added dropwise to a flask containing 5.322 g 2-hydroxyethyl methacrylate (n ≈ 4.090 · 10^{-2} mol, 1.08 eq.) at 40 °C. The mixture was stirred for 16 h. The temperature was raised to 60 °C as an IR-sample showed unreacted isocyanate. The reaction temperature was further increased after 3 h to 125 °C and stirred for 18 h. The crystalline crude product was purified by multiple dispersing steps in boiling water and rapid mixing. The water was decanted off. The colorless crystals were then dissolved in acetone and dried over $MgSO_4$. The product was isolated by evaporation of the solvent under reduced pressure.

2-[(*p*-Tolylcarbamoyl)oxy]ethyl methacrylate was isolated as colorless crystals (7.330 g, n = 2.784 · 10^{-2} mol, ***X* ≈ 73 %**).

^{1}H-NMR (300.21 MHz, acetone-d_6): δ [ppm] = 8.62 (s, 1 H, N-H), 7.43 (d, ^3J(H,H) = 8.4 Hz, 2 H, H_4), 7.10 (d, ^3J(H,H) = 8.4 Hz, 2 H, H_3), 6.14 – 6.02 (m, 1 H, $H_{11(Z)}$), 5.64 (dq, ^4J(H,H) = 3.2 Hz, ^2J(H,H) = 1.6 Hz, 1 H, $H_{11(E)}$), 4.44 – 4.31 (m, 4 H, H_7, H_8), 2.26 (s, 3 H, H_1), 1.91 (dq, ^4J(H,H) = 3.4 Hz, ^2J(H,H) = 1.6 Hz, 3 H, H_{12}).

ESI-MS: $m/z_{calc.}$ [$C_{14}H_{17}NO_4$] = 263.12 g/mol, m/z_{found} [M + Na^+] = 286.11°g/mol.

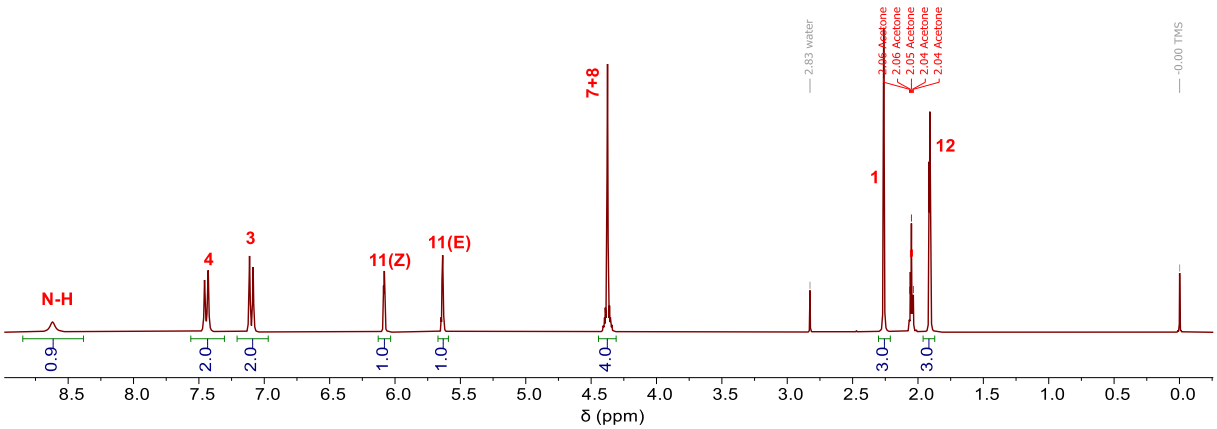

Figure 115. ^{1}H-NMR spectrum of 2-[(*p*-tolylcarbamoyl)oxy]ethyl methacrylate (acetone-d_6).

6.2.10.3 [AB]-type polymerizations

All polymerizations based on an *aza*-Michael-type polyaddition reaction using 2-[(*n*butylcarbamoyl)oxy]ethyl acrylate and 2-[(*p*-tolylcarbamoyl)oxy]ethyl acrylate were conducted as followed: Each monomer (1 eq.) was mixed with approx. 0.027 eq. catalyst and approx. 0.002 eq. radical inhibitor. The solvent-free reaction mixture was heated up to the reaction temperature while stirring. The viscosity increased continuously during the reaction as the *aza*-Michael reaction took place. The samples were dissolved in acetone-d_6 directly after sampling and analyzed using ^{1}H-NMR spectroscopy. No *aza*-Michael reaction was observed when 2-[(*n*butylcarbamoyl)oxy]ethyl acrylate was used.

The weight amounts of reactants for each reaction at a given reaction temperature are shown in Table 64 for 2-[(*n*butylcarbamoyl)oxy]ethyl acrylate and Table 65 for 2-[(*p*-tolylcarbamoyl)oxy]ethyl acrylate.

Table 64. Weights *m*, molar mass *n* and temperature *T* for reactions using 2-[(*n*butylcarbamoyl)oxy]ethyl acrylate.

T	$m_{monomer}$	$n_{monomer}$	$m_{K\ Oct}$	$n_{K\ Oct}$	m_{BHT}	n_{BHT}
[°C]	**[g]**	**[mol]**	**[g]**	**[mol]**	**[g]**	**[mol]**
110	0.504	$2.34 \cdot 10^{-3}$	0.010	$5.5 \cdot 10^{-5}$	0.001	$5 \cdot 10^{-6}$
120	0.503	$2.34 \cdot 10^{-3}$	0.010	$5.5 \cdot 10^{-5}$	0.001	$5 \cdot 10^{-6}$
130	0.499	$2.32 \cdot 10^{-3}$	0.010	$5.5 \cdot 10^{-5}$	0.001	$5 \cdot 10^{-6}$

Table 65. Weights *m*, molar mass *n* and temperature *T* for reactions using 2-[(*p*-tolylcarbamoyl)oxy]ethyl acrylate. The reaction at 130 °C was a blank-reaction without the addition of catalyst.

T	$m_{monomer}$	$n_{monomer}$	$m_{K\ Oct}$	$n_{K\ Oct}$	m_{BHT}	n_{BHT}
[°C]	**[g]**	**[mol]**	**[g]**	**[mol]**	**[g]**	**[mol]**
90	0.500	$2.00 \cdot 10^{-3}$	0.010	$5.5 \cdot 10^{-5}$	0.003	$6 \cdot 10^{-6}$
100	1.000	$4.01 \cdot 10^{-3}$	0.020	$1.1 \cdot 10^{-4}$	0.001	$5 \cdot 10^{-6}$
110	1.004	$4.03 \cdot 10^{-3}$	0.020	$1.1 \cdot 10^{-4}$	0.003	$1 \cdot 10^{-5}$
120	0.998	$4.00 \cdot 10^{-3}$	0.020	$1.1 \cdot 10^{-4}$	0.003	$1 \cdot 10^{-5}$
130	0.502	$2.01 \cdot 10^{-3}$	-	-	0.001	$5 \cdot 10^{-6}$

6.3 Surfactants

6.3.1 General synthesis of surfactants based on MoPEG-pTMI-urethane

All surfactants based on acrylate, methoxylated poly(ethylene glycol) and *para*-tolyl isocyanate were synthesized as described below. The general structure is shown in Figure 116. The weight amounts of reactants and additional reaction parameters for the preparation of each surfactant are given in the corresponding subsection.

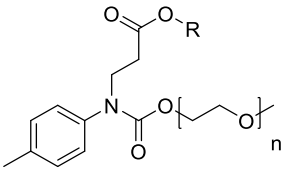

Figure 116. General backbone of all surfactants based on MoPEG and pTMI.

Para-tolyl isocyanate (2 eq.) was added to a round bottom flask containing methoxylated poly(ethylene glycol) (1 eq.), acrylate (3 eq.), 2,6-di-*tert*-butyl-*p*-cresol (0.02 eq.) and potassium octoate (0.03 eq.). The mixture was then stirred for a time, *t*, at a temperature, *T*. The crude product was dissolved in a mixture of petroleum ether and ethyl acetate (1/1 or 2/1) and filtered over silica (0.04 – 0.063 mm, eluent: petroleum ether/ethyl acetate 1/1 or 2/1). The silica was washed with a mixture of petroleum ether and ethyl acetate (1/1 or 2/1). It was subsequently slurried in acetone for at least three times. The dry and purified product was obtained after evaporation of the organic solvent at reduced pressure.

6.3.1.1 Butyl acrylate-based surfactant (S1)

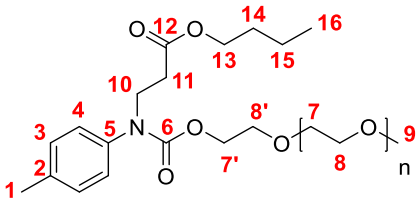

Surfactant S1

Surfactant **S1** was obtained as a colorless and low-viscosity liquid (1.193 g, $1.60 \cdot 10^{-3}$ mol, ***X* ≈ 81 %**, $R_{urethane}$ ≈ 7 %).

Table 66. Exact weights of synthesis to surfactant **S1** (*t* = 3.5 h, *T* = 90 °C).

Substance	Butyl acrylate	MoPEG500	BHT	K Oct	pTMI
***m* [g]**	0.756	1.001	0.001	0.011	0.523
***n* [mol]**	$5.82 \cdot 10^{-3}$	$1.96 \cdot 10^{-3}$	$5 \cdot 10^{-6}$	$6.1 \cdot 10^{-5}$	$3.93 \cdot 10^{-3}$

^{1}H-NMR (500.13z MHz, acetone-d_6): δ [ppm] = 7.32 – 7.13 (m, 4 H, H_3, H_4), 4.16 (t, ^3J(H,H) = 4.9 Hz, 2 H, H_7), 3.98 (t, ^3J(H,H) = 6.6 Hz, 2 H, H_{13}), 3.93 (t, ^3J(H,H) = 7.2 Hz, 2 H, H_{10}), 3.67 – 3.43 (m, 40 H, $H_{7'}$, H_8, $H_{8'}$), 3.29 (s, 3 H, H_9), 2.58 (t, ^3J(H,H) = 7.3 Hz, 2 H, H_{11}), 2.33 (s, 3 H, H_1), 1.58 – 1.48 (m, 2 H, H_{14}), 1.44 – 1.26 (m, 2 H, H_{15}), 0.90 (t, ^3J(H,H) = 7.3 Hz, 3 H, H_{16}).

ESI-MS: $m/z_{calc.}$ [$C_{36}H_{63}NO_{14}$] = 733.42 g/mol, m/z_{found} [M + H^+] = 734.43 g/mol.

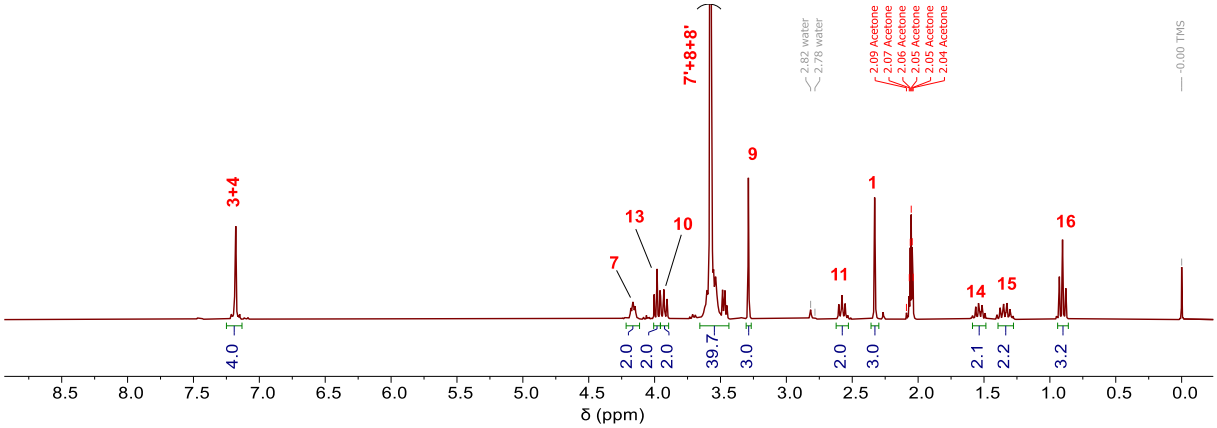

Figure 117. ^{1}H-NMR spectrum of surfactant **S1** (acetone-d_6).

6.3.1.2 Hexyl acrylate-based surfactant (S2)

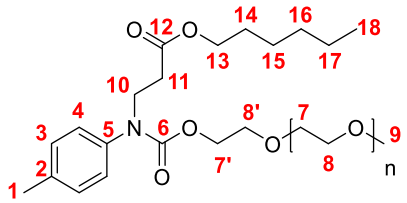

Surfactant S2

Surfactant **S2** was obtained as a colorless and low-viscosity liquid (7.866 g, $9.760\ 10^{-3}$ mol, ***X* ≈ 79 %**, $R_{urethane}$ ≈ 6 %).

Table 67. Exact weights of synthesis to surfactant S2 (t = 5 h, T = 90 °C).

Substance	Hexyl acrylate	MoPEG500	BHT	K Oct	pTMI
***m* [g]**	5.839	6.413	0.063	0.061	3.309
***n* [mol]**	$3.738 \cdot 10^{-2}$	$1.241 \cdot 10^{-2}$	$2.9 \cdot 10^{-4}$	$3.3 \cdot 10^{-4}$	$2.485 \cdot 10^{-2}$

^{1}H-NMR (300.21 MHz, acetone-d_6): δ [ppm] = 7.18 (s, 4 H, H_3, H_4), 4.20 – 4.13 (m, 2 H, $H_{7'}$), 3.98 (t, ^3J(H,H) = 6.6 Hz, 2 H, H_{13}), 3.93 (t, ^3J(H,H) = 7.4 Hz, 2 H, H_{10}), 3.66 – 3.43 (m, 42 H, H_7, H_8, $H_{8'}$), 3.29 (s, 3 H, H_9), 2.58 (t, ^3J(H,H) = 7.3 Hz, 2 H, H_{11}), 2.33 (s, 3 H, H_1), 1.63 – 1.48 (m, 2 H, H_{14}), 1.39 – 1.21 (m, 6 H, H_{15}, H_{16}, H_{17}), 0.96 – 0.81 (m, 3 H, H_{18}).

ESI-MS: $m/z_{calc.}$ [$C_{40}H_{71}NO_{15}$] = 805.48 g/mol, m/z_{found} [M + H^+] = 806.49 g/mol.

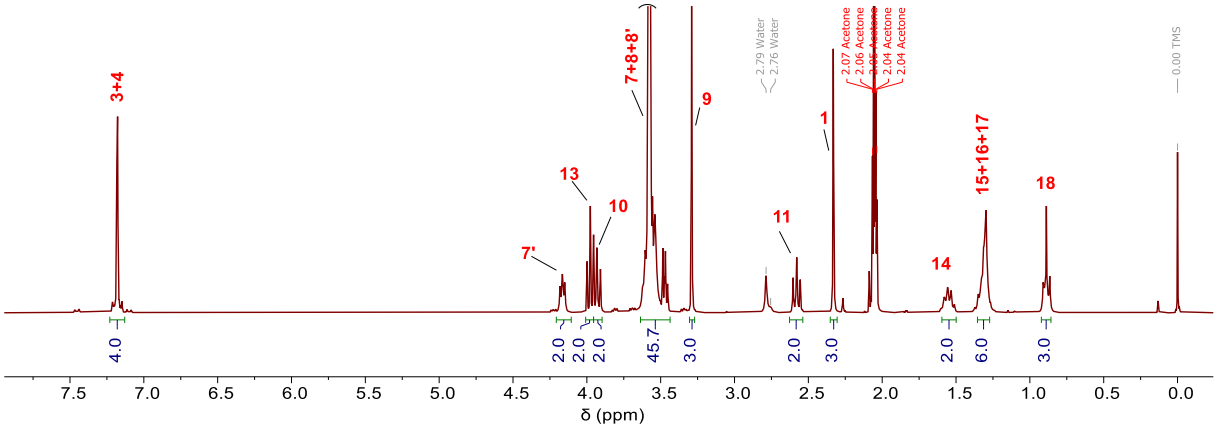

Figure 118. ^{1}H-NMR spectrum of surfactant **S2** (acetone-d_6).

6.3.1.3 Stearyl acrylate-based surfactant (S3)

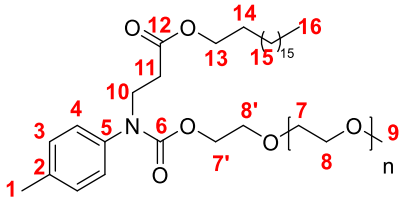

Surfactant S3

Surfactant **S3** was obtained as a colorless and medium-viscosity liquid (4.149 g, 4.258 10^{-3} mol, ***X* ≈ 83 %**, $R_{urethane}$ ≈ 5 %).

Table 68. Exact weights of synthesis to surfactant **S3** (t = 24 h, T = 90 °C).

Substance	Stearyl acrylate	MoPEG500	BHT	K Oct	pTMI
***m* [g]**	4.973	2.664	0.061	0.027	1.394
***n* [mol]**	$1.532 \cdot 10^{-2}$	$5.160 \cdot 10^{-3}$	$2.8 \cdot 10^{-4}$	$1.5 \cdot 10^{-4}$	$1.047 \cdot 10^{-2}$

^{1}H-NMR (400.13 MHz, acetone-d_6): δ [ppm] = 7.17 (s, 4 H, H_3, H_4), 4.16 (t, ^3J(H,H) = 4. 9 Hz, 2 H, $H_{7'}$), 3.97 (t, ^3J(H,H) = 6.7 Hz, 2 H, H_{13}), 3.93 (t, ^3J(H,H) = 7.2 Hz, 2 H, H_{10}), 3.66 – 3.42 (m, 42 H, H_7, H_8, $H_{8'}$), 3.29 (s, 3 H, H_9), 2.58 (t, ^3J(H,H) = 7.3 Hz, 2 H, H_{11}), 2.33 (s, 3 H, H_1), 1.56 (t, ^3J(H,H) = 6.7 Hz, 2 H, H_{14}), 1.29 (m, 30 H, H_{15}), 0.93 – 0.81 (m, 3 H, H_{16}).

ESI-MS: $m/z_{calc.}$ [$C_{52}H_{95}NO_{15}$] = 973.67 g/mol, m/z_{found} [M + H^+] = 974.68 g/mol.

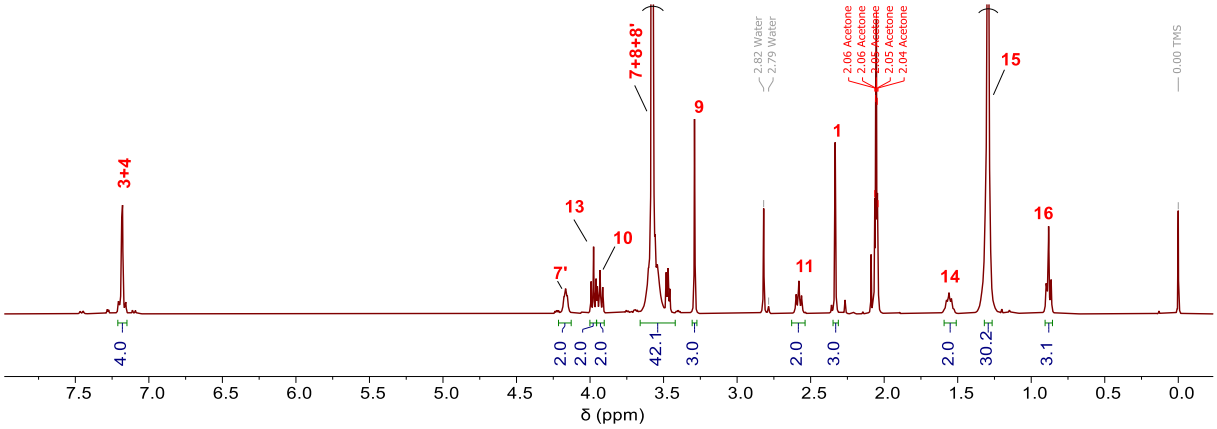

Figure 119. ^{1}H-NMR spectrum of surfactant **S3** (acetone-d_6).

6.3.1.4 2,4-Dimethyl-3-pentyl acrylate-based surfactant (S4)

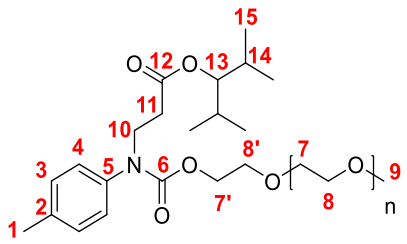

Surfactant S4

Surfactant **S4** was obtained as a colorless and low-viscosity liquid (4.112 g, 5.015 10^{-3} mol, ***X* ≈ 82 %**, $R_{urethane}$ ≈ 7 %).

Table 69. Exact weights of synthesis to surfactant **S4** (t = 8 h, T = 90 °C).

Substance	**2,4-Dimethyl-3-pentyl acrylate**	**MoPEG500**	**BHT**	**K Oct**	**pTMI**
***m* [g]**	3.116	3.153	0.008	0.030	1.635
***n* [mol]**	$1.830 \cdot 10^{-2}$	$6.100 \cdot 10^{-3}$	$4 \cdot 10^{-5}$	$1.7 \cdot 10^{-4}$	$1.830 \cdot 10^{-2}$

^{1}H-NMR (400.13 MHz, acetone-d_6): δ [ppm] = 7.19 (s, 4 H, H_3, H_4), 4.55 (t, ^3J(H,H) = 6.1 Hz, 1 H, H_{13}), 4.17 (t, ^3J(H,H) = 4.9 Hz, 2 H, $H_{7'}$), 4.00 – 3.91 (m, 2 H, H_{10}), 3.65 – 3.42 (m, 42 H, H_7, H_8, $H_{8'}$), 3.29 (s, 3 H, H_9), 2.67 (t, ^3J(H,H) = 7.8 Hz, 2 H, H_{11}), 2.33 (s, 3 H, H_1), 1.89 (dq, ^3J(H,H) = 13.4, 6.7 Hz, 2 H, H_{14}), 0.84 (dd, ^3J(H,H) = 8.8, 6.7 Hz, 12 H, H_{15}).

ESI-MS: $m/z_{calc.}$ [$C_{41}H_{73}NO_{15}$] = 819.50 g/mol, m/z_{found} [M + H^+] = 820.51 g/mol.

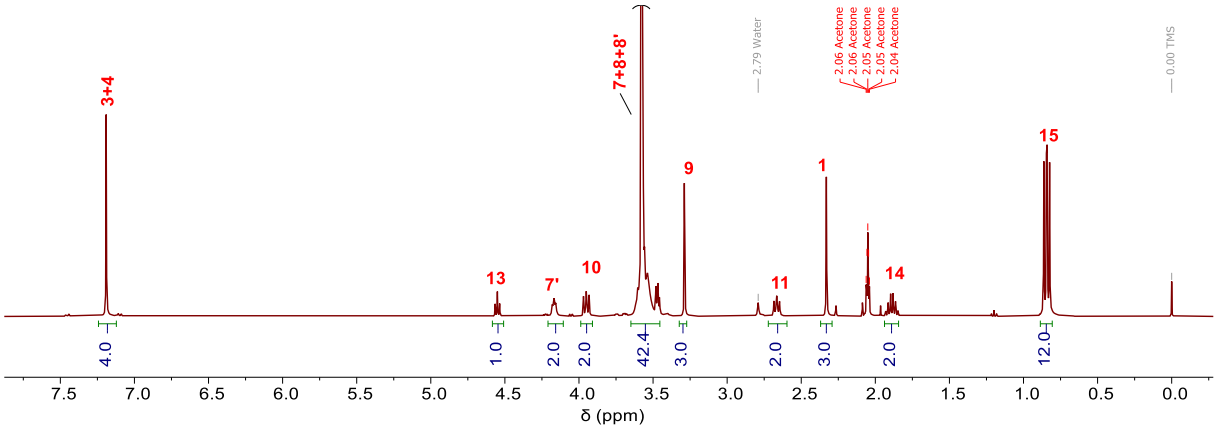

Figure 120. ^{1}H-NMR spectrum of surfactant **S4** (acetone-d_6).

6.3.1.5 2-Ethylhexyl acrylate-based surfactant (S5)

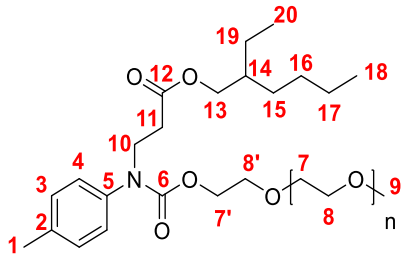

Surfactant S5

Surfactant **S5** was obtained as a colorless and medium-viscosity liquid (27.173 g, 3.2580 10^{-2} mol, ***X* ≈ 91 %**, $R_{urethane}$ ≈ 1 %).

Table 70. Exact weights of synthesis to surfactant **S5** (t = 4.5 h, T = 90 °C).

Substance	Octoyl acrylate	MoPEG500	BHT	K Oct	pTMI
***m* [g]**	19.878	18.585	0.129	0.186	9.587
***n* [mol]**	$1.079 \cdot 10^{-1}$	$3.597 \cdot 10^{-2}$	$5.86 \cdot 10^{-4}$	$1.02 \cdot 10^{-3}$	$7.180 \cdot 10^{-2}$

^{1}H-NMR (300.21 MHz, acetone-d_6): δ [ppm] = 7.17 (s, 4 H, H_3, H_4), 4.17 (t, ^{3}J(H,H) = 4.7 Hz, 2 H, $H_{7'}$), 3.95 – 3.93 (m, 2 H, H_{13}), 3.93 – 3.91 (m, 2 H, H_{10}), 3.67 – 3.42 (m, 42 H, H_7, H_8, $H_{8'}$), 3.29 (s, 3 H, H_9), 2.60 (t, ^{3}J(H,H) = 7.3 Hz, 2 H, H_{11}), 2.33 (s, 3 H, H_1), 1.51 (m, 1 H, H_{14}), 1.40 – 1.20 (m, 8 H, H_{15}, H_{16}, H_{17}, H_{19}), 0.95 – 0.83 (m, 6 H, H_{18}, H_{20}).

ESI-MS: $m/z_{calc.}$ [$C_{42}H_{75}NO_{15}$] = 833.51 g/mol, m/z_{found} [M + NH_4^+] = 851.55 g/mol.

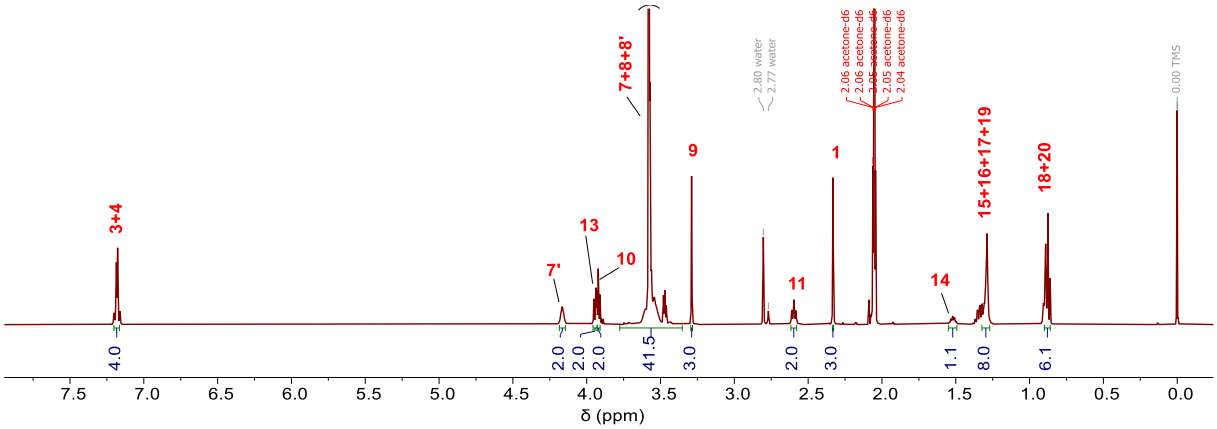

Figure 121. ^{1}H-NMR spectrum of surfactant **S5** (acetone-d_6).

6.3.1.6 4-*tert*-Butylcylcohexyl acrylate-based surfactant (S6)

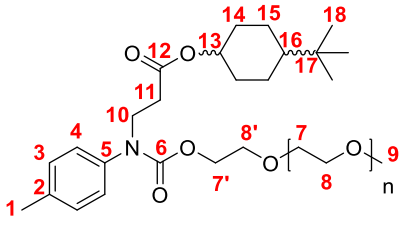

Surfactant S6

Surfactant **S6** was obtained as a colorless and low-viscosity liquid (8.669 g, 1.008 10^{-2} mol, ***X* ≈ 87 %**). The surfactant was a mixture of different enantiomers.

Table 71. Exact weights of synthesis to surfactant **S6** (*t* = 4.5 h, *T* = 90 °C).

Substance	**4-^{t}Butylcyclo-hexyl acrylate**	**MoPEG500**	**BHT**	**K Oct**	**pTMI**
***m* [g]**	7.337	6.006	0.050	0.115	3.102
***n* [mol]**	3.488 · 10^{-2}	1.163 · 10^{-2}	2.3 · 10^{-4}	6.3 · 10^{-4}	2.330 · 10^{-3}

^{1}H-NMR (500.13 MHz, acetone-d_6): δ [ppm] = 7.21 – 7.13 (m, 4 H, H_3, H_4), 4.91 (t, ^{3}J(H,H) = 2.9 Hz, 0.25 H, H_{13}), 4.52 (tt, ^{3}J(H,H) = 11.3, 4.4 Hz, 0.75 H, H_{13}), 4.16 (t, ^{3}J(H,H) = 5.0 Hz, 2 H, $H_{7'}$), 3.96 (t, ^{3}J(H,H) = 7.2 Hz, 0.5 H, H_{15}), 3.92 (t, ^{3}J(H,H) = 7.3 Hz, 1.5 H_{15}), 3.74 – 3.38 (m, 42 H, H_7, H_8, $H_{8'}$), 3.29 (s, 3 H, H_9), 2.58 (t, ^{3}J(H,H) = 7.2 Hz, 0.5 H, H_{11}), 2.53 (t, ^{3}J(H,H) = 7.2 Hz, 1.5 H, H_{11}), 2.33 (s, 3 H, H_1), 1.99 – 0.95 (m, 9 H, H_{14}, H_{15}, H_{16}), 0.86 (s, 9 H, H_{18}).

ESI-MS: $m/z_{calc.}$ [$C_{44}H_{77}NO_{15}$] = 859.53 g/mol, m/z_{found} [M + NH_4^+] = 877.568 g/mol.

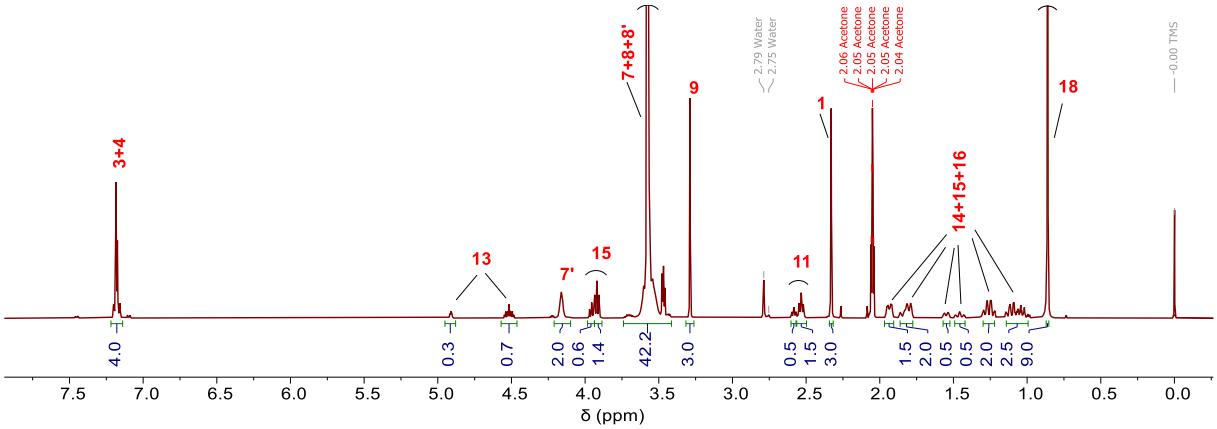

Figure 122. ^{1}H-NMR spectrum of surfactant **S6** (acetone-d_6).

6.3.1.7 Phenoxyethyl acrylate-based surfactant (S7)

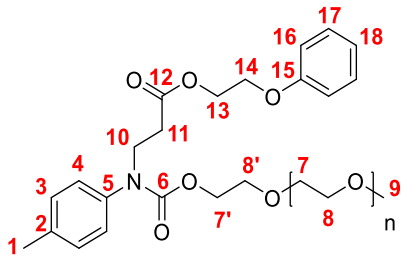

Surfactant S7

Surfactant **S7** was obtained as a colorless to slightly yellowish and low-viscosity liquid (8.168 g, 9.700 10^{-3} mol, ***X* ≈ 82 %**, $R_{urethane}$ ≈ 4 %).

Table 72. Exact weights of synthesis to surfactant **S7** (t = 5.5 h, T = 90 °C).

Substance	POEA	MoPEG500	BHT	K Oct	pTMI
***m* [g]**	6.849	6.135	0.052	0.058	3.162
***n* [mol]**	$3.560 \cdot 10^{-2}$	$1.190 \cdot 10^{-2}$	$2.4 \cdot 10^{-4}$	$3.2 \cdot 10^{-4}$	$2.375 \cdot 10^{-2}$

^{1}H-NMR (300.21 MHz, acetone-d_6): δ [ppm] = 7.33 – 7.24 (m, 2 H, H_{17}), 7.17 (s, 4 H, H_3, H_4), 7.00 – 6.86 (m, 3 H, H_{16}, H_{18}), 4.40 – 4.31 (m, 2 H, H_{13}), 4.21 – 4.10 (m, 4 H, $H_{7'}$, H_{14}), 3.95 (t, ^{3}J(H,H) = 7.2 Hz, 2 H, H_{10}), 3.66 – 3.43 (m, 42 H, H_7, H_8, $H_{8'}$), 3.29 (s, 3 H, H_9), 2.62 (t, ^{3}J(H,H) = 7.2 Hz, 2 H, H_{11}), 2.31 (s, 3 H, H_1).

ESI-MS: $m/z_{calc.}$ [$C_{42}H_{67}NO_{16}$] = 841.45 g/mol, m/z_{found} [$M+NH_4^+$] = 859.385 g/mol

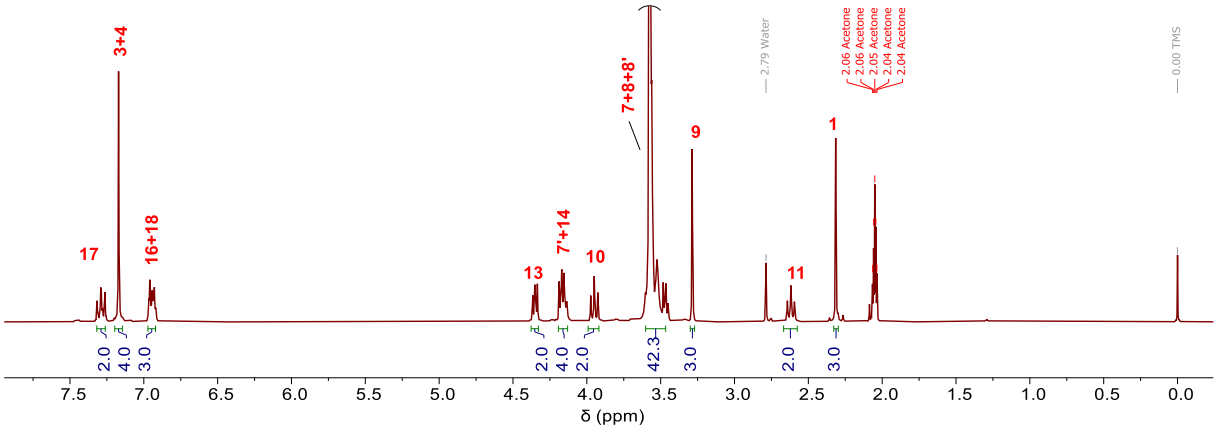

Figure 123. ^{1}H-NMR spectrum of surfactant **S7** (acetone-d_6).

6.3.1.8 2-(Methacryloyloxy)ethyl acrylate-based surfactant (S8)

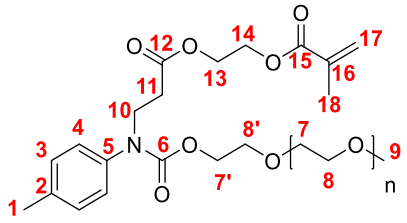

Surfactant S8

Surfactant **S8** was obtained as a colorless and low-viscosity liquid (2.313 g, 2.773 10^{-3} mol, ***X* ≈ 77 %**).

Table 73. Exact weights of synthesis to surfactant **S8** (t = 7 h, T = 90 °C).

Substance	**2-(Methacryl-oyloxy)ethyl acrylate**	**MoPEG500**	**BHT**	**K Oct**	**pTMI**
***m* [g]**	1.995	1.855	0.057	0.019	0.964
***n* [mol]**	1.083 · 10^{-2}	3.591 · 10^{-3}	2.6 · 10^{-4}	1.0 · 10^{-4}	7.24 · 10^{-3}

^{1}H-NMR (400.13 MHz, acetone-d_6): δ [ppm] = 7.18 (s, 4 H, H_3, H_4), 6.07 (m, 1 H, H_{17Z}), 5.65 (m, 1 H, H_{17E}), 4.33 – 4.24 (m, 4 H, H_{13}, H_{14}), 4.16 (t, ^{3}J(H,H) = 4.9 Hz, 2 H, $H_{7'}$), 3.94 (t, ^{3}J(H,H) = 7.3 Hz, 2 H, H_{10}), 3.67 – 3.43 (m, 42 H, H_7, H_8, $H_{8'}$), 3.29 (s, 3 H, H_9), 2.61 (t, ^{3}J(H,H) = 7.2 Hz, 2 H, H_{17}), 2.33 (s, 3 H, H_1), 1.91 (m, 3 H, H_{18}).

ESI-MS: $m/z_{calc.}$ [$C_{40}H_{67}NO_{17}$] = 833.44 g/mol, m/z_{found} [M + H^+] = 834.45 g/mol.

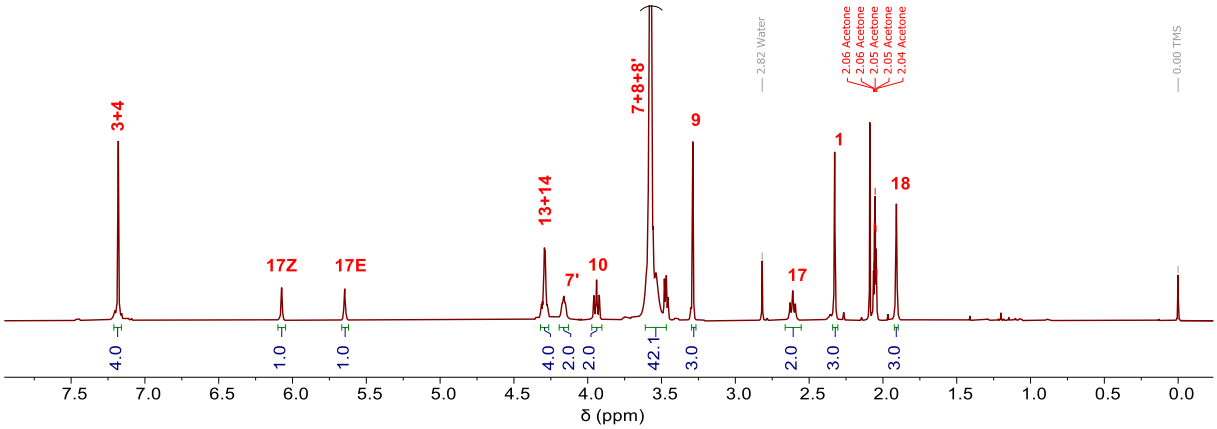

Figure 124. ^{1}H-NMR spectrum of surfactant **S8** (acetone-d_6).

6.3.1.9 2-Ethylhexyl acrylate-based surfactant (MoPEG350) (S9)

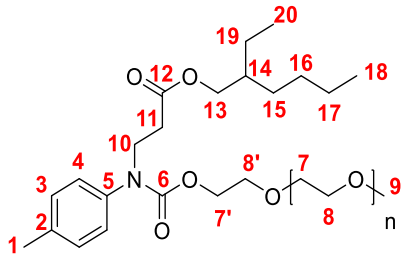

Surfactant S9

Surfactant **S9** was obtained as a colorless and low-viscosity liquid (4.393 g, 6.583 10^{-3} mol, ***X* ≈ 88 %**, $R_{urethane}$ ≈ 4 %).

Table 74. Exact weights of synthesis to surfactant **S9** (t = 7.5 h, T = 90 °C).

Substance	Octoyl acrylate	MoPEG350	BHT	K Oct	pTMI
***m* [g]**	4.146	2.629	0.010	0.038	2.018
***n* [mol]**	$2.251 \cdot 10^{-2}$	$7.511 \cdot 10^{-3}$	$4.5 \cdot 10^{-5}$	$2.1 \cdot 10^{-4}$	$1.516 \cdot 10^{-2}$

^{1}H-NMR (400.13 MHz, acetone-d_6): δ [ppm] = 7.23 – 7.12 (m, 4 H, H_3, H_4), 4.16 (t, ^{3}J(H,H) = 4.9 Hz, 2 H, $H_{7'}$), 3.99 – 3.87 (m, 4 H, H_{10}, H_{13}), 3.74 – 3.42 (m, 30 H, H_7, H_8, $H_{8'}$), 3.28 (s, 3 H, H_9), 2.59 (t, ^{3}J(H,H) = 7.3 Hz, 2 H, H_{11}), 2.33 (s, 3 H, H_1), 1.56 – 1.45 (m, 1 H, H_{14}), 1.37 – 1.23 (m, 8 H, H_{15}, H_{16}, H_{17}, H_{19}), 0.95 – 0.83 (m, 6 H, H_{18}, H_{20}).

ESI-MS: $m/z_{calc.}$ [$C_{36}H_{63}NO_{12}$] = 701.44 g/mol, m/z_{found} [M + NH_4^+] = 719.471 g/mol.

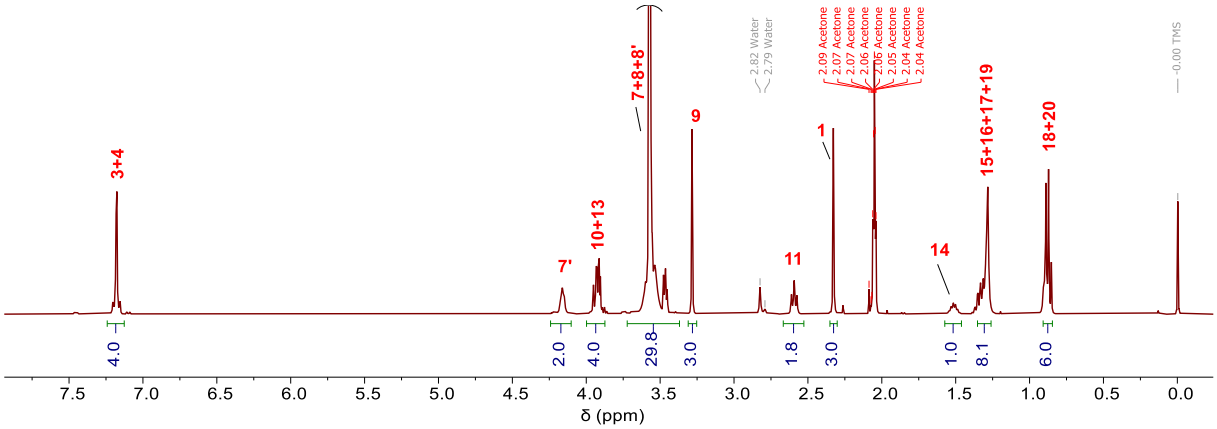

Figure 125. ^{1}H-NMR spectrum of surfactant **S9** (acetone-d_6).

6.3.1.10 2-Ethylhexyl acrylate-based surfactant (MoPEG750) (S10)

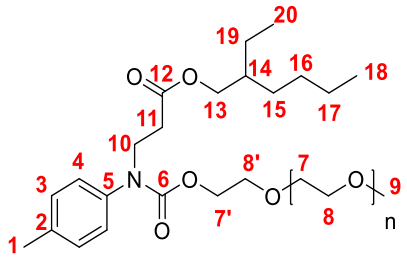

Surfactant S10

Surfactant **S10** was obtained as a colorless and medium-viscosity liquid (3.999 g, 3.747 10^{-3} mol, ***X* ≈ 80 %**, $R_{urethane}$ ≈ 5 %).

Table 75. Exact weights of synthesis to surfactant **S10** (t = 7.5 h, T = 90 °C).

Substance	Octoyl acrylate	MoPEG750	BHT	K Oct	pTMI
***m* [g]**	2.591	3.514	0.007	0.025	1.249
***n* [mol]**	$1.407 \cdot 10^{-2}$	$4.686 \cdot 10^{-3}$	$3 \cdot 10^{-5}$	$1.4 \cdot 10^{-4}$	$9.380 \cdot 10^{-3}$

^{1}H-NMR (400.13 MHz, acetone-d_6): δ [ppm] = 7.23 – 7.13 (m, 4 H, H_3, H_4), 4.17 (t, ^{3}J(H,H) = 4.9 Hz, 2 H, $H_{7'}$), 4.02 – 3.86 (m, 4 H, H_{10}, H_{13}), 3.79 – 3.37 (m, 62 H, H_7, H_8, $H_{8'}$), 3.29 (s, 3 H, H_9), 2.60 (t, ^{3}J(H,H) = 7.3 Hz, 2 H, H_{11}), 2.33 (s, 3 H, H_1), 1.56 – 1.46 (m, 1 H, H_{14}), 1.42 – 1.21 (m, 8 H, H_{15}, H_{16}, H_{17}, H_{19}), 0.97 – 0.79 (m, 6 H, H_{18}, H_{20}).

ESI-MS: $m/z_{calc.}$ [$C_{52}H_{95}NO_{20}$] = 1053.64 g/mol, m/z_{found} [M + NH_4^+] = 1071.680 g/mol.

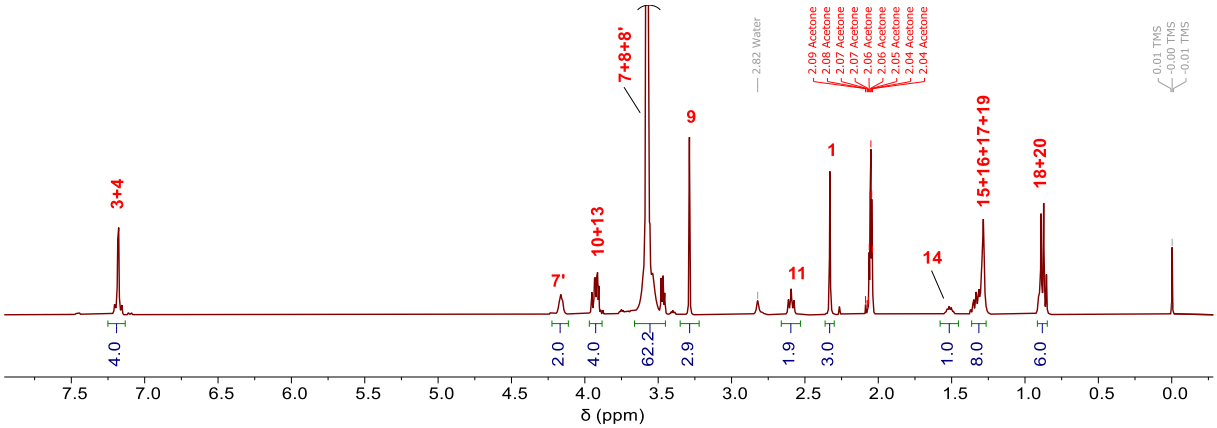

Figure 126. ^{1}H-NMR spectrum of surfactant **S10** (acetone-d_6).

6.3.1.11 Synthesis of urethane backbone

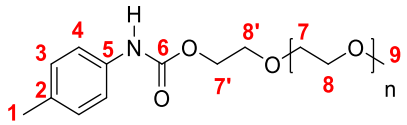

Urethane backbone

The urethane was obtained as a colorless and medium-viscosity liquid (5.332 g, 8.292 10^{-3} mol, ***X* ≈ 74 %**).

Table 76. Exact weights of synthesis to the urethane backbone (*t* = 26 h, *T* = 80 °C).

Substance	MoPEG500	pTMI
***m* [g]**	5.455	1.502
***n* [mol]**	$1.070 \cdot 10^{-2}$	$1.128 \cdot 10^{-2}$

^{1}H-NMR (300.13 MHz, acetone-d_6): δ [ppm] = 8.54 (s, 1 H, N-H), 7.45 (d, ^{3}J(H,H) = 8.5 Hz, 2 H, H_4), 7.10 (d, ^{3}J(H,H) = 8.2 Hz, 2 H, H_3), 4.30 – 4.18 (m, 2 H, $H_{7'}$), 3.75 – 3.42 (m, 46 H, H_7, H_8, $H_{8'}$), 3.26 (s, 3 H, H_9), 2.27 (s, 3 H, H_1).

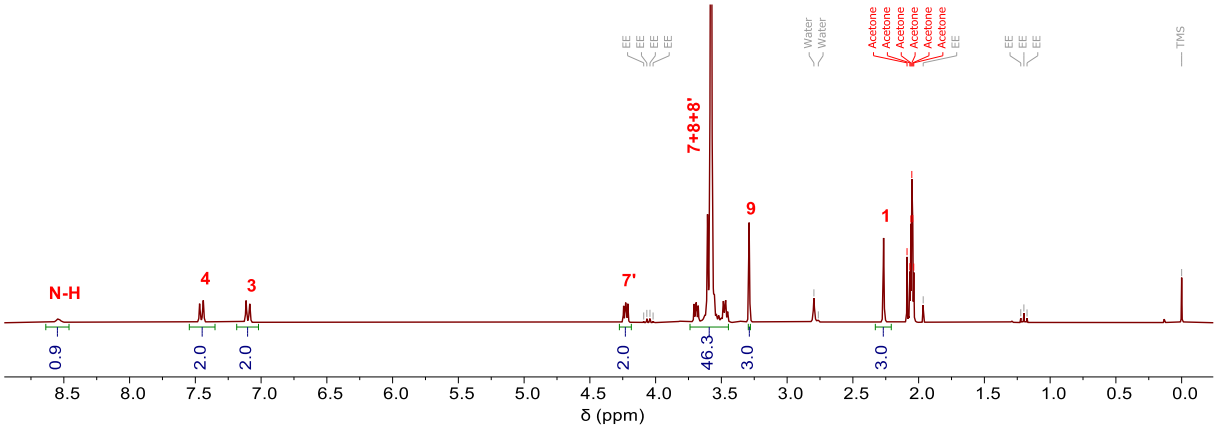

Figure 127. ^{1}H-NMR spectrum of the urethane backbone (acetone-d_6).

6.3.2 Gemini-surfactants

All gemini-surfactants based on acrylate, polyethylene glycol and *para*-tolyl isocyanate were synthesized as described below (Figure 128). The exact weights and parameters are given for each surfactant in the corresponding subsection.

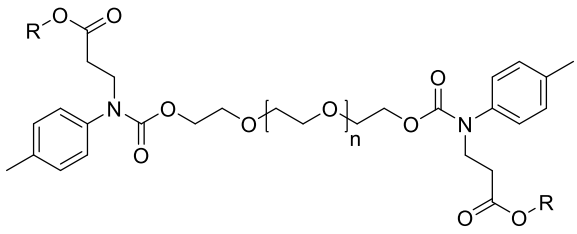

Figure 128. General backbone of gemini-surfactants based on PEG, pTMI and acrylate.

Para-tolyl isocyanate (4 eq.) was added to a round bottom flask containing polyethylene glycol ($M_n \approx 600$ g/mol, 1 eq.), acrylate (6 eq.), 2,6-di-*tert*-butyl-*p*-cresol (0.04 eq.) and potassium octoate (0.06 eq.). The mixture was stirred for a time, *t*, at a temperature, *T*. The crude product was then dissolved in a mixture of petroleum ether and ethyl acetate (1/1 or 2/1) and filtered over silica (0.04 – 0.063 mm, eluent: petroleum ether/ethyl acetate 1/1 or 2/1). The silica was washed with a mixture of petroleum ether and ethyl acetate (1/1 or 2/1). It was then slurried in acetone for at least three times. The dry and purified product was obtained after evaporation of the organic solvent at reduced pressure.

6.3.2.1 Phenoxyethyl acrylate based gemini-surfactant (S11)

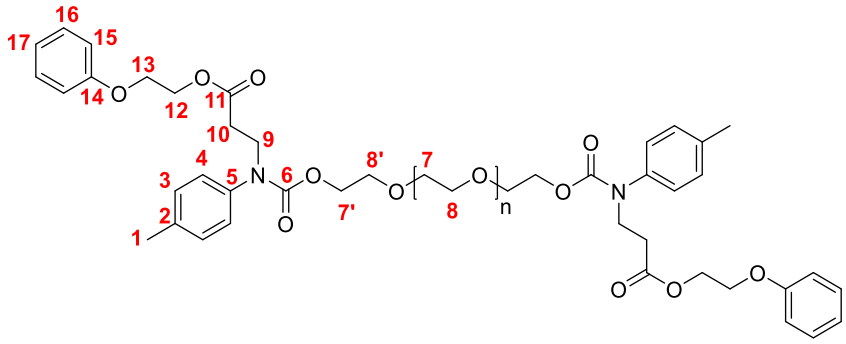

Gemini-surfactant S11

Gemini-surfactant **S11** was obtained as a colorless and medium-viscosity liquid (4.322 g, $3.481 \cdot 10^{-3}$ mol, $X \approx 86$ %).

Table 77. Exact weights of synthesis to gemini-surfactant **S11** (t = 5 h, T = 90 °C).

Substance	POEA	PEG600	BHT	K Oct	pTMI
***m* [g]**	4.644	2.425	0.053	0.041	2.183
***n* [mol]**	$2.416 \cdot 10^{-2}$	$4.041 \cdot 10^{-3}$	$2.4 \cdot 10^{-4}$	$2.3 \cdot 10^{-4}$	$1.639 \cdot 10^{-2}$

^{1}H-NMR (500.13 MHz, acetone-d_6): δ [ppm] = 7.29 (t, ^3J(H,H) = 8.0 Hz, 4 H, H_{16}), 7.21 – 7.13 (m, 8 H, H_3, H_4), 6.99 – 6.89 (m, 6 H, H_{15}, H_{17}), 4.35 (t, ^3J(H,H) = 4.5 Hz, 4 H, H_{12}), 4.20 – 4.12 (m, 8 H, $H_{7'}$, H_{13}), 3.95 (t, ^3J(H,H) = 7.2 Hz, 4 H, H_9), 3.64 – 3.48 (m, 50 H, H_7, H_8, $H_{8'}$), 2.62 (t, ^3J(H,H) = 7.2 Hz, 4 H, H_{10}), 2.31 (s, 6 H, H_1).

ESI-MS: $m/z_{calc.}$ [$C_{64}H_{92}N_2O_{22}$] = 1240.61 g/mol, m/z_{found} [M + NH_4^+] = 1258.65 g/mol.

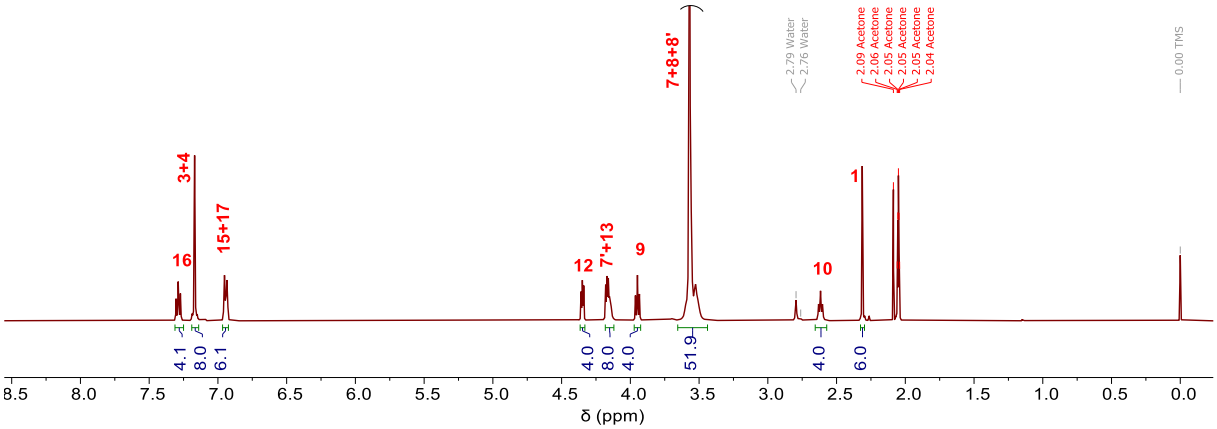

Figure 129. ^{1}H-NMR spectrum of gemini-surfactant **S11** (acetone-d_6).

6.3.2.2 2-Ethylhexyl acrylate based gemini-surfactant (S12)

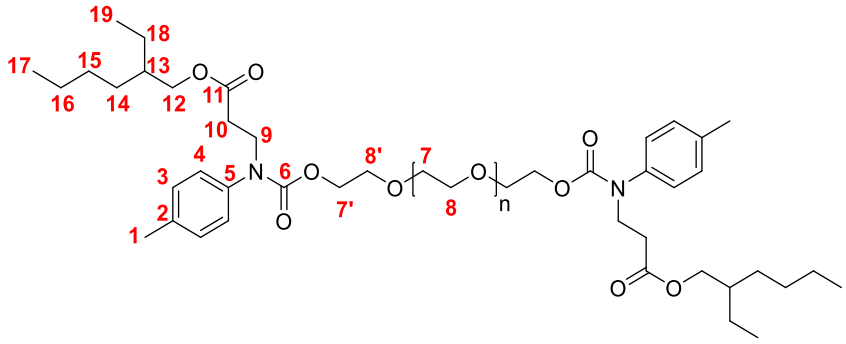

Gemini-surfactant S12

Gemini-surfactant **S12** was obtained as a colorless and medium-viscosity liquid (2.531 g, $2.096 \cdot 10^{-3}$ mol, $X \approx 87$ %).

Table 78. Exact weights of synthesis to gemini-surfactant **S12** (t = 6.5 h, T = 90 °C).

Substance	Octoyl acrylate	PEG600	BHT	K Oct	pTMI
***m* [g]**	2.683	1.450	0.005	0.025	1.305
***n* [mol]**	$1.457 \cdot 10^{-2}$	$2.417 \cdot 10^{-3}$	$2 \cdot 10^{-5}$	$1.4 \cdot 10^{-4}$	$9.808 \cdot 10^{-3}$

^{1}H-NMR (300.13 MHz, acetone-d_6): δ [ppm] = 7.21 – 7.12 (m, 8 H, H_3, H_4), 4.16 (t, ^3J(H,H) = 4.9 Hz, 4 H, H_{12}), 4.00 – 3.86 (m, H 8, $H_{7'}$, H_9), 3.67 – 3.48 (m, 50 H, H_7, H_8, $H_{8'}$), 2.59 (t, ^3J(H,H) = 7.3 Hz, 4 H, H_{10}), 2.33 (s, 6 H, H_1), 1.56 – 1.46 (m, 2 H, H_{13}), 1.39 – 1.24 (m, 16 H, H_{14}, H_{15}, H_{16}, H_{18}), 0.94 – 0.80 (m, 12 H, H_{17}, H_{19}).

ESI-MS: $m/z_{calc.}$ [$C_{64}H_{108}N_2O_{20}$] = 1224.75 g/mol, m/z_{found} [M + NH_4^+] = 1242.79 g/mol.

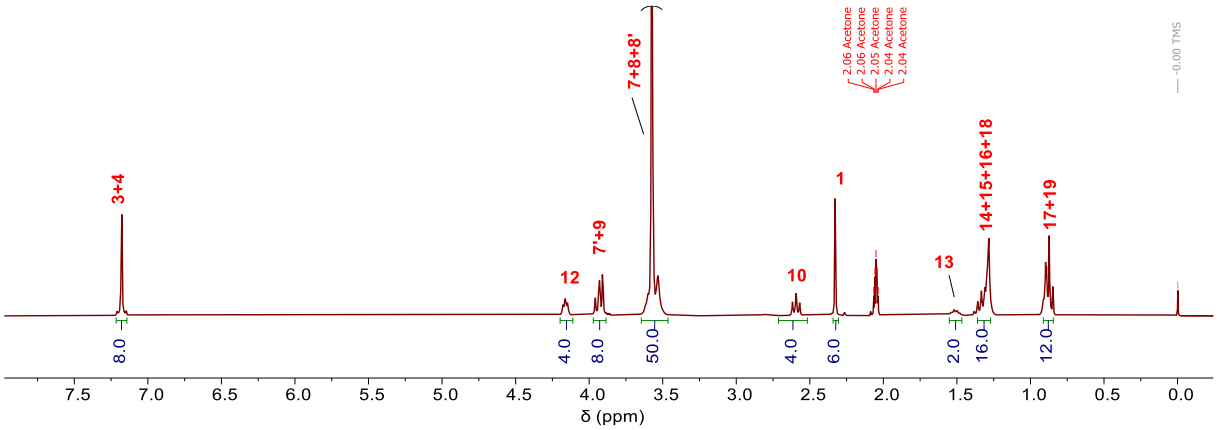

Figure 130. ^{1}H-NMR spectrum of gemini-surfactant **S12** (acetone-d_6).

6.3.3 Preparation of acrylates

6.3.3.1 2-Methylacryloyloxyethyl acrylate

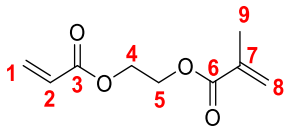

2-Methylacryloxyethyl acrylate

The preparation of 2-methylacryloxyethyl acrylate (AMA) was based on a synthesis as originally described by J. LUCHTENBERG and H. RITTER.[105] The synthesis was carried out under standard Schlenk conditions (inert gas: Ar).

10.500 g Acryloyl chloride ($1.160 \cdot 10^{-1}$ mol, 1.00 eq.) was added dropwise at about 0 to 3 °C to a solution of 12.389 g triethylamine ($1.224 \cdot 10^{-1}$ mol, 1.05 eq.) and 14.412 g 2-hydroxyethyl methacrylate ($1.107 \cdot 10^{-1}$ mol, 0.95 eq.) in dried toluene. The reaction was stirred at this temperature for 4 h and at room temperature for another 14 h. The

colorless precipitate was filtered off and the solvent was evaporated under reduced pressure. The product was purified by distillation under reduced pressure at 70 °C.

A colorless and low viscosity liquid was obtained (16.832 g, $9.1384 \cdot 10^{-2}$ mol, $X \approx 82$ %), which was stabilized by the addition of 0.151 g BHT ($6.85 \cdot 10^{-4}$ mol).

^{1}H-NMR (300.21 MHz, acetone-d_6): δ [ppm] = 6.38 (dd, ^3J(H,H) = 17.3 Hz, ^2J(H,H) = 1.7 Hz, 1 H, H_{1Z}), 6.17 (dd, ^3J(H,H) = 17.3, 10.3 Hz, 1 H, H_2), 6.10 – 6.05 (m, 1 H, H_{8Z}), 5.91 (dd, ^3J(H,H) = 10.3 Hz, ^2J(H,H) = 1.7 Hz, 1 H, H_{1E}), 5.64 (p, ^2J(H,H) = 1.6 Hz, 1 H, H_{8E}), 4.46 – 4.34 (m, 4 H, H_4, H_5), 1.95 – 1.86 (m, 3 H, H_9).

ESI-MS: $m/z_{calc.}$ [$C_{10}H_{14}O_4$] = 198.09 g/mol, m/z_{found} [M + Na^+] = 221.08 g/mol.

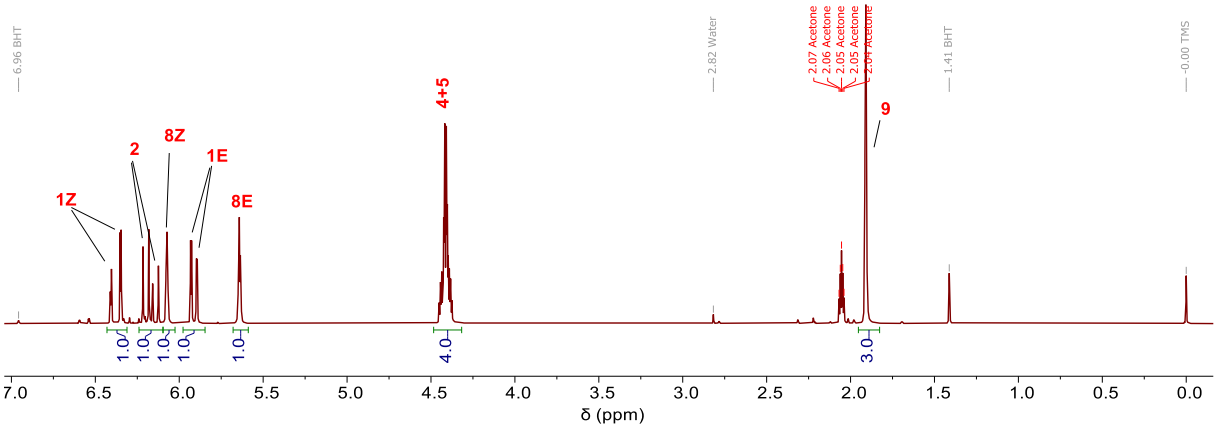

Figure 131. ^{1}H-NMR spectrum of AMA (acetone-d_6).

6.3.3.2 2,4-Dimethyl-3-pentyl acrylate

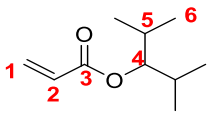

2,4-Dimethyl-3-pentyl acrylate

6.003 g Acryloyl chloride ($6.633 \cdot 10^{-2}$ mol, 1.09 eq.) was added dropwise at about 0 to 3 °C to a solution of 6.823 g triethylamine ($6.742 \cdot 10^{-2}$ mol, 1.10 eq.) and 2,4-dimethyl-3-pentanol ($6.113 \cdot 10^{-2}$ mol, 1 eq.) in dried toluene. The reaction was stirred at this temperature for 3.5 h. The colorless precipitate was filtered off and washed with toluene. 0.032 g BHT ($1.4 \cdot 10^{-4}$ mol) was added to the filtrate before the solvent was evaporated to stabilize the solution. The product was then extracted by a mixture of petroleum ether and water. The organic layer was dried over $MgSO_4$ before removal of the solvent under reduced pressure.

A colorless to slightly yellowish, low viscosity liquid was obtained (8.933 g, $5.247 \cdot 10^{-2}$ mol, $X \approx 86$ %).

^{1}H-NMR (400.13 MHz, acetone-d_6): δ [ppm] = 6.36 (dd, ^3J(H,H) = 17.3 Hz, ^2J(H,H) = 1.8 Hz, 1 H, H_{1Z}), 6.17 (dd, ^3J(H,H) = 17.3, 10.3 Hz, 1 H, H_2), 5.88 (dd, ^3J(H,H) = 10.3 Hz, ^2J(H,H) = 1.8 Hz, 1 H, H_{1E}), 4.63 (t, ^3J(H,H) = 6.1 Hz, 1 H, H_4), 1.95 (dq, ^3J(H,H) = 13.6, 6.7 Hz, 2 H, H_5), 0.88 (t, ^3J(H,H) = 6.9 Hz, 12 H, H_6).

ESI-MS: $m/z_{calc.}$ [$C_{10}H_{18}O_2$] = 170.13 g/mol, m/z_{found} [M + H^+] = 170.15 g/mol.

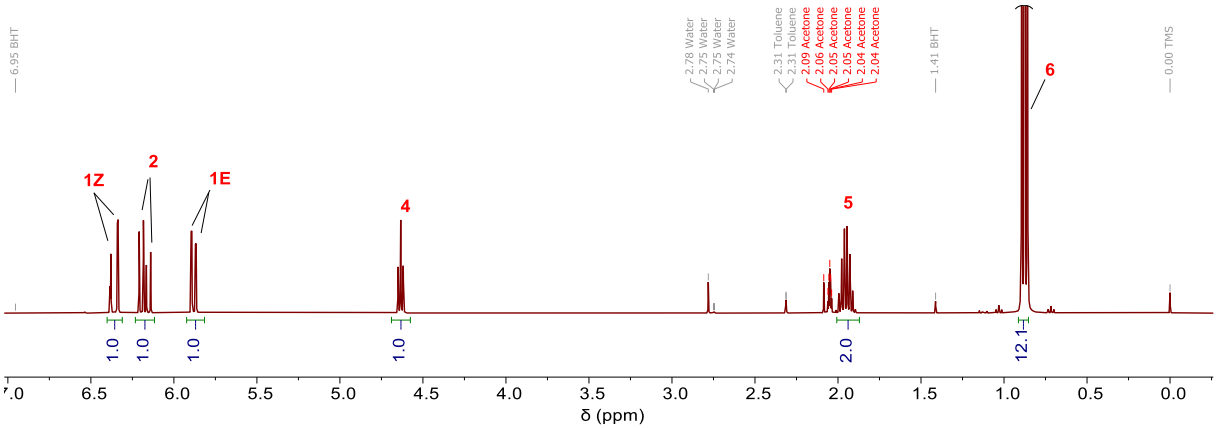

Figure 132. ^{1}H-NMR spectrum of 2,4-dimethyl-3-pentyl acrylate (acetone-d_6).

6.3.4 Preparation of PU rigid foams

All surfactants were dried prior to use over molecular sieves (4 Å) for at least three days.

The A-component was prepared from a polyether polyol-mixture (polyether 1 and polyether 2), an amine catalyst, di-ionized water and surfactant. The A-component was homogenized by vigorous shaking for about 5 min. The air bubbles in the mixture had disappeared after about 3 h and the mixture had cleared up. The B-component from polymeric MDI was then added. The Isocyanate Index of the reacting system amounted to 100. The two components were mixed using an overhead stirrer equipped with a dispersion disk at 1400 rpm for 15 s. The mixture was then poured into a cup to prepare the foam. The foam was stored at room temperature for at least 3 days to ensure complete conversion of NCO. SEM-samples were cut from the center of the foam (dimension approx. $30 \cdot 30 \cdot 3$ mm^3) and sputtered with platinum using a *Polaron SC7640 Sputter Coater* (Quorum Technologies) to obtain a conductive surface. The samples were analyzed using a *Leo 1525 Gemini* field emission scanning

microscope (LEO Electron Microscopy Inc.) using an electron beam of 10.00 kV at 32-fold magnification.

The weight amounts of the various ingredients – except that of the surfactant – required for the preparation of the three basic A-components are shown in Table 79.

Table 79. Weight amounts of all blank-sample A-components next to component no. and surfactant type (only acrylate used is shown, polyol 1 = Polyetherol 91120, polyol 2 = Polyetherol 90060, catalyst = Jeffcat ZR-70).

# (A-component)	# (surfactant)	$m_{polyol\ 1}$ [g]	$m_{polyol\ 2}$ [g]	$m_{catalyst}$ [g]	m_{water} [g]	$m_{surfactant}$ [g]
1	Blank sample	28.601	53.084	0.720	2.619	-
2	Blank sample	28.587	53.090	1.070	2.621	-
3	Blank sample	28.586	53.086	1.436	2.622	-

The molecular structure and the number average molar mass of Niax Silicone L-6900 was not known. On 100 pbw. of polyol 2 pbw. of Niax Silicone L6900 was added. The same amount was added when using the hexyl acrylate-based surfactant. All other surfactants were used at about same molar amount as the hexyl acrylate-based surfactant.

Table 80. Weight amounts of all blank-sample A-components next to component no. and surfactant type (only acrylate used is shown, AMA = 2-methylacryloyloxyethyl acrylate, POEA = phenoxyethyl acrylate, BuCyHexyl acr. = 4-*tert*-butylcyclohexyl acrylate, polyol 1 = Polyetherol 91120, polyol 2 = Polyetherol 90060).

# (A-component)	# (surfactant)	$m_{polyol\ 1}$ [g]	$m_{polyol\ 2}$ [g]	$m_{catalyst}$ [g]	m_{water} [g]	$m_{surfactant}$ [g]
4	Niax Silicone L-6900	26.904	49.958	0.674	2.463	1.634
5	Hexyl acr.	26.904	49.960	0.674	2.463	1.633
6	2-Ethylhexyl acr.	26.904	49.959	0.674	2.463	1.709
7	AMA	26.902	49.961	0.674	2.464	1.724
8	POEA	26.901	49.961	0.674	2.464	1.724
9	BuCyHexyl acr.	26.902	49.961	0.674	2.464	1.702

Table 81 contains the weight amounts of the A-component and the corresponding B-component. All formulations were reproduced once.

Table 81. Weight amounts of A-component and B-component are shown of a) first and b) second foam (reproduction).

# (A-com.)	$m_{A\text{-component}}$ [g]	$m_{B\text{-component}}$ [g]	# (A-com.)	$m_{A\text{-component}}$ [g]	$m_{B\text{-component}}$ [g]
1 – a)	35.41	45.56	**1 – b)**	35.42	45.52
2 – a)	35.41	45.52	**2 – b)**	35.41	45.51
3 – a)	35.41	45.49	**3 – b)**	35.41	45.47
4 – a)	35.41	44.69	**4 – b)**	35.41	44.69
5 – a)	35.41	44.64	**5 – b)**	35.42	44.61
6 – a)	35.41	44.60	**6 – b)**	35.41	44.59
7 – a)	35.41	44.44	**7 – b)**	35.41	44.42
8 – a)	35.41	44.60	**8 – b)**	35.41	44.58
9 – a)	35.41	44.57	**9 – b)**	35.41	44.58

6.3.5 Emulsion copolymerization of *n*-butyl acrylate and 2-ethyl-hexyl acrylate

A glass reaction calorimeter of type *RC1mx* (Mettler Toledo, V = 0.5 L) was loaded with 312 g demineralized water, 56.0 g 1-butyl acrylate (0.437 mol, 3.36 eq.), 24.0 g 2-ethylhexyl acrylate (0.130 mol, 1.00 eq.) and 3.00, 6.00 9.00 or 12.0 g surfactant **S5** (3.63, 7.25, 10.8 or 14.5 mmol). The reaction mixture was agitated using an inclined blade stirrer (6 blades, 45 °) at 400 rpm for preparing the emulsion and heated to 30 °C. The colorless emulsion was degassed with N_2 starting 30 min prior to the addition of the red-ox initiator system based on 0.830 g ascorbic acid (4.71 mmol), 13.5 mg iron (II)-sulfate (0.0889 mmol) and 0.607 g *t*butyl hydroperoxide (6.74 mmol). The reaction temperature was constantly monitored during the reaction using a PT100. A rapid increase in reaction temperature was observed. The heat development was dependent on the surfactant concentration. The fastest increase in temperature was observed at the highest surfactant concentrations. The visual appearance of the emulsion changed during the reaction from ‘milky’ to colorless-opaque. The reaction was considered finished when the temperature of the reaction mixture had come down to the starting temperature. Samples were taken after completion of the reaction for DLS- and GC-measurements.[157]

6.4 Crosslinking of oligomeric urethane

6.4.1 Preparation of difunctional urethane model systems and reactions thereof

6.4.1.1 Preparation of PEG600-based difunctional urethane

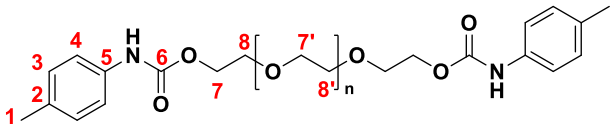

Difunctional poly(ethylene glycol) based urethane

The following reaction was carried out under an inert gas atmosphere (Ar). Toluene and PEG600 were dried prior to use over molecular sieves (4 Å) for at least three days.

6.183 g *para*-Tolyl isocyanate ($n \approx 4.644 \cdot 10^{-2}$ mol, 2.02 eq.) was added dropwise to a stirred solution of 13.854 g poly(ethylene glycol) ($M_n \approx 600$ g/mol, $n \approx 2.309 \cdot 10^{-2}$ mol, 1 eq.) in 20 mL dried toluene at 90 °C. The reaction was diluted after 23 h with 50 mL of moistened toluene to quench the non-reacted isocyanate. The liquid was filtrated to remove the precipitate. The product was obtained by evaporation of the solvent under reduced pressure.

The poly(ethylene glycol) based difunctional urethane was obtained as a clear but yellowish, medium viscosity liquid (19.883 g, $n \approx 2.295 \cdot 10^{-2}$ mol, $X \approx 99$ %).

^{1}H-NMR (300.21 MHz, acetone-d_6): δ [ppm] = 8.57 (s, 2 H, N-H), 7.62 (d, ^3J(H,H) = 8.4 Hz, 4 H, H_4), 7.10 (d, ^3J(H,H) = 8.3 Hz, 4 H, H_3), 4.34 – 4.12 (m, 4 H, H_7), 3.72 – 3.65 (m, 4 H, H_8), 3.64 – 3.48 (m, 45 H, $H_{7'}$, $H_{8'}$), 2.26 (s, 6 H, H_1).

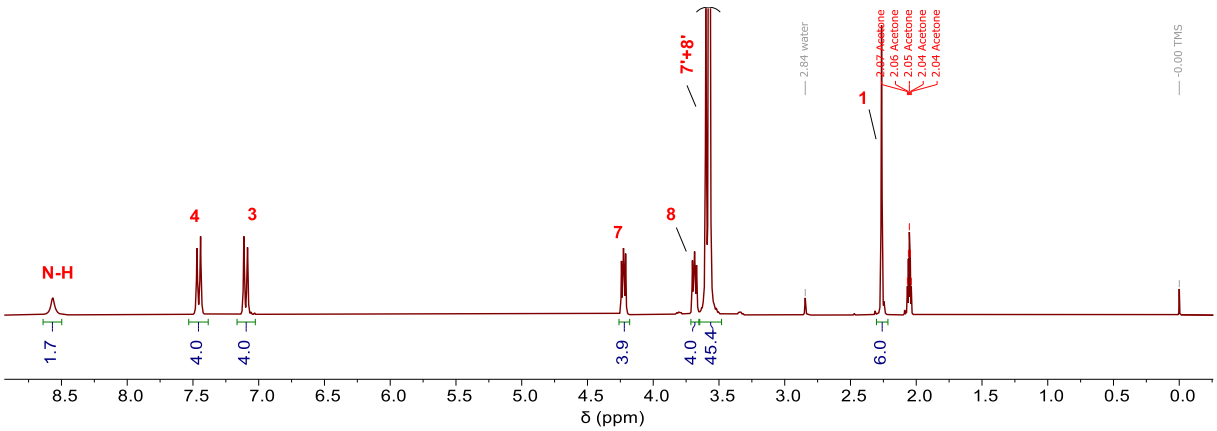

Figure 133. ^{1}H-NMR spectrum of difunctional poly(ethylene glycol) based urethane (acetone-d_6).

6.4.1.2 Preparation of PPG450-based difunctional urethane

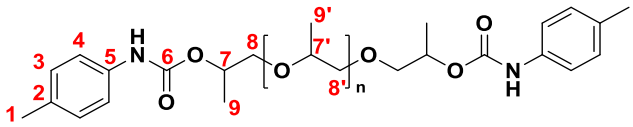

Difunctional poly(propylene glycol) based urethane

The following reaction was carried out under an inert gas atmosphere (Ar). Toluene and PPG450 (Lupranol 1200) were dried prior to use over molecular sieves (4 Å) for at least three days.

7.535 g *para*-Tolyl isocyanate ($n \approx 5.659 \cdot 10^{-2}$ mol, 2.04 eq.) was added dropwise to a stirred solution of 12.596 g poly(propylene glycol) ($M_n \approx 450$ g/mol, $n \approx 2.781 \cdot 10^{-2}$ mol, 1 eq.) in 50 mL dried toluene at 80 °C. The reaction was diluted after 21 h with 10 mL ethanol in order to quench non-reacted isocyanate and stirred at 45 °C for 1 h. The product was isolated by evaporation of the solvent under reduced pressure.

The poly(propylene glycol) based difunctional urethane was obtained as a clear but yellowish, medium viscosity liquid (no purification-steps, $X \approx 100$ %).

^{1}H-NMR (500.13z MHz, acetone-d_6): δ [ppm] = 8.44 (s, 2 H, N-H), 7.46 (d, ^3J(H,H) = 8.0 Hz, 4 H, H_4), 7.09 (d, ^3J(H,H) = 8.2 Hz, 4 H, H_3), 4.94 (q, ^3J(H,H) = 6.0 Hz, 2 H, H_7), 3.66 – 3.24 (m, 21 H, $H_{7'}$, H_8, $H_{8'}$), 2.26 (s, 6 H, H_1), 1.23 (dd, ^3J(H,H) = 6.6 Hz, 2.9 Hz, 6 H, H_9), 1.17 – 0.99 (m, 17 H, $H_{9'}$).

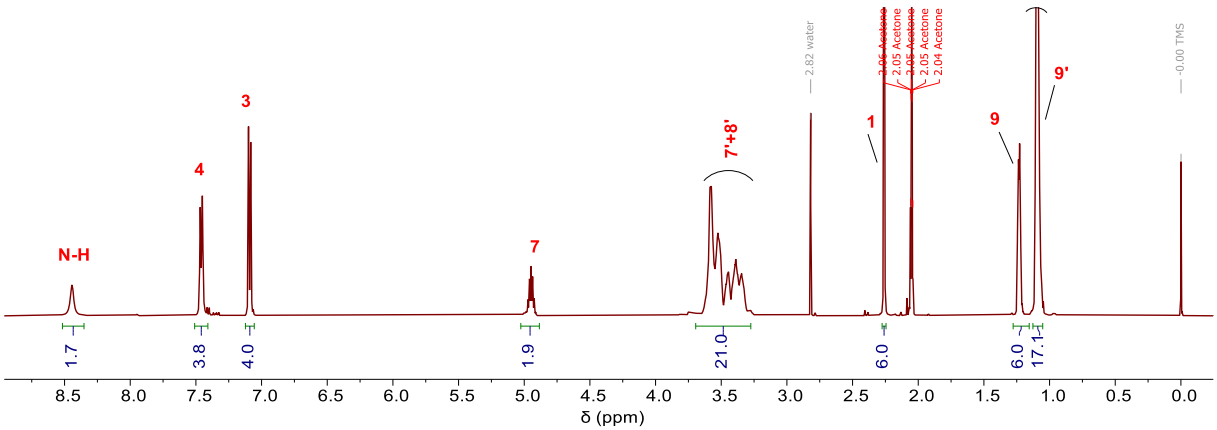

Figure 134. ^{1}H-NMR spectrum of difunctional poly(propylene glycol) based urethane (acetone-d_6).

6.4.1.3 Preparation of PTHF1400-based difunctional urethane

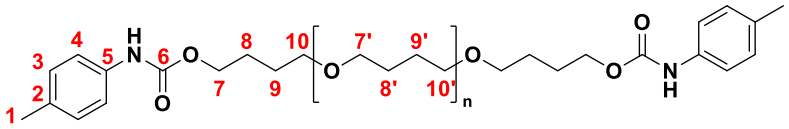

Difunctional poly(tetrahydrofuran) based urethane

The following reaction was carried out under an inert gas atmosphere (Ar). Toluene and PTHF1400 were dried prior to use over molecular sieves (4 Å) for at least three days. Before the addition of molecular sieves, PTHF1400 was molten at 40 °C. It was kept in its molten state for 3 days.

1.639 g *para*-Tolyl isocyanate ($n \approx 1.231 \cdot 10^{-2}$ mol, 2.05 eq.) was added dropwise to a stirred solution of 8.404 g poly(tetrahydrofuran) ($M_n \approx 1400$ g/mol, $n \approx 6.003 \cdot 10^{-3}$ mol, 1 eq.) in 20 mL dried toluene at 90 °C. The reaction was diluted after 4 h with 10 mL ethanol in order to quench non-reacted isocyanate. The product was isolated by evaporation of the solvent under reduced pressure.

The poly(tetrahydrofuran) based difunctional urethane was obtained as a colorless solid (no purification-steps, $X \approx 100$ %).

^{1}H-NMR (500.13 MHz, acetone-d_6): δ [ppm] = 8.47 (s, 2 H, N-H), 7.44 (d, ^3J(H,H) = 8.0 Hz, 4 H, H_4), 7.09 (d, ^3J(H,H) = 8.2 Hz, 4 H, H_3), 4.12 (t, ^3J(H,H) = 6.5 Hz. 4 H, H_7), 3.52 – 3.28 (m, 80 H, $H_{7'}$, H_{10}, $H_{10'}$), 2.26 (s, 6 H, H_1), 1.76 – 1.68 (m, 4 H, H_8), 1.68 – 1.51 (m, 80 H, $H_{8'}$, H_9, $H_{9'}$).

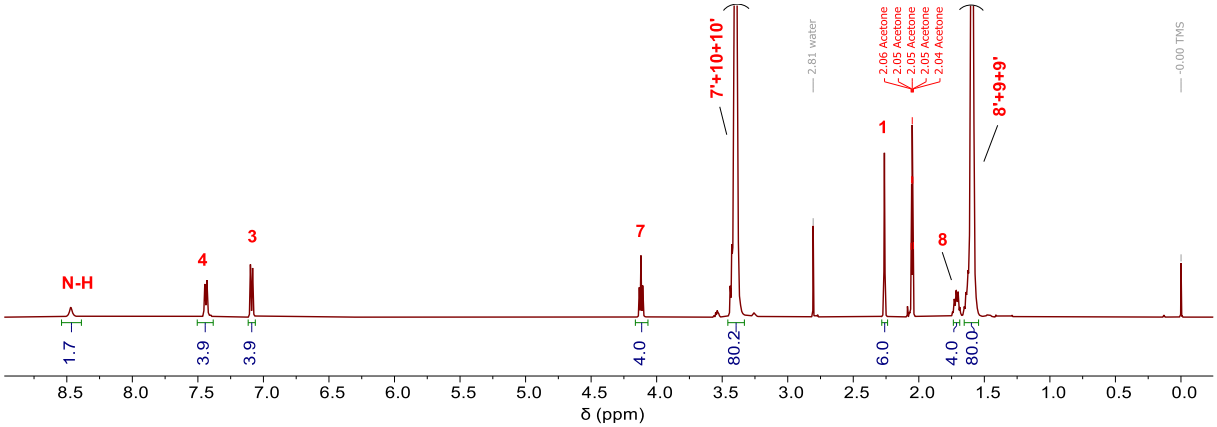

Figure 135. ^{1}H-NMR spectrum of difunctional poly(tetrahydrofuran) based urethane (acetone-d_6).

6.4.1.4 Model *aza*-Michael reactions with difunctional urethane precursors

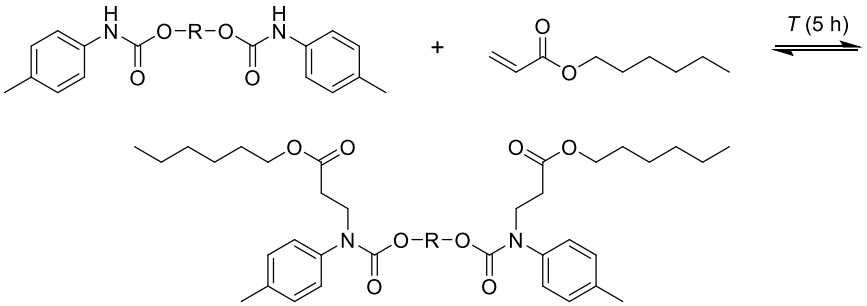

***aza*-Michael model reaction with difunctional urethane precursors**

All model reactions were conducted using the same procedure: First a masterbatch was prepared based on 1 eq. difunctional urethane precursor (PEG-DUP, PPG-DUP or PTHF-DUP, prepared as described above), 2 eq. hexyl acrylate, approx. 0.002 eq. butylated hydroxytoluene (radical inhibitor) and potassium acetate (catalyst). The masterbatch was homogenized at 80 h by stirring. Approx. 0.4 – 0.5 g was taken of each masterbatch and poured into a round bottom flask. The sealed flask was then placed in a preheated oil bath (T = 120 – 160 °C, ΔT = 10 °C) while the content was stirred. The sample was dissolved after 5 h in acetone-d_6 and analyzed by ^{1}H-NMR spectroscopy. A new masterbatch was prepared when no reaction had occurred with double the amount of catalyst and the same procedure was repeated. The lowest amount of catalyst required was approx. 0.027 equivalents. The weight amounts of the reactants for each masterbatch are shown in the following tables.

Table 82. Masterbatch based on PEG600-diurethane-precursor (PEG-DUP), HexA, BHT and K Oct. It is also given if and at which temperature a reaction was observed.

Substance	**PEG-DUP**	**HexA**	**BHT**	**K Oct**	**Reaction?**
***m* [g]**	4.004	1.444	0.002	0.025	Yes $T \geq 120$ °C
***n* [mol]**	$4.622 \cdot 10^{-3}$	$9.252 \cdot 10^{-3}$	$9 \cdot 10^{-6}$	$1.4 \cdot 10^{-4}$	
Eq.	1	2	0.002	0.029	

Table 83. Masterbatch based on PPG450-diurethane-precursor (PPG-DUP), HexA, BHT and K Oct. It is also given if and at which temperature a reaction was observed.

Substance	**PPG-DUP**	**HexA**	**BHT**	**K Oct**	**Reaction?**
***m* [g]**	3.500	1.521	0.003	0.024	Yes $T \geq 120$ °C
***n* [mol]**	$4.866 \cdot 10^{-3}$	$9.739 \cdot 10^{-3}$	$1 \cdot 10^{-5}$	$1.3 \cdot 10^{-4}$	
Eq.	1	2	0.003	0.027	

Table 84. Masterbatch based on PTHF1400-diurethane-precursor (PTHF-DUP), HexA, BHT and K Oct. It is also given if and at which temperature a reaction was observed.

Substance	PTHF-DUP	HexA	BHT	K Oct	Reaction?
***m* [g]**	4.502	0.845	0.001	0.013	No
***n* [mol]**	$2.702 \cdot 10^{-3}$	$5.44 \cdot 10^{-3}$	$6 \cdot 10^{-6}$	$6.7 \cdot 10^{-5}$	-
Eq.	1	2	0.002	0.025	

Table 85. Masterbatch based on PTHF1400-diurethane-precursor (PTHF-DUP), HexA, BHT and K Oct. It is also given if and at which temperature a reaction was observed.

Substance	PTHF-DUP	HexA	BHT	K Oct	Reaction?
***m* [g]**	4.503	0.843	0.001	0.027	Yes
***n* [mol]**	$2.702 \cdot 10^{-3}$	$5.40 \cdot 10^{-3}$	$6 \cdot 10^{-6}$	$1.5 \cdot 10^{-4}$	$T \geq 150$ °C
Eq.	1	2	0.002	0.054	

6.4.2 Chemistry of polymer forming *aza*-Michael addition reactions

The reactions were carried out under an inert gas atmosphere (Ar). Toluene and PEG600 were dried prior to use over molecular sieves (4 Å) for at least three days.

Either *para*-Tolyl isocyanate or a *para*-tolyl isocyanate/4,4'-MDI-mixture was added dropwise to a stirred solution of poly(ethylene glycol) ($M_n \approx 600$ g/mol) in dried toluene at 90 °C. The reaction was diluted after a given time with moistened toluene in order to quench the non-reacted isocyanate. The product was isolated by evaporation of the solvent under reduced pressure.

The exact weight amounts of the reactants for reactions to the model-polyurethane molecules of steps 1, 2 and 3 are shown in Table 86. NMR spectra are show in Figure 136 – Figure 138.

Table 86. Weight amounts for reactions to model-polyurethane molecules of step 1 (90 °C, 23 h), 2 (90 °C, 10 h) and 3 (90 °C, 23 h) of the proof of concept.

Substance	Step	PEG600	4,4'-MDI	pTMI
***m* [g]**	1	13.854	-	6.183 g
***n* [mol]**		$2.309 \cdot 10^{-2}$	-	$4.644 \cdot 10^{-2}$
***m* [g]**	2	13.981	2.913	3.117
***n* [mol]**		$2.330 \cdot 10^{-2}$	$1.164 \cdot 10^{-2}$	$2.340 \cdot 10^{-2}$
***m* [g]**	3	175.5	48.8	26.1
***n* [mol]**		$2.93 \cdot 10^{-1}$	$1.95 \cdot 10^{-1}$	$1.96 \cdot 10^{-1}$

^{1}H-NMR (step 1, 300.21 MHz, acetone-d_6): δ [ppm] = 8.57 (s, 2 H, N-H), 7.62 (d, ^3J(H,H) = 8.4 Hz, 4 H, H_4), 7.10 (d, ^3J(H,H) = 8.3 Hz, 4 H, H_3), 4.34 – 4.12 (m, 4 H, H_7), 3.72 – 3.65 (m, 4 H, H_8), 3.64 – 3.48 (m, 45 H, $H_{7'}$, $H_{8'}$), 2.26 (s, 6 H, H_1).

^{1}H-NMR (step 2, 300.21 MHz, acetone-d_6): δ [ppm] = 8.64 – 8.52 (m, 4 H, N-H), 7.59 – 7.37 (m, 8 H, H_4, H_{13}), 7.24 – 7.06 (m, 8 H, H_3, H_{14}), 4.22 (dd, ^3J(H,H) = 3.8, 5.7 Hz, 8 H, H_7, H_{10}), 3.87 (s, 2 H, H_{16}), 3.68 (dd, ^3J(H,H) = 3.7, 5.8 Hz, 8 H, H_8, H_9), 3.63 – 3.42 (m, 92.8 H, $H_{7'}$, $H_{8'}$), 2.26 (s, 6 H, H_1).

^{1}H-NMR (step 3, 300.21 MHz, acetone-d_6): δ [ppm] = 8.62 – 8.54 (m, 6 H, N-H), 7.47 (dd, ^3J(H,H) = 8.4, 10.9 Hz, 12 H, H_4, H_{13}), 7.12 (dd, ^3J(H,H) = 8.2, 14.0 Hz, 12 H, H_3, H_{14}), 4.22 (dd, ^3J(H,H) = 3.6, 5.8 Hz, 12 H, H_7, H_{10}), 3.87 (s, 4 H, H_{16}), 3.71 – 3.68 (m, 12 H, H_8, H_9), 3.61 – 3.49 (m, 146 H, $H_{7'}$, $H_{8'}$), 2.26 (s, 6 H, H_1).

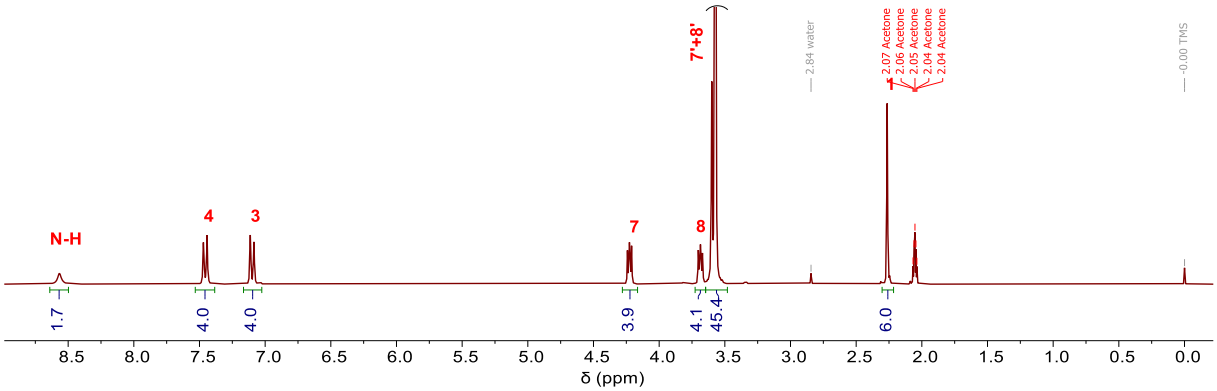

Figure 136. ^{1}H-NMR spectrum of model-polyurethane molecule of step 1 (acetone-d_6).

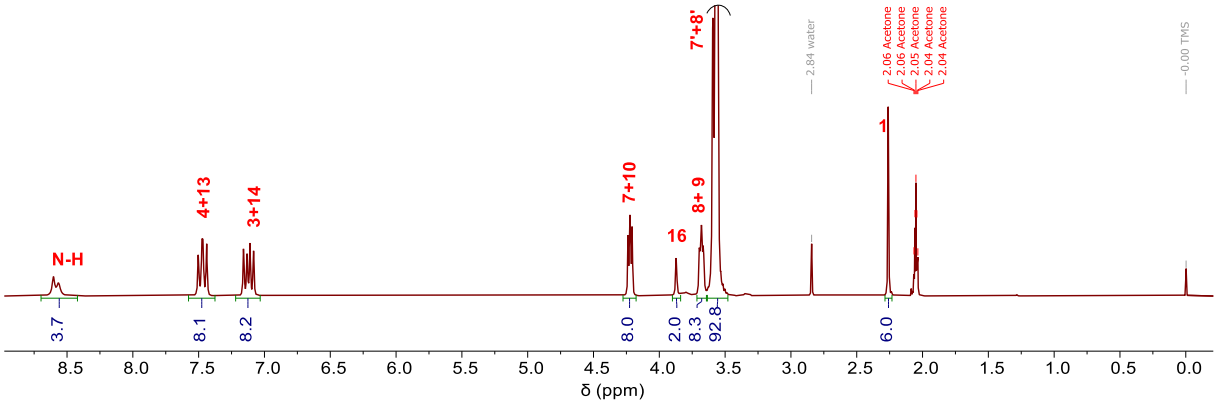

Figure 137. ^{1}H-NMR spectrum of model-polyurethane molecule of step 2 (acetone-d_6).

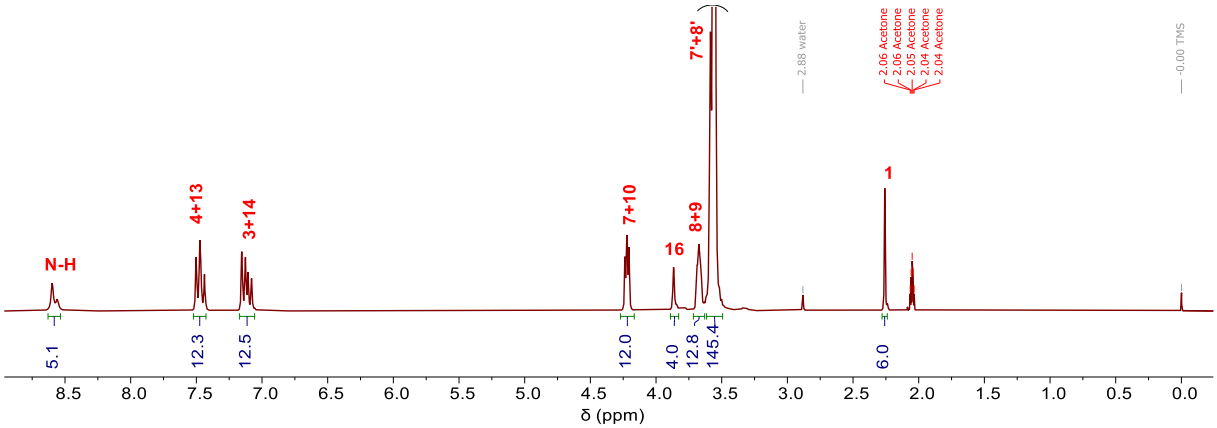

Figure 138. ^{1}H-NMR spectrum of model-polyurethane molecule of step 3 (acetone-d_6).

The above model-PU systems were subsequently reacted with acrylate according to the following protocol:

Hexyl acrylate or 1,6-hexandiol diacrylate, butylated hydroxytoluene and potassium acetate were added to the urethane precursor. The number of acrylate functionalities was equimolar to the number of carbamyl-N-H functionalities. The masterbatch was homogenized at 80 °C by stirring. Approx. 0.4 – 0.5 g of each masterbatch (step 1 and 2) were placed in a preheated oil bath (T = 120 °C) and stirred for 5 h. A sample was taken and analyzed by ^{1}H-NMR spectroscopy (Figure 64). The masterbatch for step 3 was additionally degassed using a rotary evaporator (80 °C, 20 mbar). About 10 mL of the degassed masterbatch was then poured into each of two M2-type molds and cured in an oven at 120 °C. A sample for IR spectroscopy was taken hourly for the first 7 h. The first mold was removed from the oven while the second was removed after 9 h. The material of the latter was also analyzed by IR spectroscopy (Figure 69 and Figure 70).

The exact weights for the *aza*-Michael addition reactions of steps 1, 2 and 3 are shown in Table 87.

Table 87. Weights for *aza*-Michael additions of step 1 (120 °C, 5 h), 2 (120 °C, 5 h) and 3 (120 °C, 7 – 9 h) of the proof of concept.

Substance	Step	PU	HexA/HDDA	BHT	K Oct
***m* [g]**		4.004	HexA: 1.444	0.002	0.025
***n* [mol]**	1	$4.622 \cdot 10^{-3}$	$9.252 \cdot 10^{-3}$	$9 \cdot 10^{-6}$	$1.4 \cdot 10^{-4}$
Eq.		1	2	0.002	0.029
***m* [g]**		4.999	HexA: 1.823	0.001	0.015
***n* [mol]**	2	$2.912 \cdot 10^{-3}$	$1.167 \cdot 10^{-2}$	$5 \cdot 10^{-6}$	$8.2 \cdot 10^{-5}$
Eq.		1	4	0.002	0.028

***m* [g]**		30.000	HDDA: 7.939	0.006	0.173
***n* [mol]**	3	$1.132 \cdot 10^{-2}$	$3.508 \cdot 10^{-2}$	$2 \cdot 10^{-5}$	$9.47 \cdot 10^{-4}$
Eq.		1	3	0.002	0.0836

Step 1: The conversion X_{pTMI} of the pTMI-based urethane to the corresponding *aza*-Michael adduct was calculated from ^{1}H-NMR spectroscopical data according to Equation 12 using the ratio of the urethane-based pTMI-methyl- (peak 1) to the adduct-based pTMI-methyl-group (peak a). It amounted to 64 %.

$$X_{pTMI} = \frac{\int (\text{peak a})}{\int (\text{peak 1}) + \int (\text{peak a})} \approx 0.64 \qquad \text{Equation 12}$$

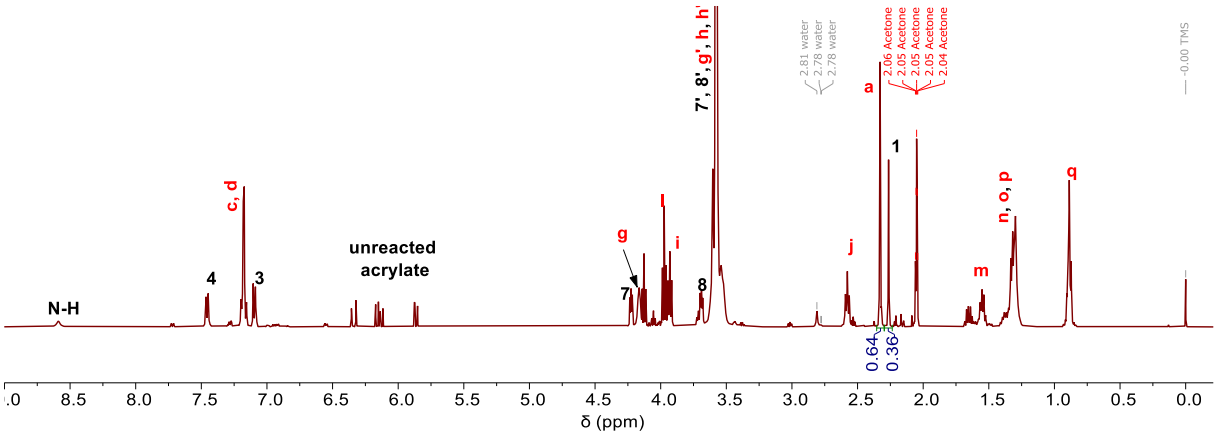

Figure 139. ^{1}H-NMR raw spectrum of step 1 (acetone-d_6). The ratio of integral (a) to (1) is 0.64 to 0.36.

Step 2: The conversion X_{pTMI} of pTMI-based urethane to the corresponding *aza*-Michael adduct was also calculated according to Equation 12 and amounted to approx. 55 %. The conversion X_{MDI} of MDI-based urethane to the corresponding *aza*-Michael adducts was calculated as follows:

1) The 4,4'-MDI based urethane groups (peak 16) decreased to one fifth of its original value, indicating that approx. 80 % of the MDI-related urethane-units were converted either to the mono- or bi-adduct.
2) Integral ∫(r + r') = 4.3 corresponds to the methylene-group in *α*-position to the former acrylic carbonyl-group of both the MDI- (peak r') and pTMI-related (peak r) adducts. With integral ∫(a) = 3.3 (3 protons) follows integral ∫(r) = 2.2 and integral ∫(r') = 2.1.
3) Integral $\int(r') = 2.1 = \int(r'_{mono}) + \int(r'_{mono\text{-}bi}) + \int(r'_{bi\text{-}bi})$ with:
    a. MDI-urethane based mono-adduct (r'_{mono}),
    b. One half of MDI-urethane based bi-adduct ($r'_{mono\text{-}bi}$),

c. The other half of MDI-urethane based bi-adduct ($r'_{bi\text{-}bi}$).

4) If 80 % of MDI-urethanes are converted to at least mono-adducts, then: integral $\int(r'_{mono}) + \int(r'_{mono\text{-}bi}) = 1.6$.
5) With integral $(r'_{bi\text{-}bi}) = \int(r') - (\int(r'_{mono}) + \int(r'_{mono\text{-}bi})) = 0.5$ follows integral $\int(r'_{mono}) = 1.1$.
6) Therefore:
   $X_{MDI\text{-}mono} = \int(r'_{mono})/\int(r') \cdot 0.8 = 0.55$ and
   $X_{MDI\text{-}bi} = \int(r'_{mono\text{-}bi})/\int(r') \cdot 0.8 = 0.25$.

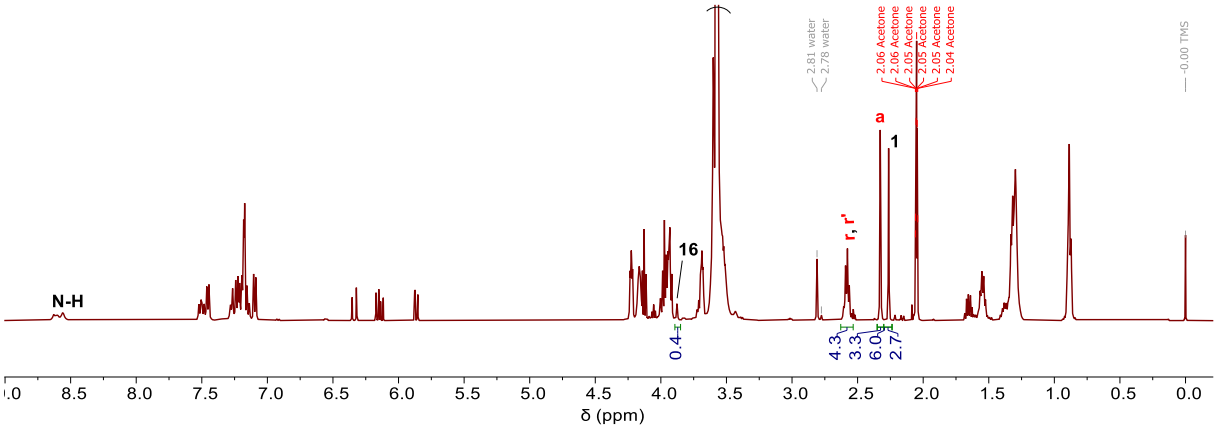

Figure 140. ^{1}H-NMR raw spectrum of step 2 (acetone-d_6). The ratio of integral (a) to (1) is 3.3 to 2.7, the ratio of (16) to (a+1) is 0.4 to 6 (instead of 2 to 6). The value of integral (r+r') is 4.3.

Step 3: No conversion was calculated based on ^{1}H-NMR measurements.

6.4.3 Preparation of PU-precursors for elastomer syntheses

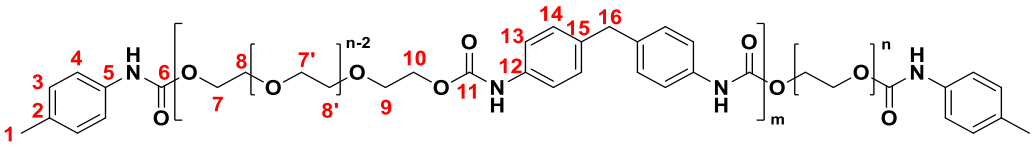

General structure of PU-precursors based on PEG600 and PEG1500

The following reactions were carried out under an inert gas atmosphere (Ar). Toluene and all ambient temperature liquid polyol-components were dried prior to use over molecular sieves (4 Å) for at least three days. At ambient temperature solid polyol-components were molten at 60 °C before molecular sieves (4 Å) were added and kept in its molten state for 3 days.

The polyol component was diluted with dried toluene and stirred at 90 °C to produce various types of PU-precursors. 4,4'-Methylene diphenyl diisocyanate and *p*-tolyl isocyanate were simultaneously homogenized at 50 °C. The isocyanate-mixture was

added dropwise to the polyol-toluene-mixture. The temperature was increased to the reflux temperature of toluene when the viscosity increased strongly (e.g., for HDI-precursor). The reaction mixture was stirred for at least another 2 h after complete addition. Toluene was removed using first a rotary evaporator (80 °C/3 mbar) followed by drying at a vacuum pump (90 °C, p << 3 mbar). The precursors were always obtained as yellowish, highly viscous liquids.

The hydroxy-terminated HDI-containing-prepolymer (HDI-prepol.) used in the synthesis of the HDI-precursor was thankfully prepared by STEFAN AUFFARTH at BASF Polyurethanes GmbH (Lemförde, Germany). 675.7 g PEG600 ($n \approx 1.13$ mol, 1 eq.), 133.8 g hexane diol (n = 1.13 mol, 1 eq.) and 0.115 g zinc octoate ($n = 3.27 \cdot 10^{-4}$ mol, 0.0004 eq.) were stirred at 110 °C under inert gas atmosphere (N_2). 190.4 g Hexane diisocyanate (n = 1.13 mol, 1 eq.) was then added dropwise. The temperature was increased stepwise with increasing viscosity of the mixture up to 125 °C. The reaction was stirred for 3 h at 120 °C after completion of the hexane diisocyanate addition. The prepolymer was obtained as a colorless, waxy solid.

The components and weight amounts used for the synthesis of PU-precursors are shown in the following tables. ^{1}H-NMR spectra of all in acetone-d_6 soluble PU-precursors are shown in Figure 141 and Figure 142.

Table 88. Preparation of PEG600-based PU-precursors with (a) 3 eq. PEG600, 2 eq. MDI and 2 eq. pTMI or (b) 4 eq. PEG600, 3 eq. MDI and 2 eq. pTMI or (c) 5 eq. PEG600, 4 eq. MDI and 2 eq. pTMI.

Substance	**#**	**PEG600**	**4,4'-MDI**	**pTMI**
***m* [g]**	(a)	175.5	48.8	26.1
***n* [mol]**		$2.93 \cdot 10^{-1}$	$1.95 \cdot 10^{-1}$	$1.96 \cdot 10^{-1}$
***m* [g]**	(b)	96.01	30.65	10.66
***n* [mol]**		$1.60 \cdot 10^{-2}$	$1.22 \cdot 10^{-1}$	$8.01 \cdot 10^{-2}$
***m* [g]**	(c)	35.16	11.73	3.13
***n* [mol]**		$5.86 \cdot 10^{-2}$	$4.69 \cdot 10^{-2}$	$2.35 \cdot 10^{-2}$

Table 89. Preparation of PEG1500- and HDI-prepolymer-based PU-precursors with (d) 4 eq. PEG1500, 3 eq. MDI and 2 eq. pTMI or (e) 4 eq. HDI-prepolymer, 3 eq. MDI and 2 eq. pTMI.

Substance	**#**	**(d) PEG1500 or (e) HDI-prepolymer**	**4,4'-MDI**	**pTMI**
***m* [g]**	(d)	85.54	10.69	3.88
***n* [mol]**		$5.70 \cdot 10^{-2}$	$4.27 \cdot 10^{-2}$	$2.91 \cdot 10^{-2}$
***m* [g]**	(e)	96.80	20.47	7.26
***n* [mol]**		$1.09 \cdot 10^{-1}$	$8.18 \cdot 10^{-2}$	$5.45 \cdot 10^{-2}$

^{1}H-NMR (PU-precursor (a), 300.21 MHz, acetone-d_6): δ [ppm] = 8.62 – 8.54 (m, 6 H, N-H), 7.47 (dd, ^3J(H,H) = 8.4, 10.9 Hz, 12 H, H_4, H_{13}), 7.12 (dd, ^3J(H,H) = 8.2, 14.0 Hz, 12 H, H_3, H_{14}), 4.22 (dd, ^3J(H,H) = 3.6, 5.8 Hz, 12 H, H_7, H_{10}), 3.87 (s, 4 H, H_{16}), 3.71 – 3.68 (m, 12 H, H_8, H_9), 3.61 – 3.49 (m, 146 H, $H_{7'}$, $H_{8'}$), 2.26 (s, 6 H, H_1).

^{1}H-NMR (PU-precursor (b), 400.13 MHz, acetone-d_6): δ [ppm] = 8.59 (m, 8 H, N-H), 7.47 (dd, ^3J(H,H) = 8.2, 14.2 Hz, 16 H, H_4, H_{13}), 7.12 (dd, ^3J(H,H) = 8.1, 19.1 Hz, 16 H, H_3, H_{14}), 4.28 – 4.15 (m, 16 H, H_7, H_{10}), 3.87 (s, 6 H, H_{16}), 3.73 – 3.64 (m, 16 H, H_8, H_9), 3.65 – 3.50 (m, 195 H, $H_{7'}$, $H_{8'}$), 2.26 (s, 6 H, H_1).

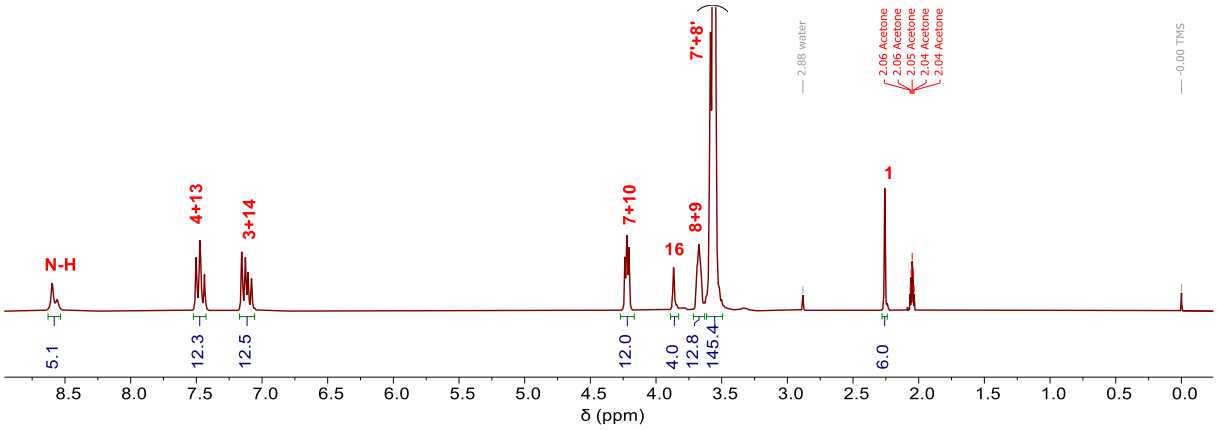

Figure 141. ^{1}H-NMR spectrum of PEG600-based PU-precursor (a) with 3 eq. PEG600, 2 eq. MDI and 2 eq. pTMI (acetone-d_6).

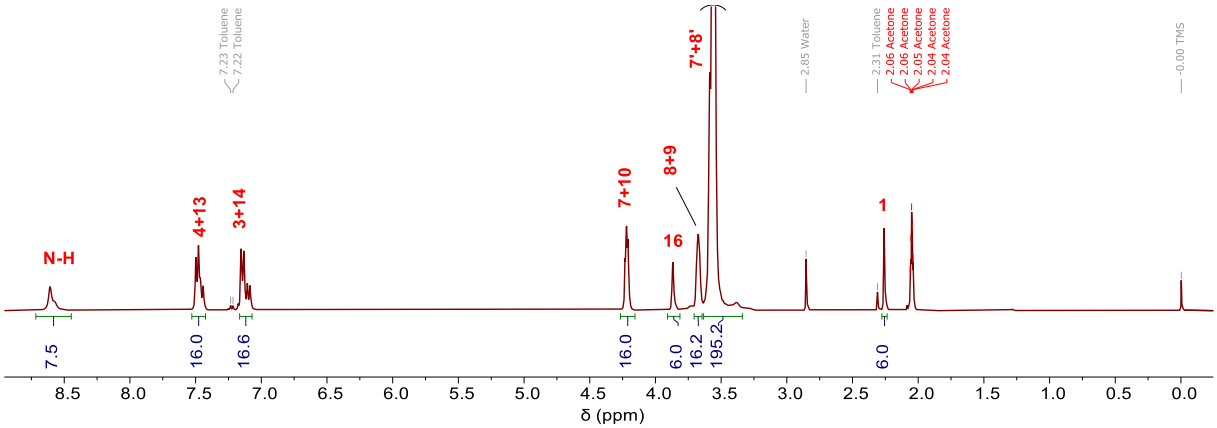

Figure 142. ^{1}H-NMR spectrum of PEG600-based PU-precursor (b) with 4 eq. PEG600, 3 eq. MDI and 2 eq. pTMI (acetone-d_6).

6.4.4 Preparation of *aza*-Michael addition-crosslinked PU-elastomers

Masterbatches containing the starting materials were prepared by liquifying the polyurethane at 80 °C. The liquid masterbatches were then mixed with polyfunctional acrylate, butylated hydroxytoluene and potassium octoate (weights in tables below). The resulting mixture was degassed using a rotary evaporator at slow rotational speed, a water bath temperature of 80 °C and reduced pressure (target pressure of $p \approx 2 – 100$ mbar). A mold was preheated to the selected reaction temperature (M1- or M2-type, Figure 73), filled up with the reactive mixture and placed in an oven. The mold was closed with a metal lid leaving a small gap between the mold and the lid. The reaction mixture was cured for a given time. The mold was then removed from the oven and cooled to room temperature before demolding.

The components and weight amounts for masterbatches of model PU-elastomers are shown in the following tables. The calculated number of N-H-groups (based on the ratio of polyol, MDI and pTMI in the precursor preparation) equaled the number of acrylate-groups.

Table 90. Influence of crosslinker functionality study: Masterbatches from PEG600-precursor (a) (2 eq. PEG600, 1.5 eq. MDI and 1 eq. pTMI), potassium octoate (K Oct), butylated hydroxytoluene (BHT) and either hexane diacrylate (HHDA), trimethylolpropane triacrylate (TMPTA) and pentaerythritol tetraacrylate (PETA). Curing at 120 °C for 5 h (HDDA), 21 h (TMPTA) and 23 h (PETA). For the precursor is $n = n(\text{N-H})/m(\text{precursor})$.

Substance	**Precursor (a)**	**Acrylate**	**K Oct**	**BHT**
***m* [g]**	10.002	HDDA: 2.686	0.063	0.002
***n* [mol]**	$2.375 \cdot 10^{-2}$	$1.187 \cdot 10^{-2}$	$3.4 \cdot 10^{-4}$	$9 \cdot 10^{-6}$
***m* [g]**	10.000	TMPTA: 2.346	0.059	0.001
***n* [mol]**	$2.375 \cdot 10^{-2}$	$7.918 \cdot 10^{-3}$	$3.2 \cdot 10^{-4}$	$5 \cdot 10^{-6}$
***m* [g]**	10.002	PETA: 2.111	0.060	0.002
***n* [mol]**	$2.375 \cdot 10^{-2}$	$5.991 \cdot 10^{-3}$	$3.3 \cdot 10^{-4}$	$9 \cdot 10^{-6}$

Table 91. Influence of urethane precursor chain length: Masterbatches from PEG600-precursor of (b) 3 eq. PEG600, 2 eq. MDI and 2 eq. pTMI or (a) 4 eq. PEG600, 3 eq. MDI and 2 eq. pTMI or (c) 5 eq. PEG600, 4 eq. MDI and 2 eq. pTMI, potassium octoate (K Oct), butylated hydroxytoluene (BHT) and hexane diacrylate (HDDA). Curing at 120 °C for 20 h. For the precursor is $n = n(\text{N-H})/m(\text{precursor})$.

Substance	**Precursor**	**HDDA**	**K Oct**	**BHT**
***m* [g]**	(b) 10.002	2.648	0.060	0.002
***n* [mol]**	$2.341 \cdot 10^{-2}$	$1.170 \cdot 10^{-2}$	$3.3 \cdot 10^{-4}$	$9 \cdot 10^{-6}$
***m* [g]**	(a) 10.002	2.649	0.059	0.002
***n* [mol]**	$2.343 \cdot 10^{-2}$	$1.171 \cdot 10^{-3}$	$3.2 \cdot 10^{-4}$	$9 \cdot 10^{-6}$
***m* [g]**	(c) 10.003	2.654	0.059	0.001
***n* [mol]**	$2.344 \cdot 10^{-2}$	$1.173 \cdot 10^{-3}$	$3.2 \cdot 10^{-4}$	$5 \cdot 10^{-6}$

Table 92. Influence of urethane precursor chain type: Masterbatches from PU-precursor of (a) 4 eq. PEG600, 3 eq. MDI and 2 eq. pTMI or (d) 4 eq. PEG1500, 3 eq. MDI and 2 eq. pTMI or (e) 4 eq. HDI-prepolymer, 3 eq. MDI and 2 eq. pTMI, potassium octoate (K Oct), butylated hydroxytoluene (BHT) and pentaerythritol tetraacrylate (PETA). For (a) curing at 120 °C/20 h, for (d) at 130 °C/20 h, for (e) at 140 °C/22 h. For the precursor is $n = n(\text{N-H})/m(\text{precursor})$.

Substance	**Precursor**	**PETA**	**K Oct**	**BHT**
***m* [g]**	(a) 10.002	2.111	0.060	0.002
***n* [mol]**	$2.375 \cdot 10^{-2}$	$5.991 \cdot 10^{-3}$	$3.3 \cdot 10^{-4}$	$9 \cdot 10^{-6}$
***m* [g]**	(d) 15.000	1.514	0.044	0.001
***n* [mol]**	$1.717 \cdot 10^{-2}$	$4.296 \cdot 10^{-3}$	$2.4 \cdot 10^{-4}$	$5 \cdot 10^{-6}$
***m* [g]**	(e) 15.010	2.315	0.064	0.002
***n* [mol]**	$2.629 \cdot 10^{-2}$	$6.571 \cdot 10^{-3}$	$3.5 \cdot 10^{-4}$	$9 \cdot 10^{-6}$

7 List of hazardous substances

Table 93. Hazardous statements for chemical compounds used in this work.[204]

Substance (CAS-No.)	GHS-Pictogram	H-Statement	P-Statement
Acetone (67-64-1)		H225-H319-H336	P210-P305+P351+P338
Acryloyl chloride (814-68-6)		H225-H290-H302+H312-H314-H330	P210-P280-P304+P340+P310-P305+P351+P338-P370+P378-P403+P235
Ascorbic acid (50-81-7)	Not a hazardous substance or mixture according to regulation (EC) no. 1272/2008.		
BHT (128-37-0)		H410	P273-P501
2-[(Butylcarbamoyl) oxy]ethyl acrylate (63225-53-6)		H315-H319-H335	P261-P305+P351+P338
4-^{t}Butylcyclohexyl acrylate (84100-23-2)		H317-H400-H410	P261-P273-P272-P280-P302+P352-P333+P313-P362+P364-P391
1-Butanol (71-36-3)		H226-H302-H315-H318-H335-H336	P210-P280-P301+P312+P330-P304+P340+P312-P305+P351+P338+P310-P403+P235
1-Butanol-d_{10} (34193-38-9)		H226-H302-H315-H318-H335-H336-H335+H336	P261-P280-P305+P351+P338
^{t}Butyl hydroperoxide (75-91-2)		H226-H242-H302-H311-H320-H314-H317-H341-H411	P210-P220-P280-P301+P330+P331-P303+P361+P353-

			P305+P351+P338-P310
15-Crown-5 ether (33100-27-5)		H302-H319	P301+P312+P330-P305+P351+P338
18-Crown-6 ether (17455-13-9)		H302	P301+P312+P330
2,4-Dimethyl-3-pentanol (600-36-2)		H226-H302-H315-H318-H335	P261-P280-P305+P351-P338
Poly (1,4-butylene adipate) (25103-87-1)	Not a hazardous substance or mixture according to regulation (EC) no. 1272/2008.		
1-Ethanol (64-17-5)		H225-H319	P210-P280-P305+P351+P338-P337+P313-P403+P235
Ethyl acetate (141-78-6)		H225-H319-H336	P210-P305+P351+P338
1-Hexanol (111-27-3)		H226-H302-H319	P210-P305+P351+P338
Hexyl acrylate (2499-95-8)		H315-H317-H319-H335-H411	P261-P273-P280-P305+P351+P338
2-Hydroxyethyl acrylate (818-61-1)		H302-P311-P314-P317-P400	P273-P280-P303+P361+P353-P304+P340+P310-P305+P351+P338-P33+P313
2-Hydroxyethyl methacrylate (868-77-9)		H315-H317-H319	P261-P264-P280-P333+P317-P337+P313-P362+P364

Iron(II) sulfate (7720-78-7)		H302-H315-H319	P301+P312+P330-P302+P352-P305+P351+P338
IsoPMDI 92140 (9016-87-9)		H315-H317-H319-H332-H334-H335-H351-H373	P280-P285-P302+P352-P305+P351+P338-P403+P233-P501
Jeffcat ZR-70 (1704-62-7)		H312-H318	P280-P305+P351+P338
K Oct (3164-85-0)		H302-H315-H319-H335	P261-P280-P301+P312
MoPEG480 acrylate (3217-1-39-4)	Not a hazardous substance or mixture according to regulation (EC) no. 1272/2008.		
MoPEG350 (9004-74-4)	Not a hazardous substance or mixture according to regulation (EC) no. 1272/2008.		
MoPEG500 (9004-74-4)	Not a hazardous substance or mixture according to regulation (EC) no. 1272/2008.		
MoPEG750 (9004-74-4)	Not a hazardous substance or mixture according to regulation (EC) no. 1272/2008.		
Niax Silicone L-6900 (-)	Not a hazardous substance or mixture according to regulation (EC) no. 1272/2008.		
Octoyl acrylate (103-11-7)		H315 -H317-H335-H412	P273-P280-P305+P351+P338-P333+P313
PEG600 (25322-68-3)	Not a hazardous substance or mixture according to regulation (EC) no. 1272/2008.		
PEG1000 (25322-68-3)	Not a hazardous substance or mixture according to regulation (EC) no. 1272/2008.		
PEG1500 (25322-68-3)	Not a hazardous substance or mixture according to regulation (EC) no. 1272/2008.		
Petroleum ether (8032-32-4)		H224-H304-H315-H336-H411	P210-P301+P310-P331-P370+P378-P403+P235

Phenoxyethyl acrylate (48145-04-6)		H317-H411	P280-P261-P273-P272-P303+P352-P333+P311-P362+P364-P391-P501
Polyetherol 90060 (-)	Not a hazardous substance or mixture according to regulation (EC) no. 1272/2008.		
Polyetherol 91120 (25322-69-4)		H302	P264-P270-P301+P312-P330-P501
1-Propanol (71-23-8)		H225-H319-H336	P210-P305+P351+P338-P370+P378-P403+P235
2-Propanol (67-63-0)		H225-H319-H336	P210-P233-P240-P241-P242-P305+P351+P338
Lupranol 1200 (25322-69-4)		H302	P264-P270-P301+P312-P330-P501
PTHF1400 (25190-06-1)		H315-H319-H335	P261-P305+P351+P338
pTMI (622-58-2)		H302+H312+H332-H315-H319-H334	P261-P280-P305+P351+P338-P342+P311
Stearyl acrylate (4813-57-4)		H315 -H319-H335-H411	P261-P273-P305+P351+P338
Toluene (108-88-3)		H225-H305-H315-H336-H361d-H373-H412	P201-P210-P273-P301+P310+P331-P302+P352-P308+P313
Triethylamine (121-44-8)		H225-H302-H311+H331-H314-H335	P210-P280-P303+P361+P353-P304+P340+P310-

			P305+P351+P338- P403+P233
THF **(109-99-9)**		H225-H302-H319- H335-H336-H351	P201-P210- P301+P312+P330- P305+P351+P338- P308+P313
2-PrOH **(67-63-0)**		H225-H319-H336	P210- P305+P351+P338- P370+P378- P403+P235
MeOH **(67-56-1)**		H225- H301+H311+H331- H370	P210-P280- P302+P352+P312- Ü304+P340+P311- P370+P378- P403+P235
HDDA **(13048-33-4)**		H315-H317-H319	P280- P305+P351+P338
TMPTA **(15625-89-5)**		H315-H317-H319	P280-P302+P352- P305+P351+P338
PETA **(4986-89-4)**		H315-H317-H319	P280- P305+P351+P338
4,4'-MDI **(101-68-8)**		H315-H317-H319- H332-H334-H335- H351-H373	P261-P280-P284- P304+P340+P312- P305+P351+P338- P342+P311
K Ac **(127-08-2)**	Not a hazardous substance or mixture according to regulation (EC) no. 1272/2008.		
Rb Ac **(536-67-7)**	Not a hazardous substance or mixture according to regulation (EC) no. 1272/2008.		
Cs Ac **(3396-11-0)**	Not a hazardous substance or mixture according to regulation (EC) no. 1272/2008.		
K Oct **(3164-85-0)**		H302-H315-H319- H335	P261-P280- P301+P312-

			P302+P352- P305+P351+P338
Rb Oct **(-)**	No CAS-number and classification was found.		
Cs Oct **(-)**	No CAS-number and classification was found.		
DABCO **(280-57-9)**		H228-H302-H315- H318	P210-P240-P280- P310+P312- P302+P352- P305+P351+P338
1-MI **(616-47-7)**		H311-H302-H314	P280-P260-P270- P264-P310- P305+P351+P338- P303+P361+P353- P304+P340- P361+P364- P301+P330+P331
DBU **(6674-22-2)**		H301-H314	P280-P260-P270- P264-P310- P305+P351+P338- P303+P361+P352- P304+P340- P301+P330+P331- P405-P501
BDMA **(103-83-3)**		H226-H301- H312+H332-H314- H411	P210-P273-P280- P301+P310+P330- P303+P361-P353- P305+P351+P338- P310
MeHQ **(150-76-5)**		H302-H317-H319- H361d-H412	P201-P273-P280- P308+P313- P333+P313- P337+P313

LiCl **(7447-41-8)**		H302-H315-H319	P280-P302+P352-P305+P351+P338-P312
2-Phenoxyethanol **(122-99-6)**		H302-H319	P305+P351+P338
BuA **(141-32-2)**		H226-H302+H312+H332-H315-H317-H319-H335-H412	P210-P261-P264-P273-P280-P370+P378
***p*-Toluidine** **(106-49-0)**		H301+H311+H331-H317-H319-H334-H351-H410	P261-P280-P284-P301+P310+P330-P304+P340+P311-P342+P311-P403+P233
Dichloromethane **(75-09-2)**		H315-H319-H336-H351	P201-P302+P352-P305+P351+P338-P308+P313
Zr(IV)*n*-butoxide **(-)**		H226-H314-H335-H336	P210-P280-P301+P330+P331-P303+P361+P353-P305+P351+P338-P310
oTMI **(614-68-6)**		H302+H312+H332-H315-H319-H334-H335	P280-P301+P312+P330-P302+P352+P312-P305+P351+P338
mTMI **(621-29-4)**		H315-H317-H319-H330-H334-H335	P280-P302+P352-P304+P340+P310-P305+P351+P338
$MgSO_4$ **(7487-88-9)**	Not a hazardous substance or mixture according to regulation (EC) no. 1272/2008.		

8 Bibliography

[1] O. Bayer, H. Rinke, W. Siefken, *Verfahren Zur Herstellung von Polyurethanen Bzw. Polyharnstoffen*, **1937**, DRP. 728981.

[2] O. Bayer, *Angew. Chemie, Ausgabe A* **1947**, *9*, 257–288.

[3] R. Geyer, J. R. Jambeck, K. L. Law, *Sci. Adv.* **2017**, *3*, 19–24.

[4] H. W. Engels, H. G. Pirkl, R. Albers, R. W. Albach, J. Krause, A. Hoffmann, H. Casselmann, J. Dormish, *Angew. Chemie - Int. Ed.* **2013**, *52*, 9422–9441.

[5] Z. R. Petrovic, J. Ferguson, *Prog. Polym. Sci.* **1991**, *16*, 695–836.

[6] E. Delebecq, J. Pascault, B. Boutevin, *Chem. Rev.* **2013**, *113*, 80–118.

[7] J. O. Akindoyo, M. D. H. Beg, S. Ghazali, M. R. Islam, N. Jeyaratnam, A. R. Yuvaraj, *RSC Adv.* **2016**, *6*, 114453–114482.

[8] A. Frick, A. Rochman, *Polym. Test.* **2004**, *23*, 413–417.

[9] C. Prisacariu, *Polyurethane Elastomers From Morphology to Mechanical Aspects*, **2011**.

[10] R. Leppkes, *Polyurethane*, Süddeutscher Verlag Onpact GmbH, München, **2012**.

[11] D. Fragiadakis, J. Runt, *Macromolecules* **2013**, *46*, 4184–4190.

[12] K. Gisselfält, B. Helgee, *Macromol. Mater. Eng.* **2003**, *288*, 265–271.

[13] T. K. Kwei, *J. Appl. Polym. Sci.* **1982**, *27*, 2891–2899.

[14] Q. Tian, I. Krakovsky, G. Yan, L. Bai, J. Liu, G. Sun, L. Rosta, B. Chen, L. Almasy, *Polymers (Basel).* **2016**, *8*, 1–12.

[15] C. S. P. Sung, N. S. Schneider, *Macromolecules* **1974**, *8*, 68–73.

[16] C. Prisacariu, E. Scortanu, B. Agapie, *Int. J. Polym. Anal. Charact.* **2012**, *17*, 312–320.

[17] A. M. Castagna, D. Fragiadakis, H. Lee, T. Choi, J. Runt, *Macromolecules* **2011**, *44*, 7831–7836.

[18] R. Bonart, *J. Macromol. Sci. , Part B* **1968**, *2*, 37–41.

[19] L. Born, H. Hespe, J. Crone, K. H. Wolf, *Colloid Polym. Sci.* **1982**, *260*, 819–828.

[20] R. Bonart, L. Morbitzer, G. Hentze, *J. Macromol. Sci. Part B* **1969**, *3*, 337–356.

[21] C. Prisacariu, E. Scortanu, *High Perform. Polym.* **2011**, *23*, 308–313.

[22] J. Reichelt, R. Reichelt, *Energieaufnehmender Druckfederkörper Und Verfahren Zur Herstellung Desselben*, **2012**, DE19700629 B4.

[23] E. GmbH, *Fahrradfedern*, **1995**, DE29515660 U1.

[24] H. L. H. Takayama, T. Tanaka, M. Harar, *Polyurethane Elastic Yarn and Production Method Thereof*, **2011**, WO2011052185.

[25] Masal Marketing & Trading, *Sole Insert for Walking Device*, **2011**, EP2342984

A1.

[26] B. Eling, Ž. Tomović, V. Schädler, *Macromol. Chem. Phys.* **2020**, 2000114.

[27] Y. Bao, J. Ma, X. Zhang, C. Shi, *J. Mater. Sci.* **2015**, *50*, 6839–6863.

[28] K. Y. Show, Y. G. Yan, J. Zhao, J. Shen, Z. X. Han, H. Y. Yao, D. J. Lee, *Bioresour. Technol.* **2020**, *317*, 123975.

[29] E. R. Braga, G. de S. Mustafa, D. de A. Pontes, L. A. M. Pontes, *Chem. Ind. Chem. Eng. Q.* **2020**, *26*, 59–69.

[30] A. S. Paula, L. G. Possato, D. R. Ratero, J. Contro, K. Keinan-Adamsky, R. R. Soares, G. Goobes, L. Martins, J. G. Nery, *Microporous Mesoporous Mater.* **2016**, *232*, 151–160.

[31] J. Chen, Y. Zhao, *J. Appl. Polym. Sci.* **2000**, *75*, 808–814.

[32] Xia Zhao, H. Hao, Y. Duan, *Polym. Sci. - Ser. A* **2020**, *62*, 184–195.

[33] Y. Chen, A. Lin, F. Gan, *Appl. Surf. Sci.* **2006**, *252*, 8635–8640.

[34] K. Li, X. Zeng, H. Li, X. Lai, *Appl. Surf. Sci.* **2014**, *298*, 214–220.

[35] S. H. Lu, G. Z. Liang, J. L. Wang, H. J. Ren, *J. Appl. Polym. Sci.* **2006**, *99*, 3195–3202.

[36] Z. Czech, R. Milker, *J. Appl. Polym. Sci.* **2003**, *87*, 182–191.

[37] E. Jablonski, T. Learner, J. Hayes, M. Golden, *Stud. Conserv.* **2003**, *48*, 3–12.

[38] M. Zou, Q. Zhao, J. Nie, Z. Zhang, *J. Appl. Polym. Sci.* **2007**, *103*, 1406–1411.

[39] T. Tamai, M. Watanabe, *J. Polym. Sci. Part A Polym. Chem.* **2006**, *44*, 273–280.

[40] I. Tissot, C. Novat, F. Lefebvre, E. Bourgeat-Lami, *Macromolecules* **2001**, *34*, 5737–5739.

[41] J. I. Amalvy, M. J. Percy, S. P. Armes, H. Wiese, *Langmuir* **2001**, *17*, 4770–4778.

[42] R. F. Linemann, T. E. Malner, R. Brandsch, G. Bar, W. Ritter, R. Mülhaupt, *Macromolecules* **1999**, *32*, 1715–1721.

[43] V. D. Athawale, M. A. Kulkarni, *Prog. Org. Coatings* **2009**, *65*, 392–400.

[44] S. D. Maurya, S. K. Kurmvanshi, S. Mohanty, S. K. Nayak, *Polym. - Plast. Technol. Eng.* **2018**, *57*, 625–656.

[45] E. S. Džunuzović, S. V. Tasić, B. R. Božić, J. V. Džunuzović, B. M. Dunjić, K. B. Jeremić, *Prog. Org. Coatings* **2012**, *74*, 158–164.

[46] B. Türel Erbay, I. E. Serhatli, *Prog. Org. Coatings* **2013**, *76*, 1–10.

[47] P. J. Peruzzo, P. S. Anbinder, O. R. Pardini, J. Vega, C. A. Costa, F. Galembeck, J. I. Amalvy, *Prog. Org. Coatings* **2011**, *72*, 429–437.

[48] B. K. Kim, J. C. Lee, *J. Appl. Polym. Sci.* **1995**, *58*, 1117–1124.

[49] E. R. Beckel, J. Nie, J. W. Stansbury, C. N. Bowman, *Macromolecules* **2004**, *37*, 4062–4069.

[50] B. M. Culbertson, L. K. Post, *Acrylic Monomers Containing Carbamate*

Functionality, **1981**, US4279833.

[51] E. Yukio Tsuge, A. Haruo Iizuka, *Ultraviolet-Hardening Urethane Acrylate Oligomer*, **1994**, US5322861.

[52] J. Kim, H. Im, C. K. Kim, **2013**, DOI 10.1021/ie303208p.

[53] C.-S. Ha, S.-J. Jung, E.-S. Kim, W.-S. Kim, S.-J. Lee, W.-J. Cho, *J. Appl. Polym. Sci.* **1996**, *62*, 1011–1021.

[54] M. Szyncher, in *Szyncher's Handb. Polyurethanes*, CRC Press, Boca Raton, **2013**, p. 597.

[55] J. Y. Kim, K. D. Suh, *Colloid Polym. Sci.* **1996**, *274*, 920–927.

[56] F. R. Mayo, *J. Am. Chem. Soc.* **1943**, *65*, 2324–2329.

[57] B. D. Mather, K. Viswanathan, K. M. Miller, T. E. Long, *Prog. Polym. Sci.* **2006**, *31*, 487–531.

[58] N. F. Albertson, *J. Am. Chem. Soc.* **1948**, *70*, 669–670.

[59] A. Genest, D. Portinha, E. Fleury, F. Ganachaud, *Prog. Polym. Sci.* **2017**, *72*, 61–110.

[60] M. Bláha, O. Trhlíková, J. Podešva, S. Abbrent, M. Steinhart, J. Dybal, M. Dušková-Smrčková, *Tetrahedron* **2017**, *74*, 58–67.

[61] J. Wang, P. Li, S. Hing, A. S. C. Chan, F. Yee, *Tetrahedron Lett.* **2012**, *53*, 2887–2889.

[62] Y. J. Wu, *Tetrahedron Lett.* **2006**, *47*, 8459–8461.

[63] J. Cabral, P. Laszlo, L. Mahé, M. T. Montaufier, S. L. Randriamahefa, *Tetrahedron Lett.* **1989**, *30*, 3969–3972.

[64] A. G. Ying, L. Liu, G. F. Wu, G. Chen, X. Z. Chen, W. D. Ye, *Tetrahedron Lett.* **2009**, *50*, 1653–1657.

[65] A. Y. Rulev, *Russ. Chem. Rev.* **2011**, *80*, 197–218.

[66] P. Wipf, Y. Kim, *Tetrahedron Lett.* **1992**, *33*, 5477–5480.

[67] P. Wipf, Y. Kim, D. M. Goldstein, *J. Am. Chem. Soc.* **1995**, *117*, 11106–11112.

[68] Mazen Es-Sayed, C. Gratkowski, N. Krass, A. I. Meyers, A. de Meijere, *Synlett* **1992**, 962.

[69] A. de Meijere, K. Ernst, B. Zuck, M. Brandl, S. I. Kozhushkov, M. Tamm, D. S. Yufit, J. A. K. Howard, T. Labahn, *Eur. J. Org. Chem.* **1999**, 3105–3115.

[70] Y. Takeuchi, S.-S. Tokuda, T. Takagi, M. Koike, H. Abe, T. Harayama, Y. Shibata, H.-S. Kim, Y. Wataya, *Heterocycles* **1999**, *51*, 1869–1875.

[71] I. J. McAlpine, R. W. Armstrong, *Tetrahedron Lett.* **2000**, *41*, 1849–1853.

[72] T. C. Wabnitz, J. Q. Yu, J. B. Spencer, *Chem. - A Eur. J.* **2004**, *10*, 484–493.

[73] T. C. Wabnitz, J. Q. Yu, J. B. Spencer, *Synlett* **2003**, 1070–1072.

[74] S. Kobayashi, K. Kakumoto, M. Sugiura, *Org. Lett.* **2002**, *4*, 1319–1322.

[75] M. J. Gaunt, J. B. Spencer, *Org. Lett.* **2001**, *3*, 25–28.

[76] Y. K. Chen, M. Yoshida, D. W. C. MacMillan, *J. Am. Chem. Soc.* **2006**, *128*, 9328–9329.

[77] L. Y. Chen, H. He, B. J. Pei, W. H. Chan, A. W. M. Lee, *Synthesis (Stuttg).* **2009**, 1573–1577.

[78] D. Enders, C. Wang, J. X. Liebich, *Chem. - A Eur. J.* **2009**, *15*, 11058–11076.

[79] S. Srinivasan, M. W. Lee, M. C. Grady, M. Soroush, A. M. Rappe, *J. Phys. Chem. A* **2010**, *114*, 7975–7983.

[80] H. Sardon, A. Pascual, D. Mecerreyes, D. Taton, H. Cramail, J. L. Hedrick, *Macromolecules* **2015**, *48*, 3153–3165.

[81] J. Otera, *Chem. Rev.* **1993**, *93*, 1449–1470.

[82] R. W. Taft, M. S. Newman, F. H. Verhoek, *J. Am. Chem. Soc.* **1950**, *72*, 4511–4519.

[83] J. H. Billman, W. T. Smith, J. L. Rendall, *J. Am. Chem. Soc.* **1947**, *69*, 2058–2059.

[84] D. J. Fortman, D. T. Sheppard, W. R. Dichtel, *Macromolecules* **2019**, *52*, 6330–6335.

[85] T. Katoh, Y. Ogawa, Y. Ohta, T. Yokozawa, *J. Polym. Sci.* **2021**, *59*, 787–797.

[86] E. Dyer, R. J. Hammond, *J. Polym. Sci. Part A Polym. Chem.* **1964**, *2*, 1–14.

[87] J. H. Saunders, J. K. Backus, *Rubber Chem. Technol.* **1966**, *39*, 461–480.

[88] G. Dijkstra, W. H. Kruizinga, R. M. Kellogg, *J. Org. Chem.* **1987**, *52*, 4230–4234.

[89] B. F. Gisin, in *Helv. Chim. Acta*, **1973**, pp. 1476–1482.

[90] S. Jaehnke, Aza-Michael-Reaktionen an Monofunktionellem Urethan Sowie Linearen Polyurethanen, Universität Hamburg, **2018**.

[91] Z. Wen, W. Hu, X. Chi, X. Wang, D. Tia, M. Wang, J. Liu, X. Ma, A. Pang, *Commun. Comput. Chem.* **2014**, *2*, 22–35.

[92] Z. Yang, H. Peng, W. Wang, T. Liu, *J. Appl. Polym. Sci.* **2010**, *116*, 2658–2667.

[93] R. A. Cageao, M. W. Lesko, *SPRAYABLE ELASTOMERIC POLYURETHANE FOAM AND PROCESS FOR ITS PRODUCTIOn*, **2010**, US 2010/0280139 A1.

[94] A. Basterretxea, Y. Haga, A. Sanchez-Sanchez, M. Isik, L. Irusta, M. Tanaka, K. Fukushima, H. Sardon, *Eur. Polym. J.* **2016**, *84*, 750–758.

[95] B. Ochiai, S. Inoue, T. Endo, *J. Polym. Sci. Part A Polym. Chem.* **2005**, *43*, 6282–6286.

[96] P. Wonner, T. Steinke, L. Vogel, S. M. Huber, *Chem. Eur. J.* **2020**, *26*, 1258–1262.

[97] A. Aneja, G. L. Wilkes, E. Yurtsever, I. Yilgor, *Polymer (Guildf).* **2002**, *44*, 757–768.

[98] M. Jalilian, H. Yeganeh, M. N. Haghighi, *Polym Int* **2008**, *57*, 1385–1394.

[99] S. K. Garg, R. Kumar, A. K. Chakraborti, *Tetrahedron Lett.* **2005**, *46*, 1721–1724.

[100] C. J. Pedersen, *J. Am. Chem. Soc.* **1967**, *89*, 7017–7036.

[101] H. K. Frensdorff, *J. Am. Chem. Soc.* **1971**, *93*, 600–606.

[102] P. Arenaz, L. Bitticks, K. H. Pannell, S. Garcia, *Mutat. Res. Toxicol.* **1992**, *280*, 109–115.

[103] L. L. Chan, K. H. Wong, J. Smid, *J. Am. Chem. Soc.* **1970**, *92*, 1955–1963.

[104] J. Lewis, B. Moore, G. Wilkinson, *J. Chem. Soc.* **1959**, *209*, 3767–3773.

[105] J. Luchtenberg, H. Ritter, *Macromol. Rapid Commun.* **1994**, *15*, 81–86.

[106] J. Alexander, J. M. Brewer, *Vaccines Containing Non-Ionic Surfactant Vesicles*, **1997**, 5,679,355.

[107] R. J. Pokorny, T. P. Klun, C. B. Walker Jr, D. B. Olson, J. M. Noyola, M. L. Toy, E. L. Schwartz, *Coating Compositions Comprising Non-Ionic Surfactant Exhibitng Reduced Fingerprind Visibility*, **2014**, 8,742,022 B2.

[108] G. Vanlerberghe, H. Sebag, *Hair Dyeing Composition Containing a Non-Ionic Surfactant*, **1976**, 3,966,398.

[109] H.-J. Butt, K. Graf, M. Kappl, in *Phys. Chem. Interfaces*, Wiley-VCH Verlag GmbH & Co. KGaA, Weinheim, **2013**, pp. 323–327.

[110] P. Atkins, J. Paula, *Physikalische Chemie*, Wiley-VCH Verlag, Weinheim, **2013**.

[111] H.-J. Butt, K. Graf, M. Kappl, in *Phys. Chem. Interfaces*, Wiley-VCH Verlag GmbH & Co. KGaA, Weinheim, **2013**, pp. 327–331.

[112] "https://www.kruss-scientific.com/fileadmin/_processed_/csm_kruss_meth_sfts_cmc_determination_1000px_en_578035a04c.png," **2020**.

[113] J. N. Israelachvili, D. J. Mitchell, B. W. Ninham, *J. Chem. Soc. Faraday Trans. 2 Mol. Chem. Phys.* **1976**, *72*, 1525–1568.

[114] T. M. Herrington, S. S. Sahi, *J. Colloid Interface Sci.* **1988**, *121*, 107–120.

[115] J. P. Conroy, C. Hall, C. A. Leng, K. Rendall, G. J. T. Tiddy, J. Walsh, G. Lindblom, *Progr. Colloid Polym. Sci.* **1990**, *82*, 253–262.

[116] W. N. Maclay, *J. Colloid Sci.* **1956**, *11*, 272–285.

[117] M. Andersson, G. Karlström, *J. Phys. Chem.* **1985**, *89*, 4957–4962.

[118] B. Lindman, B. Medronho, G. Karlström, *Curr. Opin. Colloid Interface Sci.* **2016**, *22*, 23–29.

[119] G. Karlström, *J. Phys. Chem.* **1985**, *89*, 4962–4964.

[120] V. Viti, P. Zampetti, *Chem. Phys.* **1973**, *2*, 233–238.

[121] D. J. Mitchell, G. J. T. Tiddy, L. Waring, *J. Chem. Soc., Faraday Trans. 1* **1983**, *79*, 975.

[122] K. S. Sharma, S. R. Patil, A. K. Rakshit, *Colloids Surfaces A Physicochem. Eng. Asp.* **2003**, *219*, 67–74.

[123] T. Gu, P. A. Galera-Gómez, *Colloids Surfaces A Physicochem. Eng. Asp.* **1999**, *147*, 365–370.

[124] W. C. Griffin, *J. Soc. Cosmet. Chem.* **1949**, *1*, 311–326.

[125] W. C. Griffin, *J. Soc. Cosmet. Chem.* **1954**, *5*, 249–256.

[126] C. Rodríguez-Abreu, *J. Surfactants Deterg.* **2019**, *22*, 1001–1010.

[127] L. O. Orafidiya, F. A. Oladimeji, *Int. J. Pharm.* **2002**, *237*, 241–249.

[128] Z. Liu, W. Liu, C. Lang, Y. Li, *Energy Procedia* **2019**, *158*, 5275–5280.

[129] W. El-sayed, T. G. M. Mohammad, *J. Apllied Life Sci. Int.* **2019**, *22*, 1–10.

[130] A. Carmona Hernandez, E. Vazquez Velez, J. Uruchurtu, J. G. Gonzalez Rodriguez, *ECS Trans.* **2019**, *94*, 41–51.

[131] M. P. Nieh, S. K. Kumar, R. H. Fernando, R. H. Colby, J. Katsaras, *Langmuir* **2004**, *20*, 9061–9068.

[132] R. Herrington, K. Hock, R. Autenrieth, J. Beckerdite, P. Berthevas, M. Brown, S. Burks, F. Casati, R. De Genova, J. Fosnaugh, et al., *Flexible Polyurethane Foams*, Dow Chemical, Midland, **1997**.

[133] J. Santos, N. Calero, L. A. Trujillo-Cayado, M. C. Garcia, J. Muñoz, *Colloids Surfaces B Biointerfaces* **2017**, *159*, 405–411.

[134] M. Szyncher, in *Szyncher's Handb. Polyurethanes*, CRC Press, Boca Raton, **2013**, pp. 277–279.

[135] R. M. Hill, in *Silicone Surfactants (Surfactant Sci.*, Marcel Dekker, New York, **1999**, pp. 38–39.

[136] X. D. Zhang, C. W. Macosko, H. T. Davis, *ACS Symp. Ser.* **1997**, *669*, 130–142.

[137] M. Szyncher, in *Szyncher's Handb. Polyurethanes*, CRC Press, Boca Raton, **2013**, pp. 210, 281.

[138] A. H. Baferani, R. Keshavarz, M. Asadi, A. R. Ohadi, *Adv. Polym. Technol.* **2018**, *37*, 71–83.

[139] X. D. Zhang, C. W. Macosko, H. T. Davis, A. D. Nikolov, D. T. Wasan, *J. Colloid Interface Sci.* **1999**, *215*, 270–279.

[140] C. S. Chern, *Prog. Polym. Sci.* **2006**, *31*, 443–486.

[141] R. J. Young, P. A. Lovell, in *Introd. to Polym.*, CRC Press, Boca Raton, **2011**, pp. 93–97.

[142] S. C. Thickett, R. G. Gilbert, *Polymer (Guildf).* **2007**, *48*, 6965–6991.

[143] P. A. Lovell, F. J. Schork, *Biomacromolecules* **2020**, *21*, 4396–4441.

[144] T. Cole, B. Sokull-Kluettgen, *No-Longer Polymer List, Version 2*, **2007**.

[145] A. M. Fernandez, U. Held, A. Willing, W. H. Breuer, *Prog. Org. Coatings* **2005**, *53*, 246–255.

[146] B. V. K. J. Schmidt, V. Molinari, D. Esposito, K. Tauer, M. Antonietti, *Polymer (Guildf).* **2017**, *112*, 418–426.

[147] C. N. Urbani, H. N. Nguyen, M. J. Monteiro, *Aust. J. Chem.* **2006**, *59*, 728–732.

[148] C. Patrascu, F. Gauffre, F. Nallet, R. Bordes, J. Oberdisse, N. De Lauth-Viguerie, C. Mingotaud, *ChemPhysChem* **2006**, *7*, 99–101.

[149] T. B. Nguyen, C. M. Phan, *J. Surfactants Deterg.* **2019**, *22*, 229–235.

[150] V. B. Fainerman, S. V. Lylyk, E. V. Aksenenko, A. V. Makievski, J. T. Petkov, J. Yorke, R. Miller, *Colloids Surfaces A Physicochem. Eng. Asp.* **2009**, *334*, 1–7.

[151] M. Li, Y. Rharbi, X. Huang, M. A. Winnik, *J. Colloid Interface Sci.* **2000**, *230*, 135–139.

[152] M. Fujiwara, M. Miyake, I. Hama, *Colloid Polym. Sci.* **1994**, *272*, 797–802.

[153] Z. Wang, Z. Dai, *Enzyme Microb. Technol.* **2010**, *46*, 407–418.

[154] H. Lim, S. H. Kim, B. K. Kim, *eXPRESS Polym. Lett.* **2008**, *2*, 194–200.

[155] P. Mondal, D. V Khakhar, *J. Appl. Polym. Sci.* **2004**, *93*, 2821–2829.

[156] K. Yasunaga, R. A. Neff, X. D. Zhang, C. W. Macosko, *J. Cell. Plast.* **1996**, *32*, 427–448.

[157] Q. N. Do, Synthese Und Anwendung Neuartiger Tenside Im Rahmen Der Emulsionspolymerisation, University of Hamburg, **2021**.

[158] J. L. Gardon, *J. Polym. Sci. Part A-1 Polym. Chem.* **1968**, *6*, 623–641.

[159] EUROPEAN PARLIAMENT, *Off. J. Eur. Union* **2014**, *1907/2006*.

[160] EUROPEAN PARLIAMENT, *Off. J. Eur. Union* **2020**, *2020/1149*.

[161] E. B. Richter, C. W. Macosko, *Polym. Eng. Sci.* **1978**, *18*, 1012–1018.

[162] M. Szyncher, in *Szyncher's Handb. Polyurethanes*, CRC Press, Boca Raton, **2013**, p. 52.

[163] M. F. Sonnenschein, in *Polyurethanes Sci. Technol. Mark. Trends*, **2015**, p. 113.

[164] M. A. Semsarzadeh, A. H. Navarchian, *J. Appl. Polym. Sci.* **2003**, *90*, 963–972.

[165] J. Datta, P. Kasprzyk, *Polym. Eng. Sci.* **2018**, *58*, E14–E35.

[166] D. Randall, S. Lee, Eds. , in *Polyurethane B.*, John Wiley And Sons, Inc., **2002**, p. 6.

[167] D. K. Chattopadhyay, D. C. Webster, *Prog. Polym. Sci.* **2009**, *34*, 1068–1133.

[168] G. Lu, D. M. Kalyon, I. Yilgör, E. Yilgör, *Polym. Eng. Sci.* **2003**, *43*, 1863–1877.

[169] H. Y. Mi, X. Jing, B. S. Hagerty, G. Chen, A. Huang, L. S. Turng, *Mater. Des.* **2017**, *127*, 106–114.

[170] S.-D. Z. Fei Zhao, Han-Xiong Huang, *J. Appl. Polym. Sci.* **2015**, *132*, 42511.

[171] M. Xie, J. Ge, Y. Xue, Y. Du, B. Lei, P. X. Ma, *J. Mech. Behav. Biomed. Mater.* **2015**, *51*, 163–168.

[172] Y. Okamoto, Y. Hasegawa, F. Yoshino, *Prog. Org. Coatings* **1996**, *29*, 175–182.

[173] G. Tillet, B. Boutevin, B. Ameduri, *Prog. Polym. Sci.* **2011**, *36*, 191–217.

[174] M. L. Matuszak, K. C. Frisch, S. L. Reegen, *J Polym Sci Part A-1 Polym Chem* **1973**, *11*, 1683–1690.

[175] M. W. Läubli, B. Kampus, *J. Chromatogr. A* **1995**, *706*, 103–107.

[176] S. Schantz, L. M. Torell, J. R. Stevens, *J. Appl. Phys.* **1988**, *64*, 2038–2043.

[177] A. Ballistreri, S. Foti, P. Maravigna, G. Montaudo, E. Scamporrino, *J. Polym. Sci. A1.* **1980**, *18*, 1923–1931.

[178] F. Zhao, W. Bi, S. Zhao, *J. Macromol. Sci. Part B Phys.* **2011**, *50*, 1460–1469.

[179] M. Tosaka, S. Murakami, S. Poompradub, S. Kohjiya, Y. Ikeda, S. Toki, I. Sics, B. S. Hsiao, *Macromolecules* **2004**, *37*, 3299–3309.

[180] D. W. Van Krevelen, K. Te Nijenhuis, in *Prop. Polym.*, Elsevier B.V., Amsterdam, **2009**, pp. 189–225.

[181] F. Horkay, G. McKenna, in *Phys. Prop. Polym. Handb.*, Springer Science+business Media, New York, **2007**, pp. 497–523.

[182] H. Omidian, S. A. Hashemi, F. Askari, S. Nafisi, *Iran. J. Polym. Sci. Technol.* **1994**, *3*, 115–119.

[183] Z. Petrovic, I. Javni, V. Divjakovic, *J. Polym. Sci. Part B Polym. Phys.* **1998**, *36*, 221–235.

[184] J. L. Valentín, I. Mora-Barrantes, W. Chasse, K. Saalwaächter, *Macromolecules* **2008**, *41*, 4717–4729.

[185] P. J. Flory, J. Rehner, *J. Chem. Phys.* **1943**, *11*, 512–520.

[186] C. Datta, D. Basu, A. Banerjee, *J. Appl. Polym. Sci.* **2002**, *85*, 2800–2807.

[187] M. Jacob, B. Francis, S. Thomas, *Polym. Compos.* **2006**, *27*, 671–680.

[188] R. Hagen, L. Salmén, B. Stenberg, *J. Polym. Sci. Part B Polym. Phys.* **1996**, *34*, 1997–2006.

[189] E. Saldívar-Guerra, E. Vivaldo-lima, *Handbook of Polymer Synthesis, Characterization and Processing*, Wiley-VCH Verlag, Hoboken, New Jersey, **2013**.

[190] M. Ohring, in *Eng. Mater. Sci.*, Academic Press, Inc., San Diego, **1995**, pp. 299–V.

[191] H. Stutz, K. -H Illers, J. Mertes, *J. Polym. Sci. Part B Polym. Phys.* **1990**, *28*, 1483–1498.

[192] M. Jacob, B. Francis, S. Thomas, *Polym. Compos.* **2006**, *27*, 671–680.

[193] R. J. Young, P. A. Lovell, in *Introd. to Polym.*, CRC Press, Boca Raton, **2011**, p. 10.

[194] Young, R. J., P. A. Lovell, in *Introd. to Polym.*, CRC Press, Boca Raton, **2011**, pp. 33, 34.

[195] M. M. Feldstein, G. A. Shandryuk, S. A. Kuptsov, N. A. Platé, *Polymer (Guildf).* **2000**, *41*, 5327–5338.

[196] Z. Gu, X. Zhang, C. Bao, M. Xue, H. Wang, X. Tian, *J. Macromol. Sci. Part B Phys.* **2015**, *54*, 618–627.

[197] X. Feng, G. Wang, K. Neumann, W. Yao, L. Ding, S. Li, Y. Sheng, Y. Jiang, M. Bradley, R. Zhang, *Mater. Sci. Eng. C* **2017**, *74*, 270–278.

[198] Y. L. Luo, Y. Miao, F. Xu, *Macromol. Res.* **2011**, *19*, 1233–1241.

[199] I. Hevus, A. Kohut, A. Voronov, *Macromolecules* **2010**, *43*, 7488–7494.

[200] D. Bornstein, R. J. Pazur, *Polym. Test.* **2020**, *88*, 106524.

[201] A. Barton, *Handbook of Solubility Parameters and Other Cohesion Parameters*, CRC Press, Boca Raton, **2017**.

[202] Q. Liu, M. Tian, T. Ding, R. Shi, Y. Feng, L. Zhang, D. Chen, W. Tian, **2006**, DOI 10.1002/app.

[203] A. Kumar, S. De, A. G. Samuelson, E. D. Jemmis, *Organometallics* **2008**, *27*, 955–960.

[204] “www.sigmaaldrich.com,” **2021**.

Acknowledgements

Mein erster Dank gebührt Herrn Professor Dr. Gerrit A. Luinstra. Als Doktorvater ermöglichten Sie mir eine Promotion mit großer Freiheit und Kreativität, sodass ich vieles sehen und lernen konnte – weit über das Thema dieser Promotion hinaus. Dafür danke ich Ihnen sehr.

Ebenso möchte ich mich bei Herrn Professor Dr. Berend Eling bedanken. Ich erinnere mich gerne an deine Betreuung, unsere fachlichen Diskussionen und damit verbunden mein tiefes Eintauchen in die faszinierende Chemie und Welt der Polyurethane. In Lemförde geht mein besonderer Dank an Stefan Auffarth. Ich möchte mich auch bei der BASF Polyurethanes GmbH für das Finanzieren und somit das Ermöglichen dieser Doktorarbeit im Rahmen einer Kooperation bedanken.

Ich bedanke mich ebenso bei meinen fleißigen Bacheloranten Sabrina Tamm und Andres Castro Villavicencio für eure wertvollen Beiträge zu dieser Arbeit. Ebenso danke ich Laurence Jacob und Quynh Nhi Do für eure Unterstützung.

Diese Arbeit würde es nicht geben, wenn es an der Uni Hamburg nicht so viele fleißige und kompetente Hände in den Mess- und Service-Einheiten geben würde. Danke für die unzähligen NMRs, Massen, DSCs, Mikroskopie-Bilder, Formen und Glasgeräte. Ich danke auch Kathleen Pruntsch, dass du als gute Seele die TMC am Laufen hältst. Am DESY danke ich Carsten Muhl für das Erstellen meiner Polymer-Formen.

Danken möchte ich auch euch Yannick Wencke, Jessica Redmann, Marlin Maas, Tim Beermann, Fabian Ratzke, Sabrina Tamm, Imke Schulz, Linyu Mu, Mengyu Zhang und Lasse Finzel. Mit euch war es nie langweilig und wenn ich an die Zeit im Labor und an der Uni Hamburg zurückdenke, dann sehe ich immer auch euch vor meinem inneren Auge. Natürlich danke ich auch dem gesamte Arbeitskreis Luinstra für die freundliche Aufnahme und damit verbunden die unzähligen Kaffeepausen, Feiern, Reisen und Kletterausflüge, das Grillen und Essengehen!

Zuletzt danke ich meinen Eltern für die Ermöglichung dieses Studiums und eure immerwährende Unterstützung. Mein größter Dank gebührt jedoch meiner Frau Linda. Du hast mich durch das ganze Studium mit allen Höhen und Tiefen begleitet. Ohne deinen Rückhalt und Zuspruch würde es diese Arbeit nicht geben. Und auch meiner Tochter Leonie danke ich für deine Entbehrungen, endlose Stunden musstest du schon ohne mich die Welt entdecken. Danke, dass ihr beide für mich da seid.

Declaration on oath

I hereby declare on oath that I have written the present dissertation by my own and have not used other than the acknowledged resources and aids. I hereby declare that I have not previously applied or pursued for a doctorate (Ph.D. studies).

Hamburg, 03.12.2022
(Niklas Voigt)